Understanding plant-fungal nutritional strategies using stable isotopes

Dissertation

Philipp Giesemann

Understanding plant-fungal nutritional strategies using stable isotopes

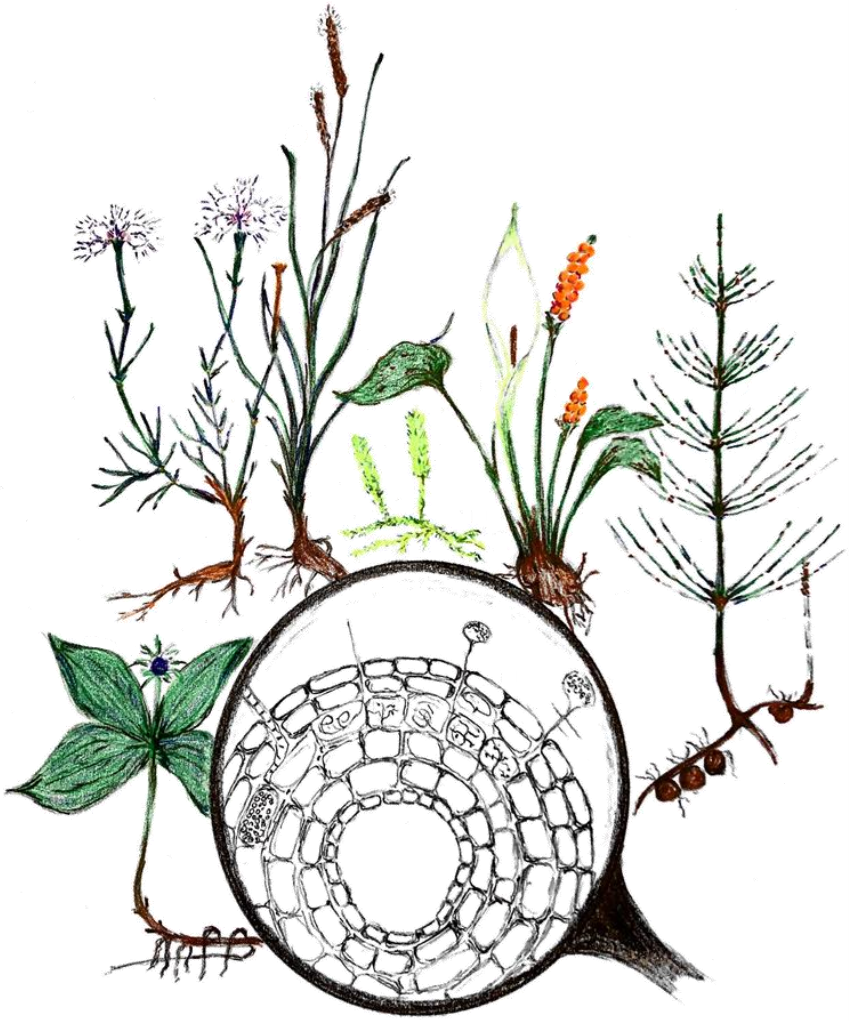

Dissertation

Philipp Giesemann

Understanding plant-fungal nutritional strategies using stable isotopes

Dissertation

Zur Erlangung des akademischen Grades

eines Doktors der Naturwissenschaften (Dr. rer. nat.)

in der Bayreuther Graduiertenschule für Mathematik und Naturwissenschaften

(BayNAT) der Universität Bayreuth

vorgelegt von

Philipp Giesemann

Geboren in Merseburg

Bayreuth, 2021

Die vorliegende Arbeit wurde in der Zeit von Januar 2017 bis Juli 2020 in Bayreuth am BayCEER – Labor für Isotopen-Biogeochemie unter Betreuung von Herrn Professor Dr. Gerhard Gebauer angefertigt.

Die Dissertation wurde von Januar 2017 bis Dezember 2019 durch ein Stipendium des Elitenetzwerks Bayern nach dem Bayerischen Eliteförderungsgesetz (BayEFG) gefördert.

Vollständiger Abdruck der von der Bayreuther Graduiertenschule für Mathematik und Naturwissenschaften (BayNAT) der Universität Bayreuth genehmigten Dissertation zur Erlangung des akademischen Grades eines Doktors der Naturwissenschaften (Dr. rer. nat.).

Dissertation eingereicht am: **29.07.2020**

Zulassung durch das Leitungsgremium: **12.08.2020**

Wissenschaftliches Kolloquium: **02.02.2021**

Amtierender Direktor: Prof. Dr. Markus Lippitz

Prüfungsausschuss:

Prof. Dr. Gerhard Gebauer (Gutachter)

Prof. Dr. Gerhard Rambold (Gutachter)

Prof. Dr. Steven Higgins (Vorsitz)

JProf. Dr. Johanna Pausch

(Weitere Gutachterin: Prof. Dr. Nicole A. Hynson)

LIST OF CONTENT

LIST OF FIGURES

The motivation of the thesis is outlined on page XV. Definitions are provided on page 19. Excursus-1 shortly summarizes findings on the *Arum*- and *Paris*-morphotypes (page 21). Excursus-2 and Excursus-3 exemplarily aggregate *evidence for mycoheterotrophy from a natural stable isotope perspective* and *from an isotope tracer and ^{14}C bomb carbon perspective* (page 26 and 27).

The cover image illustrates selected plant individuals (from left to right): *Paris quadrifolia* (Melanthiaceae), *Dianthus arenarius* (Caryophyllaceae), *Carex flacca* (Cyperaceae), *Lycopodiella inundata* (Lycopodiaceae), *Arum maculatum* (Araceae), *Equisetum arvense* (Equisetaceae). They are inhabited by a variety of root fungal partners which may reflect a variety of symbiotic characteristics. Illustration by Katrin Giesemann.

Acknowledgements

First and foremost, I express my deep gratefulness to *Gerhard Gebauer* ('doctor father') for his support on my professional career and the opportunity to work in his lab under his supervision and expertise. In addition to all guidance and professionalism, I enjoyed the nice chats we had during traveling, the working group and canteen lunches as well as at his Garden and Christmas parties. Thank you very much!

My very special, heartfelt gratitude to *Saskia Klink*. I am incredibly thankful for her professional help on samplings, manuscripts and discussions as well as the personal and moral support and love throughout my student and doctoral time. The journey we had has brought us together even closer than with anyone I know!

My warm thanks to the team of the BayCEER Laboratory of Isotope Biogeochemistry, in particular *Carina Bauer*, *Petra Eckert*, *Christine Tiroch*, *Heidi Zier* and *Isolde Baumann,* who all not only helped with their technical expertise but also made my doctoral time most enjoyable in this lovely team. I want to express special thanks to *Stefan Bindereif* for all long and intensive discussions on scientific topics, statistics and also non-scientific topics. All of it made my doctoral time more fun!

I am very thankful to *Gerhard Rambold* and *Gregor Aas* for being mentors and for their initial and final input on the doctoral project.

I thank the students *Melanie Borgwardt*, *Milena Opgenoorth* and *Lukas Seifert* for their effort on analyzing coal fossils, ferns and carnation plants, respectively. I acknowledge *Adrienne Keller*, *Franziska Zahn*, *Laura Skates* and *Theresa Rupprecht* for manuscript improvements and discussions.

I am also much obliged to the following persons: *Mechthild Kredler* and *Martin Obst* for testing around with staining applications and microscopy (light microscopy, fluorescence microscopy and confocal microscopy) and *Heiko Liebel*, *Pedro Gerstberger*, *Johannes Wagenknecht* for sharing sampling locations.

Finally, I would like to thank the *Elite Network Bavaria* and the *University of Bayreuth Graduate School* for financial support and advanced training offerings as well as all the *persons I did not mention* for their support on my personal and professional career.

My warmest thanks go to my *family* who made me what I am!

Abstract

The mycorrhizal symbiosis is widely accepted as a relationship for mutual carbon-for-nutrient trading. In contrast, hundreds of mycoheterotrophic plant species are identified subverting the usually mutual mycorrhizal symbiosis to utilize their fungal partner as an organic carbon and nitrogen source. Additionally, the focus on nutrient trading in plant-mycorrhizal fungal relationships underrates other common root fungi, such as dark septate endophytes (DSE) and fine root endophytes (FRE). The thesis hypothesizes

(i) the existence of far more mycoheterotrophic plant species than currently estimated and
(ii) a mycorrhiza-like nutritional role for DSE and FRE in plant-fungi relationships (Figure 1).

Isotope applications of the elements carbon (C), nitrogen (N) and hydrogen (H) have proven to be a valuable tool to elucidate organic and inorganic nutrient fluxes between plants and fungi. Thus, the utilization on a fungal source is evident for achlorophyllous plant species belonging to 17 plant families on either arbuscular mycorrhizal (AM) and ectomycorrhizal (EcM) fungi or on litter-decomposing and wood-decomposing fungi. The presence of fully autotrophic plant species on the one hand and achlorophyllous, fully mycoheterotrophic plant species on the other hand obliges us to postulate an intermediate strategy for chlorophyllous plant species which obtain their C energy by means of photosynthesis (autotrophy) while simultaneously channeling off organic C and N from a fungal source (mycoheterotrophy). Evidence of partial mycoheterotrophy is commonly found but yet mostly restricted to only two plant families associated with EcM fungi (Orchidaceae and Ericaceae). Full mycoheterotrophy, indeed, appears most often with AM fungi while evidence of partial mycoheterotrophy on AM fungi is very scarce. Interestingly, the AM symbiosis appears with a continuum of different fungal morphotypes with intercellular *Arum*-morphotype AM and intracellular *Paris*-morphotype AM at the ends of the continuum. So far analyzed, all fully mycoheterotrophic AM plant species appear with intracellular *Paris*-morphotype AM, thus chlorophyllous *Paris*-morphotype AM plant species are candidates for partially mycoheterotrophic nutrition. Due to the overwhelming distribution of AM plant species, the presence of partial mycoheterotrophy on AM fungi could have far-reaching implications for our understanding of plant community functioning which we might have overlooked until now. Thus, a stable isotope natural abundance approach was realized to evaluate the extent of partial mycoheterotrophy on AM fungi.

Furthermore, it is evident that the elusive DSE and FRE fungi are also commonly distributed across all plant clades while little is known about their nutritional role in plant-fungi relationships. Interestingly, DSE and FRE inhabit both mycorrhizal and non-mycorrhizal plant species. The latter might provide an opportunity to shed light onto the nutritional functions of DSE and FRE fungi in plant-fungi symbioses. In this thesis isotope applications were used to decipher a functional role in nutrient trading for the elusive DSE and FRE. Isotope tracer applications were performed to evaluate a carbon-for-nutrient trading while natural abundances were used to decipher whether either organic or inorganic soil compounds might be exchanged in the field.

In brief, the thesis consists of four manuscripts. *Manuscript 1*, *2* and *3* found plant species that were isotopically distinguished in ^{13}C, ^{2}H and frequently ^{15}N appeared either with intercellular *Arum*-morphotype AM or intracellular *Paris*-morphotype AM. The stable isotope enrichment is most likely explained by a partially mycoheterotrophic nutrition on *Paris*-morphotype AM fungi. Thus, the *Paris*-morphotype appears to be a necessary prerequisite for partial mycoheterotrophy on AM fungi. Furthermore, *Manuscript 3* and *4* provide evidence for a functional role of the ubiquitous DSE and FRE fungi in terms of plant-fungi nutrient trading. For the dual symbiosis of DSE and *Paris*-morphotype AM fungi in Equisetaceae, isotopic evidence supports an organic soil N transfer from the former and organic C transfer from the latter. Thus, organic nutrient transfer in plant-fungi symbioses may not be limited to mycoheterotrophs. This suggests DSE and FRE fungi may occupy a previously under-recognized but ecologically relevant role similar to mycorrhizas.

Summarizing, isotope natural abundance compositions supported a partially mycoheterotrophic nutrition for the *Paris*-morphotype AM-forming forest herbaceous species *Paris quadrifolia* (true lover's knot, Melanthiaceae) and *Anemone nemorosa* ('wood anemone', Ranunculaceae) (*Manuscript 1*). A literature survey of isotope natural abundance compositions resulted in 135 plant species being either achlorophyllous forming *Paris*-morphotype (13 species), chlorophyllous forming *Paris*-morphotype (63 species) or chlorophyllous forming *Arum*-morphotype (59 species). Partial mycoheterotrophy appeared frequently among the chlorophyllous *Paris*-morphotype AM plant species (31 out of 63 species under study), especially herbaceous forest seed plants and pteridophytes (*Manuscript 2* and *3*). Isotope natural abundance compositions of non-mycorrhizal plant species belonging to the plant families Equisetaceae (horsetails), Cyperaceae (sedges) and Caryophyllaceae (carnation family) supported active or passive acquisition of organic soil N compounds via DSE fungi (*Manuscript 3*). Carbon-for-nutrient trading was deciphered for a non-mycorrhizal Lycopodiaceae plant species (club moss) (*Manuscript 4*). Lab-provided inorganic nutrient tracers applied to FRE fungi were transferred towards the plant partner while the plant partner provided C in exchange. Furthermore, the isotope natural abundance of the club moss supports a transfer of organic soil N compounds in field sites.

Figure 1 **The three main questions addressed in this thesis.** Illustrations from left to right: partial mycoheterotrophy is addressed in *Mansucript 1-3*, DSE-plant symbiosis in *Manuscript 3* and FRE-plant symbiosis in *Manuscript 4*.
Abbreviations: AM, arbuscular mycorrhiza; DSE, dark septate endophyte; FRE, fine root endophyte; PMH, partial mycoheterotrophy. Drawing designed by Philipp Giesemann, produced by Katrin Giesemann.

Zusammenfassung

Mykorrhizen sind weitgehend anerkannt als Pflanze-Pilz-Symbiosen zum vorteilhaften Handel von Kohlenstoff-für-Nährstoffe. Demgegenüber stehen hunderte von mykohetertrophen Pflanzen. Diese untergraben das für gewöhnlich vorteilhafte Netzwerk und benutzen stattdessen die Pilzpartner als organische Kohlenstoff- und Stickstoffquelle. Der starke Fokus auf vorteilhafte Mykorrhizen hatte zudem zur Folge, dass andere häufige pilzliche Wurzelendophyten, wie dunkel-septierte Wurzelendophyten (DSE) und Feinwurzel-Endophyten (FRE), oft unbeachtet blieben. Die Dissertation untersucht

(i) ein häufigeres Auftreten mykoheterotropher Pflanzen als gegenwärtige Einschätzungen ergaben und
(ii) eine Mykorrhiza-ähnliche Rolle im Pflanze-Pilz-Nährstoffhandel für DSE und FRE (Abbildung 1).

Isotopenanwendungen der Elemente Kohlenstoff (C), Stickstoff (N) und Wasserstoff (H) haben sich als ein wertvolles Werkzeug etabliert, um organische und anorganische Nährstoffflüsse zwischen Pflanzen und Pilzen aufzuklären. Dabei wurden für chlorophyllfreie, vollständig mykoheterotrophe Pflanzen die Pilzpartner als organische C- und N-Quelle ausgemacht. Vollständige Mykoheterotrophie tritt in 17 Pflanzenfamilien auf. Dabei formen die Pilzpartner entweder eine arbuskuläre Mykorrhiza (AM) und Ektomykorrhiza (EcM) oder es handelt sich um streu- und holzzersetzende Pilze. Das Auftreten von einerseits vollständig photoautotrophen Pflanzen und andererseits von vollständig mykoheterotrophen Pflanzen zwingt uns, ein Zwischenstadium zu postulieren. Dieses Zwischenstadium zweigt organischen Kohlenstoff und Nährstoffe vom Pilz ab bei gleichzeitiger Fixierung von C über eigene Photosynthese. Diese partiell mykoheterotrophen Pflanzen wurden mithilfe von natürlichen Isotopenhäufigkeiten zahlreich aufgedeckt. Jedoch beschränkt sich deren kontinuierliche Dokumentation bislang auf nur zwei Pflanzenfamilien, beide sind mit EcM-Pilzen assoziiert (Orchidaceae und Ericaceae). Vollständige Mykoheterotrophie ist tatsächlich unter AM Pflanzen weitverbreitet, während die Dokumentation der partiellen Mykoheterotrophie bislang sehr selten war. Es ist zu beachten, dass die Symbiose der AM unterschiedliche morphologische Typen formt. Die Hyphenmorphologie erlaubt die Zuordnung des interzellulären *Arum*-Typ und des intrazellulären *Paris*-Typ. Diese beiden Typen stellen die Endpunkte eines ausgeprägten Kontinuums dar. Vollständige Mykoheterotrophie trat bislang ausschließlich mit dem *Paris*-Typ der AM auf. Demzufolge sollte partielle Mykoheterotrophie auch unter *Paris*-Typ AM Pflanzen mithilfe von Isotopenanwendungen zu finden sein. Das Auftreten von partiell mykoheterotrophen AM Pflanzen hätte aufgrund der schieren Verbreitung von AM Pflanzen weitreichende Konsequenzen für unser Verständnis von Pflanzengesellschaften, die möglicherweise bislang übersehen wurden.

DSE und FRE sind im Pflanzenreich weitverbreitet, dennoch ist bislang wenig über ihre Rolle im Pflanze-Pilz-Nährstoffhandel bekannt. DSE und FRE Pilze kolonisieren sowohl die Wurzeln von Mykorrhizapflanzen als auch von Pflanzenarten, die keine Mykorrhizapilze aufweisen. Die zuletzt genannten ermöglichen es, die Rolle der DSE und FRE im Pflanze-Pilz-Nährstoffhandel mithilfe von Isotopenanwendungen ans Licht zu bringen. Die Einordnung einer vom Pilz zur Verfügung gestellten organischen

oder anorganischen N-Quelle wurde mit natürlichen Isotopenhäufigkeiten aufgeklärt. Im Laborexperiment wurden Isotopen-*Tracer* angewandt, um den Handel von Kohlenstoff-für-Nährstoffe nachzuvollziehen.

Die Dissertation umfasst vier Manuskripte. *Manuskript 1*, *2* und *3* bestätigen einen Unterschied in den ^{13}C, ^{2}H und häufig in den ^{15}N Isotopensignaturen zwischen AM Pflanzenarten, die den interzellulären *Arum*-Typ oder den intrazellulären *Paris*-Typ aufweisen. Die Anreicherung im schweren ^{13}C, ^{2}H und häufig im ^{15}N Isotop ist am besten erklärt mit einer partiell mykoheterotrophen Ernährungsweise über *Paris*-Typ AM Pilze. Dies wurde in *Manuskript 1* erstmalig für die *Paris*-Typ Waldbodenpflanzen *Paris quadrifolia* (Einbeere, Melanthiaceae) und *Anemone nemorosa* (Buschwindröschen, Ranunculaceae) nachgewiesen. Eine Literaturrecherche wurde vorgenommen, um 135 *Arum*-Typ oder *Paris*-Typ AM Pflanzenarten miteinander zu vergleichen. Neben den 13 vollständig mykoheterotrophen *Paris*-Typ Arten unterstützen die Ergebnisse eine partiell mykoheterotrophe Ernährungsweise für 31 der 63 untersuchten chlorophyllhaltigen *Paris*-Typ Arten der Waldbodenvegetation, vor allem für Farne und Schachtelhalme (*Manuskript 2*, *3*). Die 59 *Arum*-Typ Arten waren isotopisch unauffällig. Der *Paris*-Typ stellt somit eine notwendige Voraussetzung für partielle Mykoheterotrophie bei AM Pflanzen dar. Darüber hinaus wurde in den *Manuskripten 3* und *4* eine funktionelle Rolle im Pflanze-Pilz-Nährstoffhandel für DSE und FRE aufgeschlüsselt. Die Isotopensignaturen ausgewählter Pflanzenarten der Equisetaceae (Schachtelhalme), Cyperaceae (Seggengewächse) und Caryophyllaceae (Nelkengewächse) unterstützen einen aktiven oder passiven Transfer von organischen Stickstoffverbindungen durch DSE (*Manuskript 3*), und für eine Art der Lycopodiaceae durch FRE (*Manuskript 4*). Ein Kohlenstoff-für-Nährstoff Handel wurde für das Bärlappgewächs im Laborexperiment gezeigt. Die Anreicherung in stabilen Isotopen legt für Equisetaceae, die sowohl mit DSE als auch mit *Paris*-Typ AM assoziiert sind, einen Gewinn von organischen Bodenstickstoff über DSE als auch einen Gewinn von organischen Kohlenstoffverbindungen über Mykoheterotrophie nahe. Ein Transfer von organischen Verbindungen in Pflanze-Pilz-Symbiosen ist deshalb nicht auf mykoheterotrophe Pflanzen beschränkt, sondern tritt wahrscheinlich auch bei Symbiosen mit Wurzelendophyten der DSE und FRE auf. Eine ökologische Rolle, ähnlich der Mykorrhiza, ist für die häufig unbeachteten DSE und FRE anzunehmen.

Abbildung 1 **Die drei in der Doktorarbeit behandelten Hauptfragestellungen.** Von links nach rechts: partielle Mykoheterotrophie wird von den *Manuskripten 1-3* behandelt, die DSE-Pflanze Symbiose in *Manuskript 3* und die FRE-Pflanze Symbiose in *Manuskript 4*.

Abkürzungen: AM, arbuskuläre Mykorrhiza; DSE, pilzliche dunkel-septierte Wurzelendophyten; FRE, pilzliche Feinwurzel-Endophyten; PMH, partielle Mykoheterotrophie. Design von Philipp Giesemann, Zeichnung von Katrin Giesemann.

Motivation

For improving their respective thriving, manifold plant-fungi nutritional relationships have evolved over time. Isotope tools greatly supported the deciphering of these nutritional relationships. At the BayCEER - Laboratory of Isotope Biogeochemistry (Bayreuth University), the conquest of the deciphering of plant-fungi nutritional relationships has resulted in a robust dataset. The database comprises stable isotope natural abundance compositions and leaf total nitrogen concentrations of thousands of putatively fully autotrophic chlorophyllous plant individuals (509 species, n = 4 647) accompanied by hundreds of partially (124 species, n = 2 123) and fully (46 species, n = 479) mycoheterotrophic specialists that partially or fully satisfy their organic carbon and nitrogen demands from a fungal source (status as of January 2020). This database provides a unique opportunity to advance our understanding on mycoheterotrophy as well as on the plant-fungi symbiosis in general. In assessing this data collection, two striking patterns emerged:

(i) a huge lack of data about partially mycoheterotrophic plants on arbuscular mycorrhiza (AM) and
(ii) unique isotopic patterns for autotrophic plants described as non-mycorrhizal.

AM is the predominant mycorrhizal type globally with >80% terrestrial plant partner species (Tedersoo *et al.*, 2020). Frequently, full mycoheterotrophs on AM have been documented (Merckx *et al.*, 2013a) while records on partial mycoheterotrophy are almost completely lacking. However, analogous to achlorophyllous holoparasitic plants, which emerged from chlorophyllous hemiparasites (Westwood *et al.*, 2010), partial mycoheterotrophy as its transitional form towards fully mycoheterotrophic nutrition is expected. This transitional form is likely evolutionarily located between a fully mutualistic mycorrhiza and the full reliance on fungal carbon. Such an intermediate nutritional strategy has been regularly documented for plant species associated with ectomycorrhizal fungi (Hynson *et al.*, 2013; Hynson *et al.*, 2016). However, a profound literature search supported the assumption that partial mycoheterotrophs on AM were greatly overlooked until now. This evidence is sustained by the presence of distinct hyphal morphologies in AM plant roots and the evidence of little phylogenetic constraints for AM plants to tap into mycoheterotrophy (Excursus-1; Perez-Lamarque *et al.*, 2020). Now, the pool of 509 putatively fully autotrophic plant species releases a robust basis for a fresh attempt to re-open a closed book.

While a wealth of knowledge about plant-fungi nutritional feedbacks exists for the mutual AM symbiosis, which mainly occur at the endophytic root-to-hyphae interface, knowledge about such nutritional relationships of other common fungal endophytes remains sparse. Among the 509 putatively fully autotrophic plant species, the majority form mycorrhizal associations while some species belonging to non-mycorrhizal plant families are also repeatedly recorded. Importantly, non-mycorrhization does not imply a lack of any fungal root endophytes (Jumpponen, 2001; Mandyam & Jumpponen, 2005; Orchard *et al.*, 2017b). Thus, these species enable a closer look at nutritional feedbacks by elusive root endophytes. Fungal root endophytes asymptomatically inhabit plant roots while a mycorrhiza-like role in nutrient trading was not shown yet in vascular plants. The robust databank serves as motivation to exemplarily study vascular plant lineages traditionally considered non-mycorrhizal to unveil a mycorrhiza-like role of their fungal root endophytes.

Synopsis

CHAPTER 1

Shortly introduces the concepts of symbiosis, mycorrhizas, plant root endophytes and mycoheterotrophy

CHAPTER 2

Synthesises the main results of the thesis, presents the author contributions to the manuscripts and lists further publications

CHAPTER 3

Manuscripts

- "I hope ecologists have more consideration of plants' heterotrophy, particularly, partial mycoheterotrophs, as well as on the nutritional role of the ubiquitous fungal root endophytes in the future."

CHAPTER 1

- "What is the unifying theme which brings together lichenologists with coral experts, entomologists with those who study mycorrhizas? The simple answer is that they are all considered to be examples of symbiosis." (D.C. Smith)

Introduction

Plant-fungi symbiosis

Autotrophy and heterotrophy are endmembers of fundamental processes on earth, represented by e.g. plants as autotrophs and fungi as heterotrophs (see Definitions). Fungi that inhabit plants have been termed fungal endophytes (Link, 1809; *endon* "within", *phyton* "plant" from Greek), forming a symbiosis (Frank, 1877; de Bary, 1878; *symbiōsis* "living together" from Greek). Symbioses fall along the parasitism-to-mutualism continuum (Johnson *et al.*, 1997).

Many fungal root endophytes form a nutritionally beneficial symbiosis termed mycorrhiza (*mykes*, "fungus", *rhiza*, "root" from Greek) (Frank, 1885; Smith & Read, 2008), and thus fall at one end of the continuum (with possibly some plasticity involved; Klironomos, 2003; Näsholm *et al.*, 2013). However, the positioning along the parasitism-to-mutualism continuum of elusive fungal endophytes, such as dark septate endophytes (DSE) and fine root endophytes (FRE), remains puzzling.

Indubitably, not all symbioses are cooperative and may instead appear exploitative. Exploiters (e.g. plant parasites) obtain a benefit without providing any advantage for the host. An extraordinary example is full mycoheterotrophy (*mykes*, "fungus", *heteros*, "another", *trophe*, "nutrition" from Greek). Fully mycoheterotrophic plants appear achlorophyllous and form exploitative mycorrhizas to cover their carbon and nutrient demands (Leake, 1994; Merckx, 2013).

Mostly, chlorophyllous plant species are treated as full photoautotrophs. What often has not been sufficiently considered is that the plant kingdom spans the full spectrum of autotrophy, heterotrophy and intermediate stages (Těšitel *et al.*, 2010; Merckx, 2013). Recent advances were made for mycoheterotrophic plants, in particular 'partial mycoheterotrophs', which may represent underappreciated intermediate stages between full autotrophy and full mycoheterotrophy (Gebauer & Meyer, 2003). Still, this knowledge remained mostly restricted to plant species from the Orchidaceae and Ericaceae. Hence, this thesis presents novel evidence of a fungi-derived carbon gain for chlorophyllous AM plant species, suggesting a substantial increase in the number of heterotrophic plants.

Definitions

Symbiosis the intimacy of organisms.

Fungal root endophytes a (mostly) symptomless symbiosis between fungi and living plant roots.

Mycorrhizas a (mostly) obligate symbiosis mainly for bidirectional nutrient trading between fungi and the living plant roots likely based on a harmonious development.

Photoautotrophy a nutritional energy acquisition by fixing carbon-dioxide with light energy to energy-rich carbohydrates, e.g. chlorophyllous plant species and algae.

Heterotrophy a nutritional energy acquisition by consumption of energy-rich substances ultimately originated from autotrophy, e.g. animals, fungi, animal-, plant- and fungi-feeding plants.

Mycoheterotrophy plant nutritional strategy secretly interlinking into mycorrhizal networks or on saprotrophic fungi to utilize on fungal organic carbon and nutrients.

Full Mycoheterotrophy achlorophyllous plants, that receive all their carbon and nutrient demand from fungal origin while devoid chlorophyll and photosynthetic abilities throughout their life span.

Partial Mycoheterotrophy chlorophyllous plants, that receive a proportion of their carbon and nutrient demand from fungal origin while photosynthesis is inherent.

Most plant species form an intimate mycorrhizal symbiosis with their fungal partners for bidirectional nutrient exchange summarized by a carbon-for-nutrient trading (Tedersoo *et al.*, 2020). This cooperation represents an ancestral steppingstone for the plants' conquest of land (Smith & Read, 2008; Strullu-Derrien *et al.*, 2018), estimated to have occurred half a billion years ago (Taylor *et al.*, 2003; Morris *et al.*, 2018). In the mycorrhizal symbiosis, the plant provides an essential carbohydrate (and frequently a lipid) source to the obligate biotrophic mycorrhizal fungi (Jakobsen & Rosendahl, 1990; Smith & Read, 2008; Wipf *et al.*, 2019). In return, the mycorrhizal fungi deliver a substantial amount of nitrogen, phosphorous and likely other mineral nutrients to the plant (Smith & Read, 2008; van der Heijden *et al.*, 2017; Wipf *et al.*, 2019). For this nutrient trading, mycorrhizas develop root-internal hyphal systems whereabout hyphae form interfaces considered for nutrient exchange. At the other hyphal end, the fungal extraradical mycelia scavenge the soil for mineral nutrients and might adhesively mobilize water (Smith & Read, 2008). Thus, the mycorrhizal fungi are capable of forming impressive belowground networks, and thereby serve to interconnect plant root systems (Finlay & Read, 1986; Kennedy *et al.*, 2003; Klein *et al.*, 2016; Wipf *et al.*, 2019).

Many mycoheterotrophic plants are exploitative, turning the tables and tapping into plant root-fungal networks to channel off organic carbon and nutrients (Merckx, 2013). Thereby, mycoheterotrophs construct either a tripartite interconnection (mycoheterotrophic plant - fungal partner - autotrophic plant partner) or directly exploit wood- and litter-decomposing fungi (Merckx, 2013; Waterman *et al.*, 2013). On an evolutionary timescale, this eventually allows mycoheterotrophs to drop endosperm production (initial mycoheterotrophy) or cease their photosynthetic activity for their entire life cycle (full mycoheterotrophy) (Merckx, 2013). Dust-like seeds, with small endosperm, do not provide sufficient endosperm energy resources to maintain the initial plant development, and are therefore dependent on fungal-derived carbon and nutrient sources (Eriksson & Kainulainen, 2011). Full mycoheterotrophy is suggested to be a point-of-no-return due to a cascade of irreversible gene-losses required for plant photosynthesis (Graham *et al.*, 2017). The 880 achlorophyllous fully mycoheterotrophic plant species so far investigated belong to 17 plant families spanning basal moss, fern and clubmoss species to seed plants such as Burmanniaceae, Orchidaceae, Thismiaceae (monocotyledons) and Ericaceae, Gentianaceae, Polygalaceae (dicotyledons) (Leake, 1994; Merckx, 2013; Merckx *et al.*, 2013a, 2013b). The evolution of full mycoheterotrophs that completely rely on a foreign carbon source suggests the existence of transitional stages. This transition can be comprehended by hemi- and holoparasitic plants relying partially or fully on carbon from neighboring plants (Westwood *et al.*, 2010). Thus, a transitional stage towards full mycoheterotrophy must also be postulated; that is, partial mycoheterotrophy, i.e. chlorophyllous plants that obtain at some point of their life a proportion of their carbon and nitrogen nutrient demand from fungi while photosynthesis is still an inherent ability.

In contrast to the profound knowledge on mutualistic AM nutritional interactions mainly happening at an root-internal plant-hyphae interface, the symbiosis of plants and common fungal endophytes, particularly DSE and FRE, remains insufficiently studied (Jumpponen, 2001; Hardoim *et al.*, 2015; Field & Pressel, 2018; Hoysted *et al.*, 2018). Similar to mycorrhizal fungi, fungal endophytes form intracellular fungal structures, while mycorrhiza-like nutrient trading has rarely been documented; examples include two vascular Antarctic

plant species associated with DSE (Hill *et al.*, 2019) and a few early diverging liverworts associated with FRE (Field *et al.*, 2015). As DSE and FRE are recognized saprotrophs and biotrophs that colonize an array of plant species globally (Jumpponen & Trappe, 1998; Orchard *et al.*, 2017b; Rimington *et al.*, 2020), their role in plant-fungi-nutritional relationships appears non-trivial, as illustrated by their potential to facilitate plant nutrient acquisition (Mandyam & Jumpponen, 2005; Newsham, 2011; Orchard *et al.*, 2017b).

Morphological features for nutrient trading

The diversity of plant and fungal species can be simplified in a structural diversity covered by endomycorrhizas (AM: arbuscular mycorrhiza, ErM: ericoid mycorrhiza, OM: orchid mycorrhiza), ectomycorrhizas (EcM) and non-mycorrhizal (NM) plant species (Smith & Read, 2008). The terrestrial plant kingdom encompasses approximately 500 000 extant species. A number beyond 1.5 million species is assumed for fungi, whilst only 100 000 species have been described (Hawksworth, 1991; Taylor *et al.*, 2003). The endomycorrhizal fungi form intracellular arbuscules, hyphal coils and pelotons while EcM fungi form a hyphal mantle around the plant root tips and an intercellular labyrinth-like 'Hartig net' (Smith & Read, 2008; Field & Pressel, 2018; Tedersoo *et al.*, 2020).

AM fungi are characterized by distinct hyphal morphologies (Gallaud, 1905). The profound reviews from Smith & Smith (1997) and Dickson *et al.* (2007) summarize the knowledge collected on *Arum*- and *Paris* AM morphotypes (Excursus-1). *Arum*- and *Paris*- AM morphotypes were first described within the roots of the herbaceous species *Arum maculatum* (Araceae) and *Paris quadrifolia* (Melanthiaceae) commonly found in European forests. These morphotypes can be distinguished by the distinctive growth of the aseptate fungal hyphae. The *Arum*-morphotype is characterized by intercellular hyphal growth along the root cortical cells (Figure 2a), while the *Paris*-morphotype has intracellularly coiling hyphae (Figure 2b). The *Arum*- and *Paris*-morphotype occupy the ends of a full continuum (Dickson, 2004). Mixed forms (intermediate types) and both types within the same plant root complete the *Arum*-to-*Paris* continuum (Dickson *et al.*, 2007). The fungal partner of AM symbioses were found to be the monophyletic Glomeromycotina (Spatafora *et al.*, 2016). These fungi are suggested to be primitive or ancestral and might have saprotrophic, algae-associated or parasitic ancestors, but seem to have lost their saprotrophic repertoire during evolution (Brundrett, 2002). Their functional diversity is suggested to be greater than the current count of "species" (Brundrett, 2002).

Excursus-1. *Short summary of Arum- and Paris-morphotype arbuscular mycorrhiza (AM)*

(i) Yet, *Arum*-morphotype AM was in focus due to the prominence of arbuscules as diagnostic AM structures. The coiling *Paris*-morphotype was frequently ignored as atypical as the criteria of AM were the presence of arbuscules (Dickson *et al.*, 2007). **(ii)** *Arum*-morphotype is dominant in early successional plants, in most herbaceous cultivars and crop plants while the *Paris*-morphotype is most dominant in late-successional stages and woodland plants (Ahulu *et al.*, 2005). **(iii)** There are indices for a plant control over morphotype development, thus species of the same genus likely form the same AM morphotype (but, the fungal genome remains to be considered; Cavagnaro *et al.*, 2001). **(iv)** *Arum*- and *Paris*-morphotype AM were recorded in mono- and dicotyledonous, woody and herbaceous plants. Almost all fern and fern-allies and all yet observed mycoheterotrophs on AM, including the achlorophyllous gametophytes of pteridophytes, share the feature of *Paris*-morphotype (Zhang *et al.*, 2004; Imhof *et al.*, 2013). **(v)** The coiling *Paris*-morphotype was once suggested as prerequisite of mycoheterotrophy on AM fungi (Imhof, 1999).

The phylogenetic sister of Glomeromycotina AM fungi, the Mucoromycotina FRE, include saprotrophic and biotrophic endogonales and *Glomus tenue* FRE (Orchard *et al.*, 2017a; Hoysted *et al.*, 2018; Walker *et al.*, 2019). Mucoromycotina FRE populate at least 40 vascular plant families (Orchard *et al.*, 2017b). Their morphological features comprise small swellings along aseptate fine branching hyphae (0.4 to 4.0 μm, diameter) and arbuscule-like structures (Figure 2c). The fine hyphae grow intercellularly and intracellularly within the cortical root space while being distinctively finer relative to coarser hyphae of AM fungi.

The ubiquitous DSE fungi have been recorded for at least 140 plant families globally from Antarctic to temperate, boreal and Arctic regions (Jumpponen & Trappe, 1998; Mandyam & Jumpponen, 2014). They enclose a polyphyletic group of saprotrophic ascomycotan fungi belonging mostly to the order of Helotiales (Jumpponen & Trappe, 1998; Mandyam & Jumpponen, 2014). DSE fungi morphologically form thick-walled, irregularly lobed intracellular microsclerotia, intracellular hyphal coils or peloton-like hyphae and intercellular hyaline or melanized septate hyphae as characteristic of DSE (Figure 2d; Melin, 1922; Jumpponen & Trappe, 1998). Intracellular colonization is often formed by hyaline hyphae, which later become melanized (Barrow & Aaltonen, 2001; Barrow, 2003; Mandyam & Jumpponen, 2014).

Distribution of AM, DSE and FRE fungal associations along the plant kingdom

Resulting from their early evolution, the distribution of the AM symbiosis is dominant, occurring in almost all terrestrial ecosystems and in almost all plant clades of different plant life forms from herbaceous species to trees (Brundrett & Tedersoo, 2018). The basal clades of liverworts, hornworts and moss species consist of approximately 16 700 species (Konrat *et al.*, 2010; Magill, 2010; Villarreal *et al.*, 2010) and the basal lycophytes and ferns consist of approximately 11 300 species (Magill, 2010; Ranker & Sundue, 2015). Liverworts, hornworts, lycophytes and ferns are predominately populated by AM fungi (Brundrett, 2002), while FRE and DSE are also documented (Jumpponen & Trappe, 1998; Orchard *et al.*, 2017b; Rimington *et al.*, 2020). Interestingly, the *Paris*-morphotype AM was documented in most, if not all, of the achlorophyllous fully mycoheterotrophic gametophytes of ferns and lycophytes as well as their chlorophyllous sporophytes (Zhang *et al.*, 2004; Imhof *et al.*, 2013). Some of the plant species belonging to the basal clades are NM, e.g. moss species (Pressel *et al.*, 2010), or facultative mycorrhizal, e.g. *Equisetum* and many ferns. The NM and facultative mycorrhizal plant species often appear with filigree, long hairs at roots or rhizoids that may contribute a similar function to that of the fine networks of extraradical fungal mycelia. The seed plant species of 1 000 gymnosperms (Christenhusz *et al.*, 2011) and 450 000 angiosperms (Pimm & Joppa, 2015) predominately form AM symbiosis, while NM occur for instance in Brassicaceae, Caryophyllaceae, Cyperaceae, and Juncaceae. An EcM occurs in Pinaceae and *Gnetum* for gymnosperms, and Betulaceae, Fagaceae and Juglandaceae are prominent examples of EcM in angiosperms (Brundrett, 2002). Among the gymnosperms and angiosperms forming AM, the distribution of *Arum*- and *Paris*-morphotype AM plant species, so far analyzed, is well-balanced (Dickson *et al.*, 2007). Conversely, according to recent works, full mycoheterotrophs on AM fungi appear with *Paris*-morphotype (Imhof *et al.*, 2013). Imhof (1999) hypothesized the hyphal morphology of the *Paris*-coiling morphotype AM could be analogous to pelotons and hyphal pegs in mycoheterotrophs on EcM fungi. Thus, partial mycoheterotrophy could

occur for *Paris*-morphotype AM, as illustrated by its occurrence in chlorophyllous angiosperms (e.g. species belonging to the Apiaceae, Gentianaceae, Ranunculaceae and Sapindaceae). While fungal root endophytes usually colonize plant species that form mycorrhizal symbioses, several authors emphasized the widespread presence of DSE and FRE in plant species considered NM, such as Caryophyllaceae, Cyperaceae, Equisetaceae and Juncaceae (Jumpponen & Trappe, 1998; Orchard *et al.*, 2017b). Plant species belonging to NM plant families may therefore represent an opportunity to study the nutritional role of DSE and FRE unbiased from mycorrhizal fungi.

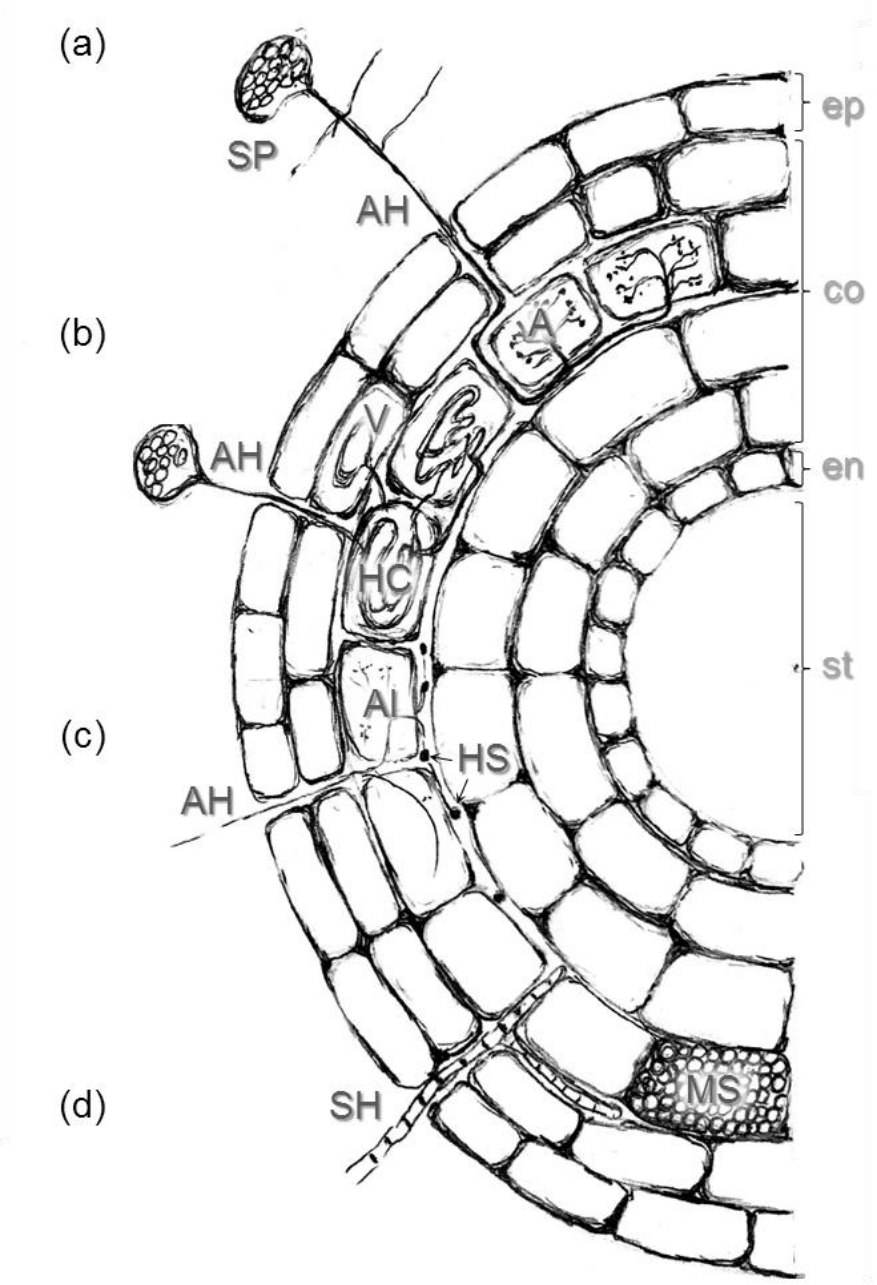

Figure 2 **Plant root colonisation by fungal partners.** Arbuscular mycorrhiza separated in *Arum*- (a) and *Paris*-morphotype (b), fine root endophytes (c) and dark septate endophytes (d) in a hypothetical plant root cross section.
Abbreviations: A, arbuscule; AH, aseptate hyphae; Al, arbuscule-like; co, inner and outer cortex; en, endodermis; ep, epidermis; HC, hyphal coil; HS, hyphal swelling (arrow); MS, microsclerotia; SH, septate hyphae; SP, spore; st, stele. Designed by Philipp Giesemann, produced by Katrin Giesemann.

Isotope applications to trace plant fungi nutritional relationships

The topics of (i) partial mycoheterotrophy on AM fungi and (ii) carbon-for-nutrient trading in DSE- and FRE-plant symbiosis addressed in this thesis can be elucidated with the powerful tool of stable isotope applications. Stable $^{13}C/^{12}C$, $^{15}N/^{14}N$ and $^{2}H/^{1}H$ isotope abundance ratios demonstrate carbon and nutrient fluxes in mycorrhizal symbioses (Excursus-2; Hynson *et al.*, 2013; Gebauer *et al.*, 2016; Gomes *et al.*, 2020). Additionally, isotope tracers successfully supported mycoheterotrophic nutrition (Excursus-3) and showed the bidirectional nutrient trading in plant-fungi symbioses (e.g. Finlay & Read, 1986; Field *et al.*, 2015, 2016; Klein *et al.*, 2016; Field & Pressel, 2018; Field *et al.*, 2019).

(i) Mycoheterotrophs cover their nutrient demand fully or partially from a carbon and nitrogen nutrient source in a completely different manner compared to that of putatively full autotrophs. As such, the stable isotope natural abundance composition of full autotrophs and both full and partial mycoheterotrophs are distinct (Excursus-2, Figure 3). The isotopic evidence of full mycoheterotrophs on EcM fungi was first shown by ^{13}C and ^{15}N enrichment (Gebauer & Meyer, 2003; Trudell *et al.*, 2003) and later by ^{2}H enrichment (Gebauer *et al.*, 2016) relative to putatively full autotrophs (Excursus-2b,c). Most provocative, ^{13}C, ^{15}N and later ^{2}H enrichment were also found for photosynthetically active C_3 plant species belonging to Orchidaceae and Ericaceae obviously deviating from the more depleted isotope composition of accompanying mycorrhizal C_3 plants (Excursus-2d). Thus, partial mycoheterotrophy was elucidated by an isotopically intermediate positioning between full autotrophs and full mycoheterotrophs. Partial mycoheterotrophs were neither visually nor morphologically distinguished from accompanying putatively full autotrophs, thus demanded an isotope approach. Similarly, Gomes *et al.* (2020) showed a ^{13}C, ^{2}H and frequently a ^{15}N enrichment for full mycoheterotrophs on *Paris*-morphotype AM belonging to Burmanniaceae, Gentianaceae, Polygalaceae, Thismiaceae and Triuridaceae spanned from Australia, New Zealand, Malaysia, and South America. The isotope enrichment was less pronounced than for mycoheterotrophs associated with EcM fungi. These findings are largely consistent with initial studies on very few species by Merckx *et al.* (2010) and Courty *et al.* (2011). Early attempts elucidating partial mycoheterotrophy on AM fungi were focused on chlorophyllous relatives of achlorophyllous full mycoheterotrophs. For instance, Merckx *et al.* (2010) focused on *Burmannia capitata* (Burmanniaceae), Cameron & Bolin (2010) focused on *Bartonia virginica* and *Obolaria virginica* (Gentianaceae) and Bolin *et al.* (2017) focused on *B. coelestis* (Burmanniaceae). So far analyzed, *B. capitata*, *B. coelestis*, *B. virginica* and *O. virginica* or their close relatives appear with *Paris*-morphotype AM. When Cameron & Bolin (2010) sampled chlorophyllous Gentianaceae and Bolin *et al.* (2017) chlorophyllous Burmanniaceae they found almost no difference in ^{13}C between the candidates of putatively partial mycoheterotrophs and their putatively full autotrophic reference plant species. However, by subsequently looking at the AM putatively full autotrophs it became obvious that the reference plants in Cameron & Bolin (2010) appeared mostly with *Paris*-morphotype AM and in Bolin *et al.* (2017) mostly with *Arum*-morphotype AM. Thus, the distribution of *Paris*-morphotype AM reference plants of *B. virginica* and *O. virginica* might have concealed the sharpness of ^{13}C and ^{15}N enrichments to elucidate partial mycoheterotrophy, as the references themselves might be partially mycoheterotrophic on *Paris*-morphotype AM fungi. A ^{13}C and frequently ^{15}N enrichment expected for partial mycoheterotrophy was clearer for

B. coelestis which appeared mostly with *Arum*-morphotype reference plants. Thus, partial mycoheterotrophy might have been overlooked frequently, and chlorophyllous *Paris*-morphotype AM plants should be the anchoring point to search for partial mycoheterotrophy on AM. Consequently, *Paris*-morphotype will be addressed as prerequisite for mycoheterotrophy in chlorophyllous AM plant species.

(ii) As mentioned above, most plant species reciprocally exchange carbon-for-nutrients with mycorrhizal partners. A minority of plant species are traditionally considered non-mycorrhizal while frequently colonized by fungal root endophytes, such as DSE and FRE. Hill *et al.* (2019) and Field *et al.* (2015) demonstrated for DSE and FRE, respectively, a carbon-for-nutrient trading in a few plant species in a controlled environment. For that, nitrogen and phosphorous tracers were applied to the fungi and retraced in the plant tissue. Further, the plant was exposed to a $^{14}CO_2$ carbon source which was retraced into the fungal tissue. In contrast to AM, the saprotrophic abilities of DSE and FRE might allow the access on ^{15}N-enriched nutrients (Caldwell *et al.*, 2000; Hoysted *et al.*, 2018). Haselwandter & Read (1982) and Upson *et al.* (2009) found a significant increase in dry weight of DSE colonized plant partners, especially when organic N was provided. However, Peterson *et al.* (2008) argued the absence of specialized nutrient transfer interfaces, perifungal membrane and interfacial matrix material for DSE. Michelsen *et al.* (1996, 1998) found plant species inhabited by DSE (therein classified 'AM/NM') to frequently appear with a ^{15}N enrichment. Thus, non-mycorrhizal plant species inhabited by DSE fungi might generally appear with a ^{15}N enrichment due to the access on ^{15}N-enriched soil organic nutrient sources actively or passively provided by DSE fungi. In contrast, mycorrhizal fungi access isotopically inconspicuous nitrate and ammonium and might translocate them to the plant partner. Field *et al.* (2015) showed a carbon-for-nutrient exchange for a FRE-liverworts symbiosis. The FRE are also widely distributed among vascular plant species, suggesting a carbon-for-nutrient trading is also likely for them. Saprotrophic abilities have been suggested for FRE (Hoysted *et al.*, 2018). Therefore, ^{15}N-enriched recalcitrant nitrogen forms might be translocated to the plant partner as well.

Thesis' Objectives

- Partial mycoheterotrophy on AM fungi was evaluated for the plant species once serving as eponym for the *Paris*-morphotype, *Paris quadrifolia* (*Manuscript 1*). A literature survey was performed to decipher the extent of partial mycoheterotrophy on AM fungi. *Paris*-morphotype AM species were compared to *Arum*-morphotype counterparts (*Manuscript 2*). Given AM is an ancient symbiosis, partial mycoheterotrophy could be an ancient nutritional strategy. Therefore, mycoheterotrophy was addressed in Equisetaceae living fossils (*Manuscript 3*).
- A literature survey and supplemental field sampling were performed to decipher the access of ^{15}N-enriched organic nitrogen via their DSE partners for non-mycorrhizal plant species (*Manuscript 3*).
- The ancient vascular plant species *Lycopodiella inundata* is exclusively inhabited by FRE. Thus, *L. inundata* were analyzed for a bidirectional carbon-for-nutrient trading with FRE partners (tracer experiment). A stable isotope natural abundance approach was realized to evaluate mycoheterotrophy for *Lycopodiella* and the nitrogen nutrient form, either ^{15}N-enriched organic or ^{15}N-inconspcious inorganic nutrients, provided by FRE in field sites (*Manuscript 4*).

***Excursus-2**. Evidence for mycoheterotrophy from a natural stable isotope perspective*

Elements identically in the number of protons and dissimilar in neutrons are termed 'isotopes'. Chemical and physical characteristics are considered almost equal while small atom mass differences are causative for 'isotope effects' in equilibrium and kinetic dynamics (Farquhar *et al.*, 1989; Ehleringer & Rundel, 1989). The isotope abundance is δ notated as $\delta^{y}X = ({}^{RSample}/_{RStandard} - 1) * 1000$ (‰) (^{y}X: ^{13}C, ^{15}N, ^{2}H, ^{18}O), whereby R is the ratio of the heavy to the respective light isotope (McKinney *et al.*, 1950). Site independency is achieved by conversion into enrichment factors ε by $\varepsilon^{y}X = \delta^{y}X_{Target} - \delta^{y}X_{Reference}$ (‰) (Preiss & Gebauer, 2008). The target plant is a plant suspected to be dissimilar by some reason from the expected mean represented by the reference plants.

(a) Plant stable ^{13}C, ^{18}O and ^{2}H isotope abundance is mostly driven by the photosynthetic pathway (Sternberg *et al.*, 1984; Farquhar *et al.*, 1989), the isotope composition of the CO_2 and H_2O sources (Farquhar *et al.*, 1982, 1989), different transpiration rates (Farquhar *et al.*, 1982, 1989; Cernusak *et al.*, 2004), microclimate (Dawson *et al.*, 2002) and alternative carbon sources (Press *et al.*, 1987; Gebauer & Meyer, 2003; Těšitel *et al.*, 2010; Gebauer *et al.*, 2016). The ^{15}N pattern is likely fixed by the nitrogen nutrient source (Hobbie & Högberg, 2012) (Figure 3). **(b) Fungi** are composed of ^{2}H-enriched secondary organic compounds that are enriched relative to autotrophic tissue (Yakir, 1992; Gebauer *et al.*, 2016; Cormier *et al.*, 2018, 2019); mycorrhizal fungi are fueled with ^{13}C-enriched carbohydrates (Figure 3), saprotrophic fungi utilize on ^{13}C-enriched cellulose, thus, they become ^{13}C-enriched. EcM and saprotrophic fungi release exoenzymes to access ^{15}N-enriched recalcitrant soil organic matter, thus, they become ^{15}N-enriched (Gebauer & Dietrich, 1993; Gleixner *et al.*, 1993; Ziegler, 1995; Mayor *et al.*, 2009; Schiebold *et al.*, 2017; Figure 3). AM fungi lack lipids synthesis (Jiang *et al.*, 2017; Keymer *et al.*, 2017; Luginbuehl *et al.*, 2017; Rich *et al.*, 2017). The mixture of ^{13}C-enriched carbohydrates and ^{13}C-depleted lipids (Gleixner *et al.*, 1993; Cormier *et al.*, 2019) might counterbalance the ^{13}C enrichment of AM fungi. Their ^{15}N enrichment should be less pronounced than this of EcM fungi as they utilize on isotopically inconspicuous nitrate and ammonium while may occupy saprotrophic capabilities (Hodge *et al.*, 2001).

(c) Full mycoheterotrophs are almost constantly characterized by a stable ^{13}C, ^{15}N and ^{2}H isotope enrichment (OM: Gebauer & Meyer, 2003; Trudell *et al.*, 2003; Hynson *et al.*, 2013; Hynson *et al.*, 2016; Gebauer *et al.*, 2016; ErM: Tedersoo *et al.*, 2007; Zimmer *et al.*, 2007, Andreas Makiola, *unpublished*; AM: Merckx *et al.*, 2010; Courty *et al.*, 2011; Gomes *et al.*, 2020) which is attributed to the simultaneous stable ^{13}C, ^{15}N and ^{2}H isotope enrichment found for many fruiting bodies (*cf.* literature above) and ^{13}C and ^{15}N enrichment (although less pronounced) found for extraradical AM mycelia (Walder *et al.*, 2012, Klink *et al.*, *unpublished*) and intraradical AM hyphae (Klink *et al.*, *unpublished*). The same applies to species that are fungal wood- or litter-decomposers (Ogura-Tsujita *et al.*, 2009; Lee *et al.*, 2015, Ogura-Tsujita *et al.*, 2018) (Figure 3). **(d) Partial mycoheterotrophs'** ^{13}C and ^{15}N enrichment in chlorophyllous orchid (Gebauer & Meyer, 2003), ericoid (Zimmer *et al.*, 2007) and in AM plant species (Cameron & Bolin, 2010; Bolin *et al.*; 2017) found mostly its place intermediate between putatively full autotrophs and obviously full mycoheterotrophs. The ^{2}H stable isotope natural abundance supports a partial mycoheterotrophy by its enrichment in orchid (Gebauer *et al.*; 2016) and ericoid mycorrhiza (Andreas Makiola, *unpublished*). Thus, partial mycoheterotrophs are suggested to simultaneously receive fungal-derived carbon and nutrients supplemented by photosynthesis by their own charge (Figure 3).

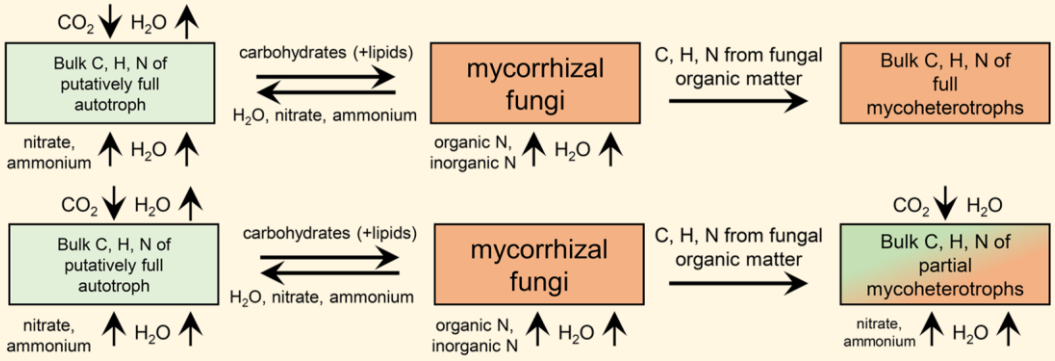

Figure 3 **The stable isotope natural abundance composition is influenced by several drivers (arrows) which might shift the isotope composition.** Autotrophy (green, relative depletion); heterotrophy (red, relative enrichment).

***Excursus-3**. Evidence for mycoheterotrophy from an isotope tracer and ^{14}C bomb carbon perspective*

Isotope tracer applications could be described by the phrase "Where does it [the tracer] come from, and where does it [the tracer] go". The tracer-based tracking of nutrients is a popular application in research on plant-fungi symbiosis (Finlay & Read, 1986; Hynson *et al.*, 2013; Field *et al.*, 2015, 2016; Klein *et al.*, 2016; Field & Pressel, 2018; Field *et al.*, 2019; Hill *et al.*, 2019), for instance:

(a) *Hypopitys monotropa* (Ericaceae) – the first record of an exploitative mycorrhiza.

The carbon source of *H. monotropa* was puzzling as parasitic structures, such as haustoria, were not observed (Curtis & Hooker, 1826; Kamienski, 1881). Kamienski (1881) hypothesized a carbon source from an ectomycorrhizal fungus which was confirmed when Björkman (1960) injected a ^{14}C-labeled glucose and ^{32}P-labeled phosphate radioisotope tracer into the phloem of spruce and pine trees. The tracer was retrieved through a mycorrhizal network in *H. monotropa* while not in accompanying heathland plants. A repetition of similar approaches confirmed the early finding by Björkman (1960) for *Corallorhiza trifida* (Orchidaceae, McKendrick *et al.*, 2000), *Aneura mirabilis* (Aneuraceae, Bidartondo *et al.*, 2003) and *Rhizanthella gardneri* (Orchidaceae, Bougoure *et al.*, 2010). Molecular approaches supported the tripartite interaction when the same fungal ribosomal DNA, as its entity, inside of tree roots and simultaneously in accompanying mycoheterotrophs was found (Taylor & Bruns, 1997; Selosse *et al.*, 2002).

(b) Bomb carbon: an elegant tool discloses the carbon source of mycoheterotrophs on saprotrophic fungi

The carbon isotopes ^{12}C, ^{13}C and ^{14}C are naturally fixed into plant biomass through photosynthesis and then potentially transferred to mycorrhizal partners. Since the mid 60th, atmospheric ^{14}C patterns decline, resulting in almost unique signatures per year. Suetsugu *et al.* (2020c) found for mycoheterotrophs on saprotrophic fungi a ^{14}C pattern of wood once synthesized decades ago (Figure 4) while mycoheterotrophs on ectomycorrhizal fungi obtained fresh carbon.

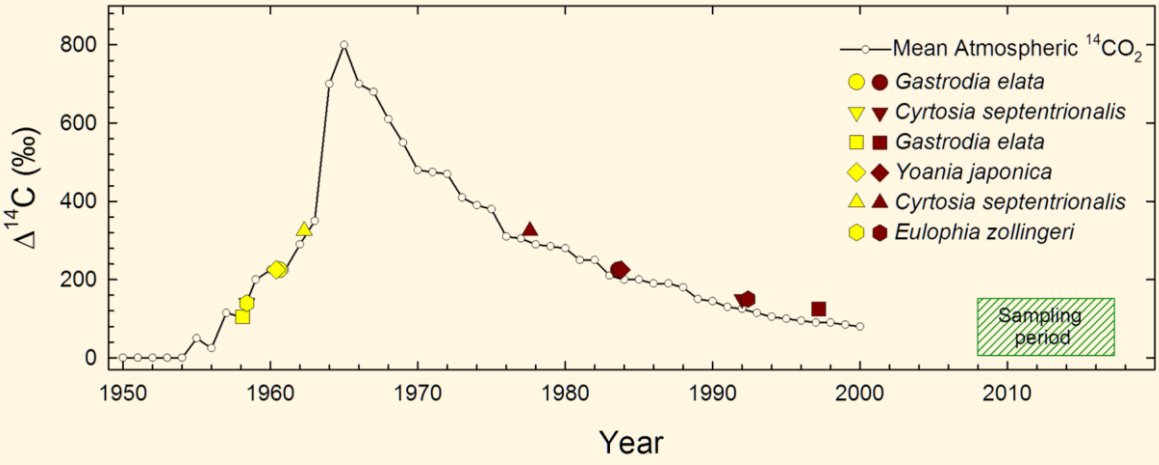

Figure 4 **Bomb carbon approach.** Mycoheterotrophic orchids on wood-decaying fungi were sampled from 2009 to 2016 (green box). The orchids' ^{14}C pattern was compared with the mean atmospheric $^{14}CO_2$ based on tree-ring analysis. The graphic indicates mycoheterotrophs on saprotrophs received a carbon source fixed in the 60th (yellow symbols, when assuming carbon utilization before the $^{14}CO_2$ peak) and 80th (red symbols, when assuming carbon utilization after the $^{14}CO_2$ peak). Data obtained from Suetsugu *et al.* (2020c).

CHAPTER 2

- "This is not so much a disappointment as a challenge to ecologists and biologists of the future. Much of the fascination of ecology and biology lies in the fact that many problems are blatant and obvious for everybody to see, while the solutions have as yet eluded us."

Mike Begon, Colin Townsend and John Harper (1990) extracted from Sieber and Grünig Microbial root endophytes (2006) as their concluding remarks about dark septate endophytes.

Synthesis

The belowground plant-fungi symbiosis attracted attention by its mutual exchange of carbon-for-nutrients omnipresent in the plant kingdom. Much was learned about the bidirectional nutrient transfers in mycorrhizas, for instance in mutual *Arum*-morphotype AM symbioses (Figure 5). Unfortunately, the *arbusculo-centric* concept of AM might have previously blinded us from the nutritional concepts hidden behind their morpho-counterpart, that is *Paris*-morphotype AM. Also, a deep focus on mycorrhizal fungi has blinded us so far from the nutritional concepts hidden behind common fungal endophytes, such as FRE and DSE. The thesis provides evidence for:

- Frequently, *Paris*-morphotype plant species are turning the tables of the mutual mycorrhizal life towards a gain of carbon from a fungal source. A continuum of *Paris*-morphotype AM plant species is evidentially deciphered, ranging from chlorophyllous fully autotrophic to chlorophyllous partially mycoheterotrophic to achlorophyllous fully mycoheterotrophic plants (Figure 5, *Manuscript 1-3*).
- DSE and FRE are actively or passively involved in a carbon-for-nutrient exchange just like mycorrhizal fungi. In striking contrast, DSE and FRE facilitate the acquisition of soil organic nutrient sources (Figure 5, *Manuscript 3-4*).

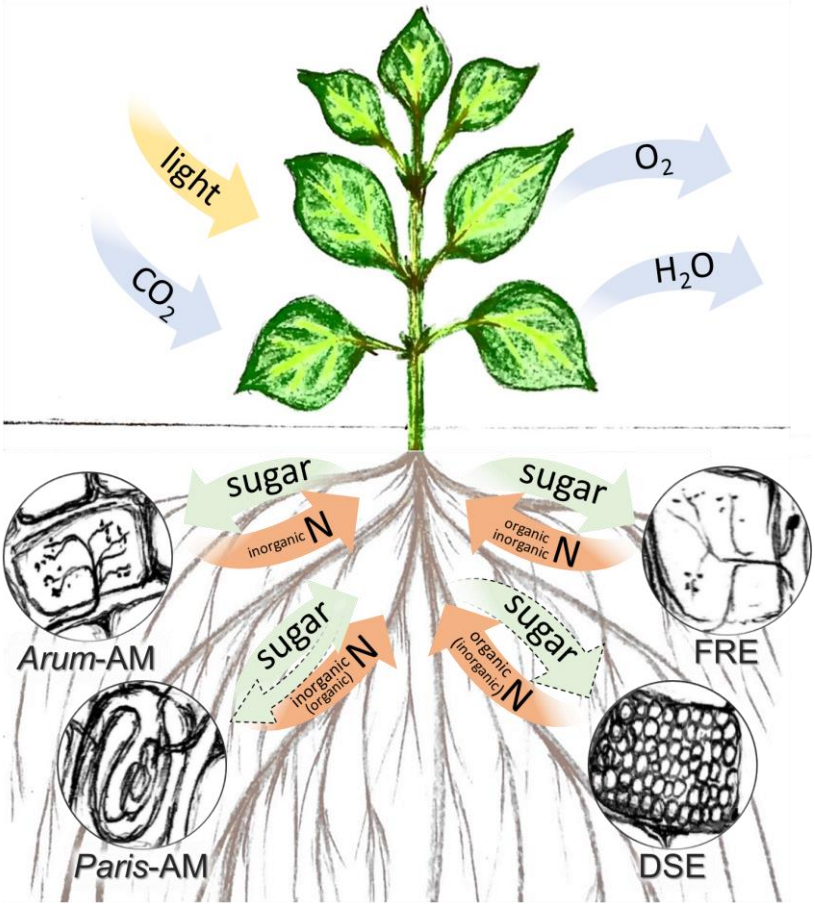

Figure 5 **Nutrient flows in plant-fungi symbiosis.**

Abbreviations: AM, arbuscular mycorrhiza; *Arum*- and *Paris*- represent morphotypes of AM; DSE, dark septate endophytes; FRE, fine root endophytes; N, either organic or inorganic nutrients; dashed line, could not be checked. Designed by Philipp Giesemann, produced by Katrin Giesemann

Manuscript 1, *2* and *3* elucidate plants that are partially mycoheterotrophic on *Paris*-coiling morphotype AM. The organic carbon and nutrient supply from a fungal source was deciphered by a conspicuous ^{13}C, ^{2}H and frequently ^{15}N isotope enrichment for chlorophyllous *Paris*-coiling morphotype AM plant species (Figure 6). This is consistent with previous studies where a ^{13}C, ^{2}H and ^{15}N isotope enrichment was commonly found for Orchidaceae and Ericaceae forming partial or full mycoheterotrophy on EcM fungi. Further, the isotope enrichment suits the pattern found for many fungi (Excursus 2). The ^{13}C, ^{2}H and frequently ^{15}N isotope enrichment of chlorophyllous *Paris*-morphotype AM is positioned intermediate between achlorophyllous full mycoheterotrophs on AM and plant species forming the morpho-counterpart, that is *Arum*-morphotype AM (Figure 6). Partial mycoheterotrophy on *Paris*-morphotype AM plant species was found for forest ground herbaceous species of seed plants *(Manuscript 1, 2)*, ferns *(Manuscript 2)* and horsetails *(Manuscript 2, 3)*. Additionally, small tree saplings and hebaceous open-land meadow species potentially also benefit from a partially mycoheterotrophic nutrition at least for a distinct period in their development *(Manuscript 2)*. The mean proportional carbon gain forms a continuum ranging from 7-93% and follows the sequence of fern > horsetail > seed plants (Figure 7).

Paris quadrifolia (*Paris*-morphotype) and *A. maculatum* (*Arum*-morphotype) are chlorophyllous forest herbaceous species common in European forests and were isotopically confronted in *Manuscript 1*. The ^{13}C, ^{2}H and frequently ^{15}N isotope enrichment of *P. quadrifolia* approaches towards an isotope enrichment known from fully mycoheterotrophic AM plants (Merckx *et al.*, 2010; Courty *et al.*, 2011; Gomes *et al.*, 2020). Additionally, *Anemone nemorosa* (*Paris*-morphotype) followed the trend in ^{13}C and ^{2}H enrichments. Following the assumption that full mycoheterotrophs meet their complete carbon demand from a fungal source, which is then mirrored by the full mycoheterotrophs ^{13}C enrichment; then approximately 50% and 24% of the carbon demand is covered from a fungal source of the here investigated individuals of *P. quadrifolia* and *A. nemorosa,* respectively (Figure 7). Thus, *P. quadrifolia* and *A. nemorosa* represent a first starting point to assume both the *Paris*-morphotype as a prerequisite for partial mycoheterotrophy and a continuum of partially mycoheterotrophic nutrition. In contrast, the *Arum*-morphotype AM reference plant species, *Fraxinus excelsior*, *Hedera helix*, *A. maculatum* and *Allium ursinum*, did not appear conspicuous in stable ^{13}C, ^{2}H and ^{15}N isotope enrichments; thus, their carbon demand assumedly is entirely derived from photosynthesis.

Intriguingly, the *Paris*-morphotype does not exclusively occur in *P. quadrifolia* and *A. nemorosa*, whilst it is, indeed, documented for at least 40% of the 861 plant species summarized in Dickson *et al.* (2007) (intermediate forms omitted). Thereafter, more than 25 publications recorded the AM morphotypes in approximately 500 plant species (intermediate forms omitted). The data on morphotype development were synthesized with stable isotope natural abundance compositions of 509 (n = 4 647) putatively autotrophic plant species (status as of January 2020). The *Manuscript 2* isotopically confronts 13 species forming full

mycoheterotrophy on *Paris*-morphotype, 63 chlorophyllous *Paris*-morphotype plant species, and 59 chlorophyllous *Arum*-morphotype plant species (Figure 6). Chlorophyllous *Paris*-morphotype plant species were hypothesized to have partially mycoheterotrophic nutrition. Thirty one of the 63 chlorophyllous *Paris*-morphotype AM plant species come along with a ^{13}C enrichment and frequently ^{2}H and ^{15}N enrichment positioned intermediate between *Paris*-morphotype full mycoheterotrophs and *Arum*-morphotype full autotrophs (Figure 6). Thus, about half of the *Paris*-morphotype plant species under study enqueue in the steadily increasing list of 124 so far known partially mycoheterotrophic plant species on EcM

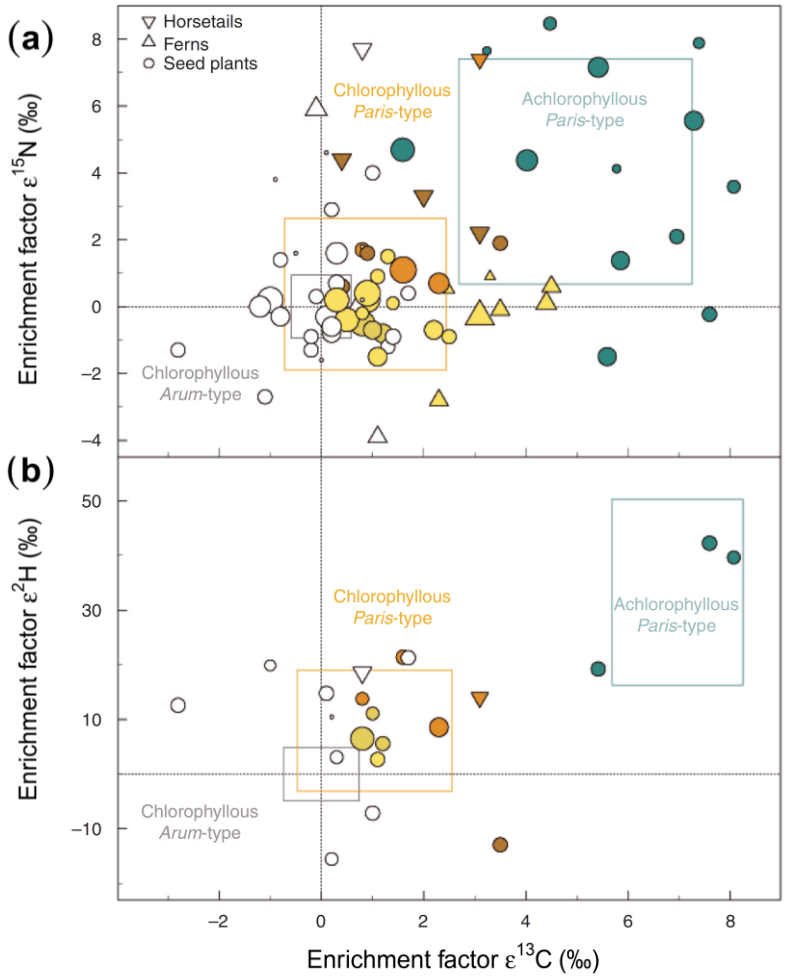

Figure 6 **(a) Carbon and nitrogen enrichment factors ($\varepsilon^{13}C$, $\varepsilon^{15}N$) and (b) carbon and hydrogen enrichment factors ($\varepsilon^{13}C$, $\varepsilon^{2}H$) for chlorophyllous *Arum*-type arbuscular mycorrhizal (AM) plant species (grey frame, SD), chlorophyllous *Paris*-type AM plant species (brownish tones, brown frame, SD) and achlorophyllous, full mycoheterotrophs on AM fungi (blue, blue frame, SD) (obtained from *Manuscript 2*).** AM morphotype assignment was obtained from literature (*cf.* Material and Methods section). Each species is represented by mean values. Standard deviations (SD) are omitted for clarity reasons. Symbol size reflects the sample size of the *Paris*-type species (n = 1 – 31, see Supplementary data Table **S3**). Each chlorophyllous *Paris*-type AM plant species was tested for significance of differences in $\varepsilon^{13}C$, $\varepsilon^{15}N$ and $\varepsilon^{2}H$ to co-occurring chlorophyllous *Arum*-type AM plant species (see Supplementary data Table **S3**). Chlorophyllous *Paris*-type AM plant species shown in coloured symbols are significant in at least one trait (^{13}C enrichment, light gold; $^{13}C+^{2}H$ enrichment, light brown; $^{13}C+^{15}N$ enrichment, dark brown, $^{13}C+^{2}H+^{15}N$ enrichment, dark gold; no significant enrichment, white). Achlorophyllous plant species were not included in the test procedure (see Gomes *et al.*, 2020). The data comprise for $^{13}C/^{15}N$: 13 achlorophyllous *Paris*-type species (n = 99), 63 chlorophyllous *Paris*-type species (n = 520) and 59 chlorophyllous *Arum*-type species (n = 530). The data comprise for ^{2}H: three achlorophyllous species (n = 14), 18 chlorophyllous *Paris*-type species (n = 100) and 15 chlorophyllous *Arum*-type species (n = 104).

and rhizoctonia fungi (*cf.* Hynson *et al.*, 2013; Hynson *et al.*, 2016; Schweiger *et al.*, 2019; status as of January 2020). Recently, the chlorophyllous gentian *Pterygocalyx volubilis* (Suetsugu *et al.*, 2020a) and sporophytes of *Ophioglossum* species (Suetsugu *et al.*, 2020b) where found partially mycoheterotrophic which strengthen the findings as well. Consequently, mycoheterotrophy is commonly distributed among chlorophyllous AM plant species. The ^{13}C relative enrichment suggests various degrees of partial mycoheterotrophy, thus a continuum of full autotrophic *Arum*- and *Paris*-morphotype AM species towards *effective* partial mycoheterotrophy on *Paris*-morphotype AM species is likely. This agrees with previous investigations on orchid and ericoid mycoheterotrophs (Hynson *et al.*, 2013). The driver for the presence of partial mycoheterotrophy might be (a) the intracellular nature of fungal hyphae and (b) the light regime.

(a) Intracellular hyphae are a common hallmark for mycoheterotrophic plants (Imhof, 1999; Imhof *et al.*, 2013), like OM forming intracellular fungal coiled 'pelotons', ErM forming intracellular 'hyphal pegs' and AM forming intracellular *Paris*-morphotype hyphal coils. To the contrary, partial or full mycoheterotrophy was not yet observed for intercellular hyphal growth, such as in *Arum*-morphotype AM (Imhof *et al.*, 2013). (b) The light regime of the forest understory may be highly variable. So far investigated, in early-seasonal stages many *Arum*-morphotype AM plant species flourish as sunlight is pouring the forest ground, e.g. *Allium*, *Bellis*, *Daphne*, *Muscari*, *Petasites*, *Prunus*, *Pulmonaria, and Rubus* (however, some *Paris*-morphotype plants thrive in early-seasonal forests as well, for instance *Anemone*). This is consistent with *Arum*-morphotype AM plant species preferentially occuring in early-successional stages shaped by scattered sun flecks (Ahulu *et al.*, 2005; Dickson *et al.*, 2007). In contrast, apparently the later the season and the later the successional stage the more *Paris*-morphotype plants thrieve in shaded habitats (Ahulu *et al.*, 2005; Dickson *et al.*, 2007). Thus, the additional carbon source from partial mycoheterotrophy might be profitable. *Paris*-morphotype AM forest understory species thriving under the shaded, closed canopy are e.g. forest ground species (*Geranium*, *Mercurialis, Oxalis*), *Acer and Liriodendron* tree saplings and ferns (*Athyrium*, *Dryopteris*, *Polypodium*) and horsetails (*Equisetum*). Many of the aforementioned *Paris*-morphotype AM plant species follow the hypothesized ^{13}C, ^{2}H and frequently ^{15}N enrichment, and thus likely are partial mycoheterotrophs, whilst *Arum*-morphotype plants remain isotopically inconspicuous. This is consistent with limited photosynthesis and lower photosynthetic rates of *Paris*-morphotype AM forest plants (Ludlow & Wolf, 1975; Wright *et al.*, 2004; Gago *et al.*, 2013; Dalke *et al.*, 2018). Most intriguing, the proportional C gain via partial mycoheterotrophy of ferns and horsetails was significantly correlated with *Ellenberg* light regime (*Manuscript 2*). Irradiance as a driver for mycoheterotrophy is in agreement with mycoheterotrophs on EcM and rhizoctonia fungi (Preiss *et al.*, 2010; Matsuda *et al.*, 2012; Schweiger *et al.*, 2019) However, the light regime might not represent the sole driver of partial mycoheterotrophy, as for instance Apiaceae, Ranunculaceae and Gentianaceae from meadow habitats also follow a partially mycoheterotrophic appearance (*cf.* consistent with rhizoctonia-associated open-land orchids, Schiebold *et al.* 2018). Summarzing, partial mycoheterotrophy is common among the group of *Paris*-morphotype AM pteridophytes and seed plant species and could serve to compensate for light-limited environments in addition to other yet unknown drivers. Partial mycoheterotrophy may have profound effects on C and N cycling and may manipulate the biodiversity and the occurrence of plant species in their habitat just as chlorophyllous hemiparasites (Quested *et al.*, 2003; Quested, 2008; Hartley *et al.*, 2015).

Recently, Perez-Lamarque *et al.* (2020) showed low phylogenetic constraints for plants to feel delighted by the downside of mycorrhizal life, i.e. mycoheterotrophic nutrition on AM fungi. This might support the here discovered appearance of partially mycoheterotrophic nutrition on AM fungi in most pteridophytes and 13 seed plant families, both mono- and dicotyledons. Now, we must consider a significant proportion of the AM plant species that reveal the morphological prerequisite (*Paris*-morphotype AM) to *efficiently* gain carbon from a fungal source. This could potentially affect up to one-third of the more than 450 000 plant species developing varying degrees of mycoheterotrophy. However, we must admit that the *Paris*-morphotype AM is not a sufficient precondition (*cf.* continuum).

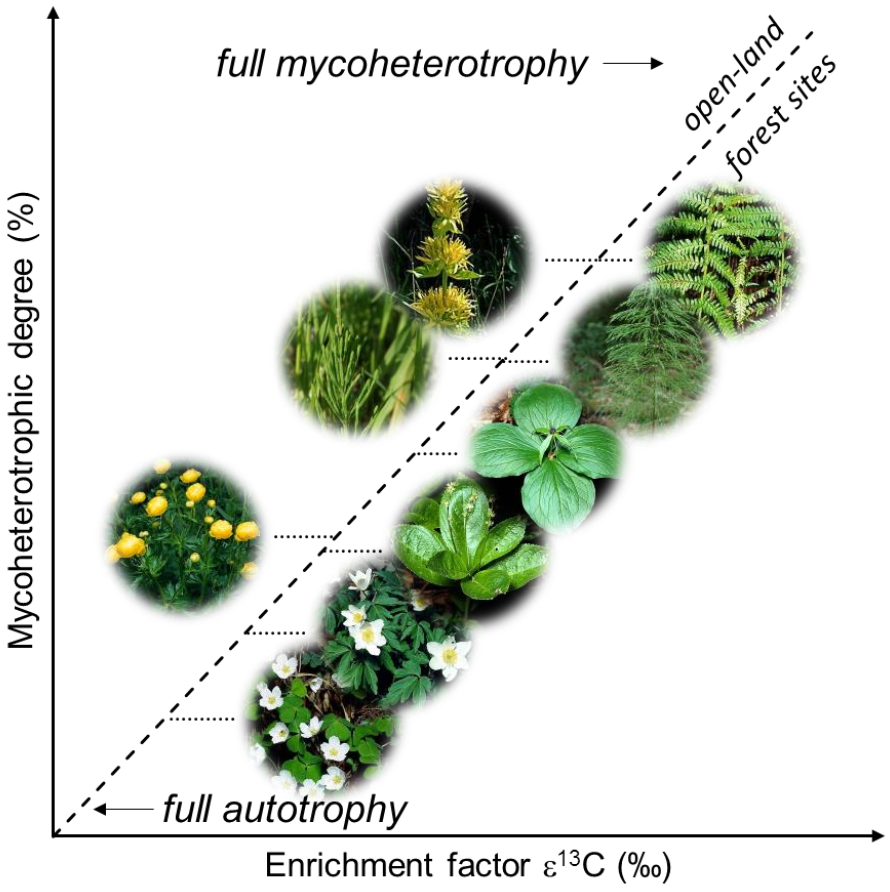

Figure 7 **The mycoheterotrophic degree [%] forms a continuum for mycoheterotrophs on arbuscular mycorrhiza (AM).** The full autotrophs are represented by the chlorophyllous plant species forming *Arum*-morphotype AM. Full mycoheterotrophy is represented by achlorophyllous AM species obtained from Merckx *et al.* (2010) and Gomes *et al.* (2020). The chlorophyllous partial mycoheterotrophs on *Paris*-morphotype AM are located intermediate. The positioning between the two-sources of full autotrophy and full mycoheterotrophy suggests a continuum of carbon acquisitions from a fungal source, exemplified by *Dryopteris filix-mas* (70±24%, n = 5), *Gentiana lutea* (70±20%, n = 5), *Equisetum arvense* (62±10%, n = 5), *E. sylvaticum* (61±13%, n = 4), *Paris quadrifolia* (45±25%, n = 13), *Trollius europaeus* (33±21%, n = 5), *Mercurialis perennis* (32±19%, n = 31), *Anemone nemorosa* (24±17%, n = 10) and *Oxalis acetosella* (20±20%, n = 10). Details outlined in *Manuscript 1* and *2*. Picture credits: horsetails © Philipp Giesemann; others © Schmeil-Fitschen *flora mobil*.

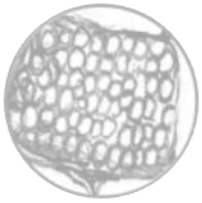

Manuscript 3 and *4* advance the current discussion on fungal root endophytes being involved in carbon-for-nutrient trading (Jumpponen, 2001; Mandyam & Jumpponen, 2005; Field & Pressel, 2018; Hoysted *et al.*, 2018). The literature survey of C, N and H isotope abundances, which fundamentally contributed to *Manuscript 2*, brought also a ^{15}N enrichment for non-mycorrhizal plant species to light (Figure 8). Interestingly, many non-mycorrhizal plant species appear with fungal root endophytes, such as DSE and FRE (Jumpponen & Trappe, 1998; Orchard *et al.*, 2017b). A ^{15}N enrichment in mycoheterotrophic plants was explained by a gain of ^{15}N-enriched organic nutrients (Hynson *et al.*, 2013; Schiebold *et al.*, 2017), and thus might be equivalent to access of ^{15}N-enriched soil organic compounds in non-mycorrhizal plants via fungal root endophytes. Plant species belonging to the Equisetaceae, Cyperaceae and Caryophyllaceae are densely colonized by DSE fungi (Jumpponen & Trappe, 1998) and selected species belonging to the Lycopodiaceae are densely colonized by FRE fungi (Rimington *et al.*, 2016). Interestingly, Equisetaceae were involved in a dual symbiosis with DSE and *Paris*-morphotype AM (Fernández *et al.*, 2008; *Manuscript 3*) and Juncaceae were involved in a dual symbiosis with FRE and AM (*Manuscript 4*). A nutritional role of DSE and FRE, that is a carbon-for-nutrient trading and, most intriguing, the facilitation of acquiring ^{15}N-enriched soil nutrients was deciphered in *Manuscript 3* and *4* (Figure 8). The ^{15}N enrichment found in Cyperaceae and Caryophyllaceae obviously provides evidence for an actively or passively translocated ^{15}N-enriched source towards the plant partner by its DSE fungi (*Manuscript 3*). The provided soil organic nitrogen source is probably rewarded in exchange for organic carbon compounds from photosynthesis. For Equisetaceae sporophytes the ^{13}C, ^{2}H and strongly pronounced ^{15}N enrichments likely support the passive or active acquisition of ^{15}N-enriched nutrients via DSE fungi while simultaneously support the acquisition of ^{13}C-enriched organic carbon via partial mycoheterotrophy from AM fungi (*Manuscript 3*). Interestingly, the isotope pattern found for full mycoheterotrophs on AM was mirrored by the achlorophyllous life form of *E. arvense*. Furthermore, in *Manuscript 4* the club moss *Lycopodiella inundata* and the rush *Juncus bulbosus,* belonging to the plant families of Lycopodiaceae and Juncaceae, respectively, were significantly ^{15}N-enriched. Thus, FRE also facilitate the acquisition of ^{15}N-enriched soil organic nitrogen compounds. Intriguingly, plant species belonging to the plant family of Juncaceae might either form separated symbioses with either FRE, AM and DSE or complex *multi-symbioses* (Jumpponen & Trappe, 1998; Orchard *et al.*, 2017b; *Manuscript 4*). Relative to accompanying mycorrhizal plant species, Juncaceae form a continuum of ^{15}N inconspicuous individuals (e.g., Motomura *et al.*, 2010; Lallemand *et al.*, 2017; Klink *et al.*, 2019) to most ^{15}N-enriched individuals (e.g., Liebel *et al.*, 2010; Gebauer *et al.*, 2016; Schiebold *et al.*, 2018; Klink *et al.*, 2019; *Manuscript 4*). This might be addressed with the nitrogen regime the fungal partners offer. A dual symbiosis of FRE-AM in liverworts efficiently translocated both nitrogen and phosphorous, respectively (Field *et al.*, 2016; Field *et al.*, 2019), thus a similar phenomenon is likely for *L. inundata* and perhaps Juncaceae which needs to be considered in future analysis.

The carbon-for-nutrient trading was evaluated for *L. inundata*. Tracer applications previously confirmed a mutual bidirectional nutrient exchange in liverworts associated with FRE (Field *et al.*, 2015, 2016; Field *et al.*, 2019). *Lycopodiella inundata* was exposed to a $^{14}CO_2$ tracer which was then retrieved in an ingrowth core colonized with FRE (Figure 9a). A small pore size mesh prevented root ingrowth. Furthermore, ^{15}N-ammonium chloride and ^{33}P-labeled orthophosphate tracers were injected into the core and later retrieved from *L. inundata* aboveground plant material (Figure 9b). Most likely, FRE linked the soil and nutrients within the core (therein, the ^{15}N and ^{33}P tracers) to the root. The tracer application provides evidence of a mutual carbon translocation from *L. inundata* to FRE, while in exchange nutrients were translocated from fungi to plant (Figure 9c,d). The bidirectional nutrient transfer is similar to that for non-vascular liverworts engaged with FRE (Field *et al.*, 2015, 2016), yet the exchange is 189- and 145-times more effective for carbon and nitrogen, respectively, in *L. inundata*. In contrast, a greater quantity of phosphorous was translocated when the plant was engaged with AM fungi compared to FRE (Field *et al.*, 2015, 2016; Field *et al.*, 2019). A similar tracer approach is recommended for plant species colonized with DSE fungi.

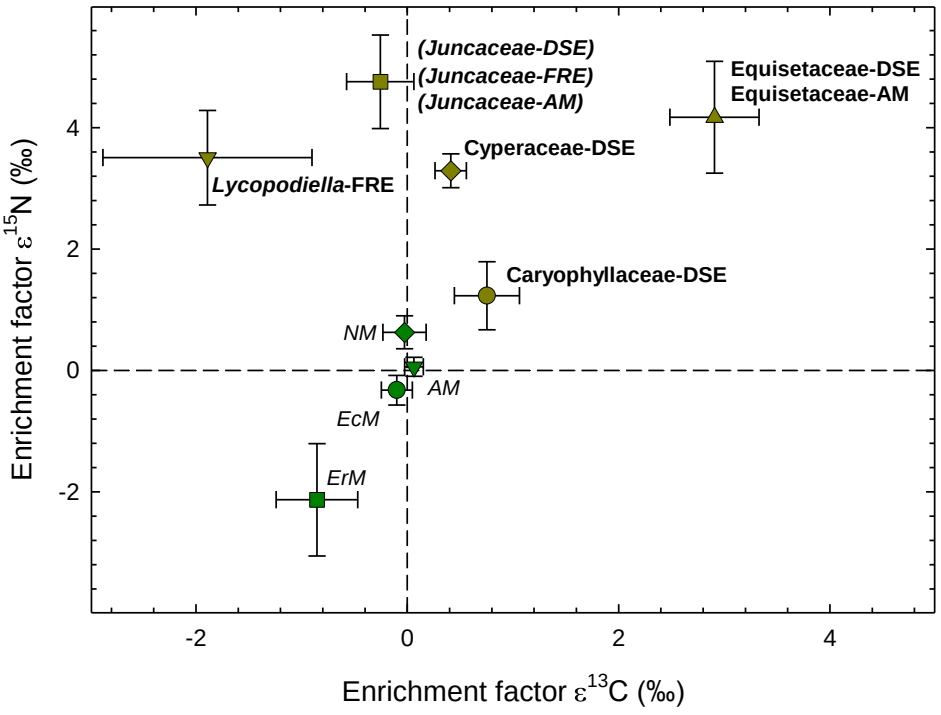

Figure 8 **Carbon and nitrogen stable isotope enrichment factors (ε^{13}C and ε^{15}N) in leaves of 37 plant species belonging to Lycopodiaceae (dark yellow triangle, *n* = 6), Equisetaceae (dark yellow pyramid, *n* = 44), Cyperaceae (dark yellow diamond, *n* = 217) and Caryophyllaceae (dark yellow circle, *n* = 48) associated with Mucoromycotina fine root endophytes (FRE) and dark septate endophytes (DSE).** Equisetaceae were additionally colonized by *Paris*-morphotype arbuscular mycorrhiza (AM). The reference plants comprise arbuscular mycorrhizal (AM, green triangle), ectomycorrhizal (EcM, green circle), ericoid mycorrhizal (ErM, green square) and non-mycorrhizal (NM, green diamond, Brassicaceae) plant species (*n* = 789). Juncaceae (dark yellow rectangle, *n* = 6) were initially sampled to contribute to the reference plants (*Manuscript 4*) but also appear with DSE fungi according to Jumpponen & Trappe (1998) and with AM and FRE according to *Manuscript 4*. All data are shown with mean values and 95% confidence interval.

In sum, the ubiquitous fungal root endophytes likely facilitate the acquisition of ^{15}N-enriched soil organic compounds in selected species belonging to the plant families of Caryophyllaceae, Cyperaceae, Equisetaceae, Juncaceae and Lycopodiaceae and potentially in numerous further plant families and species (Orchard *et al.*, 2017b). In contrast, mycorrhizal fungi might preferentially translocate isotopically inconspicuous soil ammonium and nitrate to their plant partner (Smith & Read, 2008; Field & Pressel, 2018) (Figure 8). An ecologically relevant function for the mostly underappreciated fungal root endophytes (DSE, FRE) is very likely. A possible DSE-plant mutualism supports the early investigations by Haselwandter & Read (1982) and Upson *et al.* (2009), and the recent carbon-for-nutrient tracer approach by Hill *et al.* (2019) as well as the meta-analysis of Mandyam & Jumpponen (2005) and Newsham (2011). The likely FRE-plant mutualism supports early investigations by Greenall (1963), Crush (1973a, 1973b) and Johnson (1977) (*cf.* Orchard *et al.*, 2017b) and contrasts with the weak parasitism occasionally found (*cf.* Orchard *et al.*, 2017b).

The FRE symbiosis enables new insights into early plant terrestrialisation 500 million years ago (Field & Pressel, 2018; Hoysted *et al.*, 2018). *Manuscript 4* suggests FRE are, indeed, serious symbiotic candidates facilitating early plant terrestrialisation by the advantages provided to the plant (Bidartondo *et al.*, 2011; Field & Pressel, 2018; Strullu-Derrien *et al.*, 2018). Mineral nutrient and organic nutrient acquisition by the elusive DSE and FRE could shed new perspectives on early vascular plant development as well as that of more recently evolved plants spanning from mosses to seed plants. Further, the living fossils of *Equisetum* spp. and *L. inundata* are the last recent representatives of early vascular plant species. Equisetaceae (*Manuscript 3*)

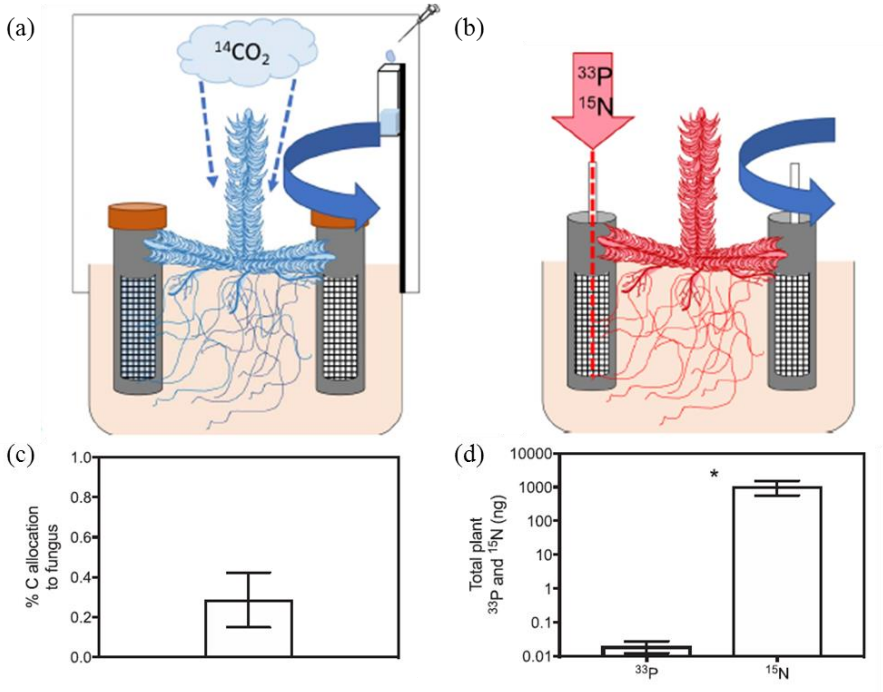

Figure 9 **Experimental design (a, b) and isotope tracer results (c, d) (obtained from *Manuscript 4*). ^{14}C allocation from plant to fungus (c) and ^{15}N and ^{33}P allocation from fungus to plant (d).** The tracer application elucidated the symbiosis between *Lycopodiella inundata* and Mucoromycotina fine root endophytes as nutritionally mutualistic. During the labelling period *L. inundata* transferred approximately 79±49 µg plant-fixed carbon and received 0.6-1% and 3-9% of the supplied ^{15}N and ^{33}P tracer, respectively. In absolute quantities more ^{15}N than ^{33}P were transferred. All data are shown with mean value and standard error.

turned the tables of mycorrhizal life towards a partially mycoheterotrophic nutrition, while partial mycoheterotrophy was not elucidated for *L. inundata* (*Manuscript 4*). This might open speculation about their thriving in the *Carboniferous coal forests*. The arborescent Equisetopsida were dominant in abundance and in species richness during the carboniferous era (approximately 300 million years ago) and emerged during the late Devionian (approximately 380 million years ago) (Burrill & Parker 1994; Feng *et al.*, 2012). The ancestors of the recent herbaceous Equisetaceae impressed with gigantism (approximately 20 m height, 25 cm in diameter; Feng *et al.*, 2012). Despite such remarkable size, they were likely literally overshadowed by gymnospermous trunks and arborescent lycopods (20- to 40 m height, 100 cm in diameter) (e.g. Gastaldo *et al.*, 2004, Krings *et al.*, 2011, Feng *et al.*, 2012). Partial mycoheterotrophy might have opened a lucrative option to thrive in shady habitats millions of years ago.

This thesis successfully addressed three research questions (Figure 1). Evidences for partial mycoheterotrophy, indeed, appears in chlorophyllous *Paris*-morphotype AM plant species. DSE and FRE actively or passively facilitate the acquisition of soil organic nutrients. FRE live in a bidirectional nutrient exchange with vascular plant species (Figure 10). Future outlooks might include:

- The factor of irradiance in partially mycoheterotrophic plants on AM needs to be investigated in the future. The role of ^{15}N isotope enrichment in mycoheterotrophs on AM needs to be deciphered as it might be linked to the functional diversity of Glomeromycotina fungi.
- The possibility of a carbon reward for the DSE fungal partner needs to be analyzed.
- The nutritional effects in FRE symbiosis on seed plant species from the monocotyledons and dicotyledons needs to be evaluated.
- If the nutritional benefits provided by DSE and FRE are further supported by additional studies, it would be worth discussing whether their status as nutritional passive root endophyte is better described, instead, by active (facultative) mycorrhizal fungi?

Figure 10 **The three main results of this thesis.** Illustrations from left to right: partial mycoheterotrophy is addressed in *Manuscript 1-3*, DSE-plant symbiosis in *Manuscript 3* and FRE-plant symbiosis in *Manuscript 4*.
Abbreviations: AM, arbuscular mycorrhiza; C, carbon; DSE, dark septate endophyte; FRE, fine root endophyte; N, nutrient; PMH, partial mycoheterotrophy. Drawing designed by Philipp Giesemann, produced by Katrin Giesemann.

Author contributions to the manuscripts

Manuscript 1

Authors	**Philipp Giesemann**, Hanne N. Rasmussen, Heiko T. Liebel, Gerhard Gebauer
Title	**Discreet heterotrophs: green plants that receive fungal carbon through *Paris*-type arbuscular mycorrhiza**
Journal	***New Phytologist***, 226, 960–966 (2020), doi:10.1111/nph.16367
PG contribution	formulation of the research question (25 %), study design (80 %), data collection (60 %), data analysis (100 %), manuscript preparation (75 %), figures, tables and literature (90 %).

PG contributed to the research design, conducted major parts of the field survey, analyzed and treated the results and wrote the first manuscript draft. HNR essentially initiated the idea for this research on the basis of an unpublished literature review. HTL helped to identify sampling locations and performed some of the sample collection. GG coordinated the project, supervised the isotope abundance analyses and supported data treatment. All coauthors contributed to the manuscript.

Manuscript 2

Authors	**Philipp Giesemann**, Hanne N. Rasmussen, Gerhard Gebauer
Title	**Partial mycoheterotrophy is common among chlorophyllous plants with *Paris*-type arbuscular mycorrhiza**
Journal	***Annals of Botany,*** XX, 1–9, doi: 10.1093/aob/mcab003
PG contribution	formulation of the research question (50 %), study design (80 %), data gathering (100 %), data analysis (100 %), manuscript preparation (75 %), figures, tables and literature (90 %).

PG surveyed data and made a synthesis, analyzed and treated the results and wrote the first manuscript draft. HNR essentially initiated the basic idea for this research originating from an unpublished literature review. GG coordinated the project, supervised the isotope abundance survey, supported data treatment and provided access to unpublished data. All authors contributed to interpretation and presentation of results in the manuscript.

Manuscript 3

Authors	**Philipp Giesemann**, David Eichenberg, Marcus Stöckel, Lukas F. Seifert, Sofia I.F. Gomes, Vincent S.F.T. Merckx, Gerhard Gebauer
Title	**Dark septate endophytes and arbuscular mycorrhizal fungi (*Paris*-morphotype) affect the stable isotope composition of 'classically' non-mycorrhizal plants**
Journal	***Functional Ecology**, 34: 2453–2466 (2020), doi.org/10.1111/1365-2435.13673*
PG contribution	formulation of the research question (25 %), study design (30 %), data collection (15 %), data analysis (100 %), manuscript preparation (40 %), figures, tables and literature (90 %).

PG comprised the data of three fieldwork campaigns, analyzed and treated the results and wrote the first manuscript draft. DE conducted the sampling of Cyperaceae, MS and PG sampled Equisetaceae, LS and PG sampled Caryophyllaceae. Microscopic and isotope analyses were performed by PG, DE, MS and LS. SG and VM were responsible for DNA analysis. GG initiated the project and coordinated the research design, supervised the isotope abundance survey and supported data treatment. All authors contributed to the manuscript.

Manuscript 4

Authors	Grace A. Hoysted, Alison S. Jacob, Jill Kowal, **Philipp Giesemann,** Martin I. Bidartondo, Jeffrey G. Duckett, Gerhard Gebauer, William R. Rimington, Sebastian Schornack, Silvia Pressel, Katie J. Field
Title	**Mucoromycotina fine root endophyte fungi form nutritional mutualisms with vascular plants**
Journal	***Plant Physiology***, 181, 565–577 (2019), doi: 10.1104/pp.19.00729
PG contribution	formulation of the research question (5 %), study design (0 %), data collection (0 %), data analysis (20 %), manuscript preparation (10 %), figures, tables and literature (10 %).

KJF, SP, SS, MIB, and JGD conceived and designed the investigation. SP, JK, JGD, MIB, ASJ, GG, and GAH collected plant material. GAH and KJF undertook the physiological analyses. ASJ, WRR, and MIB undertook the molecular analyses. SP undertook the cytological analyses with assistance from JK. PG and GG analyzed and interpreted the stable isotope data. GAH led the writing. All authors discussed results and commented on the article.

List of further publications

- Klink S, **Giesemann P**, Hubman T, Pausch J. 2020. Stable C and N isotope natural abundance of intraradical hyphae of arbuscular mycorrhizal fungi. *Mycorrhiza* **30**: 773–780.

- Bock C, Zimmermann S, Beisser D, Dinglinger SM, Engelskirchen S, **Giesemann P**, Klink S, Olefeld JL, Rahmann S, Vos M, Boenigk J, Sures B. 2019. Silver stress differentially affects growth of phototrophic and heterotrophic chrysomonad flagellate populations. *Environmental Pollution* **244**: 314–322.

- Klink S, **Giesemann P**, Gebauer G. 2019. Picky carnivorous plants? Investigating preferences for preys´ trophic levels - a stable isotope natural abundance approach with two terrestrial and two aquatic Lentibulariaceae tested in Central Europe, *Annals of Botany* **123**: 1167–1177.

- Imhof HK, Sigl R, Brauer E, Feyl S, **Giesemann P**, Klink S, Leupolz K, Löder MGJ, Löschel L, Missun J, Muszynski S, Ramsperger AFRM, Schrank I, Speck S, Steibl S, Trotter B, Winter I, Laforsch C. 2017. Spatial and temporal variation of macro-, meso- and microplastic abundance on a remote coral island of the Maldives, Indian Ocean. *Marine Pollution Bulletin* **116**: 340–347.

References

Ahulu EM, Nakata M, Nonaka M. 2005. *Arum*-and *Paris*-type arbuscular mycorrhizas in a mixed pine forest on sand dune soil in Niigata Prefecture, central Honshu, Japan. *Mycorrhiza*, **15**: 129–136.

Barrow J, Aaltonen R. 2001. Evaluation of the internal colonization of *Atriplex canescens* (Pursh) Nutt. roots by dark septate fungi and the influence of host physiological activity. *Mycorrhiza* **11**: 199–205.

Barrow JR. 2003. Atypical morphology of dark septate fungal root endophytes of *Bouteloua* in arid southwestern USA rangelands. *Mycorrhiza* **13**: 239–247.

Bidartondo MI, Bruns TD, Weiß M, Sérgio C, Read DJ. 2003. Specialized cheating of the ectomycorrhizal symbiosis by a epiparasitic liverwort. *Proceedings of the Royal Society B: Biological Sciences* **270**: 835–842.

Bidartondo MI, Read DJ, Trappe JM, Merckx V, Ligrone R, Duckett JG. 2011. The dawn of symbiosis between plants and fungi. *Biology Letters* **7**: 574–577.

Björkman E. 1960. *Monotropa hypopitys* L. – an epiparasite on tree roots. *Physiologia Plantarum* **13**: 308–327.

Bolin JF, Tennakoon KU, Majid MBA, Cameron DD. 2017. Isotopic evidence of partial mycoheterotrophy in *Burmannia coelestis* (Burmanniaceae). *Plant Species Biology* **32**: 74–80.

Bougoure JJ, Brundrett MC, Grierson PF. 2010. Carbon and nitrogen supply to the underground orchid, *Rhizanthella gardneri*. *New Phytologist* **186**: 947–956.

Brundrett MC, Tedersoo L. 2018. Evolutionary history of mycorrhizal symbioses and global host plant diversity. *New Phytologist* **220**: 1108–1115.

Brundrett MC. 2002. Coevolution of roots and mycorrhizas of land plants. *New Phytologist* **154**: 275–304.

Burrill, LC, Parker R. 1994. Field horsetail and related species, Equisetaceae. [Corvallis, Or.]: Oregon State University, Extension Service.

Caldwell BA, Jumpponen A, Trappe JM. 2000. Utilization of major detrital substrates by dark-septate, root endophytes. *Mycologia* **92**: 230–232.

Cameron DD, Bolin JF. 2010. Isotopic evidence of partial mycoheterotrophy in the Gentianaceae: *Bartonia virginica* and *Obolaria virginica* as case studies. *American Journal of Botany* **97**: 1272–1277.

Cavagnaro TR, Gao L-L, Smith FA, Smith SE. 2001. Morphology of arbuscular mycorrhizas is influenced by fungal identity. *New Phytologist* **151**: 469–475.

Cernusak LA, Pate JS, Farquhar GD. 2004. Oxygen and carbon isotope composition of parasitic plants and their hosts in southwestern Australia. *Oecologia* **139**: 199–213.

Christenhusz MJM, Reveal JL, Farjon A, Gardner MF, Mill RR, Chase MW. 2011. A new classification and linear sequence of extant gymnosperms. *Phytotaxa* **19**: 55.

Cormier M-A, Werner RA, Leuenberger MC, Kahmen A. 2019. ^{2}H-enrichment of cellulose and n-alkanes in heterotrophic plants. *Oecologia* **189**: 365–373.

Cormier M-A, Werner RA, Sauer PE, Gröcke DR, Leuenberger MC, Wieloch T, Schleucher J, Kahmen A. 2018. ^{2}H-fractionations during the biosynthesis of carbohydrates and lipids imprint a metabolic signal on the δ^{2}H values of plant organic compounds. *New Phytologist* **218**: 479–491.

Courty P-E, Walder F, Boller T, Ineichen K, Wiemken A, Rousteau A, Selosse, MA 2011. Carbon and nitrogen metabolism in mycorrhizal networks and mycoheterotrophic plants of tropical forests: a stable isotope analysis. *Plant Physiology* **156**: 952–961.

Crush JR. 1973a. Significance of endomycorrhizas in tussock grassland in Otago, New Zealand. *New Zealand Journal of Botany* **11**: 645–660.

Crush JR. 1973b. The effect of *Rhizophagus tenuis* mycorrhizas on Ryegrass, Cocksfoot and Sweet Vernal. *New Phytologist* **72**: 965–973.

Curtis W, Hooker WJ. 1826. Flora Londinensis 3.

Dalke IV, Novakovskiy AB, Maslova SP, Dubrovskiy YA. 2018. Morphological and functional traits of herbaceous plants with different functional types in the European Northeast. *Plant Ecology* **219**: 1295–1305.

Dawson TE, Mambelli S, Plamboeck AH, Templer PH, Tu KP. 2002. Stable isotopes in plant ecology. *Annual Review of Ecology and Systematics* **33**: 507–559.

de Bary A. 1878. Über Symbiose. *Tageblatt für die Versammlung deutscher Naturforscher und Aerzte* **51**: 121–126.

Dickson S, Smith FA, Smith SE. 2007. Structural differences in arbuscular mycorrhizal symbioses: More than 100 years after Gallaud, where next? *Mycorrhiza* **17**: 375–393.

Dickson S. 2004. The *Arum-Paris* continuum of mycorrhizal symbioses. *New Phytologist* **163**: 187–200.

Ehleringer JR, Rundel PW. 1989. Stable Isotopes: History, Units, and Instrumentation. In: Rundel PW, Ehleringer JR, Nagy KA. ed. *Stable Isotopes in Ecological Research. Ecological Studies (Analysis and Synthesis)*, vol 68. Springer, New York, NY, 1–15.

Eriksson O, Kainulainen K. 2011. The evolutionary ecology of dust seeds. *Perspectives in Plant Ecology, Evolution and Systematics* **13**: 73–87.

Farquhar GD, Ehleringer JR, Hubick KT. 1989. Carbon isotope discrimination and photosynthesis. *Annual Review of Plant Biology* **40**: 503–537.

Farquhar GD, O'Leary MH, Berry JA. 1982. On the relationship between carbon isotope discrimination and the intercellular carbon dioxide concentration in leaves. *Functional Plant Biology* **9**: 121.

Feng Z, Zierold T, Rößler, R. 2012. When horsetails became giants. *Chinese Science Bulletin* **57**: 1–4.

Fernández N, Messuti MI, Fontenla S. 2008. Arbuscular mycorrhizas and dark septate fungi in *Lycopodium paniculatum* (Lycopodiaceae) and *Equisetum bogotense* (Equisetaceae) in a Valdivian temperate forest of Patagonia, Argentina. *American Fern Journal* **98**: 117–127.

Field KJ, Bidartondo MI, Rimington WR, Hoysted GA, Beerling D, Cameron DD, Duckett JG, Leake JR, Pressel S. 2019. Functional complementarity of ancient plant-fungal mutualisms: Contrasting nitrogen, phosphorus and carbon exchanges between Mucoromycotina and Glomeromycotina fungal symbionts of liverworts. *New Phytologist* **223**: 908–921.

Field KJ, Pressel S. 2018. Unity in diversity: Structural and functional insights into the ancient partnerships between plants and fungi. *New Phytologist* **220**: 996–1011.

Field KJ, Rimington WR, Bidartondo MI, Allinson KE, Beerling DJ, Cameron DD, Duckett JG, Leake JR, Pressel S. 2015. First evidence of mutualism between ancient plant lineages

(Haplomitriopsida liverworts) and Mucoromycotina fungi and its response to simulated Palaeozoic changes in atmospheric CO_2. *New Phytologist* **205**: 743–756.

Field KJ, Rimington WR, Bidartondo MI, Allinson KE, Beerling DJ, Cameron DD, Duckett JG, Leake JR, Pressel S. 2016. Functional analysis of liverworts in dual symbiosis with Glomeromycota and Mucoromycotina fungi under a simulated Palaeozoic CO_2 decline. *The ISME Journal* **10**: 1514–1526.

Finlay RD, Read DJ. 1986. The structure and function of the vegetative mycelium of ectomycorrhizal plants. I. Translocation of ^{14}C-lebelled carbon between plants interconnected by a common mycelium. *New Phytologist* **103**: 143–156.

Frank AB. 1877. Über die biologischen Verhältnisse des Thalles einiger Krustenflechten. *Beitrage zur Biologie der Pflanzen* **2**: 123–200.

Frank AB. 1885. Über die auf Wurzelsymbiose beruhende Ernährung gewisser Bäume durch unterirdische Pilze. *Berichte der Deutschen Botanishen Gesellschaft* **3**: 128–145.

Gago J, Coopman RE, Cabrera HM, Hermida C, Molins A, Conesa MÀ, Galmés J, Ribas-Carbó M, Flexas J. 2013. Photosynthesis limitations in three fern species. *Physiologia Plantarum* **149**: 599–611.

Gallaud I. 1905. Études sur les mycorrhizes endotrophes. *Revue générale de botanique* **17**: 5–48; 66–83, 123–135; 223–239; 313–325; 425–433; 479–500.

Gastaldo RA, Stevanović-Walls, IM, Ware WN, Greb SF. 2004. Community heterogeneity of Early Pennsylvanian peat mires. *Geology* **32**: 693–696.

Gebauer G, Dietrich P. 1993. Nitrogen isotope ratios in different compartments of a mixed stand of spruce, larch and beech trees and of understory vegetation including fungi. *Isotopes in Environmental and Health Studies* **29**: 35–44.

Gebauer G, Meyer M. 2003. ^{15}N and ^{13}C natural abundance of autotrophic and myco-heterotrophic orchids provides insight into nitrogen and carbon gain from fungal association. *New Phytologist* **160**: 209–223.

Gebauer G, Preiss K, Gebauer AC. 2016. Partial mycoheterotrophy is more widespread among orchids than previously assumed. *New Phytologist* **211**: 11–15.

Gleixner G, Danier HJ, Werner RA, Schmidt HL. 1993. Correlations between the ^{13}C content of primary and secondary plant products in different cell compartments and that in decomposing basidiomycetes. *Plant Physiology* **102**: 1287–1290.

Gomes SIF, Merckx VSFT, Kehl J, Gebauer G. 2020. Mycoheterotrophic plants living on arbuscular mycorrhizal fungi are generally enriched in ^{13}C, ^{15}N, and ^{2}H isotopes. *Journal of Ecology* **108**: 1250–1261.

Graham SW, Lam VKY, Merckx VSFT. 2017. Plastomes on the edge: The evolutionary breakdown of mycoheterotroph plastid genomes. *New Phytologist* **214**: 48–55.

Greenall JM. 1963. The mycorrhizal endophytes of *Griselinia littoralis* (Cornaceae). *New Zealand Journal of Botany* **1**: 389–400.

Hardoim PR, van Overbeek LS, Berg G, Pirttilä AM, Compant S, Campisano A, Döring M, Sessitsch A. 2015. The Hidden World within Plants: Ecological and Evolutionary Considerations for Defining Functioning of Microbial Endophytes. *Microbiology and Molecular Biology Reviews* **79**: 293–320.

Hartley SE, Green P, Massey FP, Press MCP, Stewart JA, John EA. 2015. Hemiparasitic plant impacts animal and plant communities across four trophic levels. *Ecology* **96**: 2408–2416.

Haselwandter K, Read DJ. 1982. The significance of a root-fungus association in two *Carex* species of high-alpine plant communities. *Oecologia* **53**: 352–354.

Hawksworth DL. 1991. The fungal dimension of biodiversity: Magnitude, significance, and conservation. *Mycological Research* **95**: 641–655.

Hill PW, Broughton R, Bougoure J, Havelange W, Newsham KK, Grant H, Murphy DV, Clode P, Ramayah S, Marsden KA *et al.* 2019. Angiosperm symbioses with non-mycorrhizal fungal partners enhance N acquisition from ancient organic matter in a warming maritime Antarctic. *Biology Letters* **22**: 2111–2119.

Hobbie EA, Högberg P. 2012. Nitrogen isotopes link mycorrhizal fungi and plants to nitrogen dynamics. *New Phytologist* **196**: 367–382.

Hodge A, Campbell CD, Fitter AH. 2001. An arbuscular mycorrhizal fungus accelerates decomposition and acquires nitrogen directly from organic material. *Nature* **413**: 297–299.

Hoysted GA, Kowal J, Jacob A, Rimington WR, Duckett JG, Pressel S, Orchard S, Ryan MH, Field KJ, Bidartondo MI. 2018. A mycorrhizal revolution. *Current Opinion in Plant Biology* **44**: 1–6.

Hynson NA, Madsen TP, Selosse M-A, Adam IK, Ogura-Tsujita Y, Roy M, Gebauer G. 2013. The physiological ecology of mycoheterotrophy. In: Merckx VSFT, ed. *Mycoheterotrophy: The biology of plants living on fungi*. New York, NY: Springer, 297–342.

Hynson NA, Schiebold JM-I, Gebauer G. 2016. Plant family identity distinguishes patterns of carbon and nitrogen stable isotope abundance and nitrogen concentration in mycoheterotrophic plants associated with ectomycorrhizal fungi. *Annals of Botany* **118**: 467–479.

Imhof S, Massicotte HB, Melville LH, Peterson RL. 2013. Subterranean morphology and mycorrhizal structures. In: Merckx VSFT, ed. *Mycoheterotrophy: The biology of plants living on fungi*. New York, NY: Springer, 157–214.

Imhof S. 1999. Root morphology, anatomy and mycotrophy of the achlorophyllous *Voyria aphylla* (Jacq.) Pers. (Gentianaceae). *Mycorrhiza* **9**: 33–39.

Jakobsen I, Rosendahl L. 1990. Carbon flow into soil and external hyphae from roots of mycorrhizal cucumber plants. *New Phytologist* **115**: 77–83.

Jiang Y, Wang W, Xie Q, Liu N, Liu L, Wang D, Zhang X, Yang C, Chen X, Tang D *et al.* 2017. Plants transfer lipids to sustain colonization by mutualistic mycorrhizal and parasitic fungi. *Science* **356**: 1172–1175.

Johnson NC, Graham JH, Smith FA. 1997. Functioning of mycorrhizal associations along the mutualism-parasitism continuum. *New Phytologist* **135**: 575–585.

Johnson PN. 1977. Mycorrhizal endogonaceae in a new zealand forest. *New Phytologist* **78**: 161–170.

Jumpponen A. 2001. Dark septate endophytes - are they mycorrhizal? *Mycorrhiza* **11**: 207–211.

Jumpponen AR, Trappe JM. 1998. Dark septate endophytes: A review of facultative biotrophic root-colonizing fungi. *New Phytologist* **140**: 295–310.

Kamienski F. 1881. Die Vegetationsorgane der *Monotropa hypopitys* L. *Botanische Zeitung* **29**: 458–461.

Kennedy PG, Izzo AD, Bruns TD. 2003. There is high potential for the formation of common mycorrhizal networks between understorey and canopy trees in a mixed evergreen forest. *Journal of Ecology* **91**: 1071–1080.

Keymer A, Pimprikar P, WewerV, Huber C, BrandsM, Bucerius SL, Delaux P-M, Klingl V, Röpenack-Lahaye Ev, Wang TL *et al.* 2017. Lipid transfer from plants to arbuscular mycorrhiza fungi. *eLife* **6**: e29107.

Klein T, Siegwolf RTW, Körner C. 2016. Belowground carbon trade among tall trees in a temperate forest. *Science* **352**: 342–344.

Klink S, Giesemann P, Gebauer G. 2019. Picky carnivorous plants? Investigating preferences for preys' trophic levels–a stable isotope natural abundance approach with two terrestrial and two aquatic Lentibulariaceae tested in Central Europe. *Annals of Botany* **123**: 1167–1177.

Klironomos JN. 2003. Variation in plant response to native and exotic arbuscular mycorrhizal fungi. *Ecology* **84**: 2292–2301.

Konrat M von, **Soderstrom L, Renner MAM, Hagborg A, Briscoe L, Engel JJ. 2010.** Early Land Plants Today (ELPT): How many liverwort species are there? *Phytotaxa* **9**: 22.

Krings M, Taylor, TN, Taylor, EL, Dotzler N, Walker C. 2011. Arbuscular mycorrhizal-like fungi in Carboniferous arborescent lycopsids. *New Phytologist* **191**: 311–314.

Lallemand F, Puttsepp Ü, Lang M, Luud A, Courty P-E, Palancade C, Selosse M-A. 2017. Mixotrophy in Pyroleae (Ericaceae) from Estonian boreal forests does not vary with light or tissue age. *Annals of Botany* **120**: 361–371.

Leake JR. 1994. The biology of myco-heterotrophic ('saprophytic') plants. *New Phytologist* **127**: 171–216.

Lee Y-I, Yang C-K, Gebauer G. 2015. The importance of associations with saprotrophic non-Rhizoctonia fungi among fully mycoheterotrophic orchids is currently under-estimated: novel evidence from sub-tropical Asia. *Annals of Botany* **116**: 423–435.

Liebel HT, Bidartondo MI, Preiss K, Segreto R, Stöckel M, Rodda M, Gebauer G. 2010. C and N stable isotope signatures reveal constraints to nutritional modes in orchids from the Mediterranean and Macaronesia. *American Journal of Botany* **97**: 903–912.

Link HF. 1809. Observationes in ordines plantarum naturales. *Dissertatio I. Mag Ges Naturf Freunde Berlin*.

Ludlow CJ, Wolf FT. 1975. Photosynthesis and Respiration Rates of Ferns. *American Fern Journal* **65**: 43.

Luginbuehl LH, Menard GN, Kurup S, van Erp H, Radhakrishnan GV, Breakspear A, Oldroyd GED, Eastmond PJ. 2017. Fatty acids in arbuscular mycorrhizal fungi are synthesized by the host plant. *Science* **356**: 1175–1178.

Magill RE. 2010. Moss diversity: New look at old numbers. *Phytotaxa* **9**: 167–174.

Mandyam K, Jumpponen A. 2005. Seeking the elusive function of the root-colonising dark septate endophytic fungi. *Studies in Mycology* **53**: 173–189.

Mandyam KG, Jumpponen A. 2014. Mutualism-parasitism paradigm synthesized from results of root-endophyte models. *Frontiers in Microbiology* **5**: 776.

Matsuda Y, Shimizu S, Mori M, Ito S-I, Selosse M-A. 2012. Seasonal and environmental changes of mycorrhizal associations and heterotrophy levels in mixotrophic *Pyrola japonica* (Ericaceae) growing under different light environments. *American Journal of Botany* **99**: 1177–1188.

Mayor JR, Schuur EAG, Henkel TW. 2009. Elucidating the nutritional dynamics of fungi using stable isotopes. *Ecology Letters* **12**: 171–183.

McKendrick SL, Leake JR, Read DJ. 2000. Symbiotic germination and development of myco-heterotrophic plants in nature: transfer of carbon from ectomycorrhizal *Salix repens* and *Betula pendula* to the orchid *Corallorhiza trifida* through shared hyphal connections. *New Phytologist* **145**: 539–548.

McKinney CR, McCrea JM, Epstein S, Allen HA, Urey, HC. 1950. Improvements in mass spectrometers for the measurement of small differences in isotope abundance ratios. *Review of Scientific Instruments* **21**: 724–730.

Melin E. 1922. On the Mycorrhizas of *Pinus Silvestris* L. and *Picea Abies* Karst: A Preliminary Note. *Journal of Ecology* **9**: 254.

Merckx V, Stöckel M, Fleischmann A, Bruns TD, Gebauer G. 2010. ^{15}N and ^{13}C natural abundance of two mycoheterotrophic and a putative partially mycoheterotrophic species associated with arbuscular mycorrhizal fungi. *New Phytologist* **188**: 590–596.

Merckx VS, Freudenstein JV, Kissling J, Christenhusz MJ, Stotler RE, Crandall-Stotler B, Wickett N, Rudall PJ, Maas-van de Kamer H, Maas PM. 2013a. Taxonomy and Classification. In: Merckx VSFT, ed. *Mycoheterotrophy: The biology of plants living on fungi*. New York, NY: Springer, 19–102.

Merckx VS, Smets EF, Specht CD. 2013b. Biogeography and Conservation. In: Merckx VSFT, ed. *Mycoheterotrophy: The biology of plants living on fungi*. New York, NY: Springer, 103–156.

Merckx VS. 2013. Mycoheterotrophy: An Introduction. In: Merckx VSFT, ed. *Mycoheterotrophy: The biology of plants living on fungi*. New York, NY: Springer, 1–17.

Michelsen A, Quarmby C, Sleep D, Jonasson S. 1998. Vascular plant ^{15}N natural abundance in heath and forest tundra ecosystems is closely correlated with presence and type of mycorrhizal fungi in roots. *Oecologia* **115**: 406–418.

Michelsen A, Schmidt IK, Jonasson S, Quarmby C. Sleep D. 1996. Leaf ^{15}N abundance of subarctic plants provides field evidence that ericoid, ectomycorrhizal and non-and arbuscular mycorrhizal species access different sources of soil nitrogen. *Oecologia* **105**: 53–63.

Morris JL, Puttick MN, Clark JW, Edwards D, Kenrick P, Pressel S, Wellman CH, Yang Z, Schneider H, Donoghue PCJ. 2018. The timescale of early land plant evolution. *Proceedings of the National Academy of Sciences of the United States of America* **115**: E2274-E2283.

Motomura H, Selosse MA, Martos F, Kagawa A, Yukawa T. 2010. Mycoheterotrophy evolved from mixotrophic ancestors: evidence in *Cymbidium* (Orchidaceae). *Annals of Botany* **106**: 573–581.

Näsholm T, Högberg P, Franklin O, Metcalfe D, Keel SG, Campbell C, Hurry V, Linder S, Högberg MN. 2013. Are ectomycorrhizal fungi alleviating or aggravating nitrogen limitation of tree growth in boreal forests?. *New Phytologist* **198**: 214–221.

Newsham KK. 2011. A meta-analysis of plant responses to dark septate root endophytes. *New Phytologist* **190**: 783–793.

Ogura-Tsujita Y, Gebauer G, Hashimoto T, Umata H, Yukawa T. 2009. Evidence for novel and specialized mycorrhizal parasitism: the orchid *Gastrodia confuse* gains carbon from saprotrophic *Mycena*. *Proceedings of the Royal Society B: Biological Sciences* **276**: 761–767.

Ogura-Tsujita Y, Gebauer G, Xu H, Fukasawa Y, Umata H, Tetsuka K, Kubota M, Schweiger JM-I, Yamashita S, Maekawa N *et al.* 2018. The giant mycoheterotrophic orchid *Erythrorchis altissima* is associated mainly with a divergent set of wood-decaying fungi. *Molecular Ecology* **27**: 1324–1337.

Orchard S, Hilton S, Bending GD, Dickie IA, Standish RJ, Gleeson DB, Jeffery RP, Powell JR, Walker C, Bass D *et al.* 2017a. Fine endophytes (*Glomus tenue*) are related to Mucoromycotina, not Glomeromycota. *New Phytologist* **213**: 481–486.

Orchard S, Standish RJ, Dickie IA, Renton M, Walker C, Moot D, Ryan MH. 2017b. Fine root endophytes under scrutiny: A review of the literature on arbuscule-producing fungi recently suggested to belong to the Mucoromycotina. *Mycorrhiza* **27**: 619–638.

Perez-Lamarque B, Selosse M-A, Öpik M, Morlon H, Martos F. 2020. Cheating in arbuscular mycorrhizal mutualism: A network and phylogenetic analysis of mycoheterotrophy. *New Phytologist* **226**: 1822-1835.

Peterson RL, Wagg C, Pautler M. 2008. Associations between microfungal endophytes and roots: Do structural features indicate function? *Botany* **86**: 445–456.

Pimm SL, Joppa LN. 2015. How Many Plant Species are There, Where are They, and at What Rate are They Going Extinct? *Annals of the Missouri Botanical Garden* **100**: 170–176.

Preiss K, Adam IKU, Gebauer G. 2010. Irradiance governs exploitation of fungi: Fine-tuning of carbon gain by two partially myco-heterotrophic orchids. *Proceedings. Biological Sciences* **277**: 1333–1336.

Preiss, K, Gebauer G. 2008. A methodological approach to improve estimates of nutrient gains by partially myco-heterotrophic plants. *Isotopes in Environmental and Health Studies* **44**: 393–401.

Press MC, Shah N, Tuohy JM, Stewart GR. 1987. Carbon isotope ratios demonstrate carbon flux from C_4 host to C_3 parasite. *Plant Physiology* **85**: 1143–1145.

Pressel S, Bidartondo MI, Ligrone R, Duckett JG. 2010. Fungal symbioses in bryophytes: New insights in the Twenty First Century. *Phytotaxa* **9**: 238–253.

Quested HM, Cornelissen JHC, Press MC, Callaghan TV, Aerts R, Trosien F, Riemann P, Gwynn-Jones D, Kondratchuk A, Jonasson SE. 2003. Decomposition of sub-arctic plants with differing nitrogen economies: a functional role for hemiparasites. *Ecology* **84**: 3209–3221.

Quested HM. 2008. Parasitic plants—impacts on nutrient cycling. *Plant Soil* **311**: 269–272.

Ranker TA, Sundue MA. 2015. Why are there so few species of ferns? *Trends in Plant Science* **20**: 402–403.

Rich MK, Nouri E, Courty P-E, Reinhardt D. 2017. Diet of arbuscular mycorrhizal fungi: bread and butter? *Trends in Plant Science* **22**: 652–660.

Rimington WR, Duckett JG, Field KJ, Bidartondo MI, Pressel S. 2020. The distribution and evolution of fungal symbioses in ancient lineages of land plants. *Mycorrhiza* **30**: 23–49.

Rimington WR, Pressel S, Field KJ, Strullu-Derrien C, Duckett JG, Bidartondo MI. 2016 Chapter 2: Reappraising the origin of mycorrhizas. In Martin F, ed. *Molecular Mycorrhizal Symbiosis*. John Wiley & Sons, New York, 31–32

Schiebold JM-I, Bidartondo MI, Karasch P, Gravendeel B, Gebauer G. 2017. You are what you get from your fungi: Nitrogen stable isotope patterns in *Epipactis* species. *Annals of Botany* **119**: 1085–1095.

Schiebold JMI, Bidartondo MI, Lenhard F, Makiola A, Gebauer G. 2018. Exploiting mycorrhizas in broad daylight: Partial mycoheterotrophy is a common nutritional strategy in meadow orchids. *Journal of Ecology* **106**: 168–178.

Schweiger JM-I, Kemnade C, Bidartondo MI, Gebauer G. 2019. Light limitation and partial mycoheterotrophy in rhizoctonia-associated orchids. *Oecologia* **189**: 375–383.

Selosse M-A, Weiss M, Jany JL, Tillier A. 2002. Communities and populations of sebacinoid basidiomycetes associated with the achlorophyllous orchid *Neottia nidus-avis* (L.) L.C.M. Rich. and neighbouring treeectomycorrhizae. *Molecular Ecology* **11**: 1831−1844.

Smith FA, Smith SE. 1997. Tansley Review No. 96. Structural diversity in (vesicular)-arbuscular mycorrhizal symbioses. *New Phytologist* **137**: 373–388.

Smith SE, Read DJ. 2008. Mycorrhizal symbiosis. Amsterdam: Elsevier/Acad. Press.

Spatafora JW, Chang Y, Benny GL, Lazarus K, Smith ME, Berbee ML, Bonito G, Corradi N, Grigoriev I, Gryganskyi A *et al.* 2016. A phylum-level phylogenetic classification of zygomycete fungi based on genome-scale data. *Mycologia* **108**: 1028–1046.

Sternberg LO, DeNiro MJ, Ting IP. 1984. Carbon, hydrogen, and oxygen isotope ratios of cellulose from plants having intermediary photosynthetic modes. *Plant Physiology* **74**: 104–107.

Strullu-Derrien C, Selosse M-A, Kenrick P, Martin FM. 2018. The origin and evolution of mycorrhizal symbioses: From palaeomycology to phylogenomics. *New Phytologist* **220**: 1012–1030.

Suetsugu K, Matsubayashi J, Ogawa NO, Murata S, Sato R, Tomimatsu H. 2020a. Isotopic evidence of arbuscular mycorrhizal cheating in a grassland gentian species. *Oecologia* **192**: 929–937.

Suetsugu K, Matsubayashi J, Tayasu I. 2020c. Some mycoheterotrophic orchids depend on carbon from dead wood: novel evidence from a radiocarbon approach. *New Phytologist* **227**: 1519−1529.

Suetsugu K, Taketomi S, Tanabe AS, Haraguchi TF, Tayasu I, Toju H. 2020b. Isotopic and molecular data support mixotrophy in *Ophioglossum* at the sporophytic stage. *New Phytologist* **228**: 415−419.

Taylor DL, Bruns TD. 1997. Independent, specialized invasions of ectomycorrhizal mutualism by two nonphotosynthetic orchids. *Proceedings of the National Academy of Sciences of the United States of America* **94**: 4510−4515

Taylor TN, Klavins SD, Krings M, Taylor EL, Kerp H, Hass H. 2003. Fungi from the Rhynie chert: A view from the dark side. *Transactions of the Royal Society of Edinburgh: Earth Sciences* **94**: 457–473.

Tedersoo L, Bahram M, Zobel M. 2020. How mycorrhizal associations drive plant population and community biology. *Science* **367**.

Tedersoo L, Pellet P, Köljalg U, Selosse M-A. 2007. Parallel evolutionary paths to mycoheterotrophy in understorey Ericaceae and Orchidaceae. Ecological evidence for mixotrophy in Pyroleae. *Oecologia* **151**: 206–217.

Těšitel J, Plavcová L, Cameron DD. 2010. Interactions between hemiparasitic plants and their hosts: The importance of organic carbon transfer. *Plant Signaling & Behavior* **5**: 1072–1076.

Trudell SA, Rygiewicz PT, Edmonds RL. 2003. Nitrogen and carbon stable isotope abundances support the myco-heterotrophic nature and host-specificity of certain achlorophyllous plants. *New Phytologist* **160**: 391–401.

Upson R, Read DJ, Newsham KK. 2009. Nitrogen form influences the response of *Deschampsia antarctica* to dark septate root endophytes. *Mycorrhiza* **20**: 1–11.

van der Heijden MGA, Dombrowski N, Schlaeppi K. 2017. Continuum of root-fungal symbioses for plant nutrition. *Proceedings of the National Academy of Sciences of the United States of America* **114**: 11574–11576.

Villarreal JC, Cargill DC, Hagborg A, Soderstrom L, Renzaglia KS. 2010. A synthesis of hornwort diversity: Patterns, causes and future work. *Phytotaxa* **9**: 150.

Walder F, Niemann H, Natarajan M, Lehmann MF, Boller T, Wiemken A. 2012. Mycorrhizal networks: common goods of plants shared under unequal terms of trade. *Plant Physiology* **159**: 789–797.

Walker C, Gollotte A, Redecker D. 2018. A new genus, *Planticonsortium* (Mucoromycotina), and new combination (*P. tenue*), for the fine root endophyte, *Glomus tenue* (basionym *Rhizophagus tenuis*). *Mycorrhiza* **28**: 213–219.

Waterman RJ, Klooster MR, Hentrich H, Bidartondo MI. 2013. Species Interactions of Mycoheterotrophic Plants: Specialization and its Potential Consequences. In: Merckx VSFT, ed. *Mycoheterotrophy: The biology of plants living on fungi*. New York, NY: Springer, 267–296.

Westwood JH, Yoder JI, Timko MP, dePamphilis CW. 2010. The evolution of parasitism in plants. *Trends in Plant Science* **15**: 227–235.

Wipf D, Krajinski F, van Tuinen D, Recorbet G, Courty P-E. 2019. Trading on the arbuscular mycorrhiza market: From arbuscules to common mycorrhizal networks. *New Phytologist* **223**: 1127–1142.

Wright IJ, Reich PB, Westoby M, Ackerly DD, Baruch Z, Bongers F, Cavender-Bares J, Chapin T, Cornelissen JHC, Diemer M *et al.* 2004. The worldwide leaf economics spectrum. *Nature* **428**: 821–827.

Yakir D. 1992. Variations in the natural abundance of oxygen-18 and deuterium in plant carbohydrates. *Plant, Cell & Environment* **15**: 1005–1020.

Zhang Y, Guo LD, & Liu RJ. 2004. Arbuscular mycorrhizal fungi associated with common pteridophytes in Dujiangyan, southwest China. *Mycorrhiza* **14:** 25–30.

Ziegler H. 1995. Stable isotopes in plant physiology and ecology. In: Behnke H-D, Lüttge U, Esser K, Kadereit JW, Runge M, ed. *Progress in Botany: Structural Botany Physiology Genetics Taxonomy Geobotany*. Springer Berlin Heidelberg, Berlin, Heidelberg, 1–24.

Zimmer K, Hynson NA, Gebauer G, Allen EB, Allen MF, Read DJ. 2007. Wide geographical and ecological distribution of nitrogen and carbon gains from fungi in pyroloids and monotropoids (Ericaceae) and in orchids. *New Phytologist* **175**: 166–175.

CHAPTER 3

- "I think, unfortunately, the Paris-morphotype was wrongfully understudied for a significant amount of time. If there is ongoing support for partial mycoheterotrophy on Paris-morphotype AM fungi, we might have overlooked important mechanisms in carbon trading until now. Also, mycorrhiza-like fungal endophytes, such as DSE and FRE might play an important role in the future"

Manuscripts of this thesis

Manuscript 1

DISCREET HETEROTROPHS: GREEN PLANTS THAT RECEIVE FUNGAL CARBON THROUGH *PARIS*-TYPE ARBUSCULAR MYCORRHIZA

Philipp Giesemann[1], Hanne N. Rasmussen[2], Heiko T. Liebel[1,3], Gerhard Gebauer[1]

New Phytologist 226: 960–966 (2020), doi:10.1111/nph.16367.

[1]University of Bayreuth, Laboratory of Isotope Biogeochemistry, Bayreuth Center of Ecology and Environmental Research (BayCEER), 95440 Bayreuth, Germany

[2]Department of Geosciences and Nature Resource Management, Section of Forest, Nature and Biomass, University of Copenhagen, Rolighedsvej 23, 1958 Frederiksberg C, Copenhagen, Denmark.

[3]Biological Station Murnauer Moos, 82418 Murnau, Germany

Key words: arbuscular mycorrhiza (AM), *Arum maculatum*, *Arum*-type, mycoheterotrophy, *Paris quadrifolia*, *Paris*-type, stable isotope natural abundance.

Received, 29 October 2019; accepted, 8 December 2019; published, 14 December 2019.

New Phytologist

Forum

Letter

Discreet heterotrophs: green plants that receive fungal carbon through *Paris*-type arbuscular mycorrhiza

Arbuscular mycorrhiza (AM) represents a symbiosis between plants and Glomeromycotina fungi, and it is distributed throughout the plant kingdom and all terrestrial ecosystems. Colonization in plant roots usually takes structural form of either *Paris*- or *Arum*-type, distinguished by intracellular hyphal coils and arbuscules and exemplified by *Paris quadrifolia* and *Arum maculatum* (Gallaud, 1905; Smith & Smith, 1997; Dickson *et al.*, 2007), respectively, with a near 1 : 1 distribution among plant species (Dickson *et al.*, 2007). Extensive physiological research on the *Arum*-morphotype shows a mutualistic relationship, but the *Paris*-type has received much less attention with regard to its function (Dickson *et al.*, 2007). In this study, we show that green leaves of *P. quadrifolia* contain nearly 50% carbon of fungal origin, in striking contrast to *A. maculatum* in which carbon is entirely derived from photoassimilation. The evidence is based on stable isotope composition in the two species compared with cohabitant plant species with various types of colonization. This identifies *P. quadrifolia* as a partial mycoheterotroph on fungi, and one of the reference species, *Anemone nemorosa*, also with *Paris*-type colonization, shows evidence of similar but less pronounced carbon acquisition from fungi. Partial mycoheterotrophy could thus potentially be widespread among the roughly 100 000 plant species that are known to develop *Paris*-type AM, with far-reaching implications for our understanding of plant community functioning.

In the *Arum*-morphotype, greatly branched hyphal structures (arbuscules) develop within root cortical cells while sparsely branched hyphae run in the intercellular spaces along cell files (Gallaud, 1905; Dickson *et al.*, 2007). Arbuscules presumably are the site of mineral nutrient fluxes from fungus to plant, and together with intercellular hyphae are also involved in photosynthate transfer from plant to fungus (Smith & Smith, 1997; Dickson *et al.*, 2007; Wipf *et al.*, 2019). This morphotype is frequent among agricultural plants (Dickson *et al.*, 2007). By contrast, the *Paris*-morphotype is characterized by a dense infection with intracellular hyphal coils and few, if any, intercellular hyphae (Gallaud, 1905; Dickson *et al.*, 2007). *Paris*-type colonization is typical of forest floor herbaceous plants, and long-lived, woody and evergreen plants (Dickson *et al.*, 2007). Furthermore, many of the 880 plant species with obvious Chl-deficiency and AM (Leake, 1994; Merckx *et al.*, 2013) show *Paris*-type endomycorrhiza (Imhof *et al.*, 2013). The mycoheterotrophy, that is, parasitism on fungi, of these achlorophyllous plants is well documented, primarily by stable isotope natural abundance approaches (Hynson *et al.*, 2013). The uptake of fungal carbon in such AM plants is revealed by a significant ^{13}C enrichment, compared with photoautotrophic plants. This enrichment, however, is not as pronounced as in mycoheterotrophic plants associated with ectomycorrhizal fungi (Merckx *et al.*, 2010; Courty *et al.*, 2011).

In many types of mycorrhiza, stable isotope signatures are essential in clarifying the plant–fungus relationships, particularly in species that obviously have low or no photosynthetic capacity due to low amounts of Chl. Thus, in orchid mycorrhiza, the achlorophyllous species that associate with fungi that simultaneously form ectomycorrhizas with forest trees have been found to mirror not only carbon, but also nitrogen and hydrogen stable isotope signatures of their ^{13}C-, ^{15}N- and ^{2}H-enriched fungi (Gebauer & Meyer, 2003; Trudell *et al.*, 2003; Hynson *et al.*, 2013; Gebauer *et al.*, 2016). Furthermore, nonphotosynthetic orchid species that associate with wood- or litter-decomposing fungi are significantly enriched in ^{13}C and ^{15}N compared with autotrophic surrounding plants (Ogura-Tsujita *et al.*, 2009; Lee *et al.*, 2015; Ogura-Tsujita *et al.*, 2018), and the same applies to Chl-deficient members of Ericaceae with ericaceous mycorrhizal connection to ectomycorrhizal fungi (Tedersoo *et al.*, 2007; Zimmer *et al.*, 2007).

The driver for the enrichment in heavy isotopes of mycoheterotrophic plants appears to be the simultaneous enrichment in their mycorrhizal fungi. Ectomycorrhizal fungi become enriched in ^{13}C, ^{15}N and ^{2}H, because they gain ^{13}C-enriched carbohydrates from their tree partners (Gleixner *et al.*, 1993), have access to soil organic matter enriched in ^{15}N due to their ability to release exoenzymes (Gebauer & Dietrich, 1993; Schiebold *et al.*, 2017), and are composed of secondary organic compounds that are enriched in ^{2}H in comparison to primary photosynthetic organic compounds produced by autotrophic plants (Yakir, 1992; Gebauer *et al.*, 2016; Cormier *et al.*, 2018, 2019). Wood- or litter-decomposing fungi are enriched in ^{13}C and ^{15}N, because they use ^{13}C-enriched cellulose as a carbon source (Gleixner *et al.*, 1993) and like other fungi they access recalcitrant soil organic matter to obtain nitrogen rich in ^{15}N (Gebauer & Taylor, 1999). As a logical consequence, although not yet investigated, AM fungi should also be enriched in ^{13}C, because they gain ^{13}C-enriched carbohydrates from their green plant partners. Finding rather low ^{13}C enrichment and no detectable ^{15}N enrichment in fully mycoheterotrophic AM plants may be due to the fact that the fungal partners (Glomeromycotina) lack the ability to synthesize lipids (Jiang *et al.*, 2017; Keymer *et al.*, 2017; Luginbuehl *et al.*, 2017; Rich *et al.*, 2017) and probably exoenzymes. Thus, AM fungi are considered to gain ^{13}C-depleted lipids (Gleixner *et al.*, 1993; Cormier *et al.*, 2019) in addition to ^{13}C-enriched carbohydrates, and to use mostly isotopically inconspicuous nitrate and

ammonium as nitrogen sources. This combination of factors is expected in the end to mirror the isotopic composition of AM mycoheterotrophic plants.

Apart from obviously achlorophyllous plant species, stable isotope signatures have also shed new light on green-leaved plant species previously thought to be simply photoautotrophic (Gebauer & Meyer, 2003). In recent years a steadily increasing number of such species have been identified as 'partial mycoheterotrophs', because their stable isotope composition values lie between nonmycoheterotrophic neighboring plants and full mycoheterotrophs (Hynson *et al.*, 2013, 2016; Gebauer *et al.*, 2016). This condition is frequent within Orchidaceae (Gebauer & Meyer, 2003; Hynson *et al.*, 2013, 2016; Gebauer *et al.*, 2016) and Ericaceae (Zimmer *et al.*, 2007; Hynson *et al.*, 2009, 2013, 2016) with their particular kinds of mycorrhiza, but has only been recorded for very few species with AM (Cameron & Bolin, 2010; Bolin *et al.*, 2017).

The fact that all AM mycoheterotrophs so far investigated develop the *Paris*-morphotype (Imhof *et al.*, 2013) led us to ask whether hyphal coils are required for a fungus-to-plant carbon transmission, and whether indeed plant species with *Paris*-type mycorrhiza might potentially obtain carbon from their fungal source, having green leaves or not. This could also explain why photosynthetic rates of *P. quadrifolia* and some other *Paris*-type AM plants appear to be low compared with *Arum*-type AM plants (Dalke *et al.*, 2018). To shed light on this question, we applied stable isotope abundance analysis to the two species that once provided the very definition for the AM morphotypes, namely *A. maculatum* and *P. quadrifolia* (Gallaud, 1905). Both species are fairly common in Eurasian forest habitats, and we selected two localities where they occur together (Fig. 1a–c). Their mycorrhizal morphotypes were confirmed by microscopy of roots (Fig. 1d,e). Green leaves were collected, simultaneously with reference samples of neighboring forest ground species: *Alliaria petiolata* (nonmycorrhizal), *Allium ursinum* (*Arum*-type AM), *A. nemorosa* (*Paris*-type AM), *Fraxinus excelsior* (*Arum*-type AM), *Galium odoratum* (various) and *Hedera helix* (*Arum*-type AM) (Supporting Information Table S1).

- We hypothesized that *P. quadrifolia* would show significant enrichment in stable isotopes, ^{13}C and ^{2}H, compared with *A. maculatum* and reference plants presumed to be fully photoautotrophic, while the latter would not be distinguishable.
- We hypothesized that any difference in ^{13}C and ^{2}H isotope abundances between *P. quadrifolia* and *A. maculatum* growing under identical microclimate conditions should not be explained by differences in stomatal regulation and transpiration. To test that, we also analyzed leaf tissue for oxygen isotope abundance.

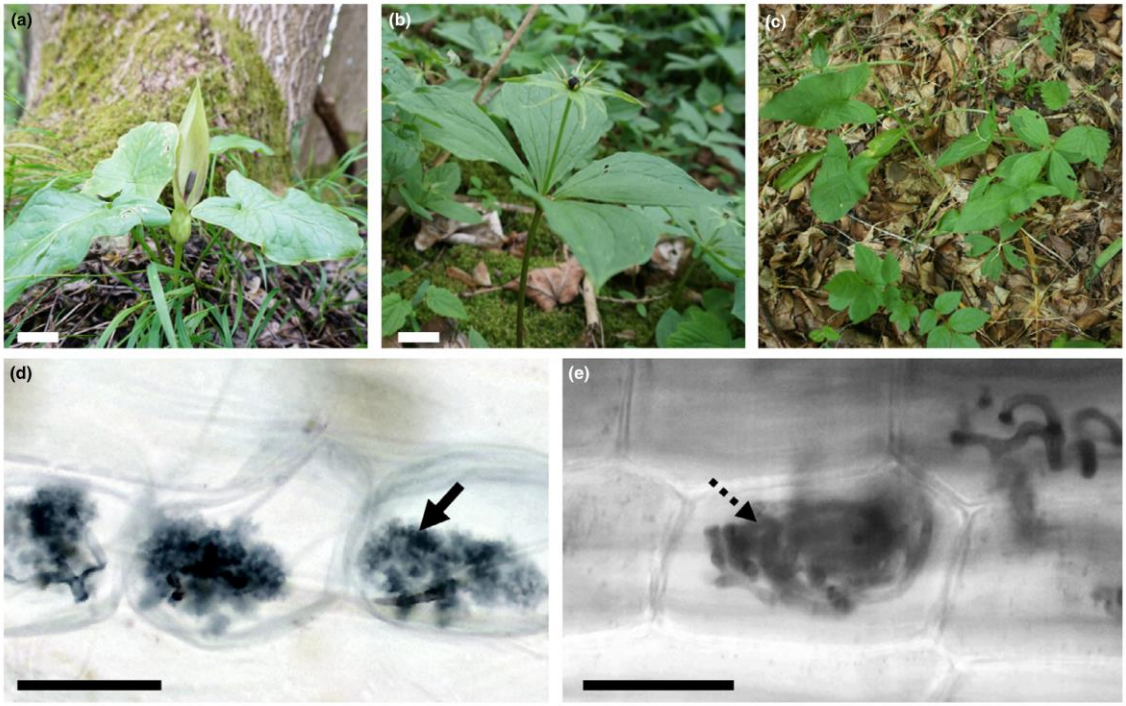

Fig. 1 *Arum*- and *Paris*-type arbuscular mycorrhiza. Habits of *Arum maculatum* (a), *Paris quadrifolia* (b) and both species growing in close proximity (c). (d) Ramified intracellular arbuscules in root cortical cells of *A. maculatum* (*Arum*-morphotype, solid arrow). (e) Dense intracellular hyphal coils in *P. quadrifolia* (*Paris*-morphotype, dashed arrow). The contrast in (d, e) is enhanced with Fiji ImageJ 1.51n. White bars, 2 cm; black bars, 50 μm.

New Phytologist

Letter Forum 3

Arum maculatum and *P. quadrifolia* (Fig. 1) were sampled in late May and early June 2017 at two sites, one in northern (49.6397°N, 11.2472°S, decimal WGS84) and one in southern Bavaria (47.6330°N, 11.1603°S), Germany. Both sites are carbonate-rich mixed temperate forests, the northern site receiving 850 mm annual precipitation, the southern site >1300 mm (Deutscher Wetterdienst, 2019). Sampling design for plant leaf material followed the approach of Gebauer & Meyer (2003), which included foliage leaf samples of *A. maculatum*, *P. quadrifolia* and three reference plant species within 1-m^2 plots each with five replicates. The reference plants cover a range of both herbaceous and woody, and deciduous and evergreen species forming AM with a range of AM-morphotypes or being nonmycorrhizal plants (Gallaud, 1905; Wang & Qiu, 2006; Dickson *et al.*, 2007; Fracchia *et al.*, 2009; Shah *et al.*, 2009; Brundrett & Tedersoo, 2019; Table S1). This set of reference plants reflects a natural variance in stable isotope abundance of chlorophyllous C_3 plants growing on shady forest floors and so far considered as completely photoautotrophic. Ten *A. maculatum* and 10 *P. quadrifolia* individuals were compared to 30 co-occurring reference plant individuals.

Plant leaf material was washed, species by species, with deionized water, oven-dried overnight, and ground to homogenous powder in a ball mill followed by storage in desiccators over silica gel until further processing (Table S2). Elemental analyzer isotope ratio mass spectrometry (EA-IRMS) was used to analyze natural relative abundances of carbon ($^{13}C:{}^{12}C$) and nitrogen ($^{15}N:{}^{14}N$) while a thermal conversion device (TC-IRMS) was used to analyze natural relative abundances of hydrogen ($^{2}H:{}^{1}H$) and oxygen isotopes ($^{18}O:{}^{16}O$) in leaves of every sampled species separately (Table S2). A memory bias was avoided by analyzing H isotope samples four times. All samples were plot-wise analyzed in identical batches to minimize an atmospheric bias by H atom exchange within the samples with water vapor in ambient air. The resulting relative isotope abundances follow the rules of the δ-notation: $\delta^{13}C$, $\delta^{15}N$, $\delta^{2}H$ or $\delta^{18}O = (R_{sample}/R_{standard} - 1) \times 1000$ (‰), whereby R is the ratio of the heavy to the respective light isotope. The site-specific δ-values were normalized to enrichment factors ε according to Preiss & Gebauer (2008) by plot-wise calculating the difference between δ values of the target plants *A. maculatum* and *P. quadrifolia* (δ_T) and the mean values of their respective neighboring reference plants (δ_{Ref}) as $\varepsilon = \delta_T - \delta_{Ref}$. The relative amount of carbon that *P. quadrifolia* received from a fungal source was quantified applying the two-source linear mixing model (Gebauer & Meyer, 2003; Hynson *et al.*, 2013). This model requires an end-member exclusively obtaining carbon through photosynthesis (our reference plants) and an end-member solely covering its carbon demand from an AM fungal source (fully mycoheterotrophic plants). For this we used the enrichment factors of the fully mycoheterotrophic AM plant species *Voyria aphylla* and *Dictyostega orobanchoides* (Merckx *et al.*, 2010). Statistical test procedures can be retraced from Table S3. All values are given as mean and SD.

Samples of target (*A. maculatum* and *P. quadrifolia*) and reference plant roots for microscopy were washed with deionized water and stored at 4°C in 70% ethanol. Staining was performed according to Phillips & Hayman (1970) and Vierheilig *et al.* (2005) (Table S4).

For the target plants our microscopic observations confirmed the presence of AM fungi based on aseptate hyphae, vesicles and, with respect to the *Arum*-morphotype, ramified arbuscules (Fig. 1d); likewise, in the *Paris*-morphotype dense hyphal coils were seen (Fig. 1e). For the reference plants, we found that their mycorrhizal status conformed with previous published records of the same species (Table S1). We found enrichment in ^{13}C (2.6 ± 0.7‰), ^{15}N (0.6 ± 0.6‰) and ^{2}H (8.8 ± 5.3‰) in *P. quadrifolia* compared with both *A. maculatum* and the group of cohabitant reference plants (Fig. 2). By definition, the sum of reference plants had a mean enrichment factor ε of zero and SD of ±1.1‰ for $\varepsilon^{13}C$, ±0.6‰ for ^{15}N and ±7.3‰ for $\varepsilon^{2}H$ (Fig. 2). Falling within the range of reference plants, *A. maculatum* individuals were inconspicuous in stable isotope enrichment, scattering in $\varepsilon^{13}C$ by 0.6 ± 0.2‰, in $\varepsilon^{15}N$ by -0.2 ± 0.9‰ and in $\varepsilon^{2}H$ by -0.7 ± 5.6‰.

Kruskal–Wallis tests found significant differences among the groups in $\varepsilon^{13}C$ ($H(2) = 24.608$, $P < 0.001$), in $\varepsilon^{15}N$ ($H(2) = 6.890$, $P = 0.03$) and in $\varepsilon^{2}H$ ($H(2) = 13.215$, $P = 0.001$). Pairwise comparisons of groups by Dunn's *post hoc* test are shown in Table 1. We detected no significant differences in ^{18}O enrichment ($H(2) = 0.402$, $P = 0.82$) or leaf total nitrogen concentrations ($H(2) = 4.608$, $P = 0.10$) between the three groups. It is notable that the only *Paris*-type species among the reference plants, *A. nemorosa*, with respect to its $\varepsilon^{13}C$ and $\varepsilon^{2}H$ pattern was closer to *P. quadrifolia* than to *A. maculatum* and all other reference plants (Fig. 2). Stable isotope patterns (δ-values) and leaf total nitrogen concentrations for each of the respective sites and all investigated plant species are given in Table S5.

In principle, relative enrichment in ^{13}C and ^{2}H can arise simultaneously by (1) different photosynthetic pathways (Sternberg *et al.*, 1984; Farquhar *et al.*, 1989); (2) differing isotopic composition in the CO_2 and H_2O sources for photosynthesis (Farquhar *et al.*, 1982, 1989); (3) different light and microclimate conditions (Dawson *et al.*, 2002); (4) different transpiration rates (Farquhar *et al.*, 1982, 1989; Cernusak *et al.*, 2004); and (5) C and H gains from sources alternative or complementary to photosynthesis (Press *et al.*, 1987; Gebauer & Meyer, 2003; Těšitel *et al.*, 2010; Hynson *et al.*, 2013; Gebauer *et al.*, 2016). However, all the plant species we investigated are known to follow the C_3 pathway of photosynthesis, and (2) and (3) are unlikely because our plant material was growing under identical light and microclimatic conditions and was collected during the same time. Because increased transpiration, as known for many hemiparasitic plants (Cernusak *et al.*, 2004), changes the oxygen isotope abundance towards depletion of ^{18}O, we tested explanation (4) by analyzing leaf tissue oxygen isotope abundances but, as stated above, found no differences. Thus, all plants investigated had similar transpiration regulation. Explanation (5) remains the most likely reason for the stable isotope pattern seen in *P. quadrifolia*.

Natural ^{13}C, ^{15}N, ^{2}H and ^{18}O isotope abundance patterns in *A. maculatum* and *P. quadrifolia* are here shown for the first time. For more than 100 years these two species have served as models for

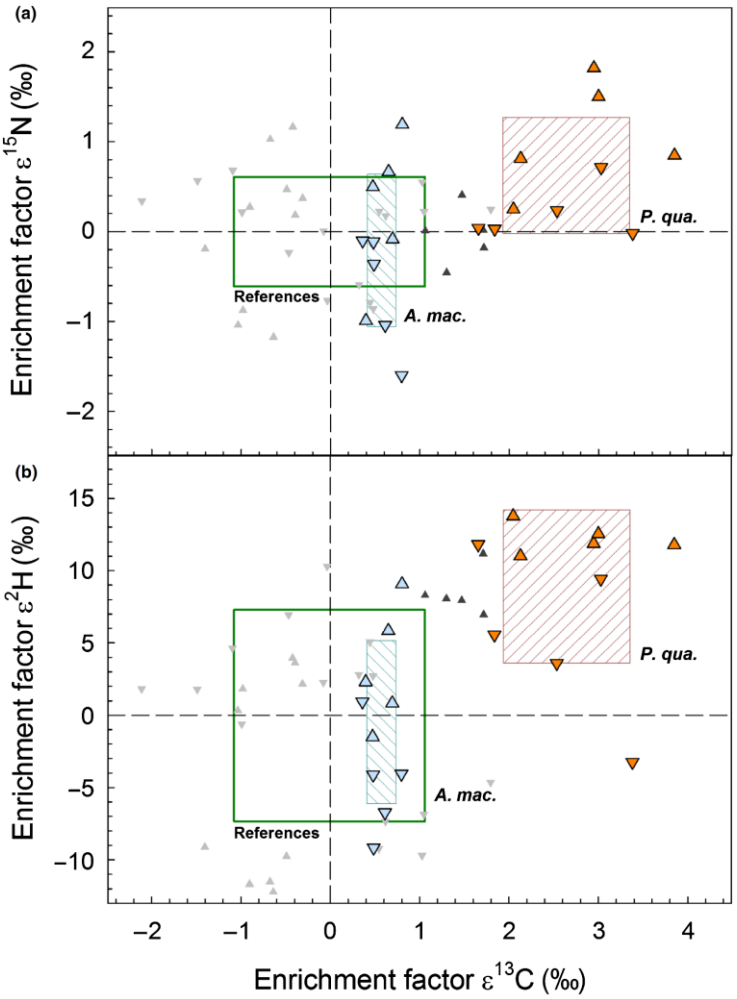

Fig. 2 Carbon and nitrogen (a) and carbon and hydrogen (b) stable isotope enrichment factors ε for *Arum maculatum* (blue triangles), *Paris quadrifolia* (red triangles). The shaded boxes indicate SD for all investigated *A. maculatum* ($n = 10$) and *P. quadrifolia* ($n = 10$). By definition, mean ε-values of the reference plants are zero, and SD is shown by green frames ($n = 30$). Upwards-triangles represent the North Bavarian site; downwards-triangles, the South Bavarian site. Dark gray symbols illustrate the reference plants forming *Paris*-type (*Anemone nemorosa*) and light gray symbols all other types (*Alliaria petiolata*, *Allium ursinum*, *Fraxinus excelsior*, *Galium odoratum*, *Hedera helix*).

Table 1 Test for differences between *Paris quadrifolia* (*P. qua.*, $n = 10$), *Arum maculatum* (*A. mac.*, $n = 10$) and neighboring plant species as references ($n = 30$) in enrichment factors ε of ^{13}C, ^{15}N and ^{2}H.

	$\varepsilon^{13}C$		$\varepsilon^{15}N$		$\varepsilon^{2}H$	
	Test statistics	*P*	Test statistics	*P*	Test statistics	*P*
P. qua. vs *A. mac.*	$Z = 2.960$	**0.003**	$Z = 2.439$	**0.022**	$Z = 3.099$	**0.002**
P. qua. vs references	$Z = 4.960$	**<0.001**	$Z = 2.261$	**0.024**	$Z = 3.400$	**0.001**
A. mac. vs references	$Z = 1.334$	0.091	$Z = 1.136$	0.233	$Z = 0.395$	0.347

Pairwise Dunn's *post hoc* tests (*Z*). Significant results are highlighted in bold.
Alliaria petiolata (nonmycorrhizal), *Allium ursinum* (*Arum*-type arbuscular mycorrhiza (AM)), *Anemone nemorosa* (*Paris*-type AM), *Fraxinus excelsior* saplings (*Arum*-type AM), *Galium odoratum* (various) and *Hedera helix* (*Arum*-type AM) served as reference plants.

New Phytologist

Letter Forum 5

the two morphotypes of AM without recognition of any functional differences between them. We found that *P. quadrifolia* was significantly enriched in heavy isotopes while *A. maculatum* resembled the reference plants. This finding is consistent with our first hypothesis and places *P. quadrifolia* as a partial mycoheterotroph because it clearly obtains carbon through mycobionts as well as by photosynthesis. By contrast, *A. maculatum* appears fully photoautotrophic and is probably engaged in a mutualistic AM relationship where it gives off carbon compounds to the mycobionts.

With respect to relative ^{13}C enrichment, *P. quadrifolia* resembles selected members of Gentianaceae (Cameron & Bolin, 2010) and Burmanniaceae (Bolin *et al.*, 2017) that are considered partial mycoheterotrophs. Their arbuscular morphotype is not known, however. Stable isotope patterns in *P. quadrifolia* also correspond to those found in several members of Orchidaceae (Gebauer & Meyer, 2003; Hynson *et al.*, 2016) and Ericaceae (Zimmer *et al.*, 2007; Hynson *et al.*, 2009, 2016) with other types of mycorrhizal association and are acknowledged as partial mycoheterotrophs.

It appears that *P. quadrifolia* obtains considerable amounts of carbon from its associated Glomeromycotina mycobionts. By applying the two-source linear mixing model using neighboring plants as fully autotrophic references receiving their C completely from photosynthesis as the lower end-members, and fully mycoheterotrophic AM plant species *V. aphylla* and *D. orobanchoides* (Merckx *et al.*, 2010) as the upper end-members, we estimate that *P. quadrifolia* received about half ($48 \pm 13\%$) of its carbon nutrients from a fungal source. This agrees with members of Gentianaceae (Cameron & Bolin, 2010) and Burmanniaceae (Bolin *et al.*, 2017) also forming AM ($44 \pm 27\%$), and is within the range found in partial mycoheterotrophic orchids and Ericaceae (Hynson *et al.*, 2013).

It was hypothesized by Imhof (1999) that intracellular hyphal growth is a prerequisite for the evolution of mycoheterotrophy (see *pelotons* in orchids, *hyphal pegs* in Ericaceae or *Paris*-type hyphal coils in achlorophyllous AM plants, Imhof *et al.*, 2013). It is known that different infection patterns may develop in different plant species by the same strain of Glomeromycotina, including the absence or presence of hyphal coils (Burleigh *et al.*, 2002). Thus, if a plant can trigger the fungus to develop intracellular coils, it may change carbon-loss into gain of fungal carbon. A selective advantage is suggested for plant control over morphotype establishment (Dickson, 2004; Dickson *et al.*, 2007). However, the process of carbon transfer from fungi to plants is yet not completely clear (Dickson *et al.*, 2007; Wipf *et al.*, 2019).

Interestingly, the ^{15}N enrichment of *P. quadrifolia*, partially mycoheterotrophic Gentianaceae (Cameron & Bolin, 2010) and Burmanniaceae (Bolin *et al.*, 2017) as well as fully mycoheterotrophic plants on AM fungi (Merckx *et al.*, 2010; Courty *et al.*, 2011; Hynson *et al.*, 2013) appears to be considerably lower than for mycoheterotrophic plants associated with fungi simultaneously forming ectomycorrhizas with neighboring forest trees (Hynson *et al.*, 2016). This suggests different nitrogen sources for mycoheterotrophs depending on whether the fungal connection is arbuscular or ectomycorrhizal. The majority of ectomycorrhizal fungi are known to access recalcitrant ^{15}N-enriched soil organic compounds through the release of exoenzymes. In this way, the hyphae become ^{15}N-enriched (Gebauer & Dietrich, 1993; Gebauer & Taylor, 1999; Mayor *et al.*, 2009) and may transfer this ^{15}N enrichment to tissues of their mycoheterotrophic plant partners. Weak or undetectable ^{15}N enrichment as in mycoheterotrophs on AM (Cameron & Bolin, 2010; Merckx *et al.*, 2010; Bolin *et al.*, 2017) – now including *P. quadrifolia* – suggests that their main nitrogen sources are ammonium and nitrate, which are less ^{15}N-enriched than organic nitrogen components in soils.

An extensive literature search showed that the significant ^{13}C and ^{15}N enrichment, which we found in *P. quadrifolia*, but not in *A. maculatum*, is confirmed by data deeply buried in two previous publications (Liebel *et al.*, 2010; Hynson *et al.*, 2015). In these cases, *P. quadrifolia* from Sweden and *Arum pictum* from Italy (closely related to *A. maculatum*) served as neighboring reference plants for orchid and Ericaceae mycoheterotrophs.

Our identification of *Paris*-morphotype AM as a partially mycoheterotrophic mode of nutrition may have far-reaching implications. Summarized data from 1895 to 2006 concerning 941 plant species from 147 families listed 59% as *Arum*-type only and 41% as *Paris*-type only (intermediate types excluded) (Dickson *et al.*, 2007). As the *Paris*-type was frequently ignored or once even classified as nonmycorrhizal, it is suggested that both morphotypes are almost equally frequent on a species level (Smith & Smith, 1997; Dickson *et al.*, 2007). This means that about half of the 200 000 AM plant species that presently are considered fully photoautotrophic could potentially gain carbon from fungi, perhaps under conditions limiting their own autotrophic carbon gain. In each of these cases, suitable sampling designs for analysis of stable isotope natural abundances may shed light on the extent to which they rely on the fungi as a carbon source. The *Paris*-type reference plant species *A. nemorosa* of the present study is a very first starting point and confirms similar enrichment in ^{13}C and ^{2}H as *P. quadrifolia*. Thus, *A. nemorosa* is apparently also partially mycoheterotrophic. Colonization patterns intermediate between the *Arum* and *Paris* morphotypes (Dickson, 2004), as well as plant species classified as nonmycorrhizal because of 'unusual *Paris*-type morphology' (Dickson *et al.*, 2007), should also be scrutinized for mycoheterotrophism. Partial mycoheterotrophy on AM fungi could be widely distributed within the plant kingdom, far beyond the currently known few members of Gentianaceae (Cameron & Bolin, 2010) and Burmanniaceae (Bolin *et al.*, 2017).

A further speculation on this finding concerns the plant species with *Arum*-type AM. Fungi belonging to Glomeromycotina are considered obligate symbionts with little capacity for saprotrophy (Lanfranco *et al.*, 2017; but see Hempel *et al.*, 2007). If so, the fungal carbon received by *P. quadrifolia* must have been acquired by the fungus via an *Arum*-type colonization within a living donor plant. A transfer of photosynthates from one green plant to another, from *Arum*- to *Paris*-type, potentially at a larger scale, would be an important mechanism for coherence in plant communities, the implications of which we have overlooked until now. By analogy to findings for partially mycoheterotrophic orchids (Preiss *et al.*, 2010), we suggest that partially mycoheterotrophic AM plants have two carbon sources, that is, from their own photosynthesis and from other plants via associated fungi. The latter source would be particularly relevant under low-light conditions. This is consistent

with the typical distribution of *Paris*-type AM (Dickson *et al.* 2007) in herbaceous plants of the forest floor and in long-lived woody plants with shaded early life stages.

Acknowledgements

We thank Christine Tiroch, Carina Bauer, Petra Eckert and Isolde Baumann (BayCEER Laboratory of Isotope Biogeochemisty) for skilful technical assistance. PG and this project was funded by the Elite Network of Bavaria. We gratefully acknowledge the Regierung von Oberbayern for authorization for plant sampling in the nature-protected South Bavarian site.

Author contributions

PG contributed to the research design, conducted major parts of the field survey, analyzed and treated the results and wrote the first manuscript draft. HNR essentially initiated the idea for this research on the basis of an unpublished literature review. HTL helped to identify sampling locations and performed some of the sample collection. GG coordinated the project, supervised the isotope abundance analyses and supported data treatment. All coauthors contributed to the manuscript.

ORCID

Gerhard Gebauer https://orcid.org/0000-0003-1577-7501
Hanne N. Rasmussen https://orcid.org/0000-0002-0181-9304

Philipp Giesemann[1], Hanne N. Rasmussen[2], Heiko T. Liebel[1,3] and Gerhard Gebauer[1]*

[1]Laboratory of Isotope Biogeochemistry, Bayreuth Center of Ecology and Environmental Research (BayCEER), University of Bayreuth, 95440 Bayreuth, Germany; [2]Department of Geosciences and Nature Resource Management, Section of Forest, Nature and Biomass, University of Copenhagen, Rolighedsvej 23, 1958 Frederiksberg C, Copenhagen, Denmark; [3]Biological Station Murnauer Moos, 82418 Murnau, Germany (*Author for correspondence: tel +49 (0)921 55 2060, email gerhard.gebauer@uni-bayreuth.de)

References

Bolin JF, Tennakoon KU, Majid MBA, Cameron DD. 2017. Isotopic evidence of partial mycoheterotrophy in *Burmannia coelestis* (Burmanniaceae). *Plant Species Biology* **32**: 74–80.

Brundrett M, Tedersoo L. 2019. Misdiagnosis of mycorrhizas and inappropriate recycling of data can lead to false conclusions. *New Phytologist* **221**: 18–24.

Burleigh SH, Cavagnaro T, Jakobsen I. 2002. Functional diversity of arbuscular mycorrhizas extends to the expression of plant genes involved in P nutrition. *Journal of Experimental Botany* **53**: 1593–1601.

Cameron DD, Bolin JF. 2010. Isotopic evidence of partial mycoheterotrophy in the Gentianaceae *Bartonia virginica* and *Obolaria virginica* as case studies. *American Journal of Botany* **97**: 1272–1277.

Cernusak LA, Pate JS, Farquhar GD. 2004. Oxygen and carbon isotope composition of parasitic plants and their hosts in southwestern Australia. *Oecologia* **139**: 199–213.

Cormier M-A, Werner RA, Leuenberger MC, Kahmen A. 2019. ^{2}H-enrichment of cellulose and n-alkanes in heterotrophic plants. *Oecologia* **189**: 365–373.

Cormier M-A, Werner RA, Sauer PE, Gröcke DR, Leuenberger MC, Wieloch T, Schleucher J, Kahmen A. 2018. ^{2}H-fractionations during the biosynthesis of carbohydrates and lipids imprint a metabolic signal on the δ^{2}H values of plant organic compounds. *New Phytologist* **218**: 479–491.

Courty P-E, Walder F, Boller T, Ineichen K, Wiemken A, Rousteau A, Selosse M-A. 2011. Carbon and nitrogen metabolism in mycorrhizal networks and mycoheterotrophic plants of tropical forests: a stable isotope analysis. *Plant Physiology* **156**: 952–961.

Dalke IV, Novakovskiy AB, Maslova SP, Dubrovskiy YA. 2018. Morphological and functional traits of herbaceous plants with different functional types in the European Northeast. *Plant Ecology* **219**: 1295–1305.

Dawson TE, Mambelli S, Plamboeck AH, Templer PH, Tu KP. 2002. Stable isotopes in plant ecology. *Annual Review of Ecology and Systematics* **33**: 507–559.

Deutscher Wetterdienst (DWD). 2019. *Climate Data Center.* [WWW document] URL https://cdc.dwd.de/portal/ [accessed 15 May 2019].

Dickson S. 2004. The *Arum–Paris* continuum of mycorrhizal symbioses. *New Phytologist* **163**: 187–200.

Dickson S, Smith FA, Smith SE. 2007. Structural differences in arbuscular mycorrhizal symbioses: more than 100 years after Gallaud, where next? *Mycorrhiza* **17**: 375–393.

Farquhar GD, Ehleringer JR, Hubick KT. 1989. Carbon isotope discrimination and photosynthesis. *Annual Review of Plant Biology* **40**: 503–537.

Farquhar GD, O'Leary MH, Berry JA. 1982. On the relationship between carbon isotope discrimination and the intercellular carbon dioxide concentration in leaves. *Functional Plant Biology* **9**: 121.

Fracchia S, Aranda A, Gopar A, Silvani V, Fernandez L, Godeas A. 2009. Mycorrhizal status of plant species in the Chaco Serrano Woodland from central Argentina. *Mycorrhiza* **19**: 205–214.

Gallaud I. 1905. Études sur les mycorrhizes endotrophes. *Revue générale de botanique* **17**: 5–48; 66–83, 123–135; 223–239; 313–325; 425–433; 479–500.

Gebauer G, Dietrich P. 1993. Nitrogen isotope ratios in different compartments of a mixed stand of spruce, larch and beech trees and of understory vegetation including fungi. *Isotopes in Environmental and Health Studies* **29**: 35–44.

Gebauer G, Meyer M. 2003. ^{15}N and ^{13}C natural abundance of autotrophic and myco-heterotrophic orchids provides insight into nitrogen and carbon gain from fungal association. *New Phytologist* **160**: 209–223.

Gebauer G, Preiss K, Gebauer AC. 2016. Partial mycoheterotrophy is more widespread among orchids than previously assumed. *New Phytologist* **211**: 11–15.

Gebauer G, Taylor AFS. 1999. ^{15}N natural abundance in fruit bodies of different functional groups of fungi in relation to substrate utilisation. *New Phytologist* **142**: 93–101.

Gleixner G, Danier HJ, Werner RA, Schmidt HL. 1993. Correlations between the ^{13}C content of primary and secondary plant products in different cell compartments and that in decomposing basidiomycetes. *Plant Physiology* **102**: 1287–1290.

Hempel S, Renker C, Buscot F. 2007. Differences in the species composition of arbuscular mycorrhizal fungi in spore, root and soil communities in a grassland ecosystem. *Environmental Microbiology* **9**: 1930–1938.

Hynson NA, Bidartondo MI, Read DJ. 2015. Are there geographic mosaics of mycorrhizal specificity and partial mycoheterotrophy? A case study in *Moneses uniflora* (Ericaceae). *New Phytologist* **208**: 1003–1007.

Hynson NA, Madsen TP, Selosse M-A, Adam IKU, Ogura-Tsujita Y, Roy M, Gebauer G. 2013. The physiological ecology of mycoheterotrophy. In: Merckx VSFT, ed. *Mycoheterotrophy. The biology of plants living on fungi.* New York, NY, USA: Springer, 297–342.

Hynson NA, Preiss K, Gebauer G, Bruns TD. 2009. Isotopic evidence of full and partial myco-heterotrophy in the plant tribe Pyroleae (Ericaceae). *New Phytologist* **182**: 719–726.

Hynson NA, Schiebold JM-I, Gebauer G. 2016. Plant family identity distinguishes patterns of carbon and nitrogen stable isotope abundance and nitrogen concentration in mycoheterotrophic plants associated with ectomycorrhizal fungi. *Annals of Botany* **118**: 467–479.

Imhof S. 1999. Root morphology, anatomy and mycotrophy of the achlorophyllous *Voyria aphylla* (Jacq.) Pers. (Gentianaceae). *Mycorrhiza* **9**: 33–39.

Imhof S, Massicotte HB, Melville LH, Peterson RL. 2013. Subterranean morphology and mycorrhizal structures. In: Merckx VSFT, ed. *Mycoheterotrophy. The biology of plants living on fungi*. New York, NY, USA: Springer, 157–214.

Jiang Y, Wang W, Xie Q, Liu N, Liu L, Wang D, Zhang X, Yang C, Chen X, Tang D *et al.* 2017. Plants transfer lipids to sustain colonization by mutualistic mycorrhizal and parasitic fungi. *Science* **356**: 1172–1175.

Keymer A, Pimprikar P, Wewer V, Huber C, Brands M, Bucerius SL, Delaux P-M, Klingl V, Röpenack-Lahaye Ev, Wang TL *et al.* 2017. Lipid transfer from plants to arbuscular mycorrhiza fungi. *eLife* **6**: e29107.

Lanfranco L, Bonfante P, Genre A. 2017. The mutualistic interaction between plants and arbuscular mycorrhizal fungi. In: Heitman J, Howlett BJ, Crous PW, Stukenbrock EH, James TY, Gow NAR, eds. *The Fungal Kingdom*. Washington, DC, USA: ASM Press, 727–748.

Leake JR. 1994. The biology of myco-heterotrophic ('saprophytic') plants. *New Phytologist* **127**: 171–216.

Lee Y-I, Yang C-K, Gebauer G. 2015. The importance of associations with saprotrophic non-Rhizoctonia fungi among fully mycoheterotrophic orchids is currently under-estimated: novel evidence from sub-tropical Asia. *Annals of Botany* **116**: 423–435.

Liebel HT, Bidartondo MI, Preiss K, Segreto R, Stöckel M, Rodda M, Gebauer G. 2010. C and N stable isotope signatures reveal constraints to nutritional modes in orchids from the Mediterranean and Macaronesia. *American Journal of Botany* **97**: 903–912.

Luginbuehl LH, Menard GN, Kurup S, van Erp H, Radhakrishnan GV, Breakspear A, Oldroyd GED, Eastmond PJ. 2017. Fatty acids in arbuscular mycorrhizal fungi are synthesized by the host plant. *Science* **356**: 1175–1178.

Mayor JR, Schuur EAG, Henkel TW. 2009. Elucidating the nutritional dynamics of fungi using stable isotopes. *Ecology Letters* **12**: 171–183.

Merckx V, Stöckel M, Fleischmann A, Bruns TD, Gebauer G. 2010. ^{15}N and ^{13}C natural abundance of two mycoheterotrophic and a putative partially mycoheterotrophic species associated with arbuscular mycorrhizal fungi. *New Phytologist* **188**: 590–596.

Merckx VSFT, Freudenstein JV, Kissling J, Christenhusz MJM, Stotler RE, Crandall-Stotler B, Wickett N, Rudall PJ, Maas-van de Kamer H, Maas PJM. 2013. Taxonomy and classification. In: Merckx VSFT, ed. *Mycoheterotrophy. The biology of plants living on fungi*. New York, NY, USA: Springer, 19–102.

Ogura-Tsujita Y, Gebauer G, Hashimoto T, Umata H, Yukawa T. 2009. Evidence for novel and specialized mycorrhizal parasitism: the orchid *Gastrodia confusa* gains carbon from saprotrophic *Mycena*. *Proceedings of the Royal Society B: Biological Sciences* **276**: 761–767.

Ogura-Tsujita Y, Gebauer G, Xu H, Fukasawa Y, Umata H, Tetsuka K, Kubota M, Schweiger JM-I, Yamashita S, Maekawa N *et al.* 2018. The giant mycoheterotrophic orchid *Erythrorchis altissima* is associated mainly with a divergent set of wood-decaying fungi. *Molecular Ecology* **27**: 1324–1337.

Phillips JM, Hayman DS. 1970. Improved procedures for clearing roots and staining parasitic and vesicular-arbuscular mycorrhizal fungi for rapid assessment of infection. *Transactions of the British Mycological Society* **55**: 158–161, IN16–IN18.

Preiss K, Adam IKU, Gebauer G. 2010. Irradiance governs exploitation of fungi: fine-tuning of carbon gain by two partially myco-heterotrophic orchids. *Proceedings of the Royal Society B: Biological Sciences* **277**: 1333–1336.

Preiss K, Gebauer G. 2008. A methodological approach to improve estimates of nutrient gains by partially myco-heterotrophic plants. *Isotopes in Environmental and Health Studies* **44**: 393–401.

Press MC, Shah N, Tuohy JM, Stewart GR. 1987. Carbon isotope ratios demonstrate carbon flux from C_4 host to C_3 parasite. *Plant Physiology* **85**: 1143–1145.

Rich MK, Nouri E, Courty P-E, Reinhardt D. 2017. Diet of arbuscular mycorrhizal fungi: bread and butter? *Trends in Plant Science* **22**: 652–660.

Schiebold JM-I, Bidartondo MI, Karasch P, Gravendeel B, Gebauer G. 2017. You are what you get from your fungi: nitrogen stable isotope patterns in *Epipactis* species. *Annals of Botany* **119**: 1085–1095.

Shah MA, Reshi ZA, Khasa D. 2009. Arbuscular mycorrhizal status of some Kashmir Himalayan alien invasive plants. *Mycorrhiza* **20**: 67–72.

Smith FA, Smith SE. 1997. Tansley Review No. 96. Structural diversity in (vesicular)–arbuscular mycorrhizal symbioses. *New Phytologist* **137**: 373–388.

Sternberg LO, DeNiro MJ, Ting IP. 1984. Carbon, hydrogen, and oxygen isotope ratios of cellulose from plants having intermediary photosynthetic modes. *Plant Physiology* **74**: 104–107.

Tedersoo L, Pellet P, Kõljalg U, Selosse M-A. 2007. Parallel evolutionary paths to mycoheterotrophy in understorey Ericaceae and Orchidaceae. Ecological evidence for mixotrophy in Pyroleae. *Oecologia* **151**: 206–217.

Těšitel J, Plavcová L, Cameron DD. 2010. Interactions between hemiparasitic plants and their hosts: the importance of organic carbon transfer. *Plant Signaling and Behavior* **5**: 1072–1076.

Trudell SA, Rygiewicz PT, Edmonds RL. 2003. Nitrogen and carbon stable isotope abundances support the myco-heterotrophic nature and host-specificity of certain achlorophyllous plants. *New Phytologist* **160**: 391–401.

Vierheilig H, Schweiger P, Brundrett M. 2005. An overview of methods for the detection and observation of arbuscular mycorrhizal fungi in roots. *Physiologia Plantarum* **125**: 393–404.

Wang B, Qiu Y-L. 2006. Phylogenetic distribution and evolution of mycorrhizas in land plants. *Mycorrhiza* **16**: 299–363.

Wipf D, Krajinski F, van Tuinen D, Recorbet G, Courty P-E. 2019. Trading on the arbuscular mycorrhiza market: from arbuscules to common mycorrhizal networks. *New Phytologist* **223**: 1127–1142.

Yakir D. 1992. Variations in the natural abundance of oxygen-18 and deuterium in plant carbohydrates. *Plant, Cell & Environment* **15**: 1005–1020.

Zimmer K, Hynson NA, Gebauer G, Allen EB, Allen MF, Read DJ. 2007. Wide geographical and ecological distribution of nitrogen and carbon gains from fungi in pyroloids and monotropoids (Ericaceae) and in orchids. *New Phytologist* **175**: 166–175.

Supporting Information

Additional Supporting Information may be found online in the Supporting Information section at the end of the article.

Table S1 The mycorrhizal type and arbuscular mycorrhizal subtype of target plant species *A. maculatum*, *P. quadrifolia* and their respective reference plants separated by sampling location.

Table S2 Equipment and substances related to stable isotope measurements and their reproducibility.

Table S3 Statistical test procedure on stable isotope enrichment factors ε.

Table S4 Root staining procedure and microphoto-documentation of hyphal structures.

Table S5 Stable isotope natural abundances in δ-values (‰) and leaf total nitrogen concentrations (mmol $g^{-1}_{\text{dry weight}}$) of the target plant species *A. maculatum*, *P. quadrifolia* and their respective reference plants.

Please note: Wiley Blackwell are not responsible for the content or functionality of any Supporting Information supplied by the authors. Any queries (other than missing material) should be directed to the *New Phytologist* Central Office.

Key words: arbuscular mycorrhiza (AM), *Arum maculatum*, *Arum*-type, myco-heterotrophy, *Paris quadrifolia*, *Paris*-type, stable isotope natural abundance.

Received, 29 October 2019; accepted, 8 December 2019.

New Phytologist Supporting Information

Discreet heterotrophs: Green plants that receive fungal carbon trhough *Paris*-type arbuscular mycorrhiza

Philipp Giesemann, Hanne N. Rasmussen, Heiko T. Liebel, Gerhard Gebauer

The following Supporting Information is available for this article:

Table S1 The mycorrhizal type and arbuscular mycorrhizal subtype of target plant species *A. maculatum*, *P. quadrifolia* and their respective reference plants separated by sampling location.

Table S2 Equipment and substances related to stable isotope measurements and their reproducibility.

Table S3 Statistical test procedure on stable isotope enrichment factors ε.

Table S4 Root staining procedure and microphoto-documentation of hyphal structures.

Table S5 Stable isotope natural abundances in δ-values [‰] and leaf total nitrogen concentrations [mmol g^{-1} dry weight] of the target plant species *A. maculatum*, *P. quadrifolia* and their respective reference plants.

Respective references

Table S1 The mycorrhizal type and arbuscular mycorrhizal subtype of target plant species *Arum maculatum* and Paris quadrifolia and their respective reference plants separated by sampling location both carbonate-rich forest sites but in North (49.6397 N, 11.2472 E, decimal WGS84) with 850 mm annual precipitation and the other in South Bavaria (47.6330 N, 11.1603 E) with 1300 mm annual precipitation (Deutscher Wetterdienst, 2019). Mycorrhizal types and AM-subtypes were classified based on literature as indicated and confirmed by own microscopic observations.

Site	Species	N	Mycorrhizal type	AM-subtype based on Genus* or species#
North Bavaria	***Arum maculatum* L.**	**5**	**AM[1]**	***Arum*-type[2,3,#]**
	***Paris quadrifolia* L.**	**5**	**AM[1]**	***Paris*-type[2,3,#]**
	Alliaria petiolata (M. Bieb.) Cavara & Grande	5	NM[1]	-
	Hedera helix L.	5	AM[1]	*Arum*-type[3,#]
	Anemone nemorosa L.	5	AM[1]	*Paris*-type[3,#]
South Bavaria	***Arum maculatum* L.**	**5**	**AM[1]**	***Arum*-type[2,3,#]**
	***Paris quadrifolia* L.**	**5**	**AM[1]**	***Paris*-type[2,3,#]**
	Allium ursinum L.	5	AM[1]	*Arum*-type[3,*]
	Fraxinus excelsior L.	5	AM[1]	*Arum*-type[3,#]
	Galium odoratum (L.) Scop.	5	various[1,3-6,*]	

AM: arbuscular mycorrhizal, NM: non-mycorrhizal, 1: Brundrett & Tedersoo (2019), 2: Gallaud (1905), 3: Dickson *et al.* (2007), 4: Wang & Qui (2006), 5: Fraccia *et al.* (2009); 6: Shah *et al.* (2009). Deutscher Wetterdienst (DWD). 2019**.** Climate Data Center. https://cdc.dwd.de/portal/ (15 May 2019).

Table S2 Equipment and substances in order to apply the stable isotope measurements and their reproducibility.

Drying temperature	105 °C
Ball mill	Retsch Schwingmühle MM2, Haan, Germany
Elemental analyzer (EA) coupled to an Isotope ratio mass spectrometer (IRMS)	
EA	1108; Carlo Erba Instruments, Milano, Italy
IRMS	delta S, Finnigan MAT, Bremen, Germany
ConFlo III interface	Thermo Fisher Scientific, Bremen, Germany
Thermal conversion (TC) coupled to an Isotope ratio mass spectrometer (IRMS)	
Thermal Conversion device (pyrolysis oven)	HTO, HEKAtech, Wegberg, Germany
IRMS	delta V advantage, Thermo Fisher Scientific, Bremen, Germany
ConFlo IV interface	Thermo Fisher Scientific, Bremen, Germany
Standard gases (Riessner, Lichtenfels, Germany) calibrated acc. to international standards	
CO_2 vs. V-PDB	ANU sucrose and NBS19 for the C isotopes
N_2 vs. N_2 in air	N1 and N2 for the N isotopes
H_2 vs. V-SMOW	CH7, V-SMOW and SLAP for H isotopes
CO vs. V-SMOW	IAEA601 and IAEA602 for the O isotopes
Provider: International Atomic Energy Agency Vienna, Austria	
Acetanilide (MERCK KGaA, Darmstadt, Germany) was used to calibrate the C/N concentrations.	
Reproducibility of isotope measurements	
$\delta^{13}C$	< 0.2 ‰
$\delta^{15}N$	< 0.2 ‰
$\delta^{2}H$	< 4.0 ‰
$\delta^{18}O$	< 0.6 ‰

Table S3 Statistical test procedure on stable isotope enrichment factors ε.

Step 1	Normal distribution	➔	Shapiro-Wilk test
	Homogeneity of variance	➔	Levene test
Most data were not normal distributed, thus non-parametric tests were applied.			
Step 2	*Arum maculatum* (n = 10) vs. *Paris quadrifolia* (n = 10) vs. Reference plants (n = 30)	➔	One-tailed Kruskal Wallis (H)
Step 3	Significant differences between the groups?	➔	Dunn's *post hoc* tests (Z)
The P-values were adjusted with Holm-Bonferroni correction.			
The significance level of $\alpha = 0.05$ was set.			

Applied Software for statistics and graphs: RStudio 1.1 (R Core Development Team, Vienna, Austria) and SigmaPlot 11.0 (Systat Software, San Jose, CA, USA)

Table S4 Root staining procedure and microphoto-documentation of hyphal structures.

	Wash out ethanol in VE-water	
Clearing:	10 % (w/v) KOH	30 min, 70 °C
Acidification:	1 % (v/v) HCl	1-3 min, RT
Stain:	1 % (w/v) trypan blue stain consisted of stain powder, 33 % (v/v) lactic acid and 33% (v/v) glycerol	overnight, RT
Microphoto-documentation	BA210LED trino, Motic, Wetzlar, Germany 3MP Moticam 3+	4x, 10x, 40x and 100x magnification

RT: room temperature

Table S5 Stable isotope natural abundances in δ-values [‰] and leaf total nitrogen concentrations [mmol g^{-1} $_{dry\ weight}$] of the target plant species *Arum maculatum* and *Paris quadrifolia* and their respective reference plants separated by sampling location (North and South Bavaria).

Site	Species (N)	δ^{13}**C**	δ^{15}**N**	δ^{2}**H**	δ^{18}**O**	**Total N**
North Bavaria	***Arum maculatum* (5)**	**-29.8** ±0.3	**-2.6** ±0.5	**-118.8** ±3.2	**24.3** ±0.4	**2.8** ±0.3
	***Paris quadrifolia* (5)**	**-27.6** ±0.8	**-1.9** ±0.3	**-100.9** ±2.3	**24.6** ±0.5	**2.3** ±0.1
	Alliaria petiolata (5)	-31.2 ±0.3	-0.1 ±0.8	-133.0 ±2.3	24.0 ±0.6	3.7 ±0.4
	Hedera helix (5)	-31.0 ±0.4	-2.9 ±0.9	-119.8 ±1.6	26.0 ±0.7	1.5 ±0.3
	Anemone nemorosa (5)	-28.9 ±0.4	-2.9 ±0.7	-113.7 ±2.5	24.0 ±0.6	2.0 ±0.2
South Bavaria	***Arum maculatum* (5)**	**-30.7** ±0.3	**-4.2** ±0.7	**-110.6** ±3.0	**23.5** ±0.3	**2.3** ±0.4
	***Paris quadrifolia* (5)**	**-28.7** ±0.6	**-3.4** ±0.5	**-100.5** ±3.3	**23.4** ±0.3	**2.0** ±0.2
	Allium ursinum (5)	-30.2 ±0.3	-3.3 ±0.4	-113.5 ±1.9	22.8 ±0.5	2.2 ±0.1
	Fraxinus excelsior (5)	-31.0 ±0.4	-4.2 ±0.6	-101.3 ±6.2	24.7 ±0.5	2.2 ±0.3
	Galium odoratum (5)	-32.5 ±0.8	-3.3 ±0.4	-103.0 ±0.3	23.1±0.5	1.9 ±0.1

Respective reference

Brundrett, M, Tedersoo, L. 2019. Misdiagnosis of mycorrhizas and inappropriate recycling of data can lead to false conclusions. *New Phytologist* **221**: 18–24.

Deutscher Wetterdienst (DWD). 2019. Climate Data Center. https://cdc.dwd.de/portal/ (15 May 2019).

Dickson, S, Smith, FA, Smith, SE. 2007. Structural differences in arbuscular mycorrhizal symbioses: more than 100 years after Gallaud, where next? *Mycorrhiza* **17**: 375–393.

Fracchia, S, Aranda, A, Gopar, A, Silvani, V, Fernandez, L, Godeas, A. 2009. Mycorrhizal status of plant species in the Chaco Serrano Woodland from central Argentina. *Mycorrhiza* **19**: 205–214.

Gallaud, I. 1905. Études sur les mycorrhizes endotrophes. *Revue générale de botanique* **17**: 5–48; 66–83, 123–135; 223–239; 313–325; 425–433; 479–500.

R Development Core Team. 2016. A language and environment for statistical computing. R Foundation for Statistical Computing, Vienna.

Shah, MA, Reshi, ZA, Khasa, D. 2009. Arbuscular mycorrhizal status of some Kashmir Himalayan alien invasive plants. *Mycorrhiza* **20**: 67–72.

SigmaPlot. Systat Software, San Jose, CA, USA.

Wang, B, Qiu, Y-L. 2006. Phylogenetic distribution and evolution of mycorrhizas in land plants. *Mycorrhiza* **16**: 299–363.

Manuscript 2

PARTIAL MYCOHETEROTROPHY IS COMMON AMONG CHLOROPHYLLOUS PLANTS WITH PARIS-TYPE ARBUSCULAR MYCORRHIZA

Philipp Giesemann[1], Hanne N. Rasmussen[2] and Gerhard Gebauer[1]

Annals of Botany XX, 1–9, doi: 10.1093/aob/mcab003.

[1]University of Bayreuth, Laboratory of Isotope Biogeochemistry, Bayreuth Center of Ecology and Environmental Research (BayCEER), 95440 Bayreuth, Germany

[2]University of Copenhagen, Institute of Geosciences and Natural Resources, Rolighedsvej 23, 1958 Frederiksberg C, Denmark.

Key words Arbuscular mycorrhiza, *Arum*-type, Ellenberg values, ferns, horsetails, mycoheterotrophy, mycorrhizal networks, *Paris*-type, seed plants, stable isotopes, ^{13}C, ^{2}H.

Received, 21 August 2020; accepted, 8 January 2021; published, 06 February 2021.

Annals of Botany **XX**: 1–9, 2021
doi: 10.1093/aob/mcab003, available online at www.academic.oup.com/aob

ANNALS OF BOTANY Founded 1887

Partial mycoheterotrophy is common among chlorophyllous plants with *Paris*-type arbuscular mycorrhiza

Philipp Giesemann[1], Hanne N. Rasmussen[2] and Gerhard Gebauer[1,*]

[1]University of Bayreuth, Laboratory of Isotope Biogeochemistry, Bayreuth Center of Ecology and Environmental Research (BayCEER), D-95440 Bayreuth, Germany, and [2]University of Copenhagen, Institute of Geosciences and Natural Resources, Rolighedsvej 23, 1958 Frederiksberg C, Denmark
** For correspondence. E-mail gerhard.gebauer@uni-bayreuth.de*

Received: 21 August 2020 Returned for revision: 10 December 2020 Editorial decision: 4 January 2021 Accepted: 8 January 2021

• **Background and Aims** An arbuscular mycorrhiza is a mutualistic symbiosis with plants as carbon providers for fungi. However, achlorophyllous arbuscular mycorrhizal species are known to obtain carbon from fungi, i.e. they are mycoheterotrophic. These species all have the *Paris* type of arbuscular mycorrhiza. Recently, two chlorophyllous *Paris*-type species proved to be partially mycoheterotrophic. In this study, we explore the frequency of this condition and its association with *Paris*-type arbuscular mycorrhiza.
• **Methods** We searched for evidence of mycoheterotrophy in all currently published ^{13}C, ^{2}H and ^{15}N stable isotope abundance patterns suited for calculations of enrichment factors, i.e. isotopic differences between neighbouring *Paris*- and *Arum*-type species. We found suitable data for 135 plant species classified into the two arbuscular mycorrhizal morphotypes.
• **Key Results** About half of the chlorophyllous *Paris*-type species tested were significantly enriched in ^{13}C and often also enriched in ^{2}H and ^{15}N, compared with co-occurring *Arum*-type species. Based on a two-source linear mixing model, the carbon gain from the fungal source ranged between 7 and 93 % with ferns > horsetails > seed plants. The seed plants represented 13 families, many without a previous record of mycoheterotrophy. The ^{13}C-enriched chlorophyllous *Paris*-type species were exclusively herbaceous perennials, with a majority of them thriving on shady forest ground.
• **Conclusions** Significant carbon acquisition from fungi appears quite common and widespread among *Paris*-type species, this arbuscular mycorrhizal morphotype probably being a pre-condition for developing varying degrees of mycoheterotrophy.

Key words: Arbuscular mycorrhiza, *Arum*-type, Ellenberg values, ferns, horsetails, mycoheterotrophy, mycorrhizal networks, *Paris*-type, seed plants, stable isotopes, ^{13}C, ^{2}H.

INTRODUCTION

A number of plant species are known to cover their energy consumption entirely or partly by parasitism. Some parasitic species transfer photosynthates from another plant through haustoria (Těšitel *et al.*, 2010; Westwood *et al.*, 2010), but many parasitize endophytic fungi ('mycoheterotrophy'; Leake, 1994; Merckx, 2013; Waterman *et al.*, 2013). Ultimately, mycoheterotrophy must be based on hyphal connection to photo-assimilating plants or to photosynthetic products in organic debris. The physiology of parasitic plants holds a considerable fascination. Access to photosynthates either directly from another plant or through hyphae can be associated with a dramatic reduction of chlorophyll and thus of photosynthetic capacity (Westwood *et al.*, 2010; Merckx, 2013), but often some photosynthetic activity is retained ('hemiparasites' or 'partial mycoheterotrophs') (Těšitel *et al.*, 2010; Hynson *et al.*, 2013).

The role that parasitic plants play in the natural habitats where they occur is generally understudied and probably underestimated (Quested *et al.*, 2003; Quested, 2008). The vast majority of parasitic plants are herbaceous, often small in stature, and the condition is thought to be confined to certain specialized plant families (e.g. Burmanniaceae, Ericaceae, Gentianaceae, Orchidaceae, Orobanchaceae, Polygalaceae, Santalaceae, Thismiaceae and Triuridaceae; Westwood *et al.*, 2010; Merckx *et al.*, 2013). In a recent study, however, we demonstrated partial mycoheterotrophy in two plant species with *Paris*-type arbuscular mycorrhiza (AM): *Paris quadrifolia* (Melanthiaceae) and *Anemone nemorosa* (Ranunculaceae) (Giesemann *et al.*, 2020*b*). Nevertheless, both plant species have the outer appearance of typical photo-assimilating plants and no close relationship with previously known mycoheterotrophic species (Giesemann *et al.*, 2020*b*). This supports the suggestion that a capacity towards mycoheterotrophy may coincide with the *Paris* type of AM, as suggested by Imhof (1999), and be more widespread than previously recognized. The impact on plant communities could thus be quite considerable, if it amounts to regular and substantial transfers of photosynthates between common plant species.

In this study, we explore the prevalence of partial mycoheterotrophy and its suspected link to the *Paris* type of AM by surveying published information. Evidence of carbon (C) gain from fungi may be found in the stable isotope

composition in leaves of the species in question, where species with mycoheterotrophy deviate characteristically in composition from the purely photo-assimilating species (Gebauer and Meyer, 2003). Thus, we extracted information on carbon (^{13}C), nitrogen (^{15}N) and hydrogen (^{2}H) stable isotope composition in plant species with AM and sorted them into three groups: chlorophyllous *Arum*-type species, chlorophyllous *Paris*-type species and achlorophyllous *Paris*-type species. The distinction into morphotypes (*Arum* vs. *Paris*) was developed by Gallaud (1905) and is based on the infection pattern of hyphae within the roots. Since then the morphotyping has been applied to a wide range of plant species. About 80 % of higher plant species are estimated to form AM, and published records suggest that the morphotypes occur with about equal frequency, with few intermediate or variable forms. Furthermore, the morphotype is mostly consistent across the species of the same genus (Dickson *et al.*, 2007). AM is based on ubiquitous fungi belonging to Glomeromycotina.

We intended to test the following hypotheses: (i) that chlorophyllous *Paris*-type AM plant species would be enriched in ^{13}C, ^{15}N and ^{2}H stable isotopes compared with chlorophyllous *Arum*-type species, but less so than the achlorophyllous *Paris*-type AM species (cf. Gomes *et al.*, 2020; Giesemann *et al.*, 2020*b*); (ii) that the proportion of C gained by photosynthesis and through fungi, respectively, would vary within the group of chlorophyllous *Paris*-type species, reflecting different degrees of reliance on mycoheterotrophy, in the same way as was found in partial mycoheterotrophs with other mycorrhizal relationships (associated with either ectomycorrhizal or saprotrophic basidio- or ascomycetes; cf. Gebauer and Meyer, 2003; Zimmer *et al.*, 2007; Hynson *et al.*, 2009; Gebauer *et al.*, 2016; Schiebold *et al.*, 2018); and (iii) that shade-adapted *Paris*-type AM plant species would show a greater reliance on fungi as their C source, and thus a higher ^{13}C and ^{2}H enrichment, than *Paris*-morphotype AM plant species adapted to full sunlight. A similar light dependence is known in partial mycoheterotrophs on ectomycorrhizal fungi (Preiss *et al.*, 2010) and on saprotrophic rhizoctonia fungi (Schweiger *et al.*, 2019).

MATERIALS AND METHODS

Distinction of species to AM morphotype

The morphotype of each chlorophyllous plant genus/species was obtained from Dickson *et al.* (2007). This information was supplemented with data from Diallo *et al.* (2001), Becerra *et al.* (2007), Menoyo *et al.* (2007), Turnau *et al.* (2008), Zubek *et al.* (2008, 2011*a*, *b*), Shah *et al.* (2009), Zubek and Błaszkowski (2009), Druva-Lusite and Ievinsh (2010), Velázquez *et al.* (2010), Burni and Hussain (2011), Kołaczek *et al.* (2013), Shi *et al.* (2013) and Nobis *et al.* (2015) (see details in Supplementary data Table S1). All achlorophyllous plant species on AM fungi were assumed to possess *Paris*-type AM, as no contradictory evidence is present so far (Dickson *et al.*, 2007; Imhof *et al.*, 2013).

Stable isotope data for plant species with known AM morphotype, nitrogen concentration and light requirement

The literature was surveyed for C, N, H and oxygen (O) stable isotope natural abundance data suitable for the calculation of the stable isotope enrichment factors, ε (see below) (Supplementary data Table S1). These factors average the effect of habitat conditions, such as microclimate, soil respiration and soil conditions, on the stable isotope composition in leaves of autotrophic C_3 plants growing together in the respective habitats. Those drivers for variations in the stable isotope composition of plants collected from different habitats may thus be disregarded (Farquhar *et al.*, 1982, 1989; Sternberg *et al.*, 1984; Ziegler, 1988; Dawson *et al.*, 2002; Cernusak *et al.*, 2004; Gebauer *et al.*, 2016). We obtained raw data of 1300 stable isotope records on $\varepsilon^{13}C/^{15}N$ and 225 on $\varepsilon^{2}H/^{18}O$ from the following publications: Gebauer and Meyer (2003), Bidartondo *et al.* (2004), Zimmer *et al.* (2007, 2008), Hynson *et al.* (2009, 2015), Cameron and Bolin (2010), Liebel *et al.* (2010, 2015), Preiss *et al.* (2010), Girlanda *et al.* (2011), Ercole *et al.* (2015), Lee *et al.* (2015), Hynson (2016), Shutoh *et al.* (2016), Schiebold *et al.* (2017, 2018), Suetsugu *et al.* (2017), Ogura-Tsujita *et al.* (2018), Giesemann *et al.* (2020*a*, *b*) and Gomes *et al.* (2020). Additionally, unpublished data from the BayCEER Laboratory of Isotope Biogeochemistry Bayreuth were kindly provided. From this data set, 155 plant individuals (22 species) forming either intermediate morphotypes or establishing both *Arum* and *Paris* type were excluded (Dickson, 2004). Raw data from Courty *et al.* (2011) not made available are the only currently published data with AM reference plants missing in our survey. Thus, 1145 stable isotope records on $\varepsilon^{13}C/^{15}N$ and 218 on $\varepsilon^{2}H/^{18}O$ were analysed (135 plant species).

The isotope data were sorted into three functional groups: 13 species of achlorophyllous, full mycoheterotrophs on *Paris*-type AM (Merckx *et al.*, 2010; Gomes *et al.*, 2020), 63 species of chlorophyllous *Paris*- and 59 species of chlorophyllous *Arum*-type AM. From this data pool, leaf N concentrations were also available for 107 plant species ($n = 890$, 12 full mycoheterotrophs, 50 chlorophyllous *Paris*-type and 45 chlorophyllous *Arum*-type). Most belonged to the temperate climate zone in Europe (e.g. Austria, Germany and Italy) but there were a few records from other continents (e.g. Australia, Japan and the USA) (Supplementary data Table S1).

We compared the *Paris*-type enrichment factor ε (target plant, TP) with neighbouring *Arum*-type species (reference plant, RP) as $\varepsilon x = \delta x_{TP} - \text{mean}(\delta x_{RP})$ ($x = {}^{13}C$, ^{15}N, ^{18}O, ^{2}H) (Preiss and Gebauer, 2008; Hynson *et al.*, 2013) [see hypotheses (i) and (ii)].

We classified the species with respect to light and temperature preferences by means of Ellenberg indicator values (Ellenberg *et al.*, 2001) which is a system of ordinally/quasi-cardinally scaled classification of plants in Central Europe, finding information on 96 *Paris*- and 149 *Arum*-type species. For a sub-set of plant species from Central Europe (81 species, $n = 787$), we had both Ellenberg indicator values and $\varepsilon^{13}C$ enrichment factors. The 41 *Paris*-type species of this sub-set ($n = 315$) were analysed for a correlation between light availability and $\varepsilon^{13}C$ enrichment factors, reflecting the degree of mycoheterotrophy [see hypothesis (iii)].

Statistical analysis

The degree of mycoheterotrophy was approximated based on the two-source linear mixing model on ^{13}C (Gebauer and Meyer, 2003; Hynson *et al.*, 2013). Plant species considered fully autotrophic (chlorophyllous *Arum*-type plant species) and plant species considered fully mycoheterotrophic (achlorophyllous *Paris*-type plant species; Merckx *et al.*, 2010; Gomes *et al.*, 2020) represent the two end members between which the partially mycoheterotrophic *Paris*-type species are expected to fall (Giesemann *et al.*, 2020*b*).

RStudio 1.1 (R Core Team, 2019) and SigmaPlot 11.0 (Systat Software, San Jose, CA, USA) were applied for data analyses. The platform from Lenhard and Lenhard (2016) was used for estimations of effect sizes (Cohen's *d*). An effect size of $d > 0.8$ is usually counted as relevant (Cohen, 1992). Shapiro–Wilk tests for normal distribution ('stats' R package by R Core Team, 2019) and Levene tests for variance homogeneity ('car' R package by Fox and Weisberg, 2019) recommended a conservative, non-parametric test procedure for the comparison between *Arum*- and *Paris*-morphotype species. The one-tailed Mann–Whitney *U*-test using the 'stats' R package was performed to evaluate differences in Ellenberg indicator values between *Arum*- and *Paris*-morphotype species. One-tailed Kruskal–Wallis *H*-tests using the 'stats' R package were applied for a comparison of full mycoheterotrophs, chlorophyllous *Paris*- and *Arum*-morphotype species as well as for chlorophyllous *Arum*- and *Paris*-morphotype species separated into ferns, horsetails and seed plants, respectively. Dunn's post-hoc (*Z*) test for multiple comparison was performed after a significant *H*-test using the 'dunn.test' R package (Dinno, 2017). *P*-values were corrected according to the sequential Holm–Bonferroni method. A linear regression (Pearson correlation, r^2_{adj}) was performed for light availability and $\varepsilon^{13}C$ enrichment of *Paris*-morphotype plant species. The critical level of significance was set to $\alpha \leq 0.05$. The data are expressed as their mean value with their s.d. ($\bar{x} \pm$ s.d.).

RESULTS

For *Arum*-morphotype AM species, as reference plants, the mean enrichment factor ε was zero by definition. Thus with standard deviation it was for $^{13}C = 0.0 \pm 0.6$ ‰, $^{15}N = 0.0 \pm 0.9$ ‰ and $^{2}H = 0.0 \pm 5.0$ ‰, while enrichments in achlorophyllous *Paris*-morphotype species were pronounced: $^{13}C = 5.0 \pm 2.3$ ‰, $^{15}N = 4.0 \pm 3.4$ ‰ and $^{2}H = 33.3 \pm 17.0$ ‰ (Fig. 1). Chlorophyllous *Paris*-type species were located between chlorophyllous *Arum*-type and achlorophyllous fully mycoheterotrophic plants, with intermediate enrichment values: $^{13}C = 0.9 \pm 1.6$ ‰, $^{15}N = 0.4 \pm 2.3$ ‰ and $^{2}H = 8.0 \pm 11.1$ ‰. (Fig. 1). These average figures cover a large variation among chlorophyllous *Paris*-type species, ranging from –2.7 ± 0.8 ‰ for *Asarum europaeum* to 4.5 ± 1.4 ‰ for *Athyrium filix-femina* in ^{13}C, from –3.9 ± 1.1 ‰ for *Asplenium ruta-muraria* to 7.7 ± 3.2 ‰ for *Equisetum palustre* in ^{15}N and from –15.5 ± 7.8 ‰ for *Gentiana bavarica* to 21.4 ± 6.4 ‰ for *Mercurialis perennis* in ^{2}H (Supplementary data Table S1).

Kruskal–Wallis tests indicated significant effects for the comparisons of *Arum*-type AM, achlorophyllous *Paris*-type AM and chlorophyllous *Paris*-type AM plants in $\varepsilon^{13}C$ [$H(2) = 330.523$, $P < 0.001$, Cohen's $d = 1.276$], $\varepsilon^{15}N$ [$H(2) = 139.422$, $P < 0.001$, Cohen's $d = 0.742$] and $\varepsilon^{2}H$ [$H(2) = 71.985$, $P < 0.001$, Cohen's $d = 1.389$]. Pairwise comparisons by Dunn's post-hoc test showed significant differences in $\varepsilon^{13}C$, $\varepsilon^{15}N$ and $\varepsilon^{2}H$ between each of the three functional groups (Table 1). Although Kruskal–Wallis test detected a significant effect between groups in ^{18}O enrichment [$H(2) = 6.001$, $P = 0.05$, Cohen's $d = 0.275$], the low Cohen's *d* value suggested that the effect was not relevant. Furthermore, no significant effect between groups was detected for leaf total N concentrations [$H(2) = 4.856$, $P = 0.09$, Cohen's $d = 0.113$]. The chlorophyllous *Paris*-type species were also consistently ^{13}C and ^{2}H enriched when *Paris*- and *Arum*-type species were separated into groups of horsetails (*Equisetum*), ferns and seed plants (Supplementary data Table S2). The ^{13}C enrichment follows the sequence ferns > horsetails > seed plants, while the limited data on ^{2}H enrichment suggest horsetails > seed plants (see below).

A total of 63 chlorophyllous *Paris*-type AM species were compared with their respective chlorophyllous *Arum*-type AM reference plants in stable isotope enrichment factors $\varepsilon^{13}C$, $\varepsilon^{15}N$ and $\varepsilon^{2}H$ (Supplementary data Table S3). Of these, 31 were found to be significantly ^{13}C enriched (Fig. 1, brownish symbols) while 32 remained inconspicuously enriched or depleted in their ^{13}C patterns (Fig. 1, white). For the group that was significantly ^{13}C enriched, a mean proportional C gain from the fungal source was calculated based on the linear two-source mixing model (Table 2). This mean proportional C gain from the fungal source ranged from 7 to 93 % (38±19 %) and follows the sequence ferns > horsetails > seed plants (Table 2).

Among the ^{13}C-enriched chlorophyllous *Paris*-type species were seven out of ten forest ferns ($\varepsilon^{13}C$ mean: 3.4 ± 1.1 ‰), four out of five forest horsetails ($\varepsilon^{13}C$ mean: 2.2 ± 1.3 ‰) and nine out of 24 forest-floor seed plants ($\varepsilon^{13}C$ mean: 1.4 ± 0.8 ‰). These species were all herbaceous perennials. In addition to ^{13}C enrichment, two species were also ^{2}H enriched (8.4 ± 3.9 ‰; *Anemone nemorosa* and *Oxalis acetosella*; Fig. 1, light brown) and four were ^{15}N enriched (2.8 ± 1.2 ‰; *Equisetum arvense*, *E. fluviatile*, *E. telmateia* and *Tamus communis*; Fig. 1, dark brown). The herbaceous forest species *Paris quadrifolia*, *Mercurialis perennis* and *Equisetum sylvaticum* turned out to be simultaneously ^{13}C (mean: 2.3 ± 0.8 ‰), ^{15}N (mean: 3.1 ± 3.8 ‰) and ^{2}H enriched (mean: 14.7 ± 6.4 ‰) (Fig. 1, dark gold).

Among the chlorophyllous *Paris*-type species that did not show significant ^{13}C enrichment, the forest perennial *Asarum europaeum* was nevertheless significantly ^{15}N and ^{2}H enriched (Supplementary data Table S3). Tree saplings of *Acer campestre* tended towards both ^{13}C and ^{15}N enrichment, and saplings of *Cornus controversa* tended towards a ^{13}C enrichment that was uncertain because of the small sample size. Saplings of *Acer pseudoplatanus* were not conspicuously ^{13}C enriched while they were significantly ^{2}H enriched.

In addition to the frequently ^{13}C-enriched chlorophyllous *Paris*-type species from forest sites, ^{13}C enrichments were also observed for 11 out of 23 herbaceous open-land species ($\varepsilon^{13}C$ mean: 1.2 ± 1.0 ‰), such as *Astrantia major*, *Gentiana lutea* and *Ligusticum mutellina*. Their conspicuousness was

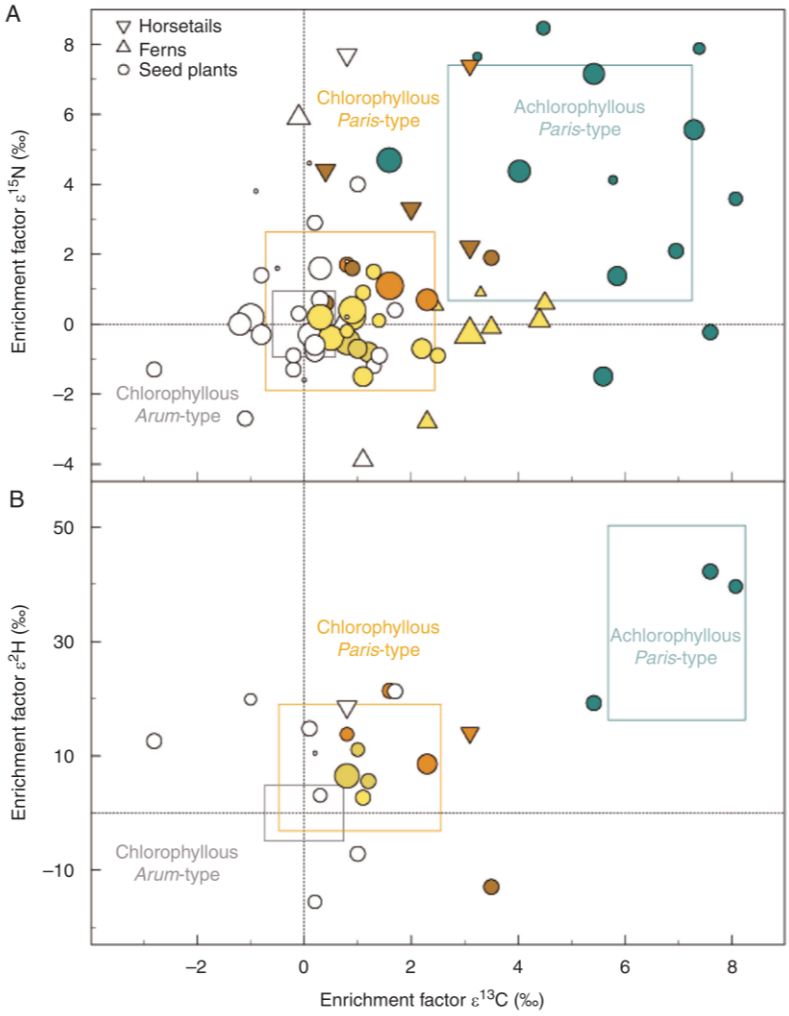

FIG. 1. (A) Carbon and nitrogen enrichment factors ($\varepsilon^{13}C$ and $\varepsilon^{15}N$) and (B) carbon and hydrogen enrichment factors ($\varepsilon^{13}C$ and $\varepsilon^{2}H$) for chlorophyllous *Arum*-type arbuscular mycorrhizal (AM) plant species (grey frame, s.d.), chlorophyllous *Paris*-type AM plant species (brownish tones, brown frame, s.d.) and achlorophyllous, full mycoheterotrophs on AM fungi (blue, blue frame, s.d.). AM morphotype assignment was obtained from the literature (see the Materials and Methods). Each species is represented by mean values and the s.d. is omitted for clarity. Symbol size reflects the sample size of the *Paris*-type species (n = 1–31, see Supplementary data Table S3). Each chlorophyllous *Paris*-type AM plant species was tested for significance of differences in $\varepsilon^{13}C$, $\varepsilon^{15}N$ and $\varepsilon^{2}H$ from co-occurring chlorophyllous *Arum*-type AM plant species (see Supplementary data Table S3). Chlorophyllous *Paris*-type AM plant species shown in coloured symbols are significant in at least one trait (^{13}C enrichment, light gold; ^{13}C + ^{2}H enrichment, light brown; ^{13}C + ^{15}N enrichment, dark brown, ^{13}C + ^{2}H + ^{15}N enrichment, dark gold; no significant enrichment, white). Achlorophyllous plant species were not included in the test procedure (see Gomes *et al.*, 2020). The data comprise for $^{13}C/^{15}N$: 13 achlorophyllous *Paris*-type species (n = 99), 63 chlorophyllous *Paris*-type species (n = 520) and 59 chlorophyllous *Arum*-type species (n = 530). The data comprise for ^{2}H: three achlorophyllous species (n = 14), 18 chlorophyllous *Paris*-type species (n = 100) and 15 chlorophyllous *Arum*-type species (n = 104).

supported by either an ^{15}N enrichment (1.3 ± 0.9 ‰, *Gentiana lutea* and *Alchemilla* sp.; Fig. 1, dark brown), an ^{2}H enrichment (6.5 ± 6.0 ‰, *Astrantia major*; Fig. 1, light brown) or both (1.7 ± 1.1 ‰ and 13.8 ± 4.4 ‰, *Ligusticum mutellina*, Fig. 1, dark gold; Table 2). The open-land species *Aquilegia atrata* and *Trollius europaeus* were found to be ^{13}C inconspicuous (0.9 ± 0.9 ‰) while a significant ^{2}H enrichment was disclosed (14.8 ± 6.3 ‰ and 21.3 ± 5.6 ‰, respectively; Supplementary data Table S3). Species that were ^{13}C enriched but where data on ^{2}H are not available could be suspected of partial mycoheterotrophic nutrition and should be further investigated (2.0 ± 1.3 ‰, e.g. *Asphodelus aestivus*, *Geranium sylvaticum*, *Meum athamanticum*, *Scandix pecten-veneris* and ferns). *Botrychium lunaria*, *Brachypodium sylvaticum*, *Molinia caerulea* and *Pimpinella saxifraga* were found to be only ^{15}N enriched, while data on ^{2}H enrichment are still missing for these species.

Ellenberg indicator values found chlorophyllous *Paris*-type species to be significantly distinguished from chlorophyllous *Arum*-type species in their preferences for light availability

TABLE 1. *Pairwise Dunn's post-hoc test (Z) for significance of differences between the three functional groups of achlorophyllous species on* Paris*-type AM (full mycoheterotrophs), chlorophyllous potentially partial mycoheterotrophs on* Paris*-type AM and chlorophyllous* Arum*-type AM plant species as references in enrichment factors $\varepsilon^{13}C$, $\varepsilon^{15}N$ and $\varepsilon^{2}H$*

	$\varepsilon^{13}C$		$\varepsilon^{15}N$		$\varepsilon^{2}H$	
	Test statistics	*P*	Test statistics	*P*	Test statistics	*P*
Achlorophyllous *Paris*-type vs. chlorophyllous *Paris*-type	$Z = 11.193$	**<0.001**	$Z = 10.384$	**<0.001**	$Z = 3.885$	**<0.001**
Achlorophyllous *Paris*-type vs. chlorophyllous *Arum*-type	$Z = 17.176$	**<0.001**	$Z = 11.772$	**<0.001**	$Z = 7.009$	**<0.001**
Chlorophyllous *Paris*-type vs. chlorophyllous *Arum*-type	$Z = 10.570$	**<0.001**	$Z = 2.451$	**0.007**	$Z = 6.331$	**<0.001**

Significances are highlighted in bold.

For $^{13}C/^{15}N$, the data comprise 13 achlorophyllous *Paris*-type species ($n = 99$), 63 chlorophyllous *Paris*-type species ($n = 520$) and 59 chlorophyllous *Arum*-type species ($n = 530$). For ^{2}H, the data comprise three achlorophyllous species ($n = 14$), 18 chlorophyllous *Paris*-type species ($n = 100$) and 15 chlorophyllous *Arum*-type species ($n = 104$).

TABLE 2. *Proportional C gain (%) of all 31 chlorophyllous* Paris*-type species that were identified as significantly different in stable isotope enrichment factors $\varepsilon^{13}C$ from neighbouring* Arum*-type species*

	***Paris*-type species**	**Family**	***n***	**Proportional C gain (%)**	
				Range	Mean s.d.
H,o	*Equisetum arvense*	Equisetaceae	5	53–81	63 ± 10
H,f	*Equisetum fluviatile*	Equisetaceae	5	6–12	9 ± 3
H,f	*Equisetum sylvaticum*	Equisetaceae	4	48–81	63 ± 14
H,f	*Equisetum telmateia*	Equisetaceae	5	12–73	41 ± 24
F,f	*Pteridium* sp.	Dennstaedtiaceae	2	64–72	68
F,f	*Blechnum* sp.	Blechnaceae	2	25–79	52
F,f	*Athyrium filix-femina*	Athyriaceae	5	69–139	93 ± 28
F,f	*Diplazium sandwichianum*	Athyriaceae	6	50–122	91 ± 30
F,f	*Dryopteris filix-mas*	Dryopteridaceae	5	33–99	73 ± 25
F,f	*Polystichum* sp.	Dryopteridaceae	16	3–113	64 ± 31
F,f	*Polypodium vulgare*	Polypodiaceae	5	30–70	48 ± 16
S,f	*Tamus communis*	Dioscoreaceae	5	–13 to 41	19 ± 22
S,f	*Paris quadrifolia*	Melanthiaceae	13	24–79	47 ± 16
S,f	*Smilax aspera*	Smilacaceae	5	5–48	26 ± 19
S,o	*Asphodelus aestivus*	Asphodelaceae	25	–16 to 91	18 ± 26
S,o	*Bromus erectus*	Poaceae	29	–7 to 54	18 ± 15
S,o	*Bromus* sp.	Poaceae	21	–42 to 50	11 ± 22
S,f	*Melica nutans*	Poaceae	4	5–42	16 ± 17
S,f	*Anemone nemorosa*	Ranunculaceae	10	–5 to 53	25 ± 17
S,o	*Ranunculus* sp.	Ranunculaceae	23	–41 to 38	7 ± 20
S,o	*Alchemilla vulgaris*	Rosaceae	4	18–36	29 ± 8
S,o	*Alchemilla* sp.	Rosaceae	6	–81 to 64	8 ± 49
S,f	*Oxalis acetosella*	Oxalidaceae	9	–9 to 59	20 ± 21
S,f	*Mercurialis perennis*	Euphorbiaceae	31	–3 to 85	33 ± 22
S,f	*Geranium sylvaticum*	Geraniaceae	5	42–66	52 ± 10
S,f	*Lysimachia nummularia*	Primulaceae	5	5–32	23 ± 11
S,o	*Gentiana lutea*	Gentianaceae	5	55–108	73 ± 21
S,o	*Astrantia major*	Apiaceae	25	–31 to 50	17 ± 19
S,o	*Ligusticum mutellina*	Apiaceae	5	13–25	16 ± 5
S,o	*Meum athamanticum*	Apiaceae	10	23–76	46 ± 17
S,o	*Scandix pecten-veneris*	Apiaceae	10	–4 to 44	22 ± 17

In total, 63 chlorophyllous *Paris*-type plant species were tested, thus 32 species were insignificantly enriched in ^{13}C (see Supplementary data Table S3 for the complete list). Nomenclature follows the sources APG IV (2016) and PPG I (2016). Family sequences are according to PPG I (2016) (pteridophytes), Haston *et al.* (2009) and APG IV (2016) (angiosperms).

F, fern; H, horsetail; S, seed plant; f, forest; o, open-land.

[$U(94,148) = 5416.5$, $P = 0.003$, Cohen's $d = 0.4$] and temperature [$H(66,111) = 2605.5$, $P < 0.001$, Cohen's $d = 0.5$]. Although the Cohen's *d* index probably penalizes the imbalance in sample size distribution, these differences tendentially indicate that *Paris*-type species occur preferentially in habitats of lower light availability and lower temperature (Supplementary data Fig. S1). Among the chlorophyllous *Paris*-type ferns and horsetails for which both Ellenberg light availability values and

ε^{13}C enrichment factors of *Paris*-type species were available, significant relationships were found to ^{13}C enrichments. This means proportionally higher C gains from the fungal source under conditions of lower light availability (Fig. 2). There was no significant correlation between Ellenberg light availability values and ε^{13}C in seed plants, which could be due to the existence of a few highly ^{13}C-enriched open-land plant species (*Gentiana lutea* and *Meum athamanticum*). Chlorophyllous *Paris*-type ferns, horsetails and seed plants from forests together were more ^{13}C enriched than open-land *Paris*-type plants [$U(148,163) = 6272.6$, $P < 0.001$, Cohen's $d = 0.9$]. This relationship also holds when only comparing seed plants that were significantly ^{13}C enriched from forests and open lands [$U(73,84) = 2368$, $P = 0.014$, Cohen's $d = 0.4$; Fig. 2].

DISCUSSION

We found that partial mycoheterotrophy is common in plants with AM. In plants with *Paris*-type AM, we found significant ^{13}C enrichment in about half of the species under study (31 out of 63 *Paris*-type species). Two of these, *Paris quadrifolia* and *Anemone nemorosa*, coincide with our previous report (Giesemann *et al.*, 2020*b*). Among some of the remaining species with *Paris*-type AM, the enrichment in ^{15}N, ^{2}H or both may suggest that some mycoheterotrophy did occur. Plant species with *Paris*-type AM might thus present a continuous range between full autotrophy and full mycoheterotrophy. Our results are in support of Imhof (1999) who suggested that hyphal growth within root cells, such as the intracellular hyphal coils of the *Paris* morphotype, is an important prerequisite for the evolution of mycoheterotrophy.

Paris-type partial mycoheterotrophy seemed to be common in the group of pteridophytes, and among seed plants we found it in 13 families, both mono- and dicotyledons. This suggests that the capacity to parasitize Glomeromycotina fungi in a *Paris*-type AM relationship is widespread in the plant kingdom and, important to note, exists among plants with fully developed leaves which up to now have been thought to be fully photo-assimilating.

Our 31 species with partial mycoheterotrophy on *Paris*-type AM add to the steadily increasing list of plant species with this kind of nutrition; currently 124 plant species are known. Most of these belong in Orchidaceae (orchid mycorrhiza) and Ericales (ericoid mycorrhiza) (Hynson *et al.*, 2013, 2016; Gebauer *et al.*, 2016; Schiebold *et al.*, 2018).

Previous discoveries of partial mycoheterotrophy on *Paris*-type AM amount to a few species with apparent physiological and evolutionary prerequisites. *Ophioglossum kawamurae*, *O. parvum* and *O. thermale* (sporophyte, Ophioglossaceae), found by Suetsugu *et al.* (2020*b*) to be partially mycoheterotrophic, belong to a family where the gametophyte generation is known to be achlorophyllous and mycoheterotrophic. Other examples belong to families known to contain achlorophyllous members: *Bartonia virginica*, *Obolaria virginica* and *Pterygocalyx volubilis* in Gentianaceae (Cameron and Bolin, 2010; Suetsugu *et al.*, 2020*a*) and *Burmannia coelestis* in Burmanniaceae (Bolin *et al.*, 2017). In view of our new records, these first few examples appear to just graze the surface of something

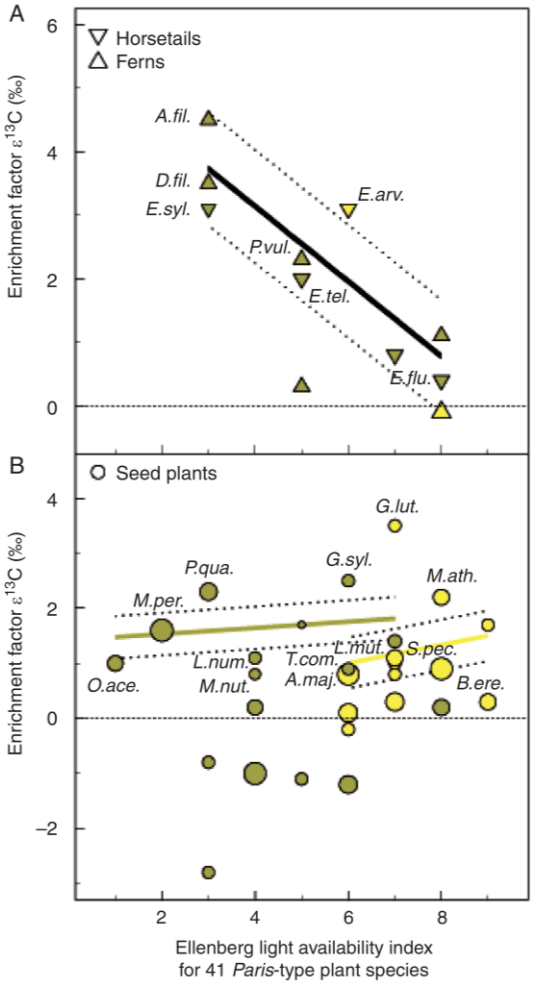

FIG. 2. Relationship between the Ellenberg light availability index and stable isotope enrichment factors ε^{13}C for 41 *Paris*-morphotype arbuscular mycorrhizal (AM) plant species. Significance of ^{13}C enrichment tested towards co-occurring *Arum*-type AM species is highlighted by species labels (see Supplementary data Table S3). (A) Pteridophytes (horsetails and ferns). A negative correlation between light and fungal carbon gain [black solid line, $t(34) = 12.8$, $r^2_{adj} = 0.7$, $P = 0.016$, dotted line: 95 % confidence intervals]. (B) Seed plant species. No clear correlation. The coloured solid lines illustrate a regression among seed plant species significantly ^{13}C enriched separated by forest habitats [dark khaki-coloured solid line and symbols; $t(73) = 0.1$, $r^2_{adj} = 0.0$, $P = 0.741$] and open lands [light khaki-coloured solid line and symbols; $t(84) = 0.1$, $r^2_{adj} = 0.0$, $P = 0.729$] (dotted 95 % confidence intervals). Ellenberg light availability index and AM morphotype were obtained from the literature (see the Materials and Methods). The single *Paris*-type AM plant species are represented by mean values. Standard deviations are omitted for clarity. Symbol size reflects the sample size of the *Paris*-type species (n = 1–31, see Supplementary data Table S3). The figure counts only *Paris*-type AM species with data on ε^{13}C and Ellenberg light availability values. *Paris*-type plant species that were significantly ^{13}C enriched: (A) A.fil. *Athyrium filix-femina*, D.fil. *Dryopteris filix-mas*, E. syl. *Equisetum sylvaticum*, P.vul. *Polypodium vulgare*, E.tel. *Equisetum telmateia*, E.arv. *Equisetum arvense*, E.flu. *Equisetum fluviatile*; (B) O.ace. *Oxalis acetosella*, M.per. *Mercurialis perennis*, P.qua. *Paris quadrifolia*, L.num. *Lysimachia nummularia*, M.nut. *Melica nutans*, G.syl. *Geranium sylvaticum*, T.com. *Tamus communis*, A.maj. *Astrantia major*, G.lut. *Gentiana lutea*, S.pec. *Scandix pecten-veneris*, L.mut. *Ligusticum mutellina*, M.ath. *Meum athamanticum*, B.ere. *Bromus erectus*.

much bigger. In surveying plants that have served as references in other studies, we were able to make an assessment without any pre-conceived expectations regarding certain species or groups. Thus, we could demonstrate significant mycoheterotrophy not only in most pteridophytes tested, but also in ten families of seed plants where it has not been recorded, or even suspected, previously (Apiaceae, Asphodelaceae, Dioscoreaceae, Euphorbiaceae, Geraniaceae, Oxalidaceae, Poaceae, Primulaceae, Rosaceae and Smilacaceae). To this list we may add two more families: Melanthiaceae and Ranunculaceae for *Paris quadrifolia* and *Anemone nemorosa* which we identified as partially mycoheterotrophic quite recently (Giesemann *et al.*, 2020*b*).

Since organic C within the fungi ultimately comes from photo-assimilating plants (either alive or as plant debris), partial mycoheterotrophy does not interact only with the fungi in question, but also with potential donor plants in the ecosystem. Since fungi belonging to the Glomeromycotina are considered to be obligate biotrophs, we should be expecting live donor plants. We found partial mycoheterotrophy only in herbaceous species with *Paris*-type AM. The woody species under study were either *Arum*-type plants, or *Paris*-type without any clear indication of mycoheterotrophy. Transfer of photosynthates from the roots of woody species could be a way for understorey AM species to compensate for a light-limited environment. The negative relationship in pteridophyte species between light and ^{13}C enrichment suggests such a mechanism and is consistent with our third hypothesis. Previous studies indicated a limited photosynthetic capacity of many ferns and horsetails (e.g. Ludlow and Wolf, 1975; Gago *et al.*, 2013; Nadal *et al.*, 2018), and photosynthetic rates lower than in corresponding *Arum*-type species were found in several *Paris*-type AM deciduous forest trees (Wright *et al.*, 2004) and *Paris*-type AM forest ground herbaceous species (Dalke *et al.*, 2018).

Some *Paris*-type AM tree saplings (*Acer campestre*, *A. pseudoplatanus* and *Cornus controversa*) did show indications towards partial mycoheterotrophy. Whether this condition only characterizes the juvenile trees or persists throughout life is a matter for future investigations.

Between herbaceous plant species, however, partial mycoheterotrophy could also be a competitive advantage in relation to species with *Arum*-type mycorrhizal connections. Partial mycoheterotrophy in some species might increase biodiversity by restricting development in other, more vigorously growing members, in analogy with the effect that hemiparasitic plant species may have on the surrounding vegetation and ecosystem (Quested *et al.*, 2003; Quested, 2008; Hartley *et al.*, 2015). Partial mycoheterotrophy may thus have profound effects with respect not only to C cycling but also to the cycling of nutrients such as N.

Interspecific and interfamilial variations in ^{15}N enrichments are known from other groups of mycoheterotrophic plants (Orchidaceae and Pyroloideae; Hynson *et al.*, 2016) and also from AM full mycoheterotrophs (Merckx *et al.*, 2010; Courty *et al.*, 2011; Gomes *et al.*, 2020). The various ^{15}N enrichments were attributed to different fungal partners that access different N nutrient sources (Schiebold *et al.*, 2017). The variations in this study of ^{15}N enrichments in the partially mycoheterotrophic species might indicate different forms of N utilized by Glomeromycotina fungi. Significant ^{15}N enrichments without any ^{13}C and ^{2}H enrichments might, however, also be attributed to a functional role in N acquisition by entirely different fungal endophytes (Hoysted *et al.*, 2019; Giesemann *et al.*, 2020*a*). In addition to stable isotope natural abundance, the total leaf N concentration has been used to differentiate between mycoheterotrophy on orchid mycorrhiza (high leaf N concentrations) and ericoid mycorrhiza (low leaf N concentrations) (Hynson *et al.*, 2016). This difference is thought to be due to different fungal matter uptake mechanisms by the various types of mycoheterotrophic plants: digestion of fungal 'pelotons' in addition to active membrane transport in orchid mycorrhiza and exclusively active membrane transport in ericoid mycorrhiza (Hynson *et al.*, 2016). Since partially mycoheterotrophic *Paris*-type AM species do not differ markedly in leaf total N concentration from fully autotrophic *Arum*-type AM species, a similar active membrane transport mechanism for the uptake of N is suggested for both. However, digestion of *Paris*-morphotype coils has also been documented (Imhof *et al.*, 2013) and life history strategies rather than fungal substrate and trophic strategies could contribute to leaf total N concentration patterns as well (cf. Hynson *et al.*, 2016).

The high diversity in partial mycoheterotrophs as found here is in agreement with the recent finding of low phylogenetic constraints for developing mycoheterotrophy (Perez-Lamarque *et al.*, 2020). A significant proportion of the AM plants, and thus also of all plant species globally, possess the required infection pattern (*Paris*-type AM) to obtain C from a fungal source. Based on these findings, partial mycoheterotrophy, indeed, is more widespread than recognized so far (Giesemann *et al.*, 2020*b*). Nonetheless, there still remain a lot of open questions to be resolved. Our current survey on the occurrence of *Paris*-type AM is mostly based on sometimes old lists from the literature that might require careful re-evaluation. A matter of further research has to be also the consideration of intermediate AM types, plant species that are able to form either *Arum*- or *Paris*-type AM and the influences of environmental conditions and AM fungal taxa on the formation of either *Arum*- or *Paris*-type AM.

We conclude that the fungal *Paris*-coiling type appears to be a necessary prerequisite for partial mycoheterotrophy in chlorophyllous AM plant species. However, not all chlorophyllous *Paris*-morphotype AM plant species turned out to be partially mycoheterotrophic.

SUPPLEMENTARY DATA

Supplementary data are available online at https://academic.oup.com/aob and consist of the following. Figure S1: Ellenberg indicator value for light availability and temperature between *Arum*- and *Paris*-type arbuscular mycorrhizal plant species. Table S1: stable isotope enrichment factors ε with s.d., leaf total N concentrations with s.d. and the arbuscular mycorrhizal type. Table S2: pairwise Dunn's post-hoc test for significance of differences between chlorophyllous *Arum*- and *Paris*-type arbuscular mycorrhizal plant species separated by groups of horsetails, ferns and seed plants in enrichment factors $\varepsilon^{13}C$, $\varepsilon^{15}N$ and $\varepsilon^{2}H$. Table S3: Mann–Whitney *U*-test for significance

of differences between chlorophyllous *Paris*-type species and their respective chlorophyllous *Arum*-type reference plant species in stable isotope enrichment factors $\varepsilon^{13}C$, $\varepsilon^{15}N$ and $\varepsilon^{2}H$.

ACKNOWLEDGEMENTS

Some species were sampled during students' field courses in 2007, 2008, 2016, and 2018 and we are grateful for the support of student field assistants. The authors thank Milena Opgenoorth for providing data on fern species, and Finn N. Rasmussen for enabling a taxonomic ordering of Table 2 and Supplementary data Table S3. The authors thank Ian Wright and Peter Reich for access to the 'GLOPNET' leaf ecomonics data set. P.G. surveyed the data and made a synthesis, analysed and treated the results, and wrote the first manuscript draft. H.N.R. essentially initiated the basic idea for this research originating from an unpublished literature review. G.G. coordinated the project, supervised the isotope abundance survey, supported data treatment and provided access to unpublished data. All authors contributed to interpretation and presentation of results in the manuscript.

FUNDING

P.G. and this project were funded by the Elite Network of Bavaria.

LITERATURE CITED

APG IV. 2016. An update of the Angiosperm Phylogeny Group classification for the orders and families of flowering plants: APG IV. *Botanical Journal of the Linnean Society* **181**: 1–20.

Becerra A, Cabello M, Chiarini F. 2007. Arbuscular mycorrhizal colonization of vascular plants from the Yungas forests, Argentina. *Annals of Forest Science* **64**: 765–772.

Bidartondo MI, Burghardt B, Gebauer G, Bruns TD, Read DJ. 2004. Changing partners in the dark: isotopic and molecular evidence of ectomycorrhizal liaisons between forest orchids and trees. *Proceedingsof the Royal Society B: Biological Sciences* **271**: 1799–1806.

Bolin JF, Tennakoon KU, Majid MBA, Cameron DD. 2017. Isotopic evidence of partial mycoheterotrophy in *Burmannia coelestis* (Burmanniaceae). *Plant Species Biology* **32**: 74–80.

Burni T, Hussain F. 2011. Diversity in arbuscular mycorrhizal morphology in some medicinal plants of family Lamiaceae. *Pakistan Journal of Botany* **43**: 1789–1792.

Cameron DD, Bolin JF. 2010. Isotopic evidence of partial mycoheterotrophy in the Gentianaceae: *Bartonia virginica* and *Obolaria virginica* as case studies. *American Journal of Botany* **97**: 1272–1277.

Cernusak LA, Pate JS, Farquhar GD. 2004. Oxygen and carbon isotope composition of parasitic plants and their hosts in southwestern Australia. *Oecologia* **139**: 199–213.

Cohen J. 1992. A power primer. *Psychological Bulletin* **112**: 155–159.

Courty PE, Walder F, Boller T, *et al.* 2011. Carbon and nitrogen metabolism in mycorrhizal networks and mycoheterotrophic plants of tropical forests: a stable isotope analysis. *Plant Physiology* **156**: 952–961.

Dalke IV, Novakovskiy AB, Maslova SP, Dubrovskiy YA. 2018. Morphological and functional traits of herbaceous plants with different functional types in the European Northeast. *Plant Ecology* **219**: 1295–1305.

Dawson TE, Mambelli S, Plamboeck AH, Templer PH, Tu KP. 2002. Stable isotopes in plant ecology. *Annual Review of Ecology and Systematics* **33**: 507–559.

Diallo A, Weber H, Imhof S. 2001. Sonderstellung der Mykorrhiza von *Mercurialis perennis* L. im Vergleich mit anderen Euphorbiaceae. *Beiträge zur Biologie der Pflanzen* **72**: 315–323.

Dickson S. 2004. The *Arum–Paris* continuum of mycorrhizal symbioses. *New Phytologist* **163**: 187–200.

Dickson S, Smith FA, Smith SE. 2007. Structural differences in arbuscular mycorrhizal symbioses: more than 100 years after Gallaud, where next? *Mycorrhiza* **17**: 375–393.

Dinno A. 2017. dunn.test: Dunn's test of multiple comparisons using rank sums. R package version 1.3.5. https://cran.r-project.org/package=dunn.test.

Druva-Lusite I, Ievinsh G. 2010. Diversity of arbuscular mycorrhizal symbiosis in plants from coastal habitats. *Environmental and Experimental Biology* **8**: 17–34.

Ellenberg H, Weber HE, Düll R, Wirth V, Werner W. 2001. *Zeigerwerte von Pflanzen in Mitteleuropa, 3., durchgesehene Auflage.* Göttingen: Verlag Erich Goltze GmbH & Co KG.

Ercole E, Adamo M, Rodda M, Gebauer G, Girlanda M, Perotto S. 2015. Temporal variation in mycorrhizal diversity and carbon and nitrogen stable isotope abundance in the wintergreen meadow orchid *Anacamptis morio*. *New Phytologist* **205**: 1308–1319.

Farquhar GD, O'Leary MH, Berry JA. 1982. On the relationship between carbon isotope discrimination and the intercellular carbon dioxide concentration in leaves. *Functional Plant Biology* **9**: 121.

Farquhar GD, Ehleringer JR, Hubick KT. 1989. Carbon isotope discrimination and photosynthesis. *Annual Review of Plant Biology* **40**: 503–537.

Fox J, Weisberg S. 2019. *An R companion to applied regression*, 3rd edn. Thousand Oaks, CA: Sage. https://socialsciences.mcmaster.ca/jfox/Books/Companion/.

Gago J, Coopman RE, Cabrera HM, *et al.* 2013. Photosynthesis limitations in three fern species. *Physiologia Plantarum* **149**: 599–611.

Gallaud I. 1905. Études sur les mycorrhizes endotrophes. *Revue générale de botanique* **17**: 5–48; 66–83, 123–135; 223–239; 313–325; 425–433; 479–500.

Gebauer G, Meyer M. 2003. ^{15}N and ^{13}C natural abundance of autotrophic and myco-heterotrophic orchids provides insight into nitrogen and carbon gain from fungal association. *New Phytologist* **160**: 209–223.

Gebauer G, Preiss K, Gebauer AC. 2016. Partial mycoheterotrophy is more widespread among orchids than previously assumed. *New Phytologist* **211**: 11–15.

Giesemann P, Eichenberg D, Stöckel M, *et al.* 2020*a*. Dark septate endophytes and arbuscular mycorrhizal fungi (*Paris*-morphotype) affect the stable isotope composition of 'classically' non-mycorrhizal plants. *Functional Ecology* **34**: 2453–2466.

Giesemann P, Rasmussen HN, Liebel HT, Gebauer G. 2020*b*. Discreet heterotrophs: green plants that receive fungal carbon through *Paris*-type arbuscular mycorrhiza. *New Phytologist* **226**: 960–966.

Girlanda M, Segreto R, Cafasso D, *et al.* 2011. Photosynthetic Mediterranean meadow orchids feature partial mycoheterotrophy and specific mycorrhizal associations. *American Journal of Botany* **98**: 1148–1163.

Gomes S, Merckx V, Kehl J, Gebauer G. 2020. Mycoheterotrophic plants living on arbuscular mycorrhizal fungi are generally enriched in ^{13}C, ^{15}N, and ^{2}H isotopes. *Journal of Ecology* **108**: 1250–1261.

Hartley SE, Green P, Massey FP, Press MC, Stewart JA, John EA. 2015. Hemiparasitic plant impacts animal and plant communities across four trophic levels. *Ecology* **96**: 2408–2416.

Haston E, Richardson JE, Stevens PF, Chase MW, Harris DJ. 2009. The Linear Angiosperm Phylogeny Group (LAPG) III: a linear sequence of the families in APG III. *Botanical Journal of the Linnean Society* **161**: 128–131.

Hoysted GA, Jacob AS, Kowal J, *et al.* 2019. Mucoromycotina fine root endophyte fungi form nutritional mutualisms with vascular plants. *Plant Physiology* **181**: 565–577.

Hynson NA. 2016. The carbon and nitrogen ecophysiologies of two endemic tropical orchids mirrors those of their temperate relatives and the local environment. *Royal Society Open Science* **3**: 160427.

Hynson NA, Preiss K, Gebauer G, Bruns TD. 2009. Isotopic evidence of full and partial myco-heterotrophy in the plant tribe Pyroleae (Ericaceae). *New Phytologist* **182**: 719–726.

Hynson NA, Madsen TP, Selosse M-A, *et al.* 2013. The physiological ecology of mycoheterotrophy. In: Merckx VSFT, ed. *Mycoheterotrophy: the biology of plants living on fungi*. New York: Springer, 297–342.

Hynson NA, Bidartondo MI, Read DJ. 2015. Are there geographic mosaics of mycorrhizal specificity and partial mycoheterotrophy? A case study in *Moneses uniflora* (Ericaceae). *New Phytologist* **208**: 1003–1007.

Hynson NA, Schiebold JM, Gebauer G. 2016. Plant family identity distinguishes patterns of carbon and nitrogen stable isotope abundance and nitrogen concentration in mycoheterotrophic plants associated with ectomycorrhizal fungi. *Annals of Botany* **118**: 467–479.

Imhof S. 1999. Root morphology, anatomy and mycotrophy of the achlorophyllous *Voyria aphylla* (Jacq.) Pers. (Gentianaceae). *Mycorrhiza* **9**: 33–39.

Imhof S, Massicotte HB, Melville LH, Peterson RL. 2013. Subterranean morphology and mycorrhizal structures. In: Merckx VSFT, ed. *Mycoheterotrophy: the biology of plants living on fungi*. New York: Springer, 157–214.

Kołaczek P, Zubek S, Błaszkowski J, Mleczko P, Margielewski W. 2013. Erosion or plant succession – How to interpret the presence of arbuscular mycorrhizal fungi (Glomeromycota) spores in pollen profiles collected from mires. *Review of Palaeobotany and Palynology* **189**: 29–37.

Leake JR. 1994. The biology of myco-heterotrophic ('saprophytic') plants. *New Phytologist* **127**: 171–216.

Lee YI, Yang CK, Gebauer G. 2015. The importance of associations with saprotrophic non-*Rhizoctonia* fungi among fully mycoheterotrophic orchids is currently under-estimated: novel evidence from sub-tropical Asia. *Annals of Botany* **116**: 423–435.

Lenhard W, Lenhard A. 2016. *Berechnung von Effektstärken*. https://www.psychometrica.de/effektstaerke.html.

Liebel HT, Bidartondo MI, Preiss K, *et al.* 2010. C and N stable isotope signatures reveal constraints to nutritional modes in orchids from the Mediterranean and Macaronesia. *American Journal of Botany* **97**: 903–912.

Liebel HT, Bidartondo MI, Gebauer G. 2015. Are carbon and nitrogen exchange between fungi and the orchid *Goodyera repens* affected by irradiance? *Annals of Botany* **115**: 251–261.

Ludlow CJ, Wolf FT. 1975. Photosynthesis and respiration rates of ferns. *American Fern Journal* **65**: 43.

Menoyo E, Beccera A, Rension D. 2007. Mycorrhizal assiciations in *Polylepsis* woodlands of Central Argentina. *Canadian Journal of Botany* **85**: 526–531.

Merckx VSFT. 2013. Mycoheterotrophy: an introduction. In: Merckx VSFT, ed. *Mycoheterotrophy: the biology of plants living on fungi*. New York: Springer, 1–17.

Merckx V, Stöckel M, Fleischmann A, Bruns TD, Gebauer G. 2010. ^{15}N and ^{13}C natural abundance of two mycoheterotrophic and a putative partially mycoheterotrophic species associated with arbuscular mycorrhizal fungi. *New Phytologist* **188**: 590–596.

Merckx VS, Freudenstein JV, Kissling J, *et al.* 2013. Taxonomy and classification. In: Merckx VSFT, ed. *Mycoheterotrophy: the biology of plants living on fungi*. New York: Springer, 19–101.

Nadal M, Flexas J, Gulías J. 2018. Possible link between photosynthesis and leaf modulus of elasticity among vascular plants: a new player in leaf traits relationships? *Ecology Letters* **21**: 1372–1379.

Nobis A, Błaszkowski J, Zubek S. 2015. Arbuscular mycorrhizal fungi associations of vascular plants confined to river valleys: towards understanding the river corridor plant distribution. *Journal of Plant Research* **128**: 127–137.

Ogura-Tsujita Y, Gebauer G, Xu H, *et al.* 2018. The giant mycoheterotrophic orchid *Erythrorchis altissima* is associated mainly with a divergent set of wood-decaying fungi. *Molecular Ecology* **27**: 1324–1337.

Perez-Lamarque B, Selosse MA, Öpik M, Morlon H, Martos F. 2020. Cheating in arbuscular mycorrhizal mutualism: a network and phylogenetic analysis of mycoheterotrophy. *New Phytologist* **226**: 1822–1835.

PPG I. 2016. A community-derived classification for extant lycophytes and ferns. *Journal of Systematics and Evolution* **54**: 563–603.

Preiss K, Adam IK, Gebauer G. 2010. Irradiance governs exploitation of fungi: fine-tuning of carbon gain by two partially myco-heterotrophic orchids. *Proceedings of the Royal Society B: Biological Sciences* **277**: 1333–1336.

Preiss K, Gebauer G. 2008. A methodological approach to improve estimates of nutrient gains by partially myco-heterotrophic plants. *Isotopes in Environmental and Health Studies* **44**: 393–401.

Quested HM. 2008. Parasitic plants – impacts on nutrient cycling. *Plant and Soil* **311**: 269–272.

Quested HM, Cornelissen JHC, Press MC, *et al.* 2003. Decomposition of sub-arctic plants with differing nitrogen economies: a functional role for hemiparasites. *Ecology* **84**: 3209–3221.

R Core Team. 2019. *R: a language and environment for statistical computing*. Vienna, Austria: R Foundation for Statistical Computing. https://www.R-project.org.

Schiebold JM, Bidartondo MI, Karasch P, Gravendeel B, Gebauer G. 2017. You are what you get from your fungi: nitrogen stable isotope patterns in *Epipactis* species. *Annals of Botany* **119**: 1085–1095.

Schiebold JM-I, Bidartondo MI, Lenhard F, Makiola A, Gebauer G. 2018. Exploiting mycorrhizas in broad daylight: partial mycoheterotrophy is a common nutritional strategy in meadow orchids. *Journal of Ecology* **106**: 168–178.

Schweiger JM, Kemnade C, Bidartondo MI, Gebauer G. 2019. Light limitation and partial mycoheterotrophy in rhizoctonia-associated orchids. *Oecologia* **189**: 375–383.

Shah MA, Reshi ZA, Khasa D. 2009. Arbuscular mycorrhizal status of some Kashmir Himalayan alien invasive plants. *Mycorrhiza* **20**: 67–72.

Shi Z, Hou X, Chen Y, Wang F, Miao Y. 2013. Foliar stoichiometry under different mycorrhizal types in relation to temperature and precipitation in grassland. *Journal of Plant Ecology* **6**: 270–276.

Shutoh K, Kaneko S, Suetsugu K, Naito YI, Kurosawa T. 2016. Variation in vegetative morphology tracks the complex genetic diversification of the mycoheterotrophic species *Pyrola japonica* sensu lato. *American Journal of Botany* **103**: 1618–1629.

Sternberg LO, DeNiro MJ, Ting IP. 1984. Carbon, hydrogen, and oxygen isotope ratios of cellulose from plants having intermediary photosynthetic modes. *Plant Physiology* **74**: 104–107.

Suetsugu K, Yamato M, Miura C, *et al.* 2017. Comparison of green and albino individuals of the partially mycoheterotrophic orchid *Epipactis helleborine* on molecular identities of mycorrhizal fungi, nutritional modes and gene expression in mycorrhizal roots. *Molecular Ecology* **26**: 1652–1669.

Suetsugu K, Matsubayashi J, Ogawa NO, Murata S, Sato R, Tomimatsu H. 2020*a*. Isotopic evidence of arbuscular mycorrhizal cheating in a grassland gentian species. *Oecologia* **192**: 929–937.

Suetsugu K, Taketomi S, Tanabe AS, Haraguchi TF, Tayasu I, Toju H. 2020*b*. Isotopic and molecular data support mixotrophy in *Ophioglossum* at the sporophytic stage. *New Phytologist* **228**: 415–419.

Těšitel J, Plavcová L, Cameron DD. 2010. Interactions between hemiparasitic plants and their hosts: the importance of organic carbon transfer. *Plant Signaling & Behavior* **5**: 1072–1076.

Turnau K, Anielska T, Ryszka P, Gawroński S, Ostachowicz B, Jurkiewicz A. 2008. Establishment of arbuscular mycorrhizal plants originating from xerothermic grasslands on heavy metal rich industrial wastes – new solution for waste revegetation. *Plant and Soil* **305**: 267–280.

Velázquez S, Biganzoli F, Cabello M. 2010. Arbuscular mycorrhizal fungi in El Palmar National Park (Entre Rios Province, Argentina) – a protected reserve. *Sydowia* **62**: 149–163.

Waterman RJ, Klooster MR, Hentrich H, Bidartondo MI. 2013. Species interactions of mycoheterotrophic plants: specialization and its potential consequences. In: Merckx VSFT, ed. *Mycoheterotrophy: the biology of plants living on fungi*. New York: Springer, 267–296.

Westwood JH, Yoder JI, Timko MP, dePamphilis CW. 2010. The evolution of parasitism in plants. *Trends in Plant Science* **15**: 227–235.

Wright IJ, Reich PB, Westoby M, *et al.* 2004. The worldwide leaf economics spectrum. *Nature* **428**: 821–827.

Ziegler H. 1988. Hydrogen isotope fractionation in plant tissues. In: Rundel PW, Ehleringer JR, Nagy KA, eds. *Stable isotopes in ecological research*. Berlin: Springer, 105–123.

Zimmer K, Hynson NA, Gebauer G, Allen EB, Allen MF, Read DJ. 2007. Wide geographical and ecological distribution of nitrogen and carbon gains from fungi in pyroloids and monotropoids (Ericaceae) and in orchids. *New Phytologist* **175**: 166–175.

Zimmer K, Meyer C, Gebauer G. 2008. The ectomycorrhizal specialist orchid *Corallorhiza trifida* is a partial myco-heterotroph. *New Phytologist* **178**: 395–400.

Zubek S, Błaszkowski J. 2009. Medicinal plants as hosts of arbuscular mycorrhizal fungi and dark septate endophytes. *Phytochemistry Reviews* **8**: 571–580.

Zubek S, Turnau K, Błaszkowski J. 2008. Arbuscular mycorrhiza of endemic and endangered plants from the Tatra Mts. *Acta Societatis Botanicorum Poloniae* **77**: 149–156.

Zubek S, Blaszkowski J, Mleczko P. 2011*a*. Arbuscular mycorrhizal and dark septate endophyte associations of medicinal plants. *Acta Societatis Botanicorum Poloniae* **80**: 285–292.

Zubek S, Nobis M, Błaszkowski J, Mleczko P, Nowak A. 2011*b*. Fungal root endophyte associations of plants endemic to the Pamir Alay Mountains of Central Asia. *Symbiosis (Philadelphia, Pa.)* **54**: 139–149.

Annals of Botany Supporting Information

Partial mycoheterotrophy is common among chlorophyllous plants with *Paris*-type arbuscular mycorrhiza

Philipp Giesemann, Hanne N. Rasmussen, Gerhard Gebauer

The following Supporting Information is available for this article:

Figure S1 *Ellenberg Indicator Value* (EIV) for light availability and temperature between *Arum*- (grey) and *Paris*-type (dark gold) arbuscular mycorrhizal (AM) plant species.

Table S1 Stable isotope enrichment factors ε (‰) with SD, leaf total N concentrations (N, mmol g^{-1}dry wt) with SD and the arbuscular mycorrhizal type (AM).

Table S2 Pairwise Dunn's *post hoc* test (Z) for significance of differences between chlorophyllous *Arum*- and *Paris*-type arbuscular mycorrhizal plant species separated by groups of horsetails, ferns and seed plants in enrichment factors $\varepsilon^{13}C$, $\varepsilon^{15}N$, $\varepsilon^{2}H$.

Table S3 Mann-Whitney *U* test for significance of differences between chlorophyllous *Paris*-type species and their respective chlorophyllous *Arum*-type reference plant species in stable isotope enrichment factors $\varepsilon^{13}C$, $\varepsilon^{15}N$, $\varepsilon^{2}H$.

Respective references

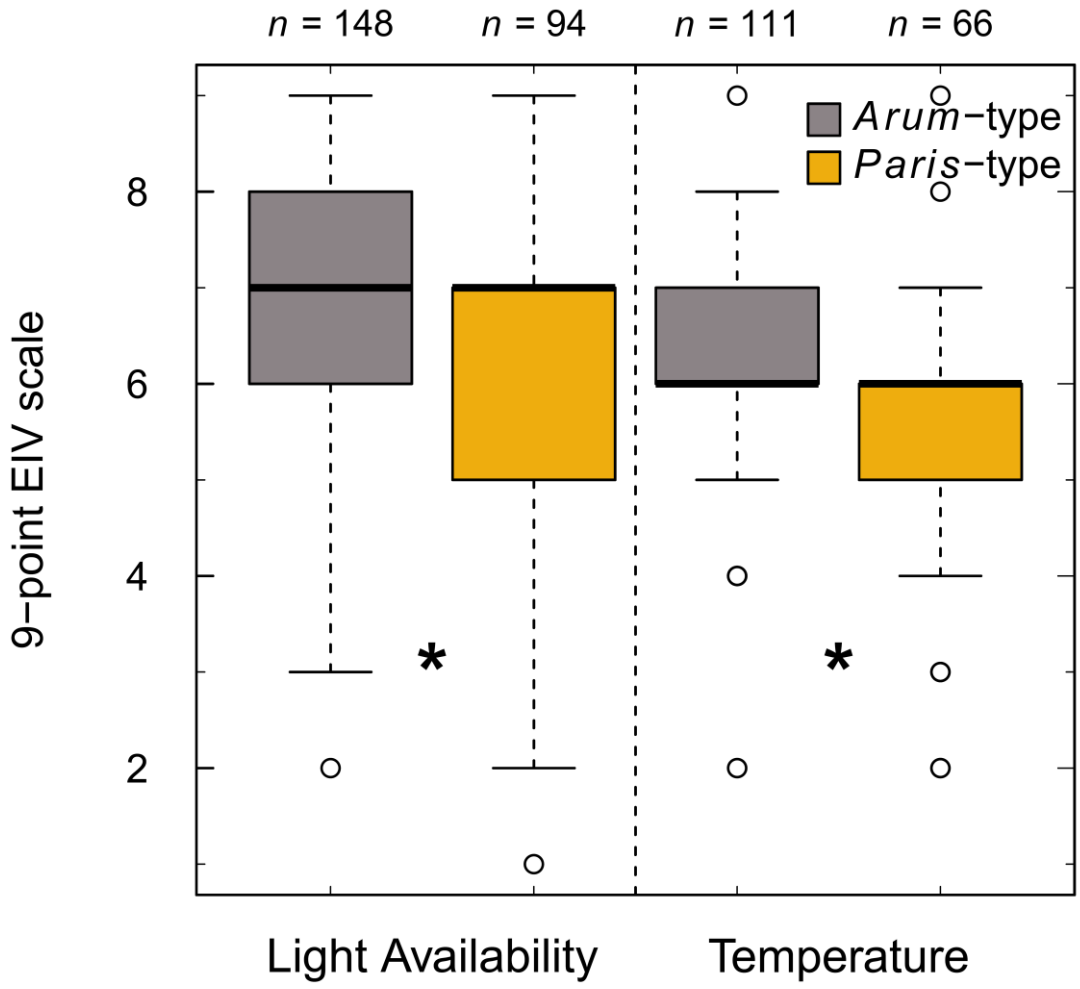

Figure S1 *Ellenberg Indicator Value* (EIV) for light availability and temperature between *Arum*- (grey) and *Paris*-type (dark gold) arbuscular mycorrhizal (AM) plant species. EIV and AM morphotype were obtained from literature (*cf.* Materials and Methods section). In both traits a significant difference was observed, *Paris*-type AM plant species occurring tendentially under lower light and temperature than *Arum*-type AM plant species ($U(148, 94) = 5416$, $P_{\text{Light Availability}} = 0.003$, Cohen's $d = 0.4$; $U(111, 66) = 2605$, $P_{\text{Temperature}} < 0.001$, Cohen's $d = 0.5$). The range of the boxes illustrate the first and third quartile, the horizontal solid lines represent the medians, the whiskers enclose data within the 1.5x interquartile range, colorless circles are data extremes.

Table S1 Stable isotope enrichment factors ε (‰) with SD, leaf total N concentrations (N, mmol g^{-1}dry wt) with SD and the arbuscular mycorrhizal type (AM). PT, *Paris*-type AM; AT, *Arum*-type AM; NA, not available.

Species (*n*)	AM-type/ literature	$\varepsilon^{13}C$ [‰]	$\varepsilon^{15}N$ [‰]	$\varepsilon^{2}H$ [‰]	$\varepsilon^{18}O$ [‰]	N	Isotope Literature
Acer campestre (2)	PT †, 1	1.7±1	1.1±1.7	NA	NA	1.4±0	Liebel *et al.*(2010)
Acer platanoides (9)	PT †, 1	0.2±0.8	-0.8±1.5	NA	NA	2.1±0.6	Gebauer and Meyer (2003), Giesemann *et al.*(2020a)
Acer pseudoplatanus (25)	PT *, 1	-1±1.2	0.2±1.3	19.9±9.9	2.5±4.6	1.3±0.3	Zimmer *et al.* (2007), Student course (2008) unpublished, Zimmer *et al.* (2008), Preiss *et al.* (2010), Schiebold *et al.* (2018)
Alchemilla alpina (10)	PT †, 2,3	0.3±0.6	-0.1±1.7	3.1±11	1.3±0.5	1.8±0.4	Student course (2008) unpublished, Student course (2018) unpublished
Alchemilla sp. (6)	PT †, 2,3	0.4±2.4	0.6±1	NA	NA	1.6±0.3	Student course (2008) unpublished
Alchemilla vulgaris (4)	PT †, 2,3	1.4±0.4	0.1±1	NA	NA	1.4±0.2	Gebauer and Meyer (2003)
Allium ursinum (5)	AT *, 1,4,5,6	0.4±0.3	0.6±0.1	-5±2	-0.9±0.3	2.2±0.1	Giesemann *et al.* (2020b)
Anagallis foemina (15)	AT †, 1,5	0±0	0±0	NA	NA	NA	Liebel *et al.* (2010)
Anemone nemorosa (10)	PT *, 1,‡	1.2±0.8	-0.8±1.3	5.6±2.4	-1.1±0.6	2.1±0.2	Giesemann *et al.*(2020a), Giesemann *et al.* (2020b)
Aquilegia atrata (15)	PT †, 7	0.1±0.8	-0.3±2.2	14.8±6.3	-0.1±1.2	1.8±0.7	Student course (2008) unpublished, Schiebold *et al.* (2018)
Arum maculatum (10)	AT *, 1,‡	0.3±0.4	-0.1±0.5	-0.8±3	-0.5±0.5	2.5±0.5	Giesemann *et al.* (2020b)
Arum pictum (5)	AT †, 1	0±0	0±0	NA	NA	1.9±0.3	Liebel *et al.* (2010)
Asarum europaeum (5)	PT *, 1	-2.8±0.8	-1.3±1	12.6±8.3	-0.7±0.7	1.4±0.2	Schiebold *et al.* (2018)
Asphodelus aestivus (25)	PT †, 1	0.9±1.3	0.2±1.2	NA	NA	NA	Liebel *et al.* (2010)
Asplenium ruta-muraria (5)	PT , ‡	1.1±1.4	-3.9±1.1	NA	NA	2±0.1	Giesemann *et al.* (2020a)
Astrantia major (25)	PT , ‡	0.8±0.9	-0.5±1	6.5±6	0.5±1.7	2±0.4	Schiebold *et al.* (2018), Student course (2018) unpublished
Athyrium filix-femina (5)	PT †, 1,‡	4.5±1.4	0.6±3.4	NA	NA	1.4±0.3	Giesemann *et al.* (2020a)
Athyrium japonicum (5)	PT †, 1	0.7±0.8	0±1.4	NA	NA	2.7±0.2	Lee *et al.* (2015)
Bellis perennis (5)	AT *, 1,‡	0±0	0±0	0±0	0±0	1.9±0.2	Student course (2018) unpublished
Blechnum sp. (2)	PT †, 3	2.5±1.9	0.5±1.5	NA	NA	0.9±0.1	Gomes *et al.* (2020)
Botrychium lunaria (6)	PT *, 1	-0.1±1.5	5.9±0.7	NA	NA	2.5±0.5	Student course (2008) unpublished
Brachypodium pinnatum (5)	PT *, 8	-0.2±1.4	-1.3±1.2	NA	NA	NA	Liebel *et al.* (2010)
Brachypodium sylvaticum (6)	PT †, 8	-0.8±0.8	1.4±1.1	NA	NA	1.6±0.5	Giesemann *et al.* (2020a)
Bromus erectus (29)	PT †, 5,8,‡	0.9±0.7	0.4±1.1	NA	NA	NA	Girlanda *et al.* (2011), Liebel *et al.* (2010)
Bromus sp. (21)	PT †, 5,8	0.5±1.1	-0.4±1.7	NA	NA	1.8±0.6	Ercole *et al.* (2015)
Buphthalmum salicifolium (1)	AT , ‡	0	0	NA	NA	1.9	Student course (2016) unpublished

Table S1 continued.

Species (*n*)	AM-type/ literature	$\varepsilon^{13}C$ [‰]	$\varepsilon^{15}N$ [‰]	$\varepsilon^{2}H$ [‰]	$\varepsilon^{18}O$ [‰]	N	Isotope Literature
Centaurea jacea (14)	AT †, 1,5,‡	-0.1±0.3	0.5±0.6	-1.8±4.2	-0.1±0.4	1.9±0.4	Schiebold *et al.* (2018)
Chrysanthemum leucanthemum (11)	AT †, 9,‡	-0.1±0.2	0.1±0.5	NA	NA	2.2±0.3	Gebauer & Meyer 2003
Colchicum autumnale (14)	PT *, 1	-1.2±1	0±1.6	NA	NA	1.6±0.1	Gebauer and Meyer (2003)
Commelina communis (9)	AT *, 1	0±0	0±0	NA	NA	3.8±0.2	Bidartondo *et al.* (2004), Giesemann *et al.* (2020a)
Convallaria majalis (27)	AT *, 1,10	0.1	-0.1	NA	NA	1.6	Lee *et al.* (2015), Suetsugu *et al.* (2017)
Cornus controversa (1)	PT †, 1	0.8	0.2	NA	NA	NA	Zimmer *et al.* (2007), Zimmer *et al.* (2008), Gebauer and Meyer (2003), Preiss *et al.* (2010), Hynson *et al.* (2015), Liebel *et al.* (2015)
Crepis vesicaria (10)	AT †, 5	0±0	0±0	NA	NA	NA	Girlanda *et al.* (2011), Liebel *et al.* (2010)
Daphne mezereum (3)	AT †, 1	0±0.1	0.3±0.7	NA	NA	2.3±0.1	Gebauer and Meyer (2003)
Diplazium sandwichianum (6)	PT †, 1	4.4±1.4	0.1±0.6	NA	NA	3±0.4	Hynson (2016)
Disporum smilacinum (1)	PT *, 1	-0.5	1.6	NA	NA	NA	Shutoh *et al.* (2016)
Dryopteris filix-mas (5)	PT , ‡	3.5±1.2	-0.1±1.8	NA	NA	1.5±0.1	Giesemann *et al.* (2020a)
Equisetum arvense (5)	PT *.†, 1	3.1±0.5	2.2±1	NA	NA	2.5±0.3	Giesemann *et al.* (2020a)
Equisetum fluviatile (5)	PT *.†, 1	0.4±0.1	4.4±1.3	NA	NA	1.9±0.2	Giesemann *et al.* (2020a)
Equisetum palustre (5)	PT *.†, 1	0.8±0.4	7.7±3.2	18.6±3	4.6±1.5	3.1±0.4	Giesemann *et al.* (2020a)
Equisetum sylvaticum (4)	PT *.†, 1	3.1±0.7	7.4±3	14±5.2	2.7±0.8	1.9±0.2	Giesemann *et al.* (2020a)
Equisetum telmateia (5)	PT *.†, 1	2±1.1	3.3±1.9	NA	NA	1.4±0.2	Giesemann *et al.* (2020a)
Erodium cicutarium (5)	AT †, 1	0±0	0±0	NA	NA	1.6±0.1	Giesemann *et al.* (2020a)
Fragaria vesca (35)	AT *, 1	0.2±0.4	0±0.8	-3±4.8	0.1±0.2	1.4±0.3	Student course (2008) unpublished, Zimmer *et al.* (2008), Student course (2016) unpublished, Schiebold *et al.* (2017), Schiebold *et al.* (2018), Giesemann *et al.* (2020a)
Fraxinus excelsior (6)	AT *, 1	-0.3±0.3	-0.2±0.4	7.1±3.5	1.1±0.3	1.9±0.8	Student course (2008) unpublished, Giesemann *et al.* (2020b)
Galium aparine (5)	AT *, 5	-0.9±0.3	0.3±0.4	NA	NA	3±0.6	Giesemann *et al.* (2020a)

Table S1
continued.

Species (*n*)	AM-type/ literature	$\varepsilon^{13}C$ [‰]	$\varepsilon^{15}N$ [‰]	$\varepsilon^{2}H$ [‰]	$\varepsilon^{18}O$ [‰]	N	Isotope Literature
Gentiana asclepiadeae (5)	PT *, 1	1±1.1	4±1	-7.1±5	0.8±1	2.2±0.2	Student course (2018) unpublished
Gentiana bavaria (5)	PT †, 1	0.2±1.3	2.9±0.7	-15.5±7.8	-5.5±10.3	1.4±0.1	Student course (2018) unpublished
Gentiana lutea (5)	PT *, 1	3.5±1	1.9±0.5	-12.9±4.7	1.7±1.6	1.6±0.2	Student course (2018) unpublished
Geranium robertianum (5)	PT †, 1,11,however 5	-1.1±0.5	-2.7±2.5	NA	NA	2.6±0.5	Liebel *et al.* (2010)
Geranium sylvaticum (5)	PT †, 1,11,however 5	2.5±0.5	-0.9±1.1	NA	NA	1.8±0.1	Gebauer and Meyer (2003)
Hedera helix (17)	AT *, 1	0±0.6	-0.1±0.6	-0.5±2.2	0.8±0.3	1.5±0.3	Liebel *et al.* (2010), Giesemann *et al.* (2020b)
Hieracium pilosella (1)	AT *, 1,8	0	0	NA	NA	2.1	Gebauer and Meyer (2003)
Holcus mollis (5)	AT †, 1	0±0	0±0	NA	NA	1.9±0.1	Giesemann *et al.* (2020a)
Homogyne alpina (5)	AT , ‡	0±0	0±0	NA	NA	1.6±0.3	Student course (2008) unpublished
Ilex macropoda (1)	PT †, 1	0.1	4.6	NA	NA	NA	Shutoh *et al.* (2016)
Impatiens parviflora (5)	AT †, 1,5	0±0	0±0	NA	NA	1.8±0.2	Schiebold *et al.* (2017)
Juniperus communis (2)	AT †, 1	0±0	0±0	NA	NA	1±0	Bidartondo *et al.* (2004)
Knautia sylvatica (10)	AT †, 9	0±0	0±0	NA	NA	1.1±0.1	Student course (2007) unpublished, Hynson *et al.* (2009)
Lamium galeobdolon (5)	AT , ‡	-0.5±0.9	1.5±1.5	NA	NA	2.4±0.3	Giesemann *et al.* (2020a)
Leontodon tuberosus (5)	AT †, 1	0±0	0±0	NA	NA	NA	Liebel *et al.* (2010)
Leptospermum sp. (2)	AT †, 1	-1.2±1.2	3.3±0.1	NA	NA	0.3±0.1	Gomes *et al.* (2020)
Ligusticum mutellina (5)	PT , ‡	0.8±0.2	1.7±1.1	13.8±4.4	0.3±0.7	2.4±0.1	Student course (2018) unpublished
Ligustrum vulgare (5)	AT *, 1	-0.3±0.4	0.4±0.3	NA	NA	NA	Liebel *et al.* (2010)
Lindera benzoin (1)	AT †, 1	0	0	NA	NA	NA	Cameron and Bolin (2010)
Lindera umbellata (1)	AT *, 1	0	0	NA	NA	NA	Shutoh *et al.* (2016)
Liriodendron tulipifera (1)	PT *, 1	0	-1.6	NA	NA	NA	Cameron and Bolin (2010)
Lysimachia nummularia (5)	PT *, 12	1.1±0.5	0.9±1.7	2.7±4.6	0.3±1.1	1.2±0.2	Giesemann *et al.* (2020a)
Lysimachia vulgaris (19)	AT *, 1	0.1±0.9	0.7±1.2	NA	NA	1.6±0.3	Bidartondo *et al.* (2004), Giesemann *et al.* (2020a)
Matteuccia struthiopteris (5)	PT , ‡	0.3±0.8	0.4±2.4	NA	NA	1.4±0.2	Giesemann *et al.* (2020a)
Melica nutans (4)	PT †, ‡,however 8	0.8±0.8	-0.2±1	NA	NA	2.1±0.1	Gebauer and Meyer (2003)
Mercurialis perennis (31)	PT *, 13,‡	1.6±1.1	1.1±1.4	21.4±6.4	0.2±1	2±0.5	Student course (2007) unpublished, Student course (2008) unpublished, Hynson *et al.* (2009), Student course (2016) unpublished, Student course (2018) unpublished

Table S1 continued.

Species (*n*)	AM-type/ literature			$\varepsilon^{13}C$ [‰]	$\varepsilon^{15}N$ [‰]	$\varepsilon^{2}H$ [‰]	$\varepsilon^{18}O$ [‰]	N	Isotope Literature
Meum athamanticum (10)	PT	,	‡	2.2±0.8	-0.7±2.8	NA	NA	2.5±0.2	Gebauer and Meyer (2003)
Molinia caerulea (7)	PT	†,	1	0.3±1.3	0.7±0.8	NA	NA	2.1±0.3	Schiebold *et al.* (2018), Giesemann *et al.* (2020a)
Myrsine seguinii (5)	PT	†,	1	1.3±1.1	-1.2±1.2	NA	NA	0.9±0.2	Ogura-Tsujita *et al.* (2018), Ogura-Tsujita *et al.* unpublished
Olearia sp. (3)	AT	†,	1	0.4±0.2	-1±0.7	NA	NA	0.9±0.1	Gomes *et al.* (2020)
Oplismenus undulatifolius (1)	AT	*,	1	0	0	NA	NA	NA	Suetsugu *et al.* (2017)
Origanum vulgaris (5)	AT	*,	14,however 1	-1.3±0.5	-0.1±1	-7.2±4.4	1.6±0.3	1.3±0.2	Student course (2018) unpublished
Oxalis acetosella (10)	PT	†,	1,5, ‡,however 1,15	1±1	-0.7±1.9	11.1±4.8	6.5±3	1.7±0.4	Liebel *et al.* (2015), Schiebold *et al.* (2018), Giesemann *et al.* (2020a)
Paederia scandens (5)	PT	*,	1	-0.2±0.9	-0.9±1.9	NA	NA	NA	Suetsugu *et al.* (2017)
Paris quadrifolia (13)	PT	*,	1,‡	2.3±0.8	0.7±0.6	8.6±4.2	-0.4±0.4	2.1±0.3	Hynson *et al.* (2015), Giesemann *et al.* (2020b)
Pimpinella saxifraga (15)	PT	†,	1,10	0.3±0.6	1.6±1.6	NA	NA	NA	Girlanda *et al.* (2011), Liebel *et al.* (2010)
Plantago lanceolata (76)	AT	*,	1,5,‡	0±0.6	-0.3±1	1.7±4.1	0.1±0.4	1.4±0.4	Gebauer and Meyer (2003), Girlanda *et al.* (2011), Liebel *et al.* (2010), Ercole *et al.* (2015), Schiebold *et al.* (2018), Giesemann *et al.* (2020a)
Plantago media (5)	AT	*,	8	1.3±0.5	0.1±1	7.2±4.4	-1.6±0.3	1.2±0.2	Student course (2018) unpublished
Plantago sp. (3)	AT	†,	1,5	0±0	0±0	NA	NA	NA	Student Course (2008) unpublished
Poa sp. (5)	AT	†,	15,‡,however 1,3,5	0±0	0±0	NA	NA	1.9±0.3	Giesemann *et al.* (2020a)
Polygala chamaebuxus (4)	AT	†,	1,‡	0±0	0±0	NA	NA	1.8±0.2	Gebauer and Meyer (2003)
Polygonatum sp. (5)	AT	†,	1	0.2±0.3	-0.8±0.8	NA	NA	2.6±0.2	Student course (2018) unpublished
Polypodium vulgare (5)	PT	,	‡	2.3±0.8	-2.8±0.8	NA	NA	1.8±0.3	Giesemann *et al.* (2020a)
Polystichum sp. (16)	PT	†,	3	3.1±1.5	-0.3±1.8	NA	NA	1.1±0.4	Gomes *et al.* (2020)
Pomaderris sp. (14)	AT	†,	1	0.2±0.9	-0.5±1.7	NA	NA	1.1±0.4	Gomes *et al.* (2020)
Potentilla erecta (32)	AT	*,	10	0±0.6	-0.1±0.4	1.3±2.4	0.4±0.8	1.8±0.3	Student course (2008) unpublished, Student course (2016) unpublished, Schiebold *et al.* (2018), Student course (2018) unpublished, Giesemann *et al.* (2020a)
Potentilla neumanniana (5)	AT	†,	4,6,8,10	1±0.2	0.7±0.1	NA	NA	NA	Liebel *et al.* (2010)
Potentilla sp. (5)	AT	†,	4,6,8,10	0.3±0.7	1.1±3.6	NA	NA	1.7±0.3	Ercole *et al.* (2015)
Prenanthes purpurea (6)	AT	,	‡	-0.2±0.2	0.6±0.8	NA	NA	2.2±0.4	Schiebold *et al.* (2018), Student course (2018) unpublished

Table S1
continued.

Species (*n*)	AM-type/ literature			$\varepsilon^{13}C$ [‰]	$\varepsilon^{15}N$ [‰]	$\varepsilon^{2}H$ [‰]	$\varepsilon^{18}O$ [‰]	N	Isotope Literature
Prunella vulgaris (5)	AT	*,	10,‡	-1±1.1	-0.1±0.3	-3.6±2.8	-1±1	1.6±0.1	Schiebold *et al.* (2018)
Prunus spinosa (7)	AT	†,	1,however 15	-0.1±0.8	0.6±1.2	NA	NA	NA	Liebel *et al.* (2010)
Psychotria serpens (5)	AT	†,	1	0±0	0±0	NA	NA	1.3±0.1	Ogura-Tsujita *et al.* (2018), Ogura-Tsujita *et al.* unpublished
Pteridium sp. (2)	PT	†,	1	3.3±0.3	0.9±1.3	NA	NA	1.6±0.7	Gomes *et al.* (2020)
Ranunculus sp. (23)	PT	†,	1,11,however 9	0.3±1	0.2±3.2	NA	NA	2±0.5	Ercole *et al.* (2015)
Rubus argutus (4)	AT	†,	1	0±0.6	0±1.4	NA	NA	2.2±0.3	Hynson (2016)
Rubus idaeus (14)	AT	†,	1	0±0	0±0	NA	NA	1.4±0.2	Giesemann *et al.* (2020a)
Salvia pratensis (21)	AT	†,	5,7,8,10,16	0.1±0.6	-0.1±0.9	NA	NA	1.7±0.4	Liebel *et al.* (2010), Ercole *et al.* (2015)
Sanguisorba minor (5)	AT	†,	6,10	-0.3±0.2	-1.1±0.3	NA	NA	NA	Liebel *et al.* (2010)
Sanguisorba sp. (10)	AT	†,	6,10	-0.2±0.7	-0.1±2.7	NA	NA	1.6±0.3	Ercole *et al.* (2015)
Scandix pecten-veneris (10)	PT	*,	5	1.1±0.8	-1.5±0.6	NA	NA	NA	Liebel *et al.* (2010)
Sesleria albicans (6)	PT	†,	9	1.4±1.9	-0.9±1.1	NA	NA	1.2±0.4	Gebauer and Meyer (2003), Bidartondo *et al.* (2004)
Smilax aspera (5)	PT	*,	1	1.3±0.9	1.5±2.3	NA	NA	1±0.3	Liebel *et al.* (2010)
Solidago virgaurea (3)	AT	*,	1	-1.6±0.2	0.5±0.1	NA	NA	2.2±0.1	Hynson *et al.* (2015)
Sorbus aucuparia (11)	PT	†,	1	0.2±0.9	-0.6±0.9	10.5	-2.8	1±0.2	Zimmer *et al.* (2007), Zimmer *et al.* (2008), Schiebold *et al.* (2018)
Tamus communis (5)	PT	*,	1	0.9±1.1	1.6±0.9	NA	NA	NA	Liebel *et al.* (2010)
Taraxacum officinalis (10)	AT	*,	1,10,‡	-0.3±0.6	0.1±1.3	5.3±5.4	-0.1±0.3	1.9±0.8	Giesemann *et al.* (2020a)
Teucrium botrys (5)	AT	*,	10	0±0	0±0	NA	NA	NA	Liebel *et al.* (2010)
Teucrium marum (5)	AT	†,	10	0±0	0±0	NA	NA	NA	Liebel *et al.* (2010)
Teucrium polium (5)	AT	†,	10	-1±0.2	-0.7±0.1	NA	NA	NA	Liebel *et al.* (2010)
Tripterospermum japonicum (1)	PT	*,	1	0.8	1.8	NA	NA	NA	Shutoh *et al.* (2016)
Trollius europaeus (5)	PT	,	‡	1.7±1	0.4±1.8	21.3±5.6	0.3±1	1.8±0.5	Schiebold *et al.* (2018)
Urtica dioica (5)	AT	*,	1,5	0.9±0.3	-0.3±0.4	NA	NA	2.8±0.5	Giesemann *et al.* (2020a)
Veronica urticifolia (1)	AT	†,	1	0	0	0	0	1.7	Schiebold *et al.* (2018)
Viburnum dilatatum (1)	PT	*,	1	-0.9	3.8	NA	NA	NA	Shutoh *et al.* (2016)
Viola arvensis (5)	PT	†,	1,4,however 7,16	-0.1±1.1	0.3±1.1	NA	NA	1.3±0.3	Giesemann *et al.* (2020a)
Viola sp. (10)	PT	†,	1,4,however 7,16	-0.8±1.2	-0.3±1.7	NA	NA	1.3±0.2	Schiebold *et al.* (2017)

Table S1
continued.

The arbuscular mycorrhizal subtype was obtained from **1** Dickson *et al.* (2007), **2** Becerra *et al.* (2007), **3** Menoyo *et al.* (2007), **4** Nobis *et al.* (2015), **5** Shah *et al.* (2009), **6** Shi *et al.* (2013), **7** Zubek *et al.* (2011b), **8** Turnau *et al.* (2008), **9** Zubek *et al.* (2008), **10** Zubek *et al.* (2011a), **11** Druva-Lusite and Ievinsh (2010), **12** Kołaczek *et al.* (2013), **13** Diallo *et al.* (2001), **14** Burni and Hussain (2011), **15** Velázquez *et al.* (2010), **16** Zubek and Błaszkowski (2009). Subtype classification on the level of species "*", and on genera "†" (*cf.* morphotype is in most cases consistent across species of the same genus; Dickson *et al.*, 2007), ‡ personal observation.

Table S2 Pairwise Dunn's *post hoc* test (Z) for significance of differences between chlorophyllous *Arum*- and *Paris*-type arbuscular mycorrhizal plant species separated by groups of horsetails, ferns and seed plants in enrichment factors $\varepsilon^{13}C$, $\varepsilon^{15}N$, $\varepsilon^{2}H$. Significances are highlighted in bold. NA, not available.

	$\varepsilon^{13}C$		**$\varepsilon^{15}N$**		**$\varepsilon^{2}H$**	
	Test statistics	*P*	Test statistics	*P*	Test statistics	*P*
Arum-type seed plants vs *Paris-type* seed plants	*Z* = -8.661	**< 0.001**	*Z* = -1.808	= 0.071	*Z* = -5.873	**< 0.001**
Paris-type ferns vs *Arum-type* seed plants	*Z* = 10.321	**< 0.001**	*Z* = -1.170	= 0.121	NA	
Paris-type horsetails vs *Arum*-type seed plants	*Z* = 6.942	**< 0.001**	*Z* = 7.853	**< 0.001**	*Z* = 5.076	**< 0.001**
Paris-type fern vs *Paris*-type seed plants	*Z* = 6.040	**< 0.001**	*Z* = -2.025	= 0.064	NA	
Paris-type horsetails vs *Paris*-type seed plants	*Z* = 4.233	**< 0.001**	*Z* = 7.256	**< 0.001**	*Z* = 2.634	**= 0.004**
Paris-type horsetails vs *Paris*-type ferns	*Z* = 0.305	= 0.380	*Z* = 7.482	**< 0.001**	NA	

The groups were significantly distinguished in ^{13}C ($H(3) = 179.42$, $P = 0$), ^{15}N ($H(3) = 65.80$, $P = 0$), ^{2}H ($H(2) = 50.64$, $P = 0$). The data comprised for $^{13}C/^{15}N$ 47 species ($n = 433$) of *Paris*-type seed plants and 11 species ($n = 63$) of *Paris*-type ferns, 5 species ($n = 24$) of *Paris*-type horsetails, and 59 species ($n = 530$) of *Arum*-type seed plants The sample sizes for ^{2}H were 16 species ($n = 91$) of *Paris*-type seed plants and 2 species ($n = 9$) of *Paris*-type horsetails, and 15 species (n = 104) of *Arum*-type seed plants.

Table S3 Mann-Whitney *U* test for significance of differences between chlorophyllous *Paris*-type species and their respective chlorophyllous *Arum*-type reference plant species in stable isotope enrichment factors $\varepsilon^{13}C$, $\varepsilon^{15}N$, $\varepsilon^{2}H$. Stable isotope enrichments were calculated relative to neighboring *Arum*-type arbuscular mycorrhizal reference plants. Significances are highlighted in bold. Nomenclature follows the sources APG IV (2016) and PPG1 (2016). Family sequence according to PPG1 (2016) (pteridophytes), Haston *et al.* (2009) and APG IV (2016) (angiosperms).

	Species	Family	n_{target}, $n_{reference}$	$\varepsilon^{13}C$		$\varepsilon^{15}N$		n_{target}, $n_{reference}$	$\varepsilon^{2}H$	
				U	*P*	U	*P*		U	*P*
H,o	*Equisetum arvense*	Equisetaceae	5 , 5	25	**0.004**	25	**0.004**	0 , 0	NA	
H,f	*Equisetum fluviatile*	Equisetaceae	5 , 5	25	**0.004**	25	**0.004**	0 , 0	NA	
H,f	*Equisetum palustre*	Equisetaceae	5 , 10	38	0.063	50	**0.001**	5 , 10	50	**0.001**
H,f	*Equisetum sylvaticum*	Equisetaceae	4 , 8	32	**0.004**	32	**0.004**	4 , 8	30	**0.011**
H,f	*Equisetum telmateia*	Equisetaceae	5 , 10	45	**0.008**	45	**0.001**	0 , 0	NA	
F,o	*Botrychium lunaria*	Ophioglossaceae	7 , 3	12	0.409	21	**0.011**	0 , 0	NA	
F,f	*Pteridium sp.*	Dennstaedtiaceae	2 , 9	18	**0.023**	11	0.362	0 , 0	NA	
F,f	*Asplenium ruta-muraria*	Aspleniaceae	5 , 5	20	0.059	0	0.998	0 , 0	NA	
F,f	*Matteuccia struthiopteris*	Onocleaceae	5 , 5	15	0.328	10	0.748	0 , 0	NA	
F,f	*Blechnum* sp.	Blechnaceae	2 , 19	36	**0.024**	23	0.338	0 , 0	NA	
F,f	*Athyrium filix-femina*	Athyriaceae	5 , 5	25	**0.004**	10	0.748	0 , 0	NA	
F,f	*Athyrium japonicum*	Athyriaceae	5 , 5	20	0.059	10	0.748	0 , 0	NA	
F,f	*Diplazium sandwichianum*	Athyriaceae	6 , 4	24	**0.007**	13	0.458	0 , 0	NA	
F,f	*Dryopteris filix-mas*	Dryopteridaceae	5 , 5	25	**0.004**	5	0.963	0 , 0	NA	
F,f	*Polystichum sp.*	Dryopteridaceae	16 , 19	283	**< 0.001**	150	0.533	0 , 0	NA	
F,f	*Polypodium vulgare*	Polypodiaceae	5 , 5	25	**0.004**	0	0.998	0 , 0	NA	
S,f	*Asarum europaeum*	Aristolochiaceae	5 , 5	0	0.508	0	0.508	5 , 5	25	**0.004**
S,f	*Liriodendron tulipifera*	Magnoliaceae	1 , 1	1	0.5	0	0.977	0 , 0	NA	
S,f	*Tamus communis*	Dioscoreaceae	5 , 10	39	**0.049**	48	**0.003**	0 , 0	NA	
S,f	*Paris quadrifolia*	Melanthiaceae	13 , 31	395	**< 0.001**	330	**< 0.001**	10 , 25	223	**< 0.001**
S,f	*Colchicum autumnale*	Colchicaceae	14 , 24	69	0.999	204	0.141	0 , 0	NA	
S,f	*Disporum smilacinum*	Colchicaceae	1 , 1	0	0.977	1	0.5	0 , 0	NA	
S,f	*Smilax aspera*	Smilacaceae	5 , 5	25	**0.004**	15	0.328	0 , 0	NA	

Table S3
continued.

	Species	Family	n_{target}, $n_{reference}$	$\varepsilon^{13}C$		$\varepsilon^{15}N$		n_{target}, $n_{reference}$	$\varepsilon^{2}H$	
				U	*P*	U	*P*		U	*P*
S,o	*Asphodelus aestivus*	Asphodelaceae	25 , 25	450	**0.002**	350	0.221	0 , 0	NA	
S,o	*Brachypodium pinnatum*	Poaceae	5 , 5	10	0.748	5	0.963	0 , 0	NA	
S,f	*Brachypodium sylvaticum*	Poaceae	5 , 5	0	0.998	21	**0.042**	0 , 0	NA	
S,o	*Bromus erectus*	Poaceae	29 , 39	909	**< 0.001**	697	0.05	0 , 0	NA	
S,o	*Bromus sp.*	Poaceae	21 , 41	596	**0.007**	345	0.9	0 , 0	NA	
S,f	*Melica nutans*	Poaceae	4 , 6	24	**0.007**	11	0.626	0 , 0	NA	
S,o	*Molinia caerulea*	Poaceae	7 , 7	42	0.707	42	**0.01**	1 , 1	1	0.5
S,f	*Sesleria albicans*	Poaceae	6 , 6	24	0.174	6	0.984	0 , 0	NA	
S,f	*Anemone nemorosa*	Ranunculaceae	10 , 15	135	**< 0.001**	25	0.998	5 , 10	47	**0.001**
S,o	*Aquilegia atrata*	Ranunculaceae	16 , 16	128	1	128	1	5 , 5	25	**0.007**
S,o	*Ranunculus sp.*	Ranunculaceae	23 , 51	759	**0.022**	560	0.624	0 , 0	NA	
S,o	*Trollius europaeus*	Ranunculaceae	5 , 10	38	0.063	30	0.291	5 , 10	50	**0.003**
S,o	*Alchemilla alpina*	Rosaceae	10 , 10	60	0.222	60	0.222	4 , 5	10	0.553
S,o	*Alchemilla* sp.	Rosaceae	6 , 5	25	**0.034**	25	**0.034**	0 , 0	NA	
S,o	*Alchemilla vulgaris*	Rosaceae	4 , 8	32	**0.004**	16	0.534	0 , 0	NA	
S,f	*Sorbus aucuparia*	Rosaceae	11 , 10	44	0.81	66	0.212	1 , 1	1	0.5
S,f	*Oxalis acetosella*	Oxalidaceae	9 , 9	72	**0.001**	18	0.985	4 , 4	16	**0.011**
S,f	*Mercurialis perennis*	Euphorbiaceae	31 , 39	1152	**< 0.001**	981	**< 0.001**	5 , 5	25	**0.004**
S,o	*Viola arvensis*	Violaceae	5 , 5	10	0.748	15	0.328	0 , 0	NA	
S,f	*Viola sp.*	Violaceae	10 , 10	10	1	50	0.516	0 , 0	NA	
S,f	*Geranium robertianum*	Geraniaceae	5 , 5	0	0.998	0	0.998	0 , 0	NA	
S,f	*Geranium sylvaticum*	Geraniaceae	5 , 10	50	**0.001**	10	0.971	0 , 0	NA	
S,f	*Acer campestre*	Sapindaceae	2 , 4	7	0.124	6	0.244	0 , 0	NA	
S,f	*Acer platanoides*	Sapindaceae	9 , 11	20	0.181	12	0.991	0 , 0	NA	
S,f	*Acer pseudoplatanus*	Sapindaceae	29 , 33	179	1	641	**0.009**	3 , 3	9	**0.032**
S,f	*Cornus controversa*	Cornaceae	1 , 1	1	0.5	1	0.5	0 , 0	NA	
S,f	*Lysimachia nummularia*	Primulaceae	5 , 10	43	**0.016**	32	0.213	5 , 10	29	0.334
S,o	*Myrsine seguinii*	Primulaceae	5 , 5	20	0.059	5	0.963	0 , 0	NA	
S,f	*Paederia scandens*	Rubiaceae	5 , 5	10	0.748	5	0.963	0 , 0	NA	
S,o	*Gentiana asclepiadeae*	Gentianaceae	5 , 5	20	0.059	25	**0.004**	5 , 5	0	0.998
S,o	*Gentiana bavarica*	Gentianaceae	5 , 5	10	0.748	25	**0.004**	4 , 5	0	0.998
S,o	*Gentiana lutea*	Gentianaceae	5 , 10	50	**0.001**	50	**0.001**	5 , 10	4	0.996

Table S3
continued.

	Species	Family	n_{target}, $n_{reference}$	$\varepsilon^{13}C$		$\varepsilon^{15}N$		n_{target}, $n_{reference}$	$\varepsilon^{2}H$	
				U	*P*	U	*P*		U	*P*
S,o	*Tripterospermum japonicum*	Gentianaceae	1 , 1	1	0.5	1	0.5	0 , 0	NA	
S,f	*Ilex macropoda*	Aquifoliaceae	1 , 1	1	0.5	1	0.5	0 , 0	NA	
S,o	*Viburnum dilatatum*	Adoxaceae	1 , 1	0	0.977	1	0.5	0 , 0	NA	
S,o	*Meum athamanticum*	Apiaceae	10 , 15	150	**< 0.001**	47	0.944	0 , 0	NA	
S,o	*Pimpinella saxifraga*	Apiaceae	15 , 15	150	0.05	195	**< 0.001**	0 , 0	NA	
S,o	*Scandix pecten-veneris*	Apiaceae	10 , 10	80	**0.009**	0	1	0 , 0	NA	
S,o	*Astrantia major*	Apiaceae	25 , 49	980	**< 0.001**	413	0.989	20 , 39	608	**< 0.001**
S,o	*Ligusticum mutellina*	Apiaceae	5 , 5	25	**0.004**	25	**0.004**	4 , 5	20	**0.005**

F, fern; H, horsetail; S, seed plant; f, forest; o, open-land; NA, not available

Respective references

Becerra A, Cabello M, Chiarini F. 2007. Arbuscular mycorrhizal colonization of vascular plants from the Yungas forests, Argentina. *Annals of Forest Science* **64**: 765–772. doi:10.1051/forest:2007056.

Bidartondo MI, Burghardt B, Gebauer G, Bruns TD, Read DJ. 2004. Changing partners in the dark: Isotopic and molecular evidence of ectomycorrhizal liaisons between forest orchids and trees. *Proceedings of the Royal Society B: Biological Sciences* **271**: 1799–1806. doi:10.1098/rspb.2004.2807.

Burni T, Hussain F. 2011. Diversity in arbuscular mycorrhizal morphology in some medicinal plants of family Lamiaceae. *Pakistan Journal of Botany* **43**: 1789–1792.

Cameron DD, Bolin JF. 2010. Isotopic evidence of partial mycoheterotrophy in the Gentianaceae *Bartonia virginica* and *Obolaria virginica* as case studies. *American Journal of Botany* **97**: 1272–1277. doi:10.3732/ajb.0900292.

Diallo A, Weber H, Imhof S. 2001. Sonderstellung der Mykorrhiza von *Mercurialis perennis* L. im Vergleich mit anderen Euphorbiaceae. *Beiträge zur Biologie der Pflanzen* **72**: 315–323.

Dickson S, Smith FA, Smith SE. 2007. Structural differences in arbuscular mycorrhizal symbioses: more than 100 years after Gallaud, where next? *Mycorrhiza* **17**: 375–393. doi:10.1007/s00572-007-0130-9.

Druva-Lusite I, Ievinsh G. 2010. Diversity of arbuscular mycorrhizal symbiosis in plants from coastal habitats. *Environmental and Experimental Biology* **8**: 17–34.

Ercole E, Adamo M, Rodda M, Gebauer G, Girlanda M, Perotto S. 2015. Temporal variation in mycorrhizal diversity and carbon and nitrogen stable isotope abundance in the wintergreen meadow orchid Anacamptis morio. *New Phytologist* **205**: 1308–1319. doi:10.1111/nph.13109.

Gebauer G, Meyer M. 2003. ^{15}N and ^{13}C natural abundance of autotrophic and myco-heterotrophic orchids provides insight into nitrogen and carbon gain from fungal association. *New Phytologist* **160**: 209–223. doi:10.1046/j.1469-8137.2003.00872.x.

Giesemann P, Eichenberg D, Stöckel M*, et al.* 2020a. Dark septate endophytes and arbuscular mycorrhizal fungi (*Paris*-morphotype) affect the stable isotope composition of 'classically' non-mycorrhizal plants. *Functional Ecology* **34**: 2453–2466. doi:10.1111/1365-2435.13673.

Giesemann P, Rasmussen HN, Liebel HT, Gebauer G. 2020b. Discreet heterotrophs: Green plants that receive fungal carbon through *Paris*-type arbuscular mycorrhiza. *New Phytologist* **226**: 960-966. doi:10.1111/nph.16367.

Girlanda M, Segreto R, Cafasso D*, et al.* 2011. Photosynthetic Mediterranean meadow orchids feature partial mycoheterotrophy and specific mycorrhizal associations. *American Journal of Botany* **98**: 1148–1163. doi:10.3732/ajb.1000486.

Gomes S, Merckx V, Kehl J, Gebauer G. 2020. Mycoheterotrophic plants living on arbuscular mycorrhizal fungi are generally enriched in ^{13}C, ^{15}N, and ^{2}H isotopes. *Journal of Ecology* **108**: 1250–1261. doi:10.1111/1365-2745.13381.

Hynson NA. 2016. The carbon and nitrogen ecophysiologies of two endemic tropical orchids mirrors those of their temperate relatives and the local environment. *Royal Society open science* **3**: 160427. doi:10.1098/rsos.160427.

Hynson NA, Bidartondo MI, Read DJ. 2015. Are there geographic mosaics of mycorrhizal specificity and partial mycoheterotrophy? A case study in *Moneses uniflora* (Ericaceae). *New Phytologist* **208**: 1003–1007. doi:10.1111/nph.13587.

Hynson NA, Preiss K, Gebauer G, Bruns TD. 2009. Isotopic evidence of full and partial myco-heterotrophy in the plant tribe Pyroleae (Ericaceae). *New Phytologist* **182**: 719–726. doi:10.1111/j.1469-8137.2009.02781.x.

Kołaczek P, Zubek S, Błaszkowski J, Mleczko P, Margielewski W. 2013. Erosion or plant succession — How to interpret the presence of arbuscular mycorrhizal fungi (Glomeromycota) spores in pollen profiles collected from mires. *Review of Palaeobotany and Palynology* **189**: 29–37. doi:10.1016/j.revpalbo.2012.11.006.

Lee Y-I, Yang C-K, Gebauer G. 2015. The importance of associations with saprotrophic non-*Rhizoctonia* fungi among fully mycoheterotrophic orchids is currently under-estimated: Novel evidence from sub-tropical Asia. *Annals of Botany* **116**: 423–435. doi:10.1093/aob/mcv085.

Liebel HT, Bidartondo MI, Gebauer G. 2015. Are carbon and nitrogen exchange between fungi and the orchid *Goodyera repens* affected by irradiance? *Annals of Botany* **115**: 251–261. doi:10.1093/aob/mcu240.

Liebel HT, Bidartondo MI, Preiss K*, et al.* 2010. C and N stable isotope signatures reveal constraints to nutritional modes in orchids from the Mediterranean and Macaronesia. *American Journal of Botany* **97**: 903–912. doi:10.3732/ajb.0900354.

Menoyo E, Beccera A, Rension D. 2007. Mycorrhizal assiciations in *Polylepsis* woodlands of Central Argentina. *Canadian Journal of Botany* **85**: 526–531. doi:10.1139/B07-042.

Nobis A, Błaszkowski J, Zubek S. 2015. Arbuscular mycorrhizal fungi associations of vascular plants confined to river valleys: Towards understanding the river corridor plant distribution. *Journal of Plant Research* **128**: 127–137. doi:10.1007/s10265-014-0680-9.

Ogura-Tsujita Y, Gebauer G, Xu H*, et al.* 2018. The giant mycoheterotrophic orchid *Erythrorchis altissima* is associated mainly with a divergent set of wood-decaying fungi. *Molecular Ecology* **27**: 1324–1337. doi:10.1111/mec.14524.

Preiss K, Adam IKU, Gebauer G. 2010. Irradiance governs exploitation of fungi: fine-tuning of carbon gain by two partially myco-heterotrophic orchids. *Proceedings of the Royal Society B: Biological Sciences* **277**: 1333–1336. doi:10.1098/rspb.2009.1966.

Schiebold JM-I, Bidartondo MI, Karasch P, Gravendeel B, Gebauer G. 2017. You are what you get from your fungi: nitrogen stable isotope patterns in *Epipactis* species. *Annals of Botany* **119**: 1085–1095. doi:10.1093/aob/mcw265.

Schiebold JM-I, Bidartondo MI, Lenhard F, Makiola A, Gebauer G. 2018. Exploiting mycorrhizas in broad daylight: Partial mycoheterotrophy is a common nutritional strategy in meadow orchids. *Journal of Ecology* **106**: 168–178. doi:10.1111/1365-2745.12831.

Shah MA, Reshi ZA, Khasa D. 2009. Arbuscular mycorrhizal status of some Kashmir Himalayan alien invasive plants. *Mycorrhiza* **20**: 67–72. doi:10.1007/s00572-009-0258-x.

Shi Z, Hou X, Chen Y, Wang F, Miao Y. 2013. Foliar stoichiometry under different mycorrhizal types in relation to temperature and precipitation in grassland. *Journal of Plant Ecology* **6**: 270–276. doi:10.1093/jpe/rts042.

Shutoh K, Kaneko S, Suetsugu K, Naito YI, Kurosawa T. 2016. Variation in vegetative morphology tracks the complex genetic diversification of the mycoheterotrophic species *Pyrola japonica* sensu lato. *American Journal of Botany* **103**: 1618–1629. doi:10.3732/ajb.1600091.

Suetsugu K, Yamato M, Miura C*, et al.* 2017. Comparison of green and albino individuals of the partially mycoheterotrophic orchid *Epipactis helleborine* on molecular identities of mycorrhizal fungi, nutritional modes and gene expression in mycorrhizal roots. *Molecular Ecology* **26**: 1652–1669. doi:10.1111/mec.14021.

Turnau K, Anielska T, Ryszka P, Gawroński S, Ostachowicz B, Jurkiewicz A. 2008. Establishment of arbuscular mycorrhizal plants originating from xerothermic grasslands on heavy metal rich industrial wastes-new solution for waste revegetation. *Plant and Soil* **305**: 267–280. doi:10.1007/s11104-008-9563-y.

Velázquez S, Biganzoli F, Cabello M. 2010. Arbuscular mycorrhizal fungi in El Palmar National Park (Entre Rios Province, Argentina) – a protected reserve. *Sydowia* **62**: 149–163.

Zimmer K, Hynson NA, Gebauer G, Allen EB, Allen MF, Read DJ. 2007. Wide geographical and ecological distribution of nitrogen and carbon gains from fungi in pyroloids and monotropoids (Ericaceae) and in orchids. *New Phytologist* **175**: 166–175. doi:10.1111/j.1469-8137.2007.02065.x.

Zimmer K, Meyer C, Gebauer G. 2008. The ectomycorrhizal specialist orchid *Corallorhiza trifida* is a partial myco-heterotroph. *New Phytologist* **178**: 395–400. doi:10.1111/j.1469-8137.2007.02362.x.

Zubek S, Blaszkowski J, Mleczko P. 2011a. Arbuscular mycorrhizal and dark septate endophyte associations of medicinal plants. *Acta Societatis Botanicorum Poloniae* **80**: 285–292. doi:10.5586/asbp.2011.033.

Zubek S, Błaszkowski J. 2009. Medicinal plants as hosts of arbuscular mycorrhizal fungi and dark septate endophytes. *Phytochemistry Reviews* **8**: 571–580. doi:10.1007/s11101-009-9135-7.

Zubek S, Nobis M, Błaszkowski J, Mleczko P, Nowak A. 2011b. Fungal root endophyte associations of plants endemic to the Pamir Alay Mountains of Central Asia. *Symbiosis* **54**: 139–149. doi:10.1007/s13199-011-0137-z.

Zubek S, Turnau K, Błaszkowski J. 2008. Arbuscular mycorrhiza of endemic and endangered plants from the Tatra Mts. *Acta Societatis Botanicorum Poloniae* **77**: 149–156. doi:10.5586/asbp.2008.019.

Manuscript 3

DARK SEPTATE ENDOPHYTES AND ARBUSCULAR MYCORRHIZAL FUNGI (*PARIS*-MORPHOTYPE) AFFECT THE STABLE ISOTOPE COMPOSITION OF 'CLASSICALLY' NON-MYCORRHIZAL PLANTS

Philipp Giesemann[1], David Eichenberg[1,#], Marcus Stöckel[1], Lukas F. Seifert[1], Sofia I.F. Gomes[1,2], Vincent S.F.T. Merckx[2,3], Gerhard Gebauer[1*]

Functional Ecology 34: 2453–2466 (2020), doi.org/10.1111/1365-2435.13673.

[1]University of Bayreuth, Laboratory of Isotope Biogeochemistry, Bayreuth Center of Ecology and Environmental Research (BayCEER), 95440 Bayreuth, Germany

[2]Naturalis Biodiversity Center, 2332AA Leiden, The Netherlands

[3]Department of Evolutionary and Population Biology, Institute for Biodiversity and Ecosystem Dynamics, University of Amsterdam, Amsterdam, The Netherlands

[#]Current address: German Centre for Integrative Biodiversity Research (iDiv), Halle-Jena-Leipzig, Deutscher Platz 5e, Leipzig, 04103, Germany

Key words: Caryophyllaceae, Cyperaceae, dark septate endophytes, Equisetaceae, mycoheterotrophy, mycorrhiza, stable isotope natural abundance

Received, 30 March 2020; accepted, 19 August 2020; published, 29 September 2020.

Received: 30 March 2020 | Accepted: 19 August 2020

DOI: 10.1111/1365-2435.13673

RESEARCH ARTICLE

Functional Ecology | BRITISH ECOLOGICAL SOCIETY

Dark septate endophytes and arbuscular mycorrhizal fungi (*Paris*-morphotype) affect the stable isotope composition of 'classically' non-mycorrhizal plants

Philipp Giesemann[1] | **David Eichenberg**[1] | **Marcus Stöckel**[1] | **Lukas F. Seifert**[1] | **Sofia I. F. Gomes**[1,2] | **Vincent S. F. T. Merckx**[2,3] | **Gerhard Gebauer**[1]

[1]Laboratory of Isotope Biogeochemistry, Bayreuth Center of Ecology and Environmental Research (BayCEER), University of Bayreuth, Bayreuth, Germany

[2]Naturalis Biodiversity Center, Leiden, The Netherlands

[3]Department of Evolutionary and Population Biology, Institute for Biodiversity and Ecosystem Dynamics, University of Amsterdam, Amsterdam, The Netherlands

Correspondence
Gerhard Gebauer
Email: gerhard.gebauer@uni-bayreuth.de

Present address
David Eichenberg, German Centre for Integrative Biodiversity Research (iDiv), Halle-Jena-Leipzig, Deutscher Platz 5e, Leipzig, 04103, Germany

Funding information
Elitenetzwerk Bayern

Handling Editor: Alison Bennett

Abstract

1. The vast majority of terrestrial plants exchange nutrients with fungal partners forming different mycorrhizal types. The minority of plants considered as non-mycorrhizal, however, are not necessarily free of any fungi, but are frequently colonized by elusive fungal endophytes, such as *dark septate endophytes* (*DSE*) or *fine root endophytes* (*FRE*). While a functional role of *FRE* in the improvement of nutrient gain was recently elucidated, the function of *DSE* is still in discussion and was here addressed for 36 plant species belonging to the families Equisetaceae, Cypereaceae and Caryophyllaceae.
2. Molecular and microscopic staining approaches were conducted to verify the presence of *DSE* in the investigated species. Stable isotope natural abundances of the elements carbon, nitrogen, hydrogen and oxygen and total nitrogen concentrations were analysed for the respective species of the target plant families and accompanying mycorrhizal and non-mycorrhizal (Brassicaceae) plant species.
3. Staining approaches confirmed the presence of *DSE* in all investigated species within the families Equisetaceae, Cyperaceae and Caryophyllaceae. A co-colonization with *Paris*-type arbuscular mycorrhiza (AM) was occasionally found by staining and molecular approaches in species of the Equisetaceae. Species of the Equisetaceae, Cyperaceae and Caryophyllaceae were significantly ^{15}N-enriched in comparison to accompanying plants. In addition, a significant ^{13}C and ^{2}H enrichment and increased total nitrogen concentrations were found for representatives of the Equisetaceae.
4. The ^{15}N enrichment found here for representatives of Equisetaceae, Cyperaceae and Caryophyllaceae provides evidence for a functional role of the ubiquitous *DSE* fungi. *DSE* fungi obviously provide access to ^{15}N-enriched soil organic compounds probably in exchange for organic carbon compounds from plant photosynthesis. As indicated by additional ^{13}C and ^{2}H enrichments, representatives of the Equisetaceae apparently gain simultaneously organic carbon compounds from

their AM fungi of the *Paris*-morphotype. Thus, species of the Equisetaceae have to be considered as partially, or in case of the achlorophyllous fertile *Equisetum arvense*, as fully mycoheterotrophic at least in some stages of their life cycle.

5. So far, mostly underappreciated fungi classified as *DSE* are suggested to occupy an ecologically relevant role similar to mycorrhizae and the occurrence of simultaneous functions of *DSE* and AM fungi in Equisetaceae is proposed.

KEYWORDS

Caryophyllaceae, Cyperaceae, dark septate endophytes, Equisetaceae, mycoheterotrophy, mycorrhiza, stable isotope natural abundance

1 | INTRODUCTION

The vast majority of terrestrial plants live in a mostly mutualistic symbiosis with fungi forming different types of mycorrhizae (Smith & Read, 2008; Tedersoo, Bahram, & Zobel, 2020). Only a small minority of terrestrial plants is considered as non-mycorrhizal. Species belonging to the families Equisetaceae (horsetails), Cyperaceae (sedges) and Caryophyllaceae (carnation family) are classical examples of plants considered as non-mycorrhizal (Brundrett & Tedersoo, 2019; Pressel, Bidartondo, Field, Rimington, & Duckett, 2016; Smith & Read, 2008). The absence of commonly known mycorrhizal partners in plants belonging to these three families, however, does not imply a general lack of fungal root endophytes. In contrary, Equisetaceae, Cyperaceae and Caryophyllaceae are all known to be colonized by *dark septate endophytes* (*DSE*, Ascomycota; Jumpponen & Trappe, 1998) and *fine root endophytes* (*FRE*, Mucoromycotina; Orchard et al., 2017; Walker, Gollotte, & Redecker, 2018). *DSE* form hyaline or melanized inter- and intracellular septate hyphae and microsclerotia (Jumpponen & Trappe, 1998; Mandyam & Jumpponen, 2005). *FRE* form arbuscule-like structures and non-septate fine branching hyphae with small vesicle-like swellings (Hoysted et al., 2019; Orchard et al., 2017). Occasionally, arbuscular mycorrhizae (AM, Glomeromycotina) were also documented in Equisetaceae interestingly forming the *Paris*-morphotype characterized by dense aseptate intracellular hyphal coils (Dhillion, 1993; Dickson, Smith, & Smith, 2007; Fernández, Messuti, & Fontenla, 2008; Hodson, Shahid, Basinger, & Kaminskyj, 2009; Koske, Friese, Olexia, & Hauke, 1985), whereas, if present, in Cyperaceae (Dickson et al., 2007; Druvca-Lusite & Ievinsh, 2010; Velázquez, Biganzoli, & Cabello, 2010) and Caryophyllaceae (Dickson et al., 2007; Druvca-Lusite & Ievinsh, 2010; Shah, Reshi, & Khasa, 2009) mainly the *Arum*-morphotype AM forming aseptate intercellular hyphae along the cortical root cell layers was recorded.

Recent investigations provide first evidence for potential functional roles of the various fungal root endophytes reported for species of the Equisetaceae, Cyperaceae and Caryophyllaceae. *FRE* were suggested to provide a mycorrhiza-like advantage mainly in grasses (Orchard et al., 2017) as well as in some phylogenetically basal plant groups, like liverworts (Field et al., 2019) and lycopods (Hoysted et al., 2019). Interestingly, Field et al. (2019) described a selective nutritional benefit for a liverwort partner simultaneously colonized by Mucoromycotina (effective nitrogen transfer) and Glomeromycotina (effective phosphorous transfer). *DSE* are ubiquitous root fungi occupying various ecosystems, however, a potential mycorrhizal, that is, beneficial, function for *DSE* is still in discussion and needs to be evaluated (Jumpponen, 2001; Jumpponen & Trappe, 1998; Mandyam & Jumpponen, 2005; Newsham, 2011). Although the first strong indication for an organic N acquisition by *DSE* was recently provided (Hill et al., 2019), in most cases they are treated as saprotrophs on dead roots. Furthermore, the *Paris*-morphotype among AM plants, as occasionally found in representatives of the Equisetaceae, was recently identified as bearing the potential for mycoheterotrophy which is in contrast to plant species forming the *Arum*-morphotype (Giesemann, Rasmussen, Liebel, & Gebauer, 2020).

Analysis of stable isotope natural abundance of the elements carbon (C), nitrogen (N) and hydrogen (H) has proven to be a valuable tool to elucidate organic C and mineral nutrient fluxes between plants and fungi in different types of mycorrhizal associations (Gebauer & Meyer, 2003; Gebauer, Preiss, & Gebauer, 2016; Giesemann, Rasmussen, et al., 2020; Merckx, Stöckel, Fleischmann, Bruns, & Gebauer, 2010; Ogura-Tsujita, Gebauer, Hashimoto, Umata, & Yukawa, 2009; Zimmer et al., 2007). Hundreds of mycoheterotrophic plant species were identified to subvert the usually mutualistic mycorrhizal symbiosis and to utilize their fungal partners as nutrient source, which allows them to produce endospermless dust seeds (initial mycoheterotrophs) or to reduce (partial mycoheterotrophs) or even cease their photosynthetic activity (full mycoheterotrophs; Hynson et al., 2013; Leake, 1994; Merckx, 2013). The draining of fungal nutrients changes the mycoheterotrophs' stable isotope natural abundance pattern towards enrichment in heavy C, N and H isotopes (Gebauer et al., 2016; Hynson et al., 2013; Hynson, Schiebold, & Gebauer, 2016) as also found for fruit bodies of many fungi (Gebauer & Dietrich, 1993; Gleixner, Danier, Werner, & Schmidt, 1993; Mayor, Schuur, & Henkel, 2009; Ziegler, 1995). This 'interlinking' in mutualistic networks has been identified as widely distributed among achlorophyllous as well as photosynthetic plant species forming orchid (Gebauer & Meyer, 2003; Hynson et al., 2013, 2016) and ericoid mycorrhizae

(Hynson et al., 2013, 2016; Lallemand et al., 2017; Tedersoo, Pellet, Kõljalg, & Selosse, 2007; Zimmer et al., 2007) and more recently in AM (Courty et al., 2011; Giesemann, Rasmussen, et al., 2020; Gomes, Merckx, Kehl, & Gebauer, 2020; Hynson et al., 2013; Merckx et al., 2010).

Due to strong global and local variations in climatic growing conditions, soil conditions and precipitation, isotope abundances of plant tissues vary depending on their growing location, that is, stable isotope abundances are site-dependent and thus, cannot directly be compared across different locations. In order to circumvent this limitation Preiss and Gebauer (2008) suggested a normalization approach referring the isotope abundances of target plants (TPs; e.g. mycoheterotrophs) to a diverse set of putatively autotrophic reference plants growing under identical micro-site conditions and thus, converting traditional isotope abundances (δ values) into enrichment factors ε. Based on this approach, a steadily increasing site-independent enrichment factor database, not only of mycoheterotrophic plants, but also of putatively autotrophic plant species has been established. Interestingly, within the group of putatively autotrophic reference plants (all following the C_3 pathway of photosynthesis), 12 species belonging to the classically as non-mycorrhizal classified families Equisetaceae, Cyperaceae and Caryophyllaceae emerged as conspicuously enriched in the heavy isotope ^{15}N (and in case of the Equisetaceae simultaneously in the heavy isotope ^{13}C).

This finding raised two hypotheses: (1) A ^{15}N enrichment is a general phenomenon among plant species belonging to the families of Equisetaceae, Cyperaceae and Caryophyllaceae. (2) This unique pattern in isotope composition is functionally related to their respective fungal endophytes. In order to test these hypotheses, we generated C and N and in some cases H and oxygen (O) stable isotope abundance data suited for enrichment factor calculations for 24 plant species belonging to the families Equisetaceae, Cyperaceae and Caryophyllaceae. We then combined the data from these 24 species with the 12 species contained in our database in order to test whether unique stable isotope abundance patterns are a general phenomenon among plant species of these three families. Furthermore, we used staining techniques and light microscopy to identify endophytic fungi in the roots of selected species from the three families. Additionally, molecular approaches for the identification of AM fungi were applied for three selected *Equisetum* species. The functional drivers leading to unique stable isotope abundance patterns among the investigated plant species are discussed.

2 | MATERIALS AND METHODS

2.1 | Plant sampling

Target plant material was collected for representatives of the Equisetaceae (six species, $n = 103$), Cyperaceae (12 species, $n = 78$) and Caryophyllaceae (six species, $n = 35$) at six different locations per family distributed in NE-Bavaria (Germany; ~49.50 to 50.20 N, ~11.20 to 11.90 E decimal WGS84). The sampling scheme followed the methodology outlined in Gebauer and Meyer (2003), which includes at least one TP species accompanied by three to six neighbouring plants as references in a 1-m^2 plot ($n = 335$, 126 and 92 reference plants associated with Equisetaceae, Cyperaceae and Caryophyllaceae TPs respectively). The reference plant material represented a variety of C_3 plants belonging to 25 plant families colonized by different mycorrhizal fungal partners (ectomycorrhiza: ECM, arbuscular mycorrhiza: AM, ericoid endomycorrhiza: ErM) or being non-mycorrhizal: NM (Brundrett & Tedersoo, 2019; Wang & Qiu, 2006).

- Plant material of Equisetaceae was sampled from May to August 2005 distributed in agricultural land (*Equisetum arvense* L.), mixed forests (*E. sylvaticum* L.) and within patchy located swamp lands (*E. fluviatile* L., *E. hyemale* L., *E. palustre* L., *E. sylvaticum*, *E. telmateia* Ehrh.) including lateral shoots and thereon scale leaves, stem and root material of the target as well as leaf, stem and root material of respective reference plant species. For *E. arvense* achlorophyllous fertile and chlorophyllous sterile plant individuals were sampled. In 2018, one site was subsequently added, aiming to compare lateral shoots and thereon scale leaf material of *Equisetum* with leaf material of a moss species. Additionally, corresponding root samples for the estimation of colonization by fungal endophytes and temporal development of colonization during the vegetation period were collected at the same sites in 2016 and 2017.
- Leaves of Cyperaceae were sampled during the vegetation periods of 2008 and 2009 in *Fagus sylvatica* dominated forests (*Carex flacca* Schreb., *C. digitate* L.), wet meadows (*C. disticha* Huds., *C. flacca*, *C. hirta* L., *C. nigra* (L.) Reichard, *C. panicea* L., *C. pallescens* L., *C. vulpina* L., *Scirpus sylvaticus* L.), chalk heath (*C. caryophyllea* Latourr) and within a swamp land surrounded by a coniferous forest (*C. nigra*, *C. vesicaria* L., *Eriophorum vaginatum* L.). In addition, corresponding root samples for staining approaches were collected at the same time.
- Leaves of Caryophyllaceae were sampled from spring to early summer 2019 in a public lawn area (*Stellaria media* (L.) Vill.), wet forest riversides (*Cerastium fontanum* Baumg., *Stellaria holostea* L., *Silene dioica* (L.) Clairv.) and vegetation-poor and sunny slopes (*Lychnis viscaria* (L.) Jess., *Saponaria officinalis* L.). Root sampling for the approximation of fungal colonization was conducted at the same time.

All root samples for the identification of fungal partners were treated equally by washing procedures, followed by fixation in 70% ethanol and storage at 4°C until further analysis.

2.2 | Stable isotope natural abundance and nitrogen concentration analysis

Plant material for isotope abundance analysis was washed with deionized water, oven-dried overnight (105°C) and ground to a homogenous powder in either a ball mill (Retsch Schwingmühle MM2) or a micro-dismembrator (B. Braun Biotech International). The samples were stored in desiccators filled with silica gel until further

processing. Isotope ratio mass spectrometry (IRMS) was applied to analyse natural relative abundances of stable C ($^{13}C/^{12}C$), N ($^{15}N/^{14}N$), H ($^{2}H/^{1}H$) and O ($^{18}O/^{16}O$) isotopes. An elemental analyser (NA 1108, Carlo Erba Instruments) coupled to an IRMS (delta S, Finnigan MAT) via a Conflo III interface (Thermo Fisher Scientific) was applied for C and N isotopes, while a thermal conversion device (HTO, HEKAtech) coupled to an IRMS (delta V advantage, Thermo Fisher Scientific) via a Conflo IV interface (Thermo Fisher Scientific) were used for H and O isotopes. Acetanilide (Merck KGaA) was used to calibrate the obtained C/N concentrations. Standard gases (Riessner) were calibrated according to international standards (CO_2 vs. V-PDB, N_2 vs. N_2 in air, H_2 and CO vs. V-SMOW), applying reference substances provided by the International Atomic Energy Agency, Vienna, Austria (ANU sucrose, CH6, CO8, NBS18 and NBS19 for the C isotopes, N1 and N2 for the N isotopes, CH7, V-SMOW and SLAP for H isotopes and IAEA601 and IAEA602 for the O isotopes). A memory bias (see Gebauer et al., 2016) was avoided by analysing H isotope samples four times. All samples were analysed plot-wise in identical batches to minimize an atmospheric bias through a potential H atom exchange within the samples with ambient air. Reproducibility of isotope measurements was always within ±4‰ for δ^2H, ±0.2‰ for $\delta^{13}C$ and $\delta^{15}N$, and ±0.6‰ for $\delta^{18}O$. The resulting relative isotope abundances follow the rules of the δ-notation: $\delta^{13}C$, $\delta^{15}N$, δ^2H and $\delta^{18}O = (R_{sample}/R_{standard} - 1) \times 1{,}000$ (‰), whereby R is the ratio of the heavy to the respective light isotope.

In order to complement the obtained field survey in NE-Bavaria, our database survey added stable isotope enrichment factors for eleven species belonging to the Cyperaceae (n = 131, *C. conica* Boott, *C. flava* L., *C. distachya Desf.*, *C halleriana* Asso, *C. remota*, *C. siderosticta* Hance, *Machaerina* sp., *Rhynchospora alba*, *Rhynchospora* sp., *Trichophorum cespitosum* (L.) Hartm. and an unidentified *Carex* species) from 10 published datasets and three unpublished field works and references ($n_{Cyperaceae}$ = 372). Additionally, the data base added one species of the Caryophyllaceae (n = 13, *Dianthus arenarius* L.) from two published datasets and one unpublished field work and references ($n_{Caryophyllaceae}$ = 73). The database survey added 28 plant families to our field survey (in total 53). Only data following the sampling design described here were included. The detailed coordinates of the sampling areas and the studies complementing our analysis can be obtained from the supplement (Tables S2, S4, S6). A complete list of plant individuals can be obtained from the data repository (Giesemann, Eichenberg, et al., 2020).

2.3 | Root staining

Roots of Equisetaceae, Cyperaceae and Caryophyllaceae were stained according to Phillips and Hayman (1970) and following recommendations from Vierheilig, Schweiger, and Brundrett (2005). In principle, the ethanol fixed roots were washed in deionized water at least three times. Afterwards, roots were cleared applying a 10% KOH (w/v) solution for 30 min at 70°C in a water bath with continuously slight panning (Köttermann 3043, Köttermann GmbH & Co.) or under carefully inverting the staining tube several times manually. If necessary, pigmented roots were bleached applying 5% (v/v) H_2O_2 and 0.5% (v/v) NH_3 solution following the protocol from Fernández et al. (2008) for 10–30 min under room temperature depending on the pigmentation of the root sample. The durations of the clearing and bleaching treatments were adjusted for several individuals if necessary, e.g. for very dark pigmented roots of Equisetaceae or very fine roots of some Cyperaceae and Caryophyllaceae plant species. Root samples were washed with deionized water after bleaching and clearing several times. Before staining, Equisetaceae and Caryophyllaceae roots were acidified with 1% (v/v) HCl and Cyperaceae were acidified with 2% (v/v) lactic acid for 5–10 min respectively. A 0.05%-1% (v/v) trypan blue staining solution in 33% (v/v) acidic glycerol and 33% (v/v) lactic acid and 33% deionized water was applied for staining over-night at room temperature. Stained roots were stored in a refrigerator in a solution of glycine/lactic acid/distilled water (3:1:3) until further analysis. Fungal colonization was determined via light microscopy and documented with either an Olympus BH (Olympus Deutschland GmbH) equipped with an Olympus C-330 camera (Olympus Deutschland GmbH) or applying BA210LED trino (Motic) equipped with the 3MP Moticam 3+. Images were observed with Cell^A 2.6 (Olympus Soft Imaging Solutions GmbH) or Fiji ImageJ 1.51n (Schindelin et al., 2012).

In principle, the quantification of fungal root colonization followed Brundrett, Bougher, Dell, Grove, and Malajczuk (1996) by the evaluation of the presence or absence of fungal structures intersecting the hair-cross of the object lens. For Equisetaceae, ten 1-cm long root fragments were observed in three replicates per species. The presence/absence of fungal structures intersecting with the hair-cross were noted. This procedure was repeated for three (*E. sylvaticum*, *E. palustre*, *E. arvense*, *E. telmateia*) to five (*E. hyemale*) observations per species in one vegetation period. The number of colonized fields of views relative to the total number of fields of views (100 per individual) represented the colonization rate. Caryophyllaceae were treated equally, applying five root fragments (50 field of views per individual). The total number of fungal structures intersecting the hair-cross were counted. For Cyperaceae, four root fragments were observed and the presence/absence of fungal structures were evaluated for the whole root fragment (50 field of views per individual). Fungal structures were blue-stained aseptate hyphae, brownish and blue-stained septate hyphae, brownish microsclerotia, blue-stained vesicles, spores and arbuscules (Figure 1).

2.4 | Molecular approaches

In order to test roots of Equisetaceae for the occurrence of AM fungi in addition to *DSE* molecular approaches were applied for three *Equisetum* species. Root tips were cleaned with water and stored on 2% CTAB buffer at −20°C until further processing. Fungal DNA

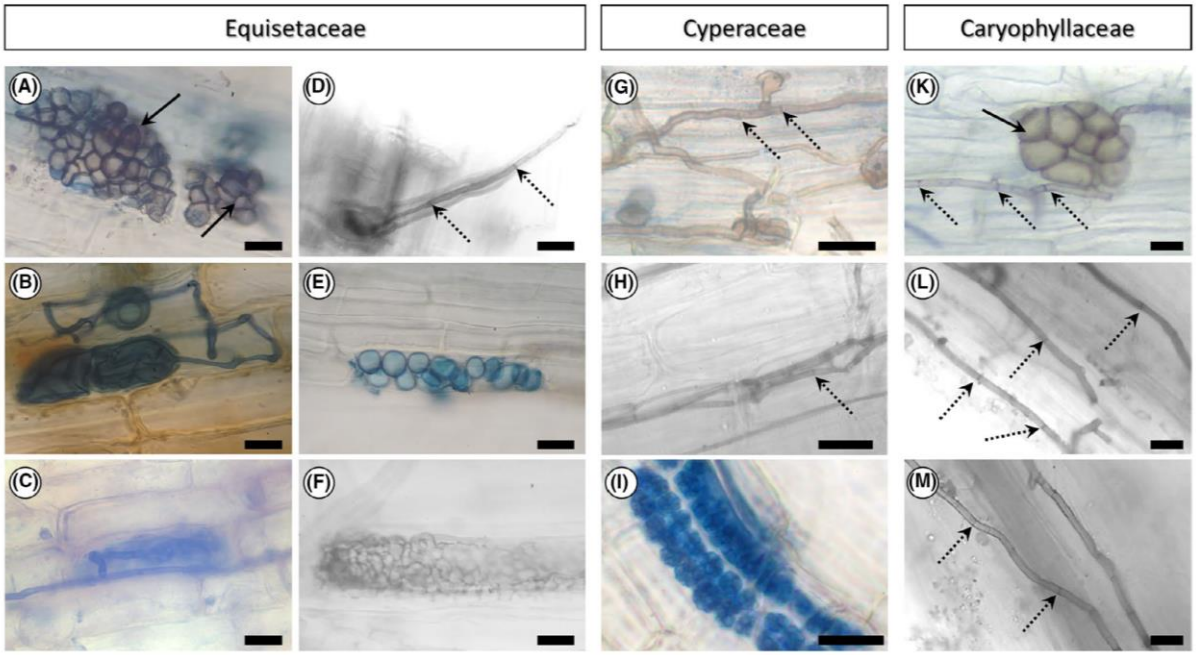

FIGURE 1 Structures of fungal root endophytes investigated in representatives of the plant families Equisetaceae, Cyperaceae and Caryophyllaceae. Dark septate fungal microsclerotia were found in all three plant families (e.g. A, K; bold arrow). Hyphae of dark septate fungal endophytes (dashed arrow) were either blue-stained or brownish and present in Equisetaceae (D), Cyperaceae (G, H) and Caryophyllaceae (L, M). Arbuscular mycorrhizal hyphae were present in Equisetaceae (e.g. B, *Paris*-type coils; C, F, *Paris*-type like structures and E vesicles- or spore-like structures). Occasionally, big colonies of the intracellular structures of Chytridiomycota fungi (I) were found in Cyperaceae and Caryophyllaceae. Scale bar: 20 μm

was extracted from root samples with the KingFisher Flex Magnetic Particle Processors (Thermo Fisher Scientific) using the NucleoMag 96 Plant Kit (Machery-Nagel). Each of the 96 aliquots in the well was assigned a unique Multiplex Identifier (MID) barcode sequence. Subsequently, amplicon libraries were created using barcode-tagged primers for the internal transcribed spacer 2 (ITS2), using the fungal specific primer fITS7 (Ihrmark et al., 2012) and ITS4 (White, Bruns, Lee, & Taylor, 1990). PCR products were purified using 0.9× NucleoMag NGS Clean-Up and Size Select beads (Macherey-Nagel) according to the manufacturer's instructions. The concentration of the individual indexed amplicons was measured with the QIAxcel using the DNA Screening kit (Qiagen), and normalized and pooled equimolar using the QIAgility robot (Qiagen). Sequencing was performed on a MiSeq Illumina platform using the paired-end 300 bp kit at BaseClear. Sequence processing was performed following the UNOISE3 algorithm (Edgar, 2016b) implemented in USearch v.11 (http://www.drive5.com/usearch/). Paired reads were assembled and passed the quality filter allowing for reads with maximum error <1.0. Followed by dereplication and filtering out singletons, the resulting sequences were used to create zero radius operational taxonomic units (zOTU), resulting in 183 zOTUs (93,883 reads) with putative chimeras removed (Blaalid et al., 2013). The taxonomic rank was assigned by BLAST search against the UNITE 8.2 database (Abarenkov et al., 2020) and with the *sintax* algorithm implemented in USearch (Edgar, 2016a) in conjunction with the UNITE database.

2.5 | Statistical analysis

Following the recommendations of Preiss and Gebauer (2008), enrichment factors ε were calculated from measured δ values by using the TP subtracted by the mean δ values of the reference plants (RP; for $\varepsilon^{13}C$, $\varepsilon^{15}N$, $\varepsilon^{2}H$ and $\varepsilon^{18}O$: $\varepsilon_{TP} = \delta_{TP}$-mean δ_{RP}), or by using already published δ values. The reference plants describe the habitat conditions and ε values reflect the relative differences to our TPs, corrected for any variations in heavy isotope enrichment due to site-specific peculiarities. This ensures that, across all samples, enrichment factors ε are independent of spatial variation; therefore, ε values can be compared across sampled populations.

The relative amount of C received from their fungal source by each single *Equisetum* individual was approximated applying the two-source linear mixing model (Gebauer & Meyer, 2003; Giesemann, Rasmussen, et al., 2020; Hynson et al., 2013). There, the reference plants are assumed to exclusively obtain C through photosynthesis while the achlorophyllous fertile stages of *E. arvense* are considered as covering their entire C demand from a fungal source. The relative amount of C received from their fungal source is shown as mean values and standard deviations for *Equisetum* species and averaged across all *Equisetum* individuals.

Data analyses were performed with RSTUDIO 1.2 (R Core Team, 2019) and SIGMAPLOT 11.0 (Systat Software, 2008). Effect sizes *d* were additionally checked according to Lenhard and Lenhard (2017).

An effect size $d \geq 0.8$ is considered as large (Cohen, 1992). Stable isotope abundances were tested for normality via Shapiro–Wilk test and homogeneity of variances via Levene test. The nonparametric tests, one-tailed Mann–Whitney *U* and one-tailed Kruskal–Wallis *H*, had to be applied for pairwise comparisons or comparisons across multiple groups respectively. In the case of a significant Kruskal–Wallis result, a post-hoc Dunn's test for multiple comparison was applied (*Z*; Dinno, 2017). *P*-values were corrected according to the sequential Holm-Bonferroni method. The critical level of significance was set to $\alpha = 0.05$. Data expression is in mean values with standard deviations ($\bar{x} \pm SD$).

3 | RESULTS

3.1 | Equisetaceae

A variety of fungal endophytes were visually documented for *Equisetum* species with *DSE* approximately more than 80% (Figure 1A–F). *DSE* remained either brown or were blue-stained but septa were very clear. Occasionally, AM forming *Paris*-type coils and vesicles were documented. The sequencing data indicated a diversity of unidentified fungi from the order Helotiales representing 51%, 40% and 29% of the reads in *E. arvense*, *E. palustre* and *E. sylvaticum* (see Figure S1 and Table S8). In addition, zOTUs identified as the *septate endophytes Phialocephala fortinii* (6% of the total reads), *Cladophialophora chaetospira* and *Tetracladium* spp. (1% of the total reads) while also AM Glomeromycotina were documented (<1% of the total reads). The total colonization rate of fungal endophytes across all here investigated *Equisetum* species was 25 ± 14%. While *Equisetum hyemale* had almost constantly low colonization rates during the year, a trend from high colonization towards almost no fungal colonization from May to August was observed for *E. palustre*, *E. sylvaticum*, *E. arvense* and *E. telmateia* (Figure S2).

By definition of the enrichment factor ε, the reference plants clustered around zero with a calculated standard deviation of ±1.1‰ for lateral shoots including scale leaves, ±1.1‰ for stems, ±1.3‰ for roots in ^{13}C and of ±1.5‰ for lateral shoots including scale leaves, ±1.1‰ for stems, ±1.3‰ for roots in ^{15}N (Figure 2). The reference plants forming AM, ECM or ErM clustered together within the range of the standard deviation of all reference plant species. The NM plant species *Brassica napus* and *Capsella bursa-pastoris* (Brassicaceae) were similar to the mycorrhizal reference plant species in ^{13}C and ^{15}N.

Six out of seven *Equisetum* species were significantly enriched in ^{13}C and ^{15}N (Figure 2) and had higher total N concentrations relative to accompanying reference plants (Table 1). This observation held true for lateral shoots including scale leaves, stems and roots (Table 1); ^{13}C enrichment increased from 2.6 ± 1.2‰, 3.2 ± 1.7‰ to 3.6 ± 1.2‰, while ^{15}N enrichment gradually decreased from 4.6 ± 3.0‰, 3.2 ± 2.8‰ to 2.3 ± 2.5‰ for lateral shoots including the scale leaves, stem and root respectively (Figure 2). The achlorophyllous, fertile stems of *E. arvense* were most enriched in ^{13}C

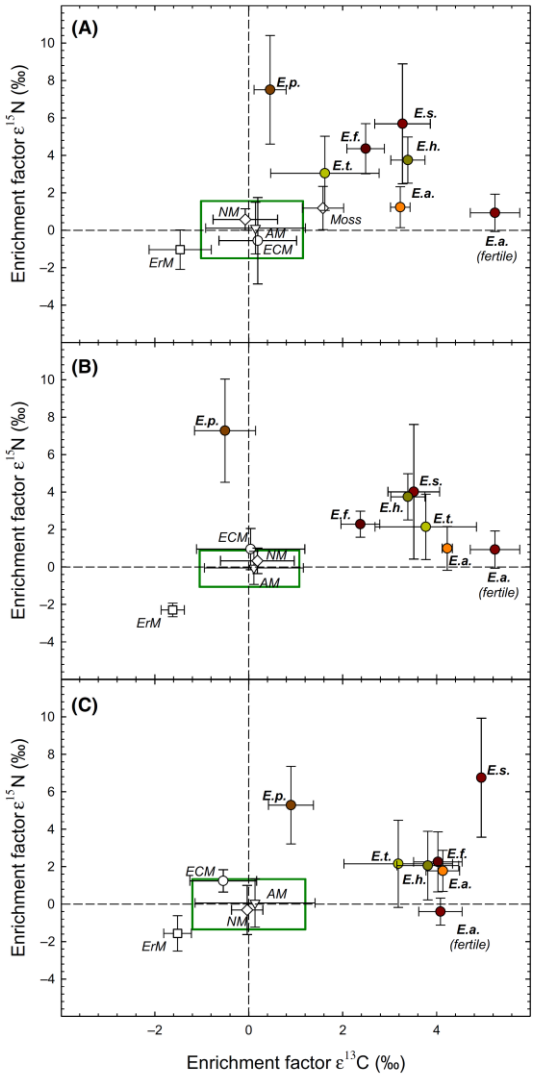

FIGURE 2 Carbon and nitrogen stable isotope enrichment factors ($\varepsilon^{13}C$ and $\varepsilon^{15}N$) in lateral shoots including the scale leaves (A: *Equisetum* spp.: $n = 34$, reference: $n = 125$), stems (B: *Equisetum* spp.: $n = 39$, reference: $n = 125$) and roots (C: *Equisetum* spp.: $n = 30$, reference: $n = 135$) of six chlorophyllous *Equisetum* species and of achlorophyllous fertile *Equisetum arvense* samples and of reference plants comprising arbuscular mycorrhizal (AM, white triangles), ectomycorrhizal (ECM, white circles), ericoid mycorrhizal (ErM white squares) and non-mycorrhizal (NM white diamonds) plant species. The green frames represent standard deviations of all reference plants. Each coloured symbol represents a single species belonging to the Equisetaceae. In the case of *E. arvense*, two different states in the life cycle (chlorophyllous sterile individuals and achlorophyllous fertile individuals) are presented separately. All data are shown with mean values and standard deviations. E.a. *Equisetum arvense* (separated by chlorophyllous sterile and achlorophyllous fertile individuals), E.f. *E. fluviatile*, E.h. *E. hyemale*, E.p. *E. palustre*, E.s. *E. sylvaticum*, E.t. *E. telmateia*. The plant lateral shoots including the scale leaves and the plant stem were pooled for *E. arvense* (fertile) and *E. hyemale*, respectively, thus shown in A and B

TABLE 1 Test for differences in enrichment factors ε of ^{13}C (‰) and ^{15}N (‰) and in total N concentrations (mmol/g_{dw}) of six chlorophyllous *Equisetum* species and their reference plants separately for three different plant organs. Mann–Whitney *U* test. Significances are highlighted in bold

Organ (N_{Equi}, N_{Ref})	$\varepsilon^{13}C$		$\varepsilon^{15}N$		Total N	
	TS	*P*	TS	*P*	TS	*P*
Leaf (34,125)	*U* = 311	**<0.001**	*U* = 318	**<0.001**	*U* = 679	**<0.001**
Stem (34,100)	*U* = 382	**<0.001**	*U* = 358	**<0.001**	*U* = 1,679	0.214
Root (25,110)	*U* = 108	**<0.001**	*U* = 541	**<0.001**	*U* = 970	**<0.001**

Note: TS: Test statistic; for $p < 0.05$, Cohen's *d* effect size is always > 1.0, except total N in roots ($d_{Cohen} = 0.7$). Leaf include the lateral shoots and thereon the scale leaves. The fertile individuals of *Equisetum arvense* were excluded as they are achlorophyllous.

(5.2 ± 0.5‰), but least enriched in ^{15}N (0.9 ± 1.0‰); while samples of *E. palustre* were the least enriched in ^{13}C (0.5 ± 0.3‰), in most cases, the most enriched in ^{15}N (7.5 ± 2.9‰). The non-mycorrhizal moss *Polytrichum commune* was significantly enriched in ^{13}C but did not differ in ^{15}N from its site-specific mycorrhizal reference plants (Table S1). *Equisetum sylvaticum* at this additional site mirrored the results already presented in Figure 2A, that is, being significantly enriched in ^{13}C and ^{15}N relative to moss and mycorrhizal plants.

The total N concentrations of the lateral shoots including the scale leaves were highest in *E. palustre*, *E. sylvaticum*, *E. arvense* and *E. fluviatile*, ranging from 1.71 to 3.7 mmol/g_{dw}, and lowest in *E. telmateia*, ranging from 1.22 to 1.57 mmol/g_{dw} when compared to their corresponding reference plants (range = 0.89 to 3.75 mmol/g_{dw}). These findings were mostly congruent also for stems and roots (Table S2). Also, the non-mycorrhizal moss *Polytrichum commune* did not differ in leaf total N concentration from its site-specific mycorrhizal reference plants but had significantly lower leaf total N concentrations than accompanying *Equisetum sylvaticum* individuals in their lateral shoots and thereon the scale leaves (Table S1).

Equisetum sylvaticum and *E. palustre* were significantly ^{2}H-enriched by 14 ± 5.4‰ ($U_{9,20} = 3$, $p = 0.001$) and significantly ^{18}O-enriched by 3.5 ± 1.7‰ ($U_{9,20} = 3$, $p = 0.001$) relative to accompanying reference plants.

Based on two-source linear mixing model calculations, the carbon received from the fungal source covered a range from 9 ± 6% in *Equisetum palustre*, 31 ± 22% in *E. telmateia*, 48 ± 7% in *E. fluviatile* to 62 ± 7% in *E. sylvaticum*, *E. arvense* and E. *hyemale*. On average, the mixing model suggests that 50 ± 22% of C across all *Equisetum* species originated from a fungal source and the remaining from photosynthesis.

3.2 | Cyperaceae

Septate hyphae and intracellular structures, either brown or blue-stained, were found in every investigated species (Figure 1G–I). In *Carex pallescens*, *C. vulpina and Scirpus sylvaticus* very few vesicle-like structures were observed (facultative mycorrhiza); however, eight out of 11 species were classified as non-mycorrhizal but *DSE* colonized. *Carex flacca* was the most pronounced example for very dense aseptate hyphae, that formed mantle-like structures which did not enter the root tissue, and spherical intraradical hyphae (probably, saprotrophic Chytridiomycetes, Terence T. McGonigle *personal communication* cf. Figure 1I). *Eriophorum vaginatum* had to be excluded from the light microscopy investigations, as the fine root structures were unusable after harsh clearing and staining procedure. All Cyperaceae species established dauciform roots, a special form of roots, often found in Cyperaceae which produces shortened club-like root structures.

Relative to reference plants composed of species forming AM, ECM, ErM or being NM and clustering around zero, with a standard deviation of ±1.0‰ in ^{13}C and of ±1.3‰ in ^{15}N (Figure 3), most species of the Cyperaceae plant family were significantly ^{15}N-enriched by 3.3 ± 2.1‰ ($U_{209,499} = 8{,}714$, $p = 0.001$, $d_{Cohen} = 1.7$), whereby ^{13}C was in the range of their references (0.4 ± 1.1‰; $U_{209,499} = 40{,}102$, $p = 0.001$, $d_{Cohen} = 0.4$; Figure 2). The effect size represented by Cohen's *d* value supports the significance in ^{15}N enrichment ($d \geq 0.8$), but not for ^{13}C ($d < 0.8$). The ^{15}N enrichment ranged from −0.2 ± 0.1‰ in *Carex siderostricta*, to 5.0 ± 1.7‰ and 5.1 ± 4.0‰ represented by *Carex vesicaria* and *T. cespitosum* respectively.

Leaf total N concentrations for Cyperaceae ranged from 0.1 to 3.0 mmol/g_{dw}, with a mean of 1.2 ± 0.4‰ mmol/g_{dw}, being slightly lower than this of the reference plants with a mean of 1.4 ± 0.5‰ mmol/g_{dw} (range = 0.5–3.0 mmol/g_{dw}; $U_{194,469} = 37{,}521$, $p < 0.001$, $d_{Cohen} = 0.3$).

Cyperaceae did not show significant enrichment in ^{2}H, when compared to their references (2.2 ± 9.3‰ vs. 0 ± 7.9‰, respectively; $U_{82,195} = 6{,}885$, $p = 0.068$, $d_{Cohen} = 0.2$). In contrast, Cyperaceae showed a significant depletion in ^{18}O relative to the reference plants (−0.5 ± 2.4‰ vs. 0 ± 1.8‰, respectively; $U_{82,194} = 6{,}600$, $p = 0.022$). However, with a Cohen's *d* value of <0.3, these differences are quite small.

3.3 | Caryophyllaceae

Colonization rates of *DSE* in the investigated Caryophyllaceae were more than twice as high when compared to their accompanying reference plants (mean 0.66 vs. 0.27 *DSE* per field of view, respectively; cf. Figure 1K–M). In contrast, aseptate hyphae, vesicles and

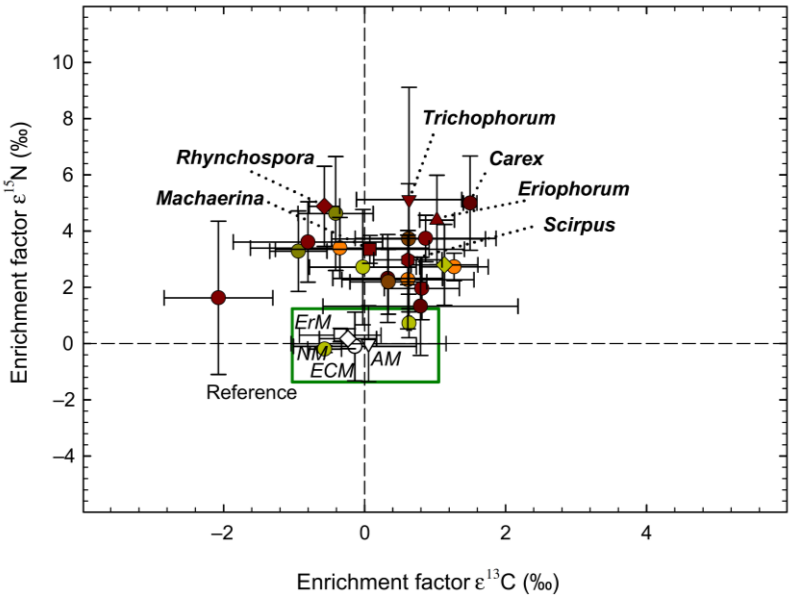

FIGURE 3 Carbon and nitrogen stable isotope enrichment factors ($\varepsilon^{13}C$ and $\varepsilon^{15}N$) in leaves of 23 plant species of the Cyperaceae ($n = 209$; coloured symbols) and of reference plants comprising arbuscular mycorrhizal (AM, white triangle), ectomycorrhizal (ECM, white circle), ericoid mycorrhizal (ErM white square) and non-mycorrhizal (NM white diamond) plant species ($n = 499$). The green frame represents the standard deviation of all reference plants. Each coloured symbol represents a single species belonging to the Cyperaceae. Identical symbols represent affiliation to identical genera as indicated. All data are shown with mean values and standard deviations

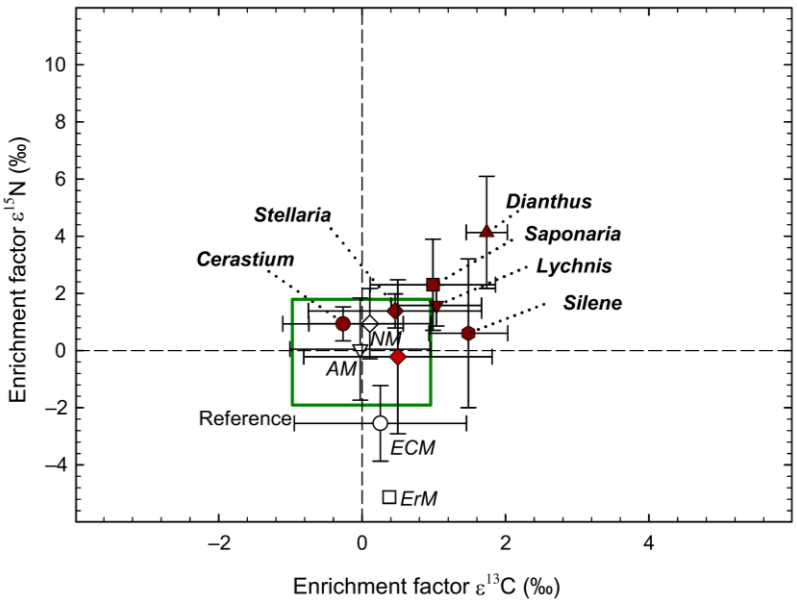

FIGURE 4 Carbon and nitrogen stable isotope enrichment factors ($\varepsilon^{13}C$ and $\varepsilon^{15}N$) in leaves of seven plant species of the Caryophyllaceae ($n = 48$) and of reference plants comprising arbuscular mycorrhizal (AM, white triangle), ectomycorrhizal (ECM, white circle), ericoid mycorrhizal (ErM white square) and non-mycorrhizal (NM white diamond) plant species ($n = 165$). The green frame represents the standard deviation of all reference plants. Each coloured symbol represents a single species belonging to the Caryophyllaceae. Identical symbols represent affiliation to identical genera as indicated. All data are shown with mean values and standard deviations

arbuscules, structures indicative for AM fungi, were more prominent in the accompanying reference plants and only in a neglectable amount in Caryophyllaceae (0.3 AM in reference plants vs. <0.05 AM per field of view in Caryophyllaceae).

Reference plants were again composed of species forming AM, ECM, ErM or were NM. Their enrichment factor ε clustered around zero with a standard deviation of ±1.0‰ in ^{13}C and of ±1.9‰ in ^{15}N (Figure 4). The NM plant species *Brassica napus* and *Capsella bursa-pastoris* (Brassicaceae) were less ^{15}N-enriched than Caryophyllaceae plant species. Most of the Caryophyllaceae species investigated in the present study were significantly enriched in ^{13}C by 0.7 ± 1.1‰ ($U_{48,165} = 2{,}394.5$, $p = 0.001$, $d_{Cohen} = 0.6$) and ^{15}N by 1.2 ± 2.0‰ ($U_{48,165} = 2055$, $p = 0.001$, $d_{Cohen} = 0.8$). While some species were considerably high ^{15}N-enriched, for example, *Dianthus arenarius* (4.1 ± 1.9‰), *S. officinalis* (2.3 ± 1.6‰), *S. media* (1.4 ± 0.6‰), few species did not significantly differ from their reference plants (Table S7). In ^{13}C, the here investigated Caryophyllaceae ranged from −0.2 ± 2.7‰ in *S. holostea* to 1.7 ± 0.3‰ in *Dianthus arenarius*.

Across all investigated Caryophyllaceae, leaf total N concentration ranged from 0.6 to 3.0 mmol/g_{dw} (mean = 1.6 ± 0.6 mmol/g_{dw}), which was in the range of the reference plants (mean = 1.7 ± 0.8 mmol/g_{dw}; range = 0.5–5.5 mmol/g_{dw}; $U_{48,165} = 3{,}485$, $p = 0.207$, $d_{Cohen} = 0.2$).

3.4 | Synopsis

In total, we investigated 36 plant species of the families Equisetaceae, Cyperaceae and Caryophyllaceae. These families are traditionally considered as non-mycorrhizal. However, we could demonstrate that these families across species are consistently colonized by fungi belonging to the *DSE*. In addition, for the Equisetaceae, we could identify microscopic structures closely resembling AM fungi forming *Paris*-type coils and vesicles; colonization by AM fungi was also confirmed by molecular data. Moreover, plants of all three families were significantly enriched in ^{15}N when compared to local reference plants, irrespective of whether these references were AM, ECM, ErM or NM. The ^{15}N enrichment was highest for Equisetaceae followed by Cyperaceae and Caryophyllaceae (Figure 5; Table 2). In addition, the plants turned out as enriched in ^{13}C, with Equisetaceae showing highest enrichment, followed by Caryophyllaceae and Cyperaceae (Figure 5; Table 2). However, effect sizes confirmed a meaningful ^{13}C enrichment only for the species belonging to the Equisetaceae. Achlorophyllous fertile stems of *E. arvense* were more enriched in ^{13}C than all other plant species here investigated. Equisetaceae

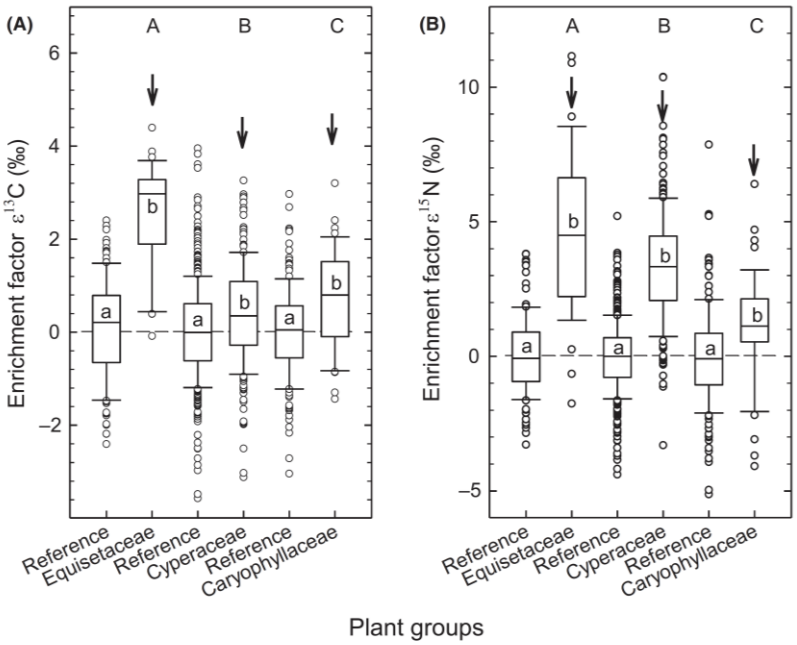

FIGURE 5 Box-and-whisker plots for stable carbon (A) and nitrogen (B) isotope enrichment factors ($\varepsilon^{13}C$ and $\varepsilon^{15}N$) of lateral shoots including the scale leaves of six plant species belonging to the Equisetaceae ($n = 34$), leaves of 23 plant species belonging to the Cyperaceae ($n = 209$) and leaves of seven plant species belonging to the Caryophyllaceae ($n = 48$) and their respective reference plants ($n = 789$, in total). The dashed line represents the mean of the reference plants. The capital letters illustrate significance of difference between the TP species belonging to Equisetaceae, Cyperaceae and Caryophyllaceae (arrow). The lower-case letters indicate significance of difference between the TP family and their respective reference plants. The reference plants were not significantly distinguished in $\varepsilon^{13}C$ and ^{15}N while significance in total N is not counted as relevant (Cohen's $d = 0.4$). The dashed line marks 0‰ enrichment. The range of the boxes illustrate the first and third quartile, the horizontal solid lines represent the medians, the whiskers enclose data within the 1.5× interquartile range, white circles are data extremes

TABLE 2 Pairwise comparison for Equisetaceae (Equi), Cyperaceae (Cype) and Caryophyllaceae (Cary) in enrichment factors ε of ^{13}C (‰), ^{15}N (‰) and of total N concentrations (mmol/g_{dw}) for leaf samples. Dunn's post hoc (*Z*) test including Bonferroni-Holm correction. Significances are highlighted in bold

	$\varepsilon^{13}C$		$\varepsilon^{15}N$		Total N	
Species (N)	**TS**	***p***	**TS**	***p***	**TS**	***p***
Equi (34) versus Cary (48)	$Z = 4.8$	**<0.001**	$Z = 6.2$	**<0.001**	$Z = 2.5$	**0.005**
Equi (34) versus Cype (209)	$Z = 7.5$	**<0.001**	$Z = 2.4$	**0.007**	$Z = 5.9$	**<0.001**
Cary (48) versus Cype (209)	$Z = 2.1$	**0.020**	$Z = -5.9$	**<0.001**	$Z = 3.3$	**0.001**

Note: TS: test statistic; Kruskal–Wallis test: $\varepsilon^{13}C$ $H(2) = 57.5$, $p = 0.001$; $\varepsilon^{15}N$ $H(2) = 46.5$, $p = 0.001$; Total N $H(2) = 40.3$, $p = 0.001$. *Equisetum* leaf include the lateral shoots and thereon the scale leaves.

also had significantly higher total N concentrations in their lateral shoots including the scale leaves when compared to their reference plants as well as to Cyperaceae and Caryophyllaceae (Figure S3), and *Equisetum* species were significantly enriched in ^{2}H in comparison to their reference plants.

The ^{13}C and ^{15}N enrichment factors and N concentrations as means and standard deviations for all investigated species of the Equisetaceae, Cyperaceae and Caryophyllaceae as well as their respective reference plants are available from the supplement (Tables S2, S4, S6) which includes also the statistics for each plot (Tables S3, S5, S7).

4 | DISCUSSION

Our investigation of natural abundances in stable N isotopes in 24 plant species belonging to the families Equisetaceae, Cyperaceae and Caryophyllaceae confirm N isotope abundances from our database for another 12 plant species of these three plant families (Tables S2, S4, S6) and earlier investigations by Michelsen, Schmidt, Jonasson, Quarmby, and Sleep (1996), Michelsen, Quarmby, Sleep, and Jonasson (1998). We show consistent ^{15}N enrichments relative to accompanying putatively autotrophic plant species forming AM, ECM, ErM or being NM. In their studies, Michelsen et al. (1996), Michelsen et al. (1998) grouped ^{15}N abundances for species belonging to the Equisetaceae, Cyperaceae and Caryophyllaceae together with species obviously capable of forming AM (e.g. *Festuca ovina*, *Geranium sylvaticum*, *Juniperus communis*, *Sorbus aucuparia* and *Trientalis europaea*), and classified them as a mixed group of NM/AM. When comparing them to co-occurring plant species forming ECM and ErM, they found that this mixed group of NM/AM plants showed enrichments in ^{15}N. Our study sheds a closer view on Michelsen's et al's data of the group classified as NM/AM and demonstrates that this group should be better separated according to two categories: the ^{15}N-enriched species belonging to the Equisetaceae, Cyperaceae and Caryophyllaceae and the plant species belonging to, for example, Apiaceae, Asteraceae, Cupressaceae, Geraniaceae, Primulaceae, Rosaceae usually forming AM (Brundrett & Tedersoo, 2019; Wang & Qiu, 2006). Thereby, the ^{15}N isotope enrichment of the majority of Michelsen's et al.'s plant species, most likely forming AM, falls back into the range of most ECM and some ErM plant species. This isotopic distinction between AM-forming plant families on the one hand and Equisetaceae, Cyperaceae and Caryophyllaceae on the other hand raises the question as to why species of the latter group are enriched in ^{15}N?

A shared feature of species belonging to Equisetaceae, Cyperaceae and Caryophyllaceae is their constant and dense colonization by *DSE* fungi as reported in the literature (Jumpponen & Trappe, 1998) and confirmed by our own microscopic and molecular findings. We therefore suggest a functional role of *DSE* in N acquisition and probably also acquisition of other mineral nutrients in analogy to the recent finding for plants colonized by *FRE* (Field et al., 2019; Hoysted et al., 2019). The site of nutrient transfer might be the fungal hyphae itself as previously demonstrated by a nanoSIMS application by Hill et al. (2019). Plants colonized by *FRE* and forming a nutritional mutualism were also enriched in ^{15}N (Hoysted et al., 2019). Our suggestion of a functional role of *DSE* fungi in nutrient acquisition is supported by early experiments by Haselwandter and Read (1982), recent findings on *DSE*-colonized *Deschampsia antarctica* (Poaceae) and *Colobanthus quitensis* (Caryophyllaceae) from Antarctica (Hill et al., 2019) and meta-analyses (Mandyam & Jumpponen, 2005; Newsham, 2011). Haselwandter and Read (1982) inoculated *Carex* species with *DSE* fungi and found a significant increase in dry weight of roots, shoots and whole plants as well as an increase in shoot phosphorous content; this effect was even higher when organic N was provided (Jumpponen & Trappe, 1998; Mandyam & Jumpponen, 2005; Upson, Read, & Newsham, 2009). The findings by Haselwandter and Read (1982) and our observation of ^{15}N enrichment are in agreement with the enzyme repertoire of *DSE* (Caldwell, Jumpponen, & Trappe, 2000) presumably allowing them to access ^{15}N-enriched soil organic compounds. Thus, *DSE* fungi may serve as providers of ^{15}N-enriched organic N compounds in Equisetaceae, Cyperaceae, Caryophyllaceae and probably other plants families and, in turn, may be rewarded by organic C compounds from plant photosynthesis. This suggestion is supported by the absence of ^{15}N enrichments found for the achlorophyllous fertile stems of *E. arvense*. These fertile stems are heterotrophic and therefore presumably cannot serve as providers of organic C and thus, there seems to be no more any mutualistic exchange in nutrients between host and fungus.

Simultaneously, the fertile stems of *E. arvense* turned out as most enriched in ^{13}C among all investigated plant samples. The enrichment in ^{13}C by the achlorophyllous fertile stems of *E. arvense* is in the typical range of ^{13}C enrichments found for fully mycoheterotrophic plants associated with AM fungi (Courty et al., 2011; Gomes et al., 2020; Merckx et al., 2010). Based on this ^{13}C enrichment found most pronounced for the achlorophyllous fertile stems of *E. arvense* and to a lower extent for all samples of chlorophyllous *Equisetum* species, we propose also an additional functional role of AM fungi for the here investigated Equisetaceae next to the function of *DSE* fungi—being aware of the fact that AM fungi were only sporadically found in our microscopic and molecular survey and that they are also only occasionally reported in the literature (Dhillion, 1993; Dickson et al., 2007; Fernández et al., 2008; Hodson et al., 2009; Koske et al., 1985). Equisetaceae are known to produce rather extensive rooting systems (Hauke, 1979). Thus, even weak fungal colonization per unit of *Equisetum* root biomass may be of significant relevance for the fungus–plant nutrient exchange on an entire plant level (van der Heijden, 2001). Importantly, AM fungal colonization by Equisetaceae always followed the *Paris*-morphotype. Hitherto, all investigated fully mycoheterotrophic plants associated with AM fungi (Imhof, Massicotte, Melville, & Peterson, 2013) and also the recently as partially mycoheterotrophic identified *Paris quadrifolia*, *Anemone nemorosa* (Giesemann, Rasmussen, et al., 2020) and *Pterygocalyx volubilis* (Suetsugu et al., 2020) always shared the *Paris*-morphotype. Based on this pattern, we suggest that the C isotope positioning between autotrophic reference plants and the achlorophyllous fertile

stems of *E. arvense* found here for six chlorophyllous *Equisetum* species indicates a partially mycoheterotrophic C gain (i.e. a simultaneous C gain from two sources, own photosynthesis and AM fungi). Based on linear two-source mixing model calculations, the proportional C gain from the fungal source by the six chlorophyllous *Equisetum* species studied here ranges in the order of 50 ± 22% with species-specific peculiarities. Similar proportional C gains from fungal sources were reported for partially mycoheterotrophic orchids and Ericaceae associated with ECM fungi (Hynson et al., 2013) and for the partially mycoheterotrophic and AM mycorrhizal *Bartonia virginica*, *Obolaria virginica*, *Pterygocalys volubilis* (Gentianaceae: Cameron & Bolin, 2010; Suetsugu et al., 2020), *Burmannia coelestris* (Burmanniaceae: Bolin, Tennakoon, Majid, & Cameron, 2017) and for *Paris quadrifolia* (Melanthiaceae) and *Anemone nemorosa* (Ranuculaceae; Giesemann, Rasmussen, et al., 2020).

Our suggestion of a partially mycoheterotrophic nutrition by chlorophyllous *Equisetum* species is supported by two other findings: (1) Significantly higher total N concentrations in all plant compartments in comparison to autotrophic reference plants. Increased total N concentrations are known as a wide-spread feature of many fully and partially mycoheterotrophic plants irrespective whether associated with fungi forming ECM (Gebauer & Meyer, 2003; Hynson et al., 2013; Stöckel, Meyer, & Gebauer, 2011) or AM (Gomes et al., 2020). (2) Significant ^{2}H enrichments in the lateral shoots including the scale leaves of the three investigated *Equisetum* species in comparison to leaves of accompanying putatively autotrophic reference plants. ^{2}H enrichment is a hallmark for heterotrophic nutrition of plants (Cormier, Werner, Leuenberger, & Kahmen, 2019; Cormier et al., 2018; Ziegler, 1994) and has been reported for fully, partially and initially mycoheterotrophic orchids, irrespective of whether associated with ECM or saprotrophic fungi of the rhizoctonia group (Gebauer et al., 2016; Schiebold, Bidartondo, Lenhard, Makiola, & Gebauer, 2018; Schweiger, Bidartondo, & Gebauer, 2018) as well as for fully and partially mycoheterotrophic plants associated with AM fungi (Giesemann, Rasmussen, et al., 2020; Gomes et al., 2020). Furthermore, our suggestion of a partially mycoheterotrophic nutrition by chlorophyllous *Equisetum* species due to significant ^{13}C and ^{2}H enrichments is supported by two previous investigations. Niu, Jiang, Gao, Li, and Liu (2003) reported on comparatively low net photosynthetic rates, high transpiration and low water use efficiency in Equisetaceae. All these factors are known to drive plants towards decreasing ^{13}C and ^{2}H abundances (Farquhar, Ehleringer, & Hubick, 1989; Ziegler, 1989) instead of the ^{13}C and ^{2}H enrichments as found here. And, in fact, Porter, Yiotis, Montañez, and McElwain (2017) found in chamber experiments under controlled conditions more negative δ^{13}C values in *Equisetum telmateia* and a couple of other ancient sporophytes in comparison to Gymnosperms and Angiosperms. Thus, our finding of ^{13}C and ^{2}H enrichments in Equisetaceae growing under natural field conditions can also not be explained by a deviating ecophysiology in photosynthesis and transpiration of these phylogenetically ancient plants.

In conclusion, plant species of the families Equisetaceae, Cyperaceae and Caryophyllaceae, traditionally considered as non-mycorrhizal turned out as conspicuous in their ^{15}N stable isotope natural abundance. Collective colonization by *DSE* and by this way access to ^{15}N-enriched organic N compounds in exchange for organic C compounds is assumed as most likely reason for this ^{15}N enrichment. This conclusion is further on supported by the absence of ^{15}N enrichments in representatives of the NM Brassicaceae. The additional enrichment in ^{13}C and ^{2}H found for green *Equisetum* species suggests them to act simultaneously as partial mycoheterotrophs on AM fungi of the *Paris*-morphotype (cf. Giesemann, Rasmussen, et al., 2020) while the achlorophyllous, fertile stems of *E. arvense* resemble a stable isotope pattern as known for fully mycoheterotrophic plants associated with AM fungi. Thus, so far, mostly underappreciated fungi classified as *DSE* are suggested to occupy an ecologically relevant role similar to mycorrhizae and the occurrence of simultaneous functions of *DSE* and AM fungi in Equisetaceae is proposed.

Our suggestion of an ecologically relevant function of *DSE* fungi should be tested in further laboratory tracer experiments as performed recently by Field et al. (2019) and Hoysted et al. (2019) when elucidating the functional role of *FRE* fungi.

ACKNOWLEDGEMENTS

P.G. and this project were funded by the Elite Network of Bavaria. The authors gratefully thank Carina Bauer, Isolde Baumann, Petra Eckert, Iris Schmiedinger, Christine Tiroch and Marga Wartinger for skilful technical assistance. We acknowledge Dr Pedro Gerstberger for plant identification in any uncertainties and localization of sampling sites. Open access funding enabled and organized by Projekt DEAL.

AUTHORS' CONTRIBUTIONS

P.G. comprised the data of three fieldwork campaigns, analysed and treated the results and wrote the first manuscript draft; D.E. conducted the sampling of Cyperaceae, M.S. and P.G. sampled Equisetaceae, L.F.S. and P.G. sampled Caryophyllaceae; Microscopic and isotope analyses were performed by P.G., D.E., M.S. and L.F.S. S.I.F.G. and V.S.F.T.M. were responsible for DNA analysis; G.G. initiated the project and coordinated the research design, supervised the isotope abundance survey and supported data treatment. All authors contributed to the manuscript.

DATA AVAILABILITY STATEMENT

Data deposited in the Dryad Digital Repository https://doi.org/10.5061/dryad.brv15dv7m (Giesemann, Eichenberg, et al., 2020).

ORCID

Sofia I. F. Gomes https://orcid.org/0000-0001-7218-1531
Vincent S. F. T. Merckx https://orcid.org/0000-0002-3959-8623
Gerhard Gebauer https://orcid.org/0000-0003-1577-7501

REFERENCES

Abarenkov, K., Zirk, A., Piirmann, T., Pöhönen, R., Ivanov, F., Nilsson, R. H., & Kõljalg, U. (2020). *UNITE general FASTA release for fungi*. UNITE Community. https://doi.org/10.15156/BIO/786369

Blaalid, R., Kumar, S., Nilsson, R. H., Abarenkov, K., Kirk, P. M., & Kauserud, H. (2013). ITS1 versus ITS2 as DNA metabarcodes for fungi. *Molecular Ecology Resources*, *13*, 218–224. https://doi.org/10.1111/1755-0998.12065

Bolin, J. F., Tennakoon, K. U., Majid, M. B. A., & Cameron, D. D. (2017). Isotopic evidence of partial mycoheterotrophy in *Burmannia coelestis* (Burmanniaceae). *Plant Species Biology*, *32*, 74–80.

Brundrett, M., Bougher, N., Dell, B., Grove, T., & Malajczuk, N. (1996). *Working with mycorrhizas in forestry and agriculture*. Canberra: Australian Centre for International Agricultural Research.

Brundrett, M., & Tedersoo, L. (2019). Misdiagnosis of mycorrhizas and inappropriate recycling of data can lead to false conclusions. *New Phytologist*, *221*, 18–24. https://doi.org/10.1111/nph.15440

Caldwell, B. A., Jumpponen, A., & Trappe, J. M. (2000). Utilization of major detrital substrates by dark-septate, root endophytes. *Mycologia*, *92*, 230–232. https://doi.org/10.1080/00275514.2000.12061149

Cameron, D. D., & Bolin, J. F. (2010). Isotopic evidence of partial mycoheterotrophy in the Gentianaceae: *Bartonia virginica* and *Obolaria virginica* as case studies. *American Journal of Botany*, *97*, 1272–1277.

Cohen, J. (1992). A power primer. *Psychological Bulletin*, *112*, 155–159. https://doi.org/10.1037/0033-2909.112.1.155

Cormier, M.-A., Werner, R. A., Leuenberger, M. C., & Kahmen, A. (2019). ^{2}H-enrichment of cellulose and n-alkanes in heterotrophic plants. *Oecologia*, *189*, 365–373. https://doi.org/10.1007/s00442-019-04338-8

Cormier, M.-A., Werner, R. A., Sauer, P. E., Gröcke, D. R., Leuenberger, M. C., Wieloch, T., … Kahmen, A. (2018). ^{2}H-fractionations during the biosynthesis of carbohydrates and lipids imprint a metabolic signal on the δ^{2}H values of plant organic compounds. *New Phytologist*, *218*, 479–491.

Courty, P.-E., Walder, F., Boller, T., Ineichen, K., Wiemken, A., Rousteau, A., & Selosse, M.-A. (2011). Carbon and nitrogen metabolism in mycorrhizal networks and mycoheterotrophic plants of tropical forests: A stable isotope analysis. *Plant Physiology*, *156*, 952–961. https://doi.org/10.1104/pp.111.177618

Dhillion, S. S. (1993). Vesicular-arbuscular mycorrhizas of *Equisetum* species in Norway and the U.S.A.: Occurrence and mycotrophy. *Mycological Research*, *97*, 656–660. https://doi.org/10.1016/S0953-7562(09)80142-1

Dickson, S., Smith, F. A., & Smith, S. E. (2007). Structural differences in arbuscular mycorrhizal symbioses: More than 100 years after Gallaud, where next? *Mycorrhiza*, *17*, 375–393.

Dinno, A. (2017). *dunn.test: Dunn's test of multiple comparisons using rank sums*. Retrieved from https://cran.r-project.org/web/packages/dunn.test/dunn.test.pdf

Druvca-Lusite, I., & Ievinsh, G. (2010). Diversity of arbuscular mycorrhizal symbiosis in plants from coastal habitats. *Environmental and Experimental Biology*, *8*.

Edgar, R. C. (2016a). SINTAX: A simple non-bayesian taxonomy classifier for 16S and ITS sequences. *bioRxiv*, 74161.

Edgar, R. C. (2016b). UNOISE2: Improved error-correction for Illumina 16S and ITS amplicon sequencing. *bioRxiv*, 081257.

Farquhar, G. D., Ehleringer, J. R., & Hubick, K. T. (1989). Carbon isotopic discrimination and photosynthesis. *Annual Review of Plant Biology*, *40*, 503–537.

Fernández, N., Messuti, M. I., & Fontenla, S. (2008). Arbuscular mycorrhizas and dark septate fungi in *Lycopodium paniculatum* (Lycopodiaceae) and *Equisetum bogotense* (Equisetaceae) in a valdivian temperate forest of Patagonia, Argentina. *American Fern Journal*, *98*, 117–127. https://doi.org/10.1640/0002-8444(2008)98[117:AMADSF]2.0.CO;2

Field, K. J., Bidartondo, M. I., Rimington, W. R., Hoysted, G. A., Beerling, D., Cameron, D. D., … Pressel, S. (2019). Functional complementarity of ancient plant-fungal mutualisms: Contrasting nitrogen, phosphorus and carbon exchanges between Mucoromycotina and Glomeromycotina fungal symbionts of liverworts. *New Phytologist*, *223*, 908–921. https://doi.org/10.1111/nph.15819

Gebauer, G., & Dietrich, P. (1993). Nitrogen isotope ratios in different compartments of a mixed stand of spruce, larch and beech trees and of understorey vegetation including fungi. *Isotopenpraxis Isotopes in Environmental and Health Studies*, *29*, 35–44. https://doi.org/10.1080/10256019308046133

Gebauer, G., & Meyer, M. (2003). ^{15}N and ^{13}C natural abundance of autotrophic and myco-heterotrophic orchids provides insight into nitrogen and carbon gain from fungal association. *New Phytologist*, *160*, 209–223. https://doi.org/10.1046/j.1469-8137.2003.00872.x

Gebauer, G., Preiss, K., & Gebauer, A. C. (2016). Partial mycoheterotrophy is more widespread among orchids than previously assumed. *New Phytologist*, *211*, 11–15. https://doi.org/10.1111/nph.13865

Giesemann, P., Eichenberg, D., Stöckel, M., Seifert, L. F., Gomes, S. I. F., Merckx, V. S. F. T., & Gebauer, G. (2020). Data from: Dark septate endophytes and arbuscular mycorrhizal fungi (*Paris*-morphotype) affect the stable isotope composition of 'classically' non-mycorrhizal plants. *Dryad Digital Repository*, https://doi.org/10.5061/dryad.brv15dv7m

Giesemann, P., Rasmussen, H. N., Liebel, H. T., & Gebauer, G. (2020). Discreet heterotrophs: Green plants that receive fungal carbon through *Paris*-type arbuscular mycorrhiza. *New Phytologist*, *226*, 960–966.

Gleixner, G., Danier, H. J., Werner, R. A., & Schmidt, H. L. (1993). Correlations between the ^{13}C content of primary and secondary plant products in different cell compartments and that in decomposing basidiomycetes. *Plant Physiology*, *102*, 1287–1290. https://doi.org/10.1104/pp.102.4.1287

Gomes, S. I., Merckx, V. S., Kehl, J., & Gebauer, G. (2020). Mycoheterotrophic plants living on arbuscular mycorrhizal fungi are generally enriched in ^{13}C, ^{15}N, and ^{2}H isotopes. *Journal of Ecology*, *108*, 1250–1261.

Haselwandter, K., & Read, D. J. (1982). The significance of a root-fungus association in two *Carex* species of high-alpine plant communities. *Oecologia*, *53*, 352–354. https://doi.org/10.1007/BF00389012

Hauke, R. L. (1979). A taxonomic monograph of *Equisetum* subgenus equisetum. *Nova Hedwigia*, *30*, 385–456. https://doi.org/10.1127/nova.hedwigia/30/1979/385

Hill, P. W., Broughton, R., Bougoure, J., Havelange, W., Newsham, K. K., Grant, H., … Jones, D. L. (2019). Angiosperm symbioses with non-mycorrhizal fungal partners enhance N acquisition from ancient organic matter in a warming maritime Antarctic. *Ecology Letters*, *22*, 2111–2119. https://doi.org/10.1111/ele.13399

Hodson, E., Shahid, F., Basinger, J., & Kaminskyj, S. (2009). Fungal endorhizal associates of *Equisetum* species from Western and Arctic Canada. *Mycological Progress*, *8*, 19–27. https://doi.org/10.1007/s11557-008-0574-0

Hoysted, G. A., Jacob, A. S., Kowal, J., Giesemann, P., Bidartondo, M. I., Duckett, J. G., … Field, K. J. (2019). Mucoromycotina fine root endophyte fungi form nutritional mutualisms with vascular plants. *Plant Physiology*, *181*, 565–577. https://doi.org/10.1104/pp.19.00729

Hynson, N. A., Madsen, T. P., Selosse, M. A., Adam, I. K., Ogura-Tsujita, Y., Roy, M., & Gebauer, G. (2013). The Physiological ecology of mycoheterotrophy. In V. S. Merckx (Ed.), *Mycoheterotrophy* (pp. 297–342). New York, NY: Springer.

Hynson, N. A., Schiebold, J.-M.-I., & Gebauer, G. (2016). Plant family identity distinguishes patterns of carbon and nitrogen stable isotope abundance and nitrogen concentration in mycoheterotrophic plants associated with ectomycorrhizal fungi. *Annals of Botany*, *118*, 467–479. https://doi.org/10.1093/aob/mcw119

Ihrmark, K., Bödeker, I. T. M., Cruz-Martinez, K., Friberg, H., Kubartova, A., Schenck, J., … Lindahl, B. D. (2012). New primers to amplify the fungal ITS2 region – Evaluation by 454-sequencing of artificial

and natural communities. *FEMS Microbiology Ecology*, *82*, 666–677. https://doi.org/10.1111/j.1574-6941.2012.01437.x

Imhof, S., Massicotte, H. B., Melville, L. H., & Peterson, R. L. (2013). Subterranean morphology and mycorrhizal structures. In V. S. Merckx (Ed.), *Mycoheterotrophy* (pp. 157–214). New York, NY: Springer.

Jumpponen, A. (2001). Dark septate endophytes – Are they mycorrhizal? *Mycorrhiza*, *11*, 207–211. https://doi.org/10.1007/s005720100112

Jumpponen, A. R. I., & Trappe, J. M. (1998). Dark septate endophytes: A review of facultative biotrophic root-colonizing fungi. *New Phytologist*, *140*, 295–310. https://doi.org/10.1046/j.1469-8137.1998.00265.x

Koske, R. E., Friese, C. F., Olexia, P. D., & Hauke, R. L. (1985). Vesicular-arbuscular mycorrhizas in *Equisetum*. *Transactions of the British Mycological Society*, *85*, 350–353. https://doi.org/10.1016/S0007-1536(85)80202-3

Lallemand, F., Puttsepp, Ü., Lang, M., Luud, A., Courty, P.-E., Palancade, C., & Selosse, M.-A. (2017). Mixotrophy in Pyroleae (Ericaceae) from Estonian boreal forests does not vary with light or tissue age. *Annals of Botany*, *120*, 361–371. https://doi.org/10.1093/aob/mcx054

Leake, J. R. (1994). The biology of myco-heterotrophic ('saprophytic') plants. *New Phytologist*, *127*, 171–216. https://doi.org/10.1111/j.1469-8137.1994.tb04272.x

Lenhard, W., & Lenhard, A. (2017). *Computation of effect sizes*. Unpublished. Retrieved from http://www.psychometrica.de/effect_size.html

Mandyam, K., & Jumpponen, A. (2005). Seeking the elusive function of the root-colonising dark septate endophytic fungi. *Studies in Mycology*, *53*, 173–189. https://doi.org/10.3114/sim.53.1.173

Mayor, J. R., Schuur, E. A. G., & Henkel, T. W. (2009). Elucidating the nutritional dynamics of fungi using stable isotopes. *Ecology Letters*, *12*, 171–183. https://doi.org/10.1111/j.1461-0248.2008.01265.x

Merckx, V. S. (2013). Mycoheterotrophy: An introduction. In V. S. Merckx (Ed.), *Mycoheterotrophy* (pp. 1–17). New York, NY: Springer.

Merckx, V., Stöckel, M., Fleischmann, A., Bruns, T. D., & Gebauer, G. (2010). ^{15}N and ^{13}C natural abundance of two mycoheterotrophic and a putative partially mycoheterotrophic species associated with arbuscular mycorrhizal fungi. *New Phytologist*, *188*, 590–596. https://doi.org/10.1111/j.1469-8137.2010.03365.x

Michelsen, A., Quarmby, C., Sleep, D., & Jonasson, S. (1998). Vascular plant ^{15}N natural abundance in heath and forest tundra ecosystems is closely correlated with presence and type of mycorrhizal fungi in roots. *Oecologia*, *115*, 406–418. https://doi.org/10.1007/s004420050535

Michelsen, A., Schmidt, I. K., Jonasson, S., Quarmby, C., & Sleep, D. (1996). Leaf ^{15}N abundance of subarctic plants provides field evidence that ericoid, ectomycorrhizal and non-and arbuscular mycorrhizal species access different sources of soil nitrogen. *Oecologia*, *105*, 53–63. https://doi.org/10.1007/BF00328791

Newsham, K. K. (2011). A meta-analysis of plant responses to dark septate root endophytes. *New Phytologist*, *190*, 783–793. https://doi.org/10.1111/j.1469-8137.2010.03611.x

Niu, S., Jiang, G., Gao, L., Li, Y., & Liu, M. (2003). Comparison of gas exchange traits of different plant species in Hunshandak sand area. *Acta Phytoecological Sinica*, *27*, 318–324.

Ogura-Tsujita, Y., Gebauer, G., Hashimoto, T., Umata, H., & Yukawa, T. (2009). Evidence for novel and specialized mycorrhizal parasitism: The orchid *Gastrodia confusa* gains carbon from saprotrophic *Mycena*. *Proceedings of the Royal Society B: Biological Sciences*, *276*, 761–767.

Orchard, S., Hilton, S., Bending, G. D., Dickie, I. A., Standish, R. J., Gleeson, D. B., … Ryan, M. H. (2017). Fine endophytes (*Glomus tenue*) are related to Mucoromycotina, not Glomeromycota. *New Phytologist*, *213*, 481–486.

Phillips, J. M., & Hayman, D. S. (1970). Improved procedures for clearing roots and staining parasitic and vesicular-arbuscular mycorrhizal fungi for rapid assessment of infection. *Transactions of the British Mycological Society*, *55*, 158-IN18. https://doi.org/10.1016/S0007-1536(70)80110-3

Porter, A. S., Yiotis, C., Montañez, I. P., & McElwain, J. C. (2017). Evolutionary differences in $\Delta^{13}C$ detected between spore and seed bearing plants following exposure to a range of atmospheric O_2:CO_2 ratios; implications for paleoatmosphere reconstruction. *Geochimica et Cosmochimica Acta*, *213*, 517–533. https://doi.org/10.1016/j.gca.2017.07.007

Preiss, K., & Gebauer, G. (2008). A methodological approach to improve estimates of nutrient gains by partially myco-heterotrophic plants. *Isotopenpraxis Isotopes in Environmental and Health Studies*, *44*, 393–401. https://doi.org/10.1080/10256010802507458

Pressel, S., Bidartondo, M. I., Field, K. J., Rimington, W. R., & Duckett, J. G. (2016). Pteridophyte fungal associations: Current knowledge and future perspectives. *Journal of Systematics and Evolution*, *54*, 666–678.

R Core Team. (2019). *R: A language and environment for sttistical computing*. Vienna, Austria: R Foundation for Statistical Computing.

Schiebold, J.-M.-I., Bidartondo, M. I., Lenhard, F., Makiola, A., & Gebauer, G. (2018). Exploiting mycorrhizas in broad daylight: Partial mycoheterotrophy is a common nutritional strategy in meadow orchids. *Journal of Ecology*, *106*, 168–178. https://doi.org/10.1111/1365-2745.12831

Schindelin, J., Arganda-Carreras, I., Frise, E., Kaynig, V., Longair, M., Pietzsch, T., … Cardona, A. (2012). Fiji: An open-source platform for biological-image analysis. *Nature Methods*, *9*, 676–682. https://doi.org/10.1038/nmeth.2019

Schweiger, J.-M.-I., Bidartondo, M. I., & Gebauer, G. (2018). Stable isotope signatures of underground seedlings reveal the organic matter gained by adult orchids from mycorrhizal fungi. *Functional Ecology*, *32*, 870–881. https://doi.org/10.1111/1365-2435.13042

Shah, M. A., Reshi, Z. A., & Khasa, D. (2009). Arbuscular mycorrhizal status of some Kashmir Himalayan alien invasive plants. *Mycorrhiza*, *20*, 67–72. https://doi.org/10.1007/s00572-009-0258-x

Smith, S. E., & Read, D. J. (2008). *Mycorrhizal symbiosis*. Amsterdam, The Netherlands: Elsevier/Academic Press.

Stöckel, M., Meyer, C., & Gebauer, G. (2011). The degree of mycoheterotrophic carbon gain in green, variegated and vegetative albino individuals of *Cephalanthera damasonium* is related to leaf chlorophyll concentrations. *New Phytologist*, *189*, 790–796. https://doi.org/10.1111/j.1469-8137.2010.03510.x

Suetsugu, K., Matsubayashi, J., Ogawa, N. O., Murata, S., Sato, R., & Tomimatsu, H. (2020). Isotopic evidence of arbuscular mycorrhizal cheating in a grassland gentian species. *Oecologia*, *192*, 929–937. https://doi.org/10.1007/s00442-020-04631-x

Systat Software. (2008). *SigmaPlot*. Version 11 (Copyright 2008). San Jose, CA: Systat Software, Inc.

Tedersoo, L., Bahram, M., & Zobel, M. (2020). How mycorrhizal associations drive plant population and community biology. *Science*, *367*, eaba1223. https://doi.org/10.1126/science.aba1223

Tedersoo, L., Pellet, P., Kõljalg, U., & Selosse, M.-A. (2007). Parallel evolutionary paths to mycoheterotrophy in understorey Ericaceae and Orchidaceae: Ecological evidence for mixotrophy in Pyroleae. *Oecologia*, *151*, 206–217. https://doi.org/10.1007/s00442-006-0581-2

Upson, R., Read, D. J., & Newsham, K. K. (2009). Nitrogen form influences the response of *Deschampsia antarctica* to dark septate root endophytes. *Mycorrhiza*, *20*, 1–11. https://doi.org/10.1007/s00572-009-0260-3

van der Heijden, E. W. (2001). Differential benefits of arbuscular mycorrhizal and ectomycorrhizal infection of *Salix repens*. *Mycorrhiza*, *10*, 185–193. https://doi.org/10.1007/s005720000077

Velázquez, M. S., Biganzoli, F., & Cabello, M. N. (2010). Arbuscular mycorrhizal fungi in El Palmar National Park (Entre Rios Province, Argentina) – A protected reserve. *Sydowia*, *62*, 149–163.

Vierheilig, H., Schweiger, P., & Brundrett, M. (2005). An overview of methods for the detection and observation of arbuscular mycorrhizal

fungi in roots. *Physiologia Plantarum*, *125*, 393–404. https://doi.org/10.1111/j.1399-3054.2005.00564.x

Walker, C., Gollotte, A., & Redecker, D. (2018). A new genus, *Planticonsortium* (Mucoromycotina), and new combination (*P. tenue*), for the fine root endophyte, *Glomus tenue* (basionym *Rhizophagus tenuis*). *Mycorrhiza*, *28*, 213–219. https://doi.org/10.1007/s00572-017-0815-7

Wang, B., & Qiu, Y.-L. (2006). Phylogenetic distribution and evolution of mycorrhizas in land plants. *Mycorrhiza*, *16*, 299–363. https://doi.org/10.1007/s00572-005-0033-6

White, T. J., Bruns, T., Lee, S., & Taylor, J. (1990). Amplification and direct sequencing of fungal ribosomal RNA genes for phylogenetics. In M. Innis, D. Gelfand, J. Sininsky, & T. White (Eds.), *PCR protocols: A guide to methods and applications* (pp. 315–332). San Diego, CA: Academic Press.

Ziegler, H. (1989). Hydrogen isotope fractionation in plant tissues. In P. W. Rundel, J. R. Ehleringer, & K. A. Nagy (Eds.) *Stable isotopes in ecological research. Ecological studies 68* (pp. 105–123). Berlin, Germany: Springer.

Ziegler, H. (1995). Stable isotopes in plant physiology and ecology. In H.-D. Behnke, U. Lüttge, K. Esser, J. W. Kadereit, & M. Runge (Eds.), *Progress in botany: Structural botany physiology genetics taxonomy geobotany/Fortschritte der Botanik Struktur Physiologie Genetik Systematik Geobotanik* (pp. 1–24). Berlin, Heidelberg: Springer Berlin Heidelberg.

Ziegler, H. (1994). Deuterium content in organic material of hosts and their parasites. In Schulze, E.-D., & Caldwell, M. M. (Eds.), *Ecophysiology of photosynthesis. Ecological studies 100* (pp. 393–408). Berlin, Germany: Springer.

Zimmer, K., Hynson, N. A., Gebauer, G., Allen, E. B., Allen, M. F., & Read, D. J. (2007). Wide geographical and ecological distribution of nitrogen and carbon gains from fungi in pyroloids and monotropoids (Ericaceae) and in orchids. *New Phytologist*, *175*, 166–175. https://doi.org/10.1111/j.1469-8137.2007.02065.x

SUPPORTING INFORMATION

Additional supporting information may be found online in the Supporting Information section.

How to cite this article: Giesemann P, Eichenberg D, Stöckel M, et al. Dark septate endophytes and arbuscular mycorrhizal fungi (*Paris*-morphotype) affect the stable isotope composition of 'classically' non-mycorrhizal plants. *Funct Ecol*. 2020;34: 2453–2466. https://doi.org/10.1111/1365-2435.13673

Funtional Ecology Supporting Information

Dark septate endophytes and arbuscular mycorrhizal fungi (*Paris*-morphotype) affect the stable isotope composition of 'classically' non-mycorrhizal plants

Philipp Giesemann, David Eichenberg, Marcus Stöckel, Lukas F. Seifert, Sofia I.F. Gomes, Vincent S.F.T. Merckx, Gerhard Gebauer

The following Supporting Information is available for this article:

Figure S1 Pie charts of dark septate fungal endophytes and Glomeromycotina in the three plant species belonging to the Equisetaceae.

Figure S2 Total root endophyte colonization (%) in Equisetaceae.

Figure S3 Leaf total N concentrations [mmol/g_{dw}] of the target plant families relative to their reference plants.

Table S1 Test for pairwise comparison between *Equisetum sylvaticum*, moss and reference plants in enrichment factors ε of ^{13}C [‰], ^{15}N [‰] and leaf total N concentrations [mmol/g_{dw}].

Table S2 Stable isotope natural abundances in δ-values [‰] and total N concentrations [mmol/g_{dw}] of Equisetaceae and their respective reference plants as mean value.

Table S3 Test for differences between Equisetaceae and their respective reference plants in enrichment factors ε of ^{13}C [‰], ^{15}N [‰] and total N concentrations [mmol/g_{dw}].

Table S4 Stable isotope natural abundances in δ-values [‰] and leaf total N concentrations [mmol/g_{dw}] of Cyperaceae and their respective reference plants as mean value.

Table S5 Test for differences between Cyperaceae species and their respective reference plants in enrichment factors ε of ^{13}C [‰], ^{15}N [‰] and leaf total N concentrations [mmol/g_{dw}].

Table S6 Stable isotope natural abundances in δ-values [‰] and leaf total N concentrations [mmol/g_{dw}] of Caryophyllaceae and their respective reference plants as mean value.

Table S7 Test for differences between Caryophyllaceae species and their respective reference plants in enrichment factors ε of ^{13}C [‰], ^{15}N [‰] and leaf total N concentrations [mmol/g_{dw}].

Table S8. Fungal endophytes in three plant species belonging to the Equisetaceae.

Respective references

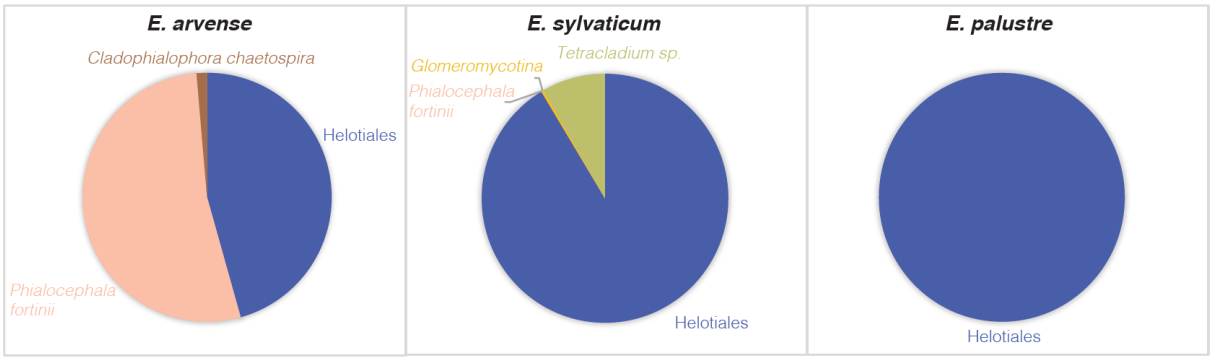

Figure S1 Pie charts of dark septate fungal endophytes and Glomeromycotina in the three plant species belonging to the Equisetaceae.

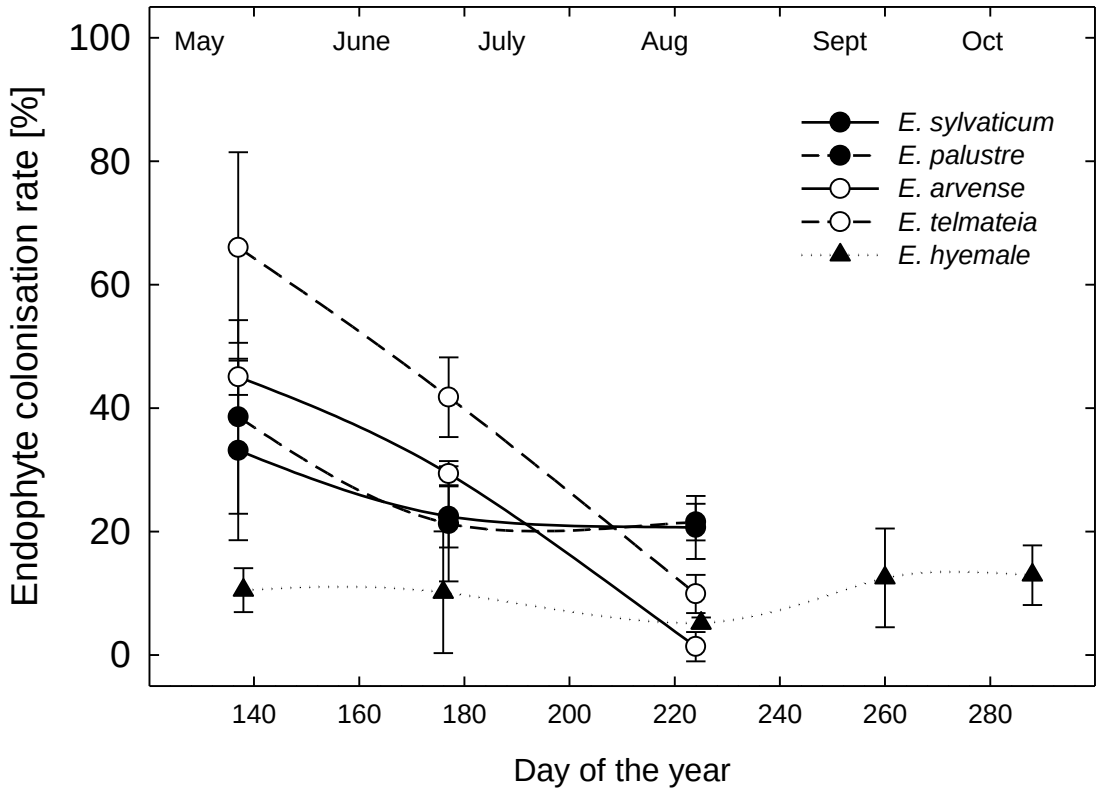

Figure S2 Total root endophyte colonization (%) in five Equisetaceae species from May to November.

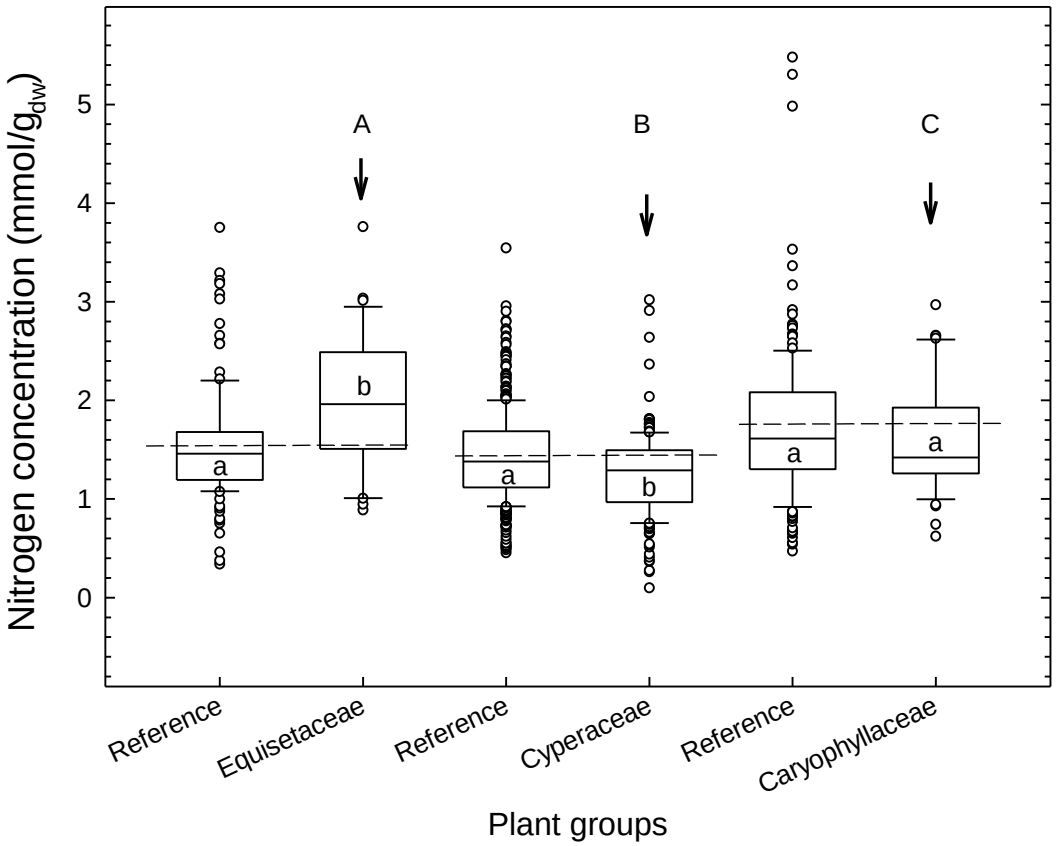

Figure S3 Leaf total N concentrations [mmol/g_{dw}] of six plant species belonging to Equisetaceae (n = 34), 22 plant species belonging to Cyperaceae (n = 194) and seven plant species belonging to Caryophyllaceae (n = 48) relative to their reference plants (n = 734, in total). The capital letters illustrate significance of difference between the target plant species belonging to Equisetaceae, Cyperaceae and Caryophyllaceae (arrow). The lower-case letters indicate significance of difference between the target plant families and their respective reference plants *Equisetum* leaf material includes the lateral shoot and thereon the scale leaves. The range of the boxes illustrate the first and third quartile, the horizontal solid lines represent the medians, the whiskers enclose data within the 1.5x interquartile range, white circles are data extremes.

Table S1 Test for pairwise comparison between *Equisetum sylvaticum* (Equi), *moss* (*Polytrichum commune*) and reference plants (Ref) in enrichment factors ε of ^{13}C [‰], ^{15}N [‰] for leaf samples and leaf total N concentrations [mmol/g_{dw}]. Dunn *post hoc* test (Z). Significances are highlighted in bold.

Species (N)	**$\varepsilon^{13}C$**		**$\varepsilon^{15}N$**		**Total N**	
	TS	*P*	TS	*P*	TS	*P*
Equi (5) *vs*. Moss (5)	$Z = 0$	**= 0.008**	$Z = 0$	**= 0.016**	$Z = 1$	**= 0.032**
Equi (5) *vs*. Ref (15)	$Z = 0$	**= 0.003**	$Z = 0$	**< 0.001**	$Z = 0$	**< 0.001**
Ref (15) *vs*. Moss (5)	$Z = 3$	**= 0.006**	$Z = 27$	= 0.383	$Z = 22$	= 0.190

TS: Test statistic. *Equisetum* leaf material includes the lateral shoot and thereon the scale leaves.

Table S2 Stable isotope natural abundances in δ-values [‰] and leaf total N concentrations [mmol/g_{dw}] of six species belonging to the Equisetaceae and their respective reference plants as mean value per plant organ. The relative enrichment ε [‰] to the mean of reference plants was calculated. Data are shown in mean ± SD.

Species	Organ	Carbon ^{13}C isotope abundance [‰]			Nitrogen ^{15}N isotope abundance [‰]			N [mmol gdw^{-1}]	
	(N_{Equi}, N_{Ref})	Equisetaceae	Reference	ε	Equisetaceae	Reference	ε	Equisetaceae	Reference
Equisetum arvense	L (5,25)	-26.6 ± 0.3	-29.8 ± 0.7	3.2 ± 0.2	3.9 ± 0.8	2.7 ± 1.2	1.2 ± 1.0	2.5 ± 0.3	1.5 ± 0.3
49.8902°N, 11.6139°E	S (5,25)	-25.3 ± 0.2	-29.5 ± 0.7	4.2 ± 0.1	3.1 ± 0.8	2.1 ± 1.3	1.0 ± 1.0	1.7 ± 0.2	1.0 ± 0.1
	R (5,20)	-24.9 ± 0.2	-29.0 ± 0.4	4.1 ± 0.3	2.1 ± 0.9	0.3 ± 1.6	1.8 ± 1.0	1.4 ± 0.4	0.5 ± 0.2
E. arvense (fertile)	-	- - -	- - -	- - -	- - -	- - -	- - -	- - -	- - -
49.8902°N, 11.6139°E	S (5,25)	-24.3 ± 0.6	-29.5 ± 0.7	5.2 ± 0.5	3.0 ± 1.5	2.1 ± 1.3	0.9 ± 1.0	2.2 ± 0.4	1.0 ± 0.1
	R (5,25)	-24.9 ± 0.5	-28.9 ± 0.4	4.1 ± 0.5	-0.3 ± 1.2	0.1 ± 1.6	-0.4 ± 0.7	1.6 ± 0.2	0.6 ± 0.2
E. fluviatile	L (5,15)	-28.9 ± 0.4	-31.3 ± 1.5	2.5 ± 0.4	2.9 ± 1.1	-1.3 ± 1.2	4.4 ± 1.2	1.9 ± 0.2	1.3 ± 0.5
49.8806°N, 11.6089°E	S (5,15)	-27.7 ± 0.2	-30.1 ± 1.6	2.4 ± 2.3	1.2 ± 0.8	-1.1 ± 1.1	2.3 ± 0.6	1.1 ± 0.1	0.5 ± 0.1
	R (5,15)	-26.6 ± 0.2	-29.9 ± 2.6	4.0 ± 0.5	0.8 ± 1.4	-1.6 ± 1.7	2.3 ± 1.4	1.1 ± 0.2	0.6 ± 0.2
E. hyemale	-	- - -	- - -	- - -	- - -	- - -	- - -	- - -	- - -
49.7658°N, 11.4643°E	S (5,15)	-28.6 ± 0.3	-32.0 ± 0.7	3.4 ± 0.3	1.5 ± 0.4	-2.3 ± 1.1	3.7 ± 1.1	0.7 ± 0.1	1.3 ± 0.3
	R (5,20)	-28.2 ± 0.4	-31.9 ± 0.8	3.8 ± 0.5	-0.9 ± 1.5	-2.8 ± 1.0	2.1 ± 1.6	1.0 ± 0.1	1.5 ± 0.2
E. palustre	L (5,20)	-29.4 ± 0.3	-29.8 ± 1.0	0.5 ± 0.3	3.0 ± 2.2	-4.5 ± 1.7	7.5 ± 2.6	3.1 ± 0.4	1.2 ± 0.2
49.8739°N, 11.6057°E	S (5,15)	-29.3 ± 0.4	-28.8 ± 0.9	-0.5 ± 0.6	2.1 ± 2.5	-5.2 ± 1.2	7.3 ± 2.5	1.6 ± 0.1	0.7 ± 0.2
	R (3,19)	-29.0 ± 0.5	-29.7 ± 1.1	0.9 ± 0.4	1.9 ± 1.5	-3.8 ± 1.8	5.3 ± 1.7	1.7 ± 0.1	0.5 ± 0.1
E. sylvaticum	L (4,20)	-27.2 ± 0.5	-29.8 ± 1.0	2.8 ± 0.6	3.2 ± 2.0	-4.5 ± 1.7	7.3 ± 2.3	1.9 ± 0.2	1.2 ± 0.2
49.8739°N, 11.6057°E	S (4, 15)	-25.8 ± 0.4	-28.8 ± 0.9	3.3 ± 0.6	2.3 ± 1.9	-5.2 ± 1.2	7.1 ± 1.5	0.9 ± 0.2	0.7 ± 0.2
	R (2,19)	-25.2	-29.7 ± 1.1	5.0	3.5	-3.8 ± 1.8	6.7	1.7	0.5 ± 0.1
E. sylvaticum	L (5,25)	-28.8 ± 0.6	-32.1 ± 1.3	3.4 ± 0.2	-2.1 ± 1.8	-4.6 ± 2.2	2.5 ± 2.5	2.2 ± 0.3	1.7 ± 0.5
49.8739°N, 11.6057°E	S (5, 20)	-28.4 ± 0.4	-32.1 ± 1.5	3.7 ± 0.3	-3.1 ± 2.1	-4.6 ± 1.8	1.5 ± 2.2	0.9 ± 0.1	0.8 ± 0.2
	-	- - -	- - -	- - -	- - -	- - -	- - -	- - -	- - -
E. sylvaticum	L (5,20)	-27.2 ± 0.5	-31.9 ± 1.1	3.6 ± 0.5	-6.2 ± 2.2	3.2 ± 2.3	7.6 ± 0.6	1.0 ± 0.1	1.0 ± 0.1
49.9234°N, 11.5495°E									
E. telmateia	L (5,15)	-28.4 ± 0.9	-30.0 ± 1.0	1.6 ± 1.0	3.1 ± 1.5	0.0 ± 0.9	3.0 ± 1.8	1.4 ± 0.2	2.4 ± 0.8
49.9488°N, 11.6539°E	S (5,10)	-26.1 ± 0.9	-29.9 ± 0.6	3.8 ± 1.0	0.9 ± 1.3	-1.3 ± 1.5	2.1 ± 1.6	0.3 ± 0.1	1.6 ± 0.4
	R (5,15)	-26.4 ± 0.9	-29.6 ± 0.9	3.2 ± 1.0	0.9 ± 1.8	-1.2 ± 1.2	2.2 ± 2.1	0.6 ± 0.2	1.3 ± 0.6

L: lateral shoots and thereon the scale leaves (n = 34,125), S: stem (n = 39,125), R: root (n = 30,135). Reference plants were *Aegopodium podagraria* (AM), *Ajuga reptans* (AM), *Brassica napus* (NM), *Capsella bursa-pastoris* (NM), *Cirsium palustre* (AM), *Erodium cicutarium* (AM), *Filipendula ulmaria* (AM), *Fragaria vesca* (AM),*Galium aparine* (AM), *Lycopus europaeus* (AM), *Lysimachia nummularia* (AM), *Lysimachia vulgaris* (AM), *Oxalis acetosella* (AM), *Picea abies* (ECM), *Sorbus aucuparia* (ECM), *Stellaria media* (NM), *Taraxacum officinale* (AM), *Trientalis europaea* (AM), *Urtica dioica* (AM), *Vaccinium myrtillus* (ErM), *Viola arvensis* (AM), *Viola* sp. (AM). AM arbuscular mycorrhiza, ECM Ectomycorrhiza, ErM ericoid mycorrhiza, NM non-mycorrhiza

Table S3 Test for differences between six species belonging to the Equisetaceae and their respective reference plants in enrichment factors ε of ^{13}C [‰] and ^{15}N [‰], and total N concentrations [mmol/g_{dw}] per plant organ. Mann-Whitney-U test. Significances are bold marked.

Species	Organ (N_{Equi}, $N_{Ref.}$)	$\varepsilon^{13}C$		$\varepsilon^{15}N$		Total N	
		TS	*P*	TS	*P*	TS	*P*
E. arvense	L (5,25)	*U* = 0	**< 0.001**	*U* = 20	**= 0.019**	*U* = 1	**< 0.001**
49.8902°N, 11.6139°E	S (5,25)	*U* = 0	**< 0.001**	*U* = 26	**= 0.045**	*U* = 0	**< 0.001**
	R (5,20)	*U* = 0	**< 0.001**	*U* = 14	**= 0.016**	*U* = 1	**< 0.001**
E. arvense (fertile)	-	-	-	-	-	-	-
49.8902°N, 11.6139°E	S (5,25)	*U* = 0	**< 0.001**	*U* = 35	= 0.133	*U* = 0	**< 0.001**
	R (5,25)	*U* = 0	**< 0.001**	*U* = 47	= 0404	*U* = 0	**< 0.001**
E. fluviatile	L (5,15)	*U*= 5	**= 0.005**	*U* = 0	**= 0.001**	*U* = 16	= 0.067
49.8806°N, 11.6089°E	S (5,15)	*U* = 11	**= 0.023**	*U* = 2	**= 0.002**	*U* = 0	**= 0.001**
	R (5,15)	*U* = 0	**= 0.001**	*U* = 8	**= 0.011**	*U* = 2	**= 0.002**
E. hyemale	-	-	-	-	-	-	-
49.7658°N, 11.4643°E	S (5,15)	*U* = 0	**= 0.001**	*U* = 0	**= 0.001**	*U* = 0	**= 0.001**
	R (5,20)	*U* = 0	**< 0.001**	*U* = 13	**= 0.040**	*U* = 1	**< 0.001**
E. palustre	L (5,20)	*U* = 38	= 0.440	*U* = 0	**< 0.001**	*U* = 0	**< 0.001**
49.8739°N, 11.6057°E	S (5,15)	*U* = 24	= 0.260	*U* = 0	**= 0.001**	*U* = 0	**= 0.001**
	R (3,19)	*U* = 14	= 0.180	*U* = 1	**= 0.010**	*U* = 0	**= 0.007**
E. sylvaticum	L (4,20)	*U* = 0	**= 0.002**	*U* = 0	**= 0.002**	*U* = 0	**< 0.002**
49.8739°N, 11.6057°E	S (4, 15)	*U* = 0	**= 0.003**	*U* = 0	**= 0.003**	*U* = 14	= 0.121
	R (2,19)	*U* = 0	**= 0.027**	*U* = 1	**= 0.036**	*U* = 0	**= 0.027**
E. sylvaticum	L (5,25)	*U* = 0	**< 0.001**	*U* = 30	= 0.075	*U* = 22	**= 0.026**
49.8739°N, 11.6057°E	S (5, 20)	*U* = 0	**< 0.001**	*U* = 26	= 0.110	*U* = 28	= 0.144
	-	-	-	-	-	-	-
E. sylvaticum	L (5,20)	*U* = 0	**< 0.001**	*U* = 0	**< 0.001**	*U* = 1	**< 0.001**
49.9234°N, 11.5495°E							
E. telmateia	L (5,15)	*U* = 5	**= 0.005**	*U* = 6	**< 0.006**	*U* = 6	**= 0.007**
49.9488°N, 11.6539°E	S (5,10)	*U* = 0	**= 0.003**	*U* = 7	**= 0.032**	*U* = 0	**= 0.003**
	R (5,15)	*U* = 0	**= 0.001**	*U* = 13	**= 0.036**	*U* = 7	**= 0.009**

TS: Test statistic, L: lateral shoots and thereon the scale leaves, S: stem, R: root. Reference plants were *Aegopodium podagraria* (AM), *Ajuga reptans* (AM), *Brassica napus* (NM), *Capsella bursa-pastoris* (NM), *Cirsium palustre* (AM), *Erodium cicutarium* (AM), *Filipendula ulmaria* (AM), *Fragaria vesca* (AM), *Galium aparine* (AM), *Lycopus europaeus* (AM), *Lysimachia nummularia* (AM), *Lysimachia vulgaris* (AM), *Oxalis acetosella* (AM), *Picea abies* (ECM), *Sorbus aucuparia* (ECM), *Stellaria media* (NM), *Taraxacum officinale* (AM), *Trientalis europaea* (AM), *Urtica dioica* (AM), *Vaccinium myrtillus* (ErM), *Viola arvensis* (AM), *Viola* sp. (AM). AM arbuscular mycorrhiza, ECM Ectomycorrhiza, ErM ericoid mycorrhiza, NM non-mycorrhiza

Table S4 Stable isotope natural abundances in δ-values [‰] and leaf total N concentrations [mmol/g_{dw}] of 23 species belonging to the Cyperaceae (n = 209) and their respective reference plants (n = 499) as mean value. The relative enrichment ε [‰] to the mean value of accompanying reference plants was calculated for isotope data. Data are shown in mean ± SD.

Species	N_{Cype}, $N_{Ref.}$		Leaf carbon ^{13}C isotope abundance [‰]			Leaf nitrogen ^{15}N isotope abundance [‰]			N [mmol gdw^{-1}]	
			Cyperaceae	Reference	ε	Cyperaceae	Reference	ε	Cyperaceae	Reference
Carex caryophyllea 50.1210°N, 11.8621°E	5,15	1	-27.6 ± 0.6	-28.5 ± 0.8	0.8 ± 0.5	-1.3 ± 1.0	-3.2 ± 0.9	2.0 ± 1.1	0.8 ± 0.1	1.0 ± 0.2
C. conica 35.0561°N, 140.0264°E	2,97	2	-32.3	-33.0 ± 1.6	0.6	-3.3	-4.0 ± 1.5	0.7	1.1	1.4 ± 0.5
C. digitata 49.6850°N, 11.3207°E	5,15	1	-30.8 ± 0.3	-30.7 ± 0.6	-0.1 ± 0.2	-2.6 ± 1.8	-4.6 ± 1.6	2.0 ± 2.1	1.1 ± 0.2	1.5 ± 0.4
C. digitata 49.6187°N, 11.4200°E	5,21	1	-28.9 ± 1.3	-29.5 ± 1.5	1.7 ± 1.5	-4.0 ± 1.4	-6.0 ± 1.4	0.6 ± 1.1	0.9 ± 0.2	1.7 ± 0.3
C. disticha 35.0561°N, 140.0264°E	5,30	1	-28.2 ± 0.6	-29.0 ± 1.2	0.8 ± 0.9	-0.9 ± 1.6	-2.4 ± 2.3	2.2 ± 1.9	1.6 ± 0.1	1.6 ± 0.3
C. disticha 49.9065°N, 11.6210°E	1,26	1	-29.3	-29.3 ± 0.9	-0.2	3.5	1.0 ± 1.7	2.8	0.9	1.5 ± 0.3
C. distachya 39.7405°N, 9.5729°E	5,10	3	-34.0 ± 0.5	-32.0 ± 0.8	-2.1 ± 0.8	0.3 ± 3.3	-1.3 ± 1.3	1.6 ± 2.7	1.1 ± 0.2	0.9 ± 0.2
C. flacca 35.0561°N, 140.0264°E	5,30	1	-29.6 ± 0.9	-29.0 ± 1.2	-0.6 ± 0.9	-1.2 ± 1.6	-2.4 ± 2.3	0.6 ± 2.6	1.5 ± 0.2	1.6 ± 0.3
C. flacca 49.6850°N, 11.3207°E	5,15	1	-31.6 ± 0.6	-30.7 ± 0.6	-0.9 ± 0.7	-2.0 ± 1.9	-4.6 ± 1.6	2.6 ± 1.3	1.3 ± 0.3	1.5 ± 0.4
C. flacca 49.6187°N, 11.4200°E	5,21	1	-29.9 ± 1.0	-29.5 ± 1.5	1.0 ± 0.8	-1.9 ± 0.9	-6.0 ± 1.4	3.6 ± 1.9	0.8 ± 0.1	1.7 ± 0.3
C. flacca 49.6715°N, 11.3893°E	10,20	4	-31.2 ± 1.2	-32.1 ± 1.1	1.2 ± 1.0	0.6 ± 4.8	-3.4 ± 2.8	4.1 ± 2.7	1.5 ± 0.3	1.8 ± 0.5
C. flacca 49.6667° N, 11.3833°E	27,57	5	-32.5 ± 0.7	-32.4 ± 1.2	0.2 ± 0.7	-1.4 ± 1.2	-5.2 ± 1.7	3.8 ± 1.4	1.5 ± 0.1	1.7 ± 0.5
C. flacca 49.6715°N, 11.3893°E	27,20	6	-32.3 ± 0.7	-33.0 ± 1.2	0.6 ± 0.4	-1.2 ± 1.1	-5.8 ± 1.4	4.6 ± 1.1	1.5 ± 0.1	1.3 ± 0.2
C. flacca 58.3333° N, 22.3000°E	19,64	7	-28.5 ± 1.0	-30.1 ± 1.2	1.6 ± 0.9	2.4 ± 1.8	-1.5 ± 2.1	4.0 ± 1.8	1.0 ± 0.3	1.3 ± 0.3
C. flava 47.1500°N, 9.800°E	5,34	8	-26.8 ± 0.6	-26.4 ± 0.8	-0.4 ± 0.5	1.2 ± 1.9	-4.3 ± 2.6	4.6 ± 2.0	1.1 ± 0.3	1.3 ± 0.4
C. hallerana 39.7405°N, 9.5729°E	5,20	3	-28.9 ± 0.8	-29.7 ± 1.4	0.9 ± 1.0	-4.4 ± 0.8	-8.2 ± 1.4	NA	NA	0.9 ± 0.2
C. hirta 49.9065°N, 11.6210°E	5,26	1	-30.0 ± 0.4	-29.3 ± 0.9	-0.7 ± 0.2	4.9 ± 0.8	1.0 ± 1.7	3.5 ± 2.1	1.2 ± 0.2	1.5 ± 0.3
C. hirta 35.0561°N, 140.0264°E	1,30	1	-28.8	-29.0 ± 1.2	0.2	-1.2	-2.4 ± 2.3	1.4	1.6	1.6 ± 0.3
C. hirta 44.38256°N, 8.2562°E	5,20	3	-28.9 ± 0.6	-29.1 ± 0.6	0.3 ± 0.8	1.1 ± 0.6	-1.2 ± 2.3	NA	NA	0.9 ± 0.2

Table S4 continued.

Species	N_{Cype}, $N_{Ref.}$		Leaf carbon ^{13}C isotope abundance [‰]			Leaf nitrogen ^{15}N isotope abundance [‰]			N [mmol gdw^{-1}]	
			Cyperaceae	Reference	ε	Cyperaceae	Reference	ε	Cyperaceae	Reference
C. hirta 44.3800°N, 8.2600°E	5,10	9	-29.5 ± 0.6	-29.8 ± 0.6	0.3 ± 0.8	1.1 ± 0.6	-1.4 ± 2.2	NA	NA	±
C. nigra 35.0561°N, 140.0264°E	5,30	1	-28.6 ± 0.7	-29.0 ± 1.2	0.4 ± 0.8	-0.4 ± 0.6	-2.4 ± 2.3	2.5 ± 0.8	1.4 ± 0.1	1.6 ± 0.3
C. nigra 50.0522°N, 11.0097°E	5,34	1	-28.8 ± 0.7	-28.8 ± 0.7	0.3 ± 0.8	-0.3 ± 2.3	-1.4 ± 2.5	2.1 ± 2.2	1.5 ± 0.1	1.7 ± 0.3
Carex sp. 49.9500° N, 11.6500°E	8,10	11	-32.1 ± 0.5	-32.3 ± 0.5	0.2 ± 0.4	-0.6 ± 0.4	-4.2 ± 1.3	3.5 ± 1.2	1.2 ± 0.1	0.9 ± 0.3
C. pallescens 35.0561°N, 140.0264°E	5,30	1	-28.7 ± 0.6	-29.0 ± 1.2	0.3 ± 0.5	-0.7 ± 0.8	-2.4 ± 2.3	2.2 ± 1.2	1.5 ± 0.1	1.6 ± 0.3
C. panicea 35.0561°N, 140.0264°E	5,30	1	-29.9 ± 0.6	-29.0 ± 1.2	-0.9 ± 0.4	0.4 ± 1.1	-2.4 ± 2.3	3.3 ± 1.4	1.5 ± 0.5	1.6 ± 0.3
C. remota 49.9523° N, 11.6239°E	5,10	10	-28.6 ± 0.7	-27.8 ± 0.8	-0.8 ± 1.1	1.5 ± 1.3	-2.1 ± 1.5	3.6 ± 1.4	1.0 ± 0.3	0.9 ± 0.4
C. siderosticta 35.0561°N, 140.0264°E	3,97	2	-33.5 ± 0.2	-33.0 ± 1.6	-0.6 ± 0.2	-4.2 ± 0.1	-4.0 ± 1.5	-0.2 ± 0.1	2.9 ± 0.2	1.4 ± 0.5
C. vesicaria 50.0522°N, 11.0097°E	5,34	1	-28.7 ± 0.3	-28.8 ± 0.7	0.2 ± 0.5	1.8 ± 1.6	-1.4 ± 2.5	5.0 ± 1.7	1.5 ± 0.1	1.7 ± 0.3
C. vulpina 49.9065°N, 11.6210°E	3,26	1	-28.3 ± 0.4	-29.3 ± 0.9	1.3 ± 0.5	3.3 ± 1.2	1.0 ± 1.7	2.7 ± 0.5	1.0 ± 0.1	1.5 ± 0.3
Eriophorum vaginatum 50.0522°N, 11.0097°E	4,34	1	-28.0 ± 0.4	-28.8 ± 0.7	1.0 ± 0.2	1.3 ± 1.9	-1.4 ± 2.5	4.4 ± 1.6	1.3 ± 0.1	1.7 ± 0.3
Machaerina sp. 21.9747°N, -159.4948°E	3,6	12	-29.1 ± 1.3	-29.2 ± 1.5	0.1 ± 1.3	2.8 ± 0.5	-0.5 ± 2.4	3.3 ± 0.5	0.6 ± 0.1	1.0 ± 0.3
Rynchospora alba 47.1500°N, 9.800°E	3,34	8	-27.2 ± 0.9	-26.4 ± 0.8	-0.6 ± 0.2	0.7 ± 1.3	-4.3 ± 2.6	4.9 ± 1.4	1.1 ± 0.3	1.3 ± 0.4
Rynchospora sp. 4.1963°N, -52.1491°E	8,8	13	-29.9 ± 0.3	-31.1 ± 0.4	1.1 ± 0.5	1.1 ± 0.6	-1.7 ± 1.5	2.8 ± 1.4	0.8 ± 0.1	1.4 ± 0.1
Scirpus sylvaticus 49.9065°N, 11.6210°E	8,26	1	-27.5 ± 0.9	-29.3 ± 0.9	0.8 ± 0.5	5.1 ± 0.9	1.0 ± 1.7	2.7 ± 0.7	0.8 ± 0.4	1.5 ± 0.3
Trichophorum cespitosum 47.1500°N, 9.800°E	9,34	8	-25.8 ± 0.8	-26.4 ± 0.8	-0.6 ± 0.2	0.3 ± 1.7	-4.3 ± 2.6	4.9 ± 1.4	1.4 ± 0.2	1.3 ± 0.4

[1]This study (samples were collected in the area of NE-Bavaria), [2] Motomura *et al.* (2010), [3] Liebel *et al.* (2010), [4] Preiss, Adam & Gebauer (2010), [5] Gebauer, Preiss & Gebauer (2016), [6] Gerhard Gebauer, unpublished, [7] Fay *et al.* (2018), [8] Schiebold *et al.* (2018), [9] Girlanda *et al.* (2011), [10] Michael Schwanfelder, unpublished, [11] Schweiger *et al.* (2018), [12] Hynson (2016), [13] Merckx *et al.* (2010). Some plots include more than one Cyperaceae species, thus the reference plants are doubled mentioned but with same mean values. Reference plants were *Acer pseudoplatanus* (AM), *Anthericum ramosum* (AM), *Ardisia japonica* (AM), *Arisaema aequinoctiale* (AM), *Aucuba japonica* (AM), *Brachypodium sylvaticum* (AM), *Caltha palustris* (AM), *Castanea crenata* (ECM),

Table S4
continued.

Castanopsis sieboldii (ECM), *Centaurea cyanus* (AM), *Centaurea nigra* (AM), *Cephalotaxus harringtonia* (AM), *Chamaecyparis obtusa* (AM), *Cinnamomum tenuifolium* (AM), *Clidemia hirta* (AM), *Colchicum autumnale* (AM), *Convallaria majalis* (AM), *Crataegus monogyna* (ECM), *Cryptomeria japonica* (AM), *Damnacanthus indicus* (AM), *Dendropanax trifidus* (AM), *Deutzia scabra* (AM), *Dioscorea japonica* (AM), *Dryopteris pacifica* (AM), *Elaeagnus macrophylla* (AM), *Eriobotrya japonica* (AM), *Euphorbia cyparissias* (AM), *Eurya japonica* (AM), *Fagus sylvatica* (ECM), *Ficus erecta* (AM), *Filipendula ulmaria* (AM), *Filipendula vulgaris* (AM), *Fragaria vesca* (AM), *Fraxinus excelsior* (AM), *Hedera rhombea* (AM), *Helianthemum nummularium* (ECM), *Holcus lanatus* (AM), *Holcus mollis* (AM), *Ilex serrata* (AM), *Ipomoea leprieurii* (NM), *Leontodon hispidus* (AM), *Lilium auratum* (AM), *Lithocarpus edulis* (ECM), *Lysimachia vulgaris* (AM), *Machilus thunbergii* (AM), *Molinia caerulea* (AM), *Nardus stricta* (AM), *Neolitsea sericea* (AM), *Ophiopogon japonicus* (AM), *Oplismenus undulatifolius* (AM), *Padus grayana* (AM), *Peperomia* sp. (AM), *Picea abies* (ECM), *Pilosella officinarum* (AM), *Pinus nigra* (ECM), *Piper kadsura* (AM), *Plantago lanceolatum* (AM), *Pleioblastus chino* (AM), *Polygala chamaebuxus* (AM), *Polygonatum odoratum* (AM), *Polygonum lapathifolium* (NM), *Potentilla erecta* (AM), *Pteris cretica* (AM), *Quercus ilex* (ECM), *Quercus infectoria* (ECM), *Ranunculus acris* (AM), *Ranunculus bulbosus* (AM), *Ranunculus flammula* (AM), *Sanguisorba officinalis* (AM), *Smilax china* (AM), *Stegnogramma pozoi* (AM), *Teucrium polium* (AM), *Thymus vulgaris* (AM), *Trachelospermum asiaticum* (AM), *Vaccinium uliginosum* (ErM), *Viburnum tinus* (AM). AM arbuscular mycorrhiza, ECM Ectomycorrhiza, ErM ericoid mycorrhiza, NM non-mycorrhiza

Table S5 Test for differences between 23 species belonging to the Cyperaceae and their respective reference plants in enrichment factors ε of ^{13}C [‰] and ^{15}N [‰], and leaf total N concentrations [mmol/g_{dw}]. Mann-Whitney-U test. Significances are bold marked.

Species	N_{Cype}, $N_{Ref.}$		$\varepsilon^{13}C$		$\varepsilon^{15}N$		Total N	
			TS	*P*	TS	*P*	TS	*P*
Carex caryophyllea 50.0522°N, 11.0097°E	5,15	1	*U* = 13	**= 0.036**	*U* = 6	**= 0.007**	*U* = 6	**= 0.007**
C. conica 35.0561°N, 140.0264°E	2,97	2	*U* = 60	= 0.364	*U* = 62	= 0.384	*U* = 7	= 0.391
C. digitata 49.6850°N, 11.3207°E	5,15	1	*U* = 30	= 0.541	*U* = 15	**= 0.050**	*U* = 12	**= 0.029**
C. digitata 49.6187°N, 11.4200°E	5,21	1	*U* = 28	= 0.117	*U* = 33	= 0.215	*U* = 1	**= 0.000**
C. disticha 35.0561°N, 140.0264°E	5,30	1	*U* = 45	= 0.164	*U* = 34	**= 0.050**	*U* = 67	= 0.724
C. disticha 49.9065°N, 11.6210°E	1,26	1	*U* = 10	= 0.748	*U* = 0	= 0.109	*U* = 1	= 0.140
C. distachya 39.7405°N, 9.5729°E	5,10	3	*U* = 2	**= 0.006**	*U* = 16	= 0.298	*U* = 18	= 0.426
C. flacca 35.0561°N, 140.0264°E	5,30	1	*U* = 53	= 0.311	*U* = 51	= 0.268	*U* = 55	= 0.358
C. flacca 49.6850°N, 11.3207°E	5,15	1	*U* = 10	**= 0.018**	*U* = 3	**= 0.003**	*U* = 26	= 0.337
C. flacca 49.6187°N, 11.4200°E	5,21	1	*U* = 28	= 0.117	*U* = 0	**= 0.001**	*U* = 0	**= 0.000**
C. flacca 49.6715°N, 11.3893°E	10,20	4	*U* = 29	**= 0.002**	*U* = 18	**= 0.001**	*U* = 73	= 0.244
C. flacca 49.6667° N, 11.3833°E	27,57	5	*U* = 664	= 0.314	*U* = 35	**= 0.001**	*U* = 668	= 0.333
C. flacca 49.6715°N, 11.3893°E	27,20	6	*U* = 46	**= 0.040**	*U* = 0	**= 0.001**	*U* = 36	**= 0.011**
C. flacca 58.3333° N, 22.3000°E	19,64	7	*U* = 168	**= 0.001**	*U* = 41	**= 0.001**	*U* = 351	**= 0.005**
C. flava 47.1500°N, 9.800°E	5,34	8	*U* = 50	= 0.147	*U* = 1	**= 0.001**	*U* = 48	= 0.125
C. hallerana 44.3825°N, 8.2562°E	5,20	3	*U* = 24	= 0.083	*U* = 0	**= 0.001**	*NA*	
C. hirta 49.9065°N, 11.6210°E	5,26	1	*U* = 29	= 0.057	*U* = 8	**= 0.002**	*U* = 24	**= 0.030**
C. hirta 35.0561°N, 140.0264°E	1,30	1	*U* = 12	= 0.780	*U* = 4	= 0.240	*U* = 15	= 0.955

Table S5
continued.

Species	N_{Cype}, $N_{Ref.}$		$\varepsilon^{13}C$		$\varepsilon^{15}N$		Total N	
			TS	*P*	TS	*P*	TS	*P*
C. hirta 44.3825°N, 8.2562°E	5,20	3	*U* = 43	= 0.659	*U* = 13	**= 0.013**	*NA*	
C. hirta 44.3800°N, 8.2600°E	5,10	9	*U* = 22	= 0.759	*U* = 6	**= 0.023**	*NA*	
C. nigra 35.0561°N, 140.0264°E	5,30	1	*U* = 57	= 0.409	*U* = 15	**= 0.005**	*U* = 24	= 0.195
C. nigra 50.1210°N, 11.8621°E	5,34	1	*U* = 41	= 0.564	*U* = 12	**= 0.011**	*U* = 7	**= 0.004**
Carex sp. 49.9500° N, 11.6500°E	8,10	11	*U* = 15	= 0.245	*U* = 0	**= 0.003**	*U* = 7	= 0.098
C. pallescens 35.0561°N, 140.0264°E	5,30	1	*U* = 54	= 0.334	*U* = 16	**= 0.006**	*U* = 61	= 0.525
C. panicea 35.0561°N, 140.0264°E	5,30	1	*U* = 41	= 0.114	*U* = 11	**= 0.003**	*U* = 51	= 0.268
C. remota 49.9523° N, 11.6239°E	5,10	10	*U* = 12	= 0.216	*U* = 0	**= 0.003**	*U* = 20	= 0.582
C. siderosticta 35.0561°N, 140.0264°E	3,97	2	*U* = 113	= 0.518	*U* = 134	= 0.824	*U* = 9	**= 0.006**
C. vesicaria 50.1210°N, 11.8621°E	5,34	1	*U* = 40	= 0.519	*U* = 0	**= 0.001**	*U* = 7	**= 0.004**
C. vulpina 49.9065°N, 11.6210°E	3,26	1	*U* = 6	**= 0.020**	*U* = 3	**= 0.011**	*U* = 7	**= 0.024**
Eriophorum vaginatum 50.1210°N, 11.8621°E	4,34	1	*U* = 8	**= 0.015**	*U* = 0	**= 0.002**	*U* = 0	**= 0.002**
Machaerina sp. 21.9747°N, -159.4948°E	3,6	12	*U* = 9	= 1.000	*U* = 0	**= 0.024**	*U* = 2	= 0.095
Rynchospora alba 47.1500°N, 9.800°E	3,34	8	*U* = 17	= 0.062	*U* = 1	**= 0.006**	*U* = 30	= 0.254
Rynchospora sp. 4.1963°N, -52.1491°E	8,8	13	*U* = 0	**= 0.001**	*U* = 0	**= 0.001**	*U* = 0	**= 0.001**
Scirpus sylvaticus 49.9065°N, 11.6210°E	8,26	1	*U* = 26	= 0.120	*U* = 2	**= 0.003**	*U* = 17	**= 0.035**
Trichophorum cespitosum 47.1500°N, 9.800°E	9,34	8	*U* = 74	**= 0.019**	*U* = 24	**= 0.001**	*U* = 17	= 0.893

Table S5
continued.

TS: Test statistic; [1]This study (samples were collected in the area of NE-Bavaria), [2] Motomura *et al.* (2010), [3] Liebel *et al.* (2010), [4] Preiss, Adam & Gebauer (2010), [5] Gebauer, Preiss & Gebauer (2016), [6] Gerhard Gebauer, unpublished, [7] Fay *et al.* (2018), [8] Schiebold *et al.* (2018), [9] Girlanda *et al.* (2011), [10] Michael Schwanfelder, unpublished, [11] Schweiger, Bidartondo & Gebauer (2018), [12] Hynson (2016), [13] Merckx *et al.* (2010). Some plots include more than one Cyperaceae species, thus the reference plants are doubled mentioned but with same mean values. Reference plants were *Acer pseudoplatanus* (AM), *Anthericum ramosum* (AM), *Arachniodes standishii* (AM), *Ardisia japonica* (AM), *Arisaema aequinoctiale* (AM), *Aucuba japonica* (AM), *Brachypodium sylvaticum* (AM), *Caltha palustris* (AM), *Castanea crenata* (ECM), *Castanopsis sieboldii* (ECM), *Centaurea cyanus* (AM), *Centaurea nigra* (AM), *Cephalotaxus harringtonia* (AM), *Chamaecyparis obtusa* (AM), *Cinnamomum tenuifolium* (AM), *Clidemia hirta* (AM), *Colchicum autumnale* (AM), *Convallaria majalis* (AM), *Crataegus monogyna* (ECM), *Cryptomeria japonica* (AM), *Damnacanthus indicus* (AM), *Dendropanax trifidus* (AM), *Deutzia scabra* (AM), *Dioscorea japonica* (AM), *Dryopteris pacifica* (AM), *Elaeagnus macrophylla* (AM), *Eriobotrya japonica* (AM), *Euphorbia cyparissias* (AM), *Eurya japonica* (AM), *Fagus sylvatica* (ECM), *Ficus erecta* (AM), *Filipendula ulmaria* (AM), *Filipendula vulgaris* (AM), *Fragaria vesca* (AM), *Fraxinus excelsior* (AM), *Hedera rhombea* (AM), *Helianthemum nummularium* (ECM), *Holcus lanatus* (AM), *Holcus mollis* (AM), *Ilex serrata* (AM), *Ipomoea leprieurii* (NM), *Leontodon hispidus* (AM), *Lilium auratum* (AM), *Lithocarpus edulis* (ECM), *Lysimachia vulgaris* (AM), *Machilus thunbergii* (AM), *Molinia caerulea* (AM), *Nardus stricta* (AM), *Neolitsea sericea* (AM), *Ophiopogon japonicus* (AM), *Oplismenus undulatifolius* (AM), *Padus grayana* (AM), *Peperomia* sp. (AM), *Picea abies* (ECM), *Pilosella officinarum* (AM), *Pinus nigra* (ECM), *Piper kadsura* (AM), *Plantago lanceolatum* (AM), *Pleioblastus chino* (AM), *Polygala chamaebuxus* (AM), *Polygonatum odoratum* (AM), *Polygonum lapathifolium* (NM), *Potentilla erecta* (AM), *Pteris cretica* (AM), *Quercus ilex* (ECM), *Quercus infectoria* (ECM), *Ranunculus acris* (AM), *Ranunculus bulbosus* (AM), *Ranunculus flammula* (AM), *Sanguisorba officinalis* (AM), *Smilax china* (AM), *Stegnogramma pozoi* (AM), *Teucrium polium* (AM), *Thymus vulgaris* (AM), *Trachelospermum asiaticum* (AM), *Vaccinium uliginosum* (ErM), *Viburnum tinus* (AM). AM arbuscular mycorrhiza, ECM Ectomycorrhiza, ErM ericoid mycorrhiza, NM non-mycorrhiza

Table S6 Stable isotope natural abundances in δ-values [‰] and leaf total N concentrations [mmol/g_{dw}] of seven plant species belonging to the Caryophyllaceae (n = 48) and their respective reference plants (n = 165) as mean value. The relative enrichment ε [‰] to the mean value of accompanying reference plants was calculated for isotope data. Data are shown in mean ± SD.

Species	$N_{Cary.}$, $N_{Ref.}$		Leaf carbon ^{13}C isotope abundance [‰]			Leaf nitrogen ^{15}N isotope abundance [‰]			N [mmol gdw^{-1}]	
			Caryophyllaceae	Reference	ε	Caryophyllaceae	Reference	ε	Caryophyllaceae	Reference
Cerastium fontanum 49.9205°N, 11.6366°E	5,15	1	-29.8 ± 0.9	-29.5 ± 1.5	-0.3 ± 0.8	0.9 ± 0.6	-0.1 ± 0.9	0.9 ± 0.6	1.7 ± 0.6	1.4 ± 0.2
Dianthus arenarius 58.2122°N, 22.2103°E	3,38	2	-28.8 ± 0.3	-30.5 ± 1.4	1.7 ± 0.3	1.5 ± 2.0	-2.7 ± 3.2	4.1 ± 2.0	0.8 ± 0.2	1.0 ± 0.3
Lychnis viscaria 49.9207°N, 11.6352°E	5,15	1	-28.4 ± 0.7	-29.6 ± 0.5	1.2 ± 0.8	0.0 ± 1.4	-1.7 ± 1.0	1.7 ± 1.0	1.2 ± 0.1	1.8 ± 0.4
Lychnis viscaria 49.6500° N, 11.4417°E	5,15	3	-26.9 ± 0.4	-27.8 ± 0.9	0.9 ± 0.5	-2.6 ± 0.3	-4.0 ± 1.6	1.5 ± 0.3	1.5 ± 0.3	1.8 ± 0.3
Saponaria officinalis 49.9212° N, 11.6366°E	5,15	1	-28.4 ± 0.4	-29.4 ± 0.7	1.0 ± 0.9	3.4 ± 0.7	1.0 ± 1.6	2.3 ± 1.6	1.7 ± 0.1	1.8 ± 0.4
Stellaria media 49.9294° N, 11.6366°E	5,17	1	-27.6 ± 0.6	-29.1 ± 0.8	0.7 ± 1.4	3.9 ± 1.7	2.2 ± 1.7	0.8 ± 1.5	1.5 ± 0.4	1.8 ± 0.5
Stellaria media 49.8902°N, 11.6139°E	5,20	4	-30.3 ± 0.3	-29.7 ± 0.7	-0.6 ± 0.4	3.6 ± 1.2	2.5 ± 1.2	1.2 ± 0.6	1.3 ± 0.1	1.7 ± 0.3
Stellaria holostea 49.9523° N, 11.6239°E	5,15	1	-27.8 ± 0.9	-29.1 ± 1.1	1.2 ± 1.3	-0.6 ± 2.6	0.5 ± 2.4	1.1 ± 3.6	2.0 ± 0.5	3.2 ± 1.2
Stellaria holostea 49.9486° N, 11.6366°E	5,15	1	-28.3 ± 1.0	-28.0 ± 0.8	-0.2 ± 0.9	-3.7 ± 1.3	-4.4 ± 1.1	0.7 ± 1.2	1.6 ± 0.3	2.4 ± 0.3
Silene dioica 49.9523° N, 11.6239°E	5,15	1	-27.6 ± 0.4	-29.1 ± 1.1	1.5 ± 0.5	3.9 ± 2.6	0.5 ± 2.4	0.6 ± 2.6	2.7 ± 0.2	3.2 ± 1.2

[1] This study (samples were collected in the area of NE-Bavaria), [2] Lallemand *et al.* (2017) [3] Gebauer & Meyer (2003),[4] unpublished field work. Reference plants were *Acer platanoides* (AM), *Achillea millefolium* (AM), *Ajuga reptans* (AM), *Alliaria petiolata* (NM), *Anemone nemorosa* (AM), *Berberis vulgaris* (AM), *Capsella bursa-pastoris* (NM), Eridium cicutarium (AM), *Fragaria vesca* (AM), *Frangula alnus* (ECM), *Galium album* (AM), *Galium aparine* (NM), *Galium boreale* (AM), *Galium pomeranicum* (AM), *Galium verum* (AM), *Glechoma hederacea* (AM), *Hieracium umbellatum* (AM), *Humulus lupulus* (AM), *Lamium galeobdolon* (AM), *Lamium purpurea* (AM), *Leucanthemum vulgare* (AM), *Luzula pilosa* (AM), *Plantago lanceolata* (AM), *Polygala vulgaris* (AM), *Potentilla reptans* (AM), *Quercus robur* (ECM), *Rumex acetosa* (NM), *Sanguisorba minor* (AM), *Sorbus aucuparia* (ECM), *Taraxacum officinale* (AM), *Thymus serpyllum* (AM), *Vaccinium vitis-idaea* (ErM), Viola arvensis (AM), *Viola rupestris* (AM). AM arbuscular mycorrhiza, ECM Ectomycorrhiza, ErM ericoid mycorrhiza, NM non-mycorrhiza

Table S7 Test for differences between seven plant species belonging to the Caryophyllaceae and their respective reference plants in enrichment factors ε of ^{13}C [‰] and ^{15}N [‰], and leaf total N concentrations [mmol/g_{dw}]. Mann-Whitney-U test. Significances are bold marked.

Species	$N_{Cary,}$ $N_{Ref.}$		**ε^{13}C**		**ε^{15}N**		**Total N**	
			TS	*P*	TS	*P*	TS	*P*
Cerastium fontanum 49.9205°N, 11.6366°E	5,15	[1]	*U* = 32	= 0.663	*U* = 23	**= 0.036**	*U* = 23	= 0.222
Dianthus arenarius 49.9206°N, 11.6352°E	3,38	[2]	*U* = 15	**= 0.038**	*U* = 21	= 0.059	*U* = 29	= 0.169
Lychnis viscaria 49.9207°N, 11.6352°E	5,15	[1]	*U* = 6	**= 0.007**	*U* = 1	**= 0.002**	*U* = 4	**= 0.004**
Lychnis viscaria 49.9205° N, 11.6366°E	5,15	[3]	*U* = 11	**= 0.023**	*U* = 11	**= 0.023**	*U* = 11	**= 0.023**
Saponaria officinalis 49.9212° N, 11.6366°E	5,15	[1]	*U* = 10	**= 0.018**	*U* = 5	**= 0.005**	*U* = 26	= 0.337
Stellaria media 49.9294° N, 11.6366°E	5,17	[1]	*U* = 7	**= 0.006**	*U* = 12	**= 0.019**	*U* = 3	**= 0.002**
Stellaria media 49.8902°N, 11.6139°E	5,20	[4]	*U* = 18	**= 0.032**	*U* = 13	= 0.159	*U* = 19	**= 0.001**
Stellaria holostea 49.9523° N, 11.6281°E	5,15	[1]	*U* = 22	= 0.190	*U* = 28	= 0.432	*U* = 11	**= 0.023**
Stellaria holostea 49.9486° N, 11.6366°E	5,15	[1]	*U* = 28	= 0.432	*U* = 22	= 0.190	*U* = 1	**= 0.002**
Silene dioica 49.9523° N, 11.6239°E	5,15	[1]	*U* = 8	**= 0.011**	*U* = 30	= 0.541	*U* = 29	= 0.485

TS: Test statistic, [1] This study (samples were collected in the area of NE-Bavaria), [2] Lallemand *et al.* (2017) [3] Gebauer & Meyer (2003),[4] unpublished field work. Reference plants were *Acer platanoides* (AM), *Achillea millefolium* (AM), *Ajuga reptans* (AM), *Alliaria petiolata* (NM), *Anemone nemorosa* (AM), *Berberis vulgaris* (AM), *Capsella bursa-pastoris* (NM), Eridium cicutarium (AM), *Fragaria vesca* (AM), *Frangula alnus* (ECM), *Galium album* (AM), *Galium aparine* (NM), *Galium boreale* (AM), *Galium pomeranicum* (AM), *Galium verum* (AM), *Glechoma hederacea* (AM), *Hieracium umbellatum* (AM), *Humulus lupulus* (AM), *Lamium galeobdolon* (AM), *Lamium purpurea* (AM), *Leucanthemum vulgare* (AM), *Luzula pilosa* (AM), *Plantago lanceolata* (AM), *Polygala vulgaris* (AM), *Potentilla reptans* (AM), *Quercus robur* (ECM), *Rumex acetosa* (NM), *Sanguisorba minor* (AM), *Sorbus aucuparia* (ECM), *Taraxacum officinale* (AM), *Thymus serpyllum* (AM), *Vaccinium vitis-idaea* (ErM), Viola arvensis (AM), *Viola rupestris* (AM). AM arbuscular mycorrhiza, ECM Ectomycorrhiza, ErM ericoid mycorrhiza, NM non-mycorrhiza

Table S8 Fungal endophytes in three plant species belonging to the Equisetaceae based on a molecular approach (183 zOTU in total; 93,883 reads in total). A complete list can be obtained from the repository.

zOTU	*E. arvense reads*	*E. sylvaticum reads*	*E. palustre reads*	GenBank	align *length*	Identification acc to BestHit		Comment
zOTU104	0	70	0	KJ827902	280	Helotiales sp.	96.4	putative root endophyte[3]
zOTU12	2035	0	0	UDB020374	238	*Phialocephala fortinii*	98.3	DSE[1]
zOTU121	51	0	0	KF359558	305	*Cladophialophora chaetospira*	100	DSE[2]
zOTU133	34	0	0	KF359558	305	*Cladophialophora chaetospira*	99.7	DSE[2]
zOTU14	1819	0	0	EU046055	281	Helotiales sp.	99.6	putative root endophyte[3]
zOTU165	26	0	0	EU035406	305	*Cladophialophora chaetospira*	99.7	DSE[2]
zOTU174	23	0	0	EU035406	305	*Cladophialophora chaetospira*	99.3	DSE[2]
zOTU177	0	16	0	DQ294955	341	Glomeromycotina sp.	81.5	AM
zOTU179	16	0	0	UDB020374	239	*Phialocephala fortinii*	98.7	DSE[1]
zOTU180	26	0	0	UDB020374	239	*Phialocephala fortinii*	98.7	DSE[1]
zOTU185	0	16	0	DQ294955	341	Glomeromycotina sp.	81.2	AM
zOTU19	0	145	1010	EF644169	279	Helotiales sp.	99.6	putative root endophyte[3]
zOTU2	0	125	6341	KC965195	277	Helotiales sp.	99.3	putative root endophyte[3]
zOTU21	0	1046	0	KJ827529	279	Helotiales sp.	100	putative root endophyte[3]
zOTU22	1178	0	0	EU046055	281	Helotiales sp.	100	putative root endophyte[3]
zOTU24	0	115	793	EF644169	279	Helotiales sp.	100	putative root endophyte[3]
zOTU27	874	0	0	LT608540	200	Helotiales sp.	100	putative root endophyte[3]
zOTU3	0	5127	7	MF487029	276	Helotiales sp.	98.9	putative root endophyte[3]
zOTU30	0	744	0	FJ000375	280	*Tetracladium furcatum*	100	DSE[4]
zOTU32	0	160	453	MF487029	276	Helotiales sp.	98.9	putative root endophyte[3]
zOTU33	648	0	0	LT608540	200	Helotiales sp.	100	putative root endophyte[3]

Table S8 continued.

zOTU-	*E. arvense reads*	*E. sylvaticum reads*	*E. palustre reads*	GenBank	align *length*	Identification acc to BestHit		Comment
zOTU4	0	106	4843	KC965195	277	Helotiales sp.	99.6	putative root endophyte[3]
zOTU42	0	113	343	MF487029	276	Helotiales sp.	99.3	putative root endophyte[3]
zOTU6	0	3650	6	MF487029	276	Helotiales sp.	99.3	putative root endophyte[3]
zOTU72	181	0	0	UDB020374	239	*Phialocephala fortinii*	97.9	DSE[1]
zOTU79	0	117	0	EU516942	280	Tetracladium sp.	99.3	DSE[4]
zOTU8	2860	1	0	UDB020374	238	*Phialocephala fortinii*	98.3	DSE[1]
zOTU80	0	0	119	HG937139	277	Helotiales sp.	99.3	putative root endophyte[3]
zOTU81	128	0	0	UDB020374	239	*Phialocephala fortinii*	97.9	DSE[1]
zOTU84	0	0	98	HG937139	277	Helotiales sp.	99.6	putative root endophyte[3]
zOTU88	0	112	0	EU516942	280	*Tetracladium* sp.	99.6	DSE[4]

Roots of Equisetum individuals (n = 3 per species) were pooled for DNA analyses. In all species septate hyphae and microsclerotia as well as *Paris*-like coils and few aseptate hyphae were microscopically documented. 1 Surono & Narisawa (2017), 2 Usui, Takashima & Narisawa (2016), 3 Tedersoo *et al.* (2009), 4 Raviraja, Sridhar & Barlocher (1996). Doubles in GenBank ID are grey marked.

Respective references

Fay, M.F., Feustel, M., Newlands, C. & Gebauer, G. (2018) Inferring the mycorrhizal status of introduced plants of *Cypripedium calceolus* (Orchidaceae) in northern England using stable isotope analysis. *Botanical Journal of the Linnean Society*, **186**, 587–590.

Gebauer, G. & Meyer, M. (2003) ^{15}N and ^{13}C natural abundance of autotrophic and myco-heterotrophic orchids provides insight into nitrogen and carbon gain from fungal association. *New Phytologist*, **160**, 209–223.

Gebauer, G., Preiss, K. & Gebauer, A.C. (2016) Partial mycoheterotrophy is more widespread among orchids than previously assumed. *New Phytologist*, **211**, 11–15.

Girlanda, M., Segreto, R., Cafasso, D., Liebel, H.T., Rodda, M., Ercole, E., Cozzolino, S., Gebauer, G. & Perotto, S. (2011) Photosynthetic Mediterranean meadow orchids feature partial mycoheterotrophy and specific mycorrhizal associations. *American Journal of Botany*, **98**, 1148–1163.

Hynson, N.A. (2016) The carbon and nitrogen ecophysiologies of two endemic tropical orchids mirrors those of their temperate relatives and the local environment. *Royal Society open science*, **3**, 160427.

Lallemand, F., Puttsepp, Ü., Lang, M., Luud, A., Courty, P.-E., Palancade, C. & Selosse, M.-A. (2017) Mixotrophy in Pyroleae (Ericaceae) from Estonian boreal forests does not vary with light or tissue age. *Annals of Botany*, **120**, 361–371.

Liebel, H.T., Bidartondo, M.I., Preiss, K., Segreto, R., Stöckel, M., Rodda, M. & Gebauer, G. (2010) C and N stable isotope signatures reveal constraints to nutritional modes in orchids from the Mediterranean and Macaronesia. *American Journal of Botany*, **97**, 903–912.

Merckx, V., Stöckel, M., Fleischmann, A., Bruns, T.D. & Gebauer, G. (2010) ^{15}N and ^{13}C natural abundance of two mycoheterotrophic and a putative partially mycoheterotrophic species associated with arbuscular mycorrhizal fungi. *New Phytologist*, **188**, 590–596.

Motomura, H., Selosse, M.-A., Martos, F., Kagawa, A. & Yukawa, T. (2010) Mycoheterotrophy evolved from mixotrophic ancestors: Evidence in *Cymbidium* (Orchidaceae). *Annals of Botany*, **106**, 573–581.

Preiss, K., Adam, I.K.U. & Gebauer, G. (2010) Irradiance governs exploitation of fungi: Fine-tuning of carbon gain by two partially myco-heterotrophic orchids. *Proceedings. Biological sciences*, **277**, 1333–1336.

Raviraja, N., Sridhar, K. & Barlocher, F. (1996) Endophytic aquatic hyphomycetes of roots of plantation crops and ferns from India. *SYDOWIA-HORN*, **48**, 152–160.

Schiebold, J.M.-I., Bidartondo, M.I., Lenhard, F., Makiola, A. & Gebauer, G. (2018) Exploiting mycorrhizas in broad daylight: Partial mycoheterotrophy is a common nutritional strategy in meadow orchids. *Journal of Ecology*, **106**, 168–178.

Schweiger, J.M.-I., Bidartondo, M.I. & Gebauer, G. (2018) Stable isotope signatures of underground seedlings reveal the organic matter gained by adult orchids from mycorrhizal fungi. *Functional Ecology*, **32**, 870–881.

Surono & Narisawa, K. (2017) The dark septate endophytic fungus *Phialocephala fortinii* is a potential decomposer of soil organic compounds and a promoter of *Asparagus officinalis* growth. *Fungal Ecology*, **28**, 1–10.

Tedersoo, L., Pärtel, K., Jairus, T., Gates, G., Põldmaa, K. & Tamm, H. (2009) Ascomycetes associated with ectomycorrhizas: Molecular diversity and ecology with particular reference to the Helotiales. *Environmental Microbiology*, **11**, 3166–3178.

Usui, E., Takashima, Y. & Narisawa, K. (2016) *Cladophialophora inabaensis* sp. nov., a New Species among the Dark Septate Endophytes from a Secondary Forest in Tottori, Japan. *Microbes and environments*, **31**, 357–360.

Manuscript 4

MUCOROMYCOTINA FINE ROOT ENDOPHYTE FUNGI FORM NUTRITIONAL MUTUALISMS WITH VASCULAR PLANTS

Grace A. Hoysted[a], Alison S. Jacob[b,c], Jill Kowal[d], **Philipp Giesemann**[e], Martin I. Bidartondo[b,c], Jeffrey G. Duckett[d], Gerhard Gebauer[e], William R. Rimington[b,c,d], Sebastian Schornack[f], Silvia Pressel[d], Katie J. Field[a]

Plant Physiology 181: 565–577 (2019), doi:10.1104/pp.19.00729.

[a]Centre for Plant Sciences, Faculty of Biological Sciences, Universioty of Leeds, LS2 9JT, United Kingdom

[b]Comparative Plant & Fungal Biology, Royal Botanic Gardens, Kew, Richmond Tw9 3DS, United Kingdom

[c]Department of Life Sciences, Imperial College London, London, SW7 2AZ, United Kingdom

[d]Department of Life Sciences, Natural Histroy Museum, London, SW7 5BD, United Kingdom

[e]Laboratory of Isotope Biogeochemistry, Bayreuth Center of Ecology and Environmental Research, University of Bayreuth, 95440 Bayreuth, Germany

[f]Sainsbury Laboratory, University of Cambridge, Cambridge, CB2 1LR, United Kingdom

Key words: Arbuscular mycorrhizas, Endogonales, fine root endophyte (FRE), lycophytes, Mucoromycotina, mutualism, nitrogen, carbon, plant-fungus symbiosis, vascular plants.

Received, 17 June 2019; accepted, 22 July 2019; published, 29 July 2019.

Mucoromycotina Fine Root Endophyte Fungi Form Nutritional Mutualisms with Vascular Plants[1][OPEN]

Grace A. Hoysted,[a] Alison S. Jacob,[b,c] Jill Kowal,[d] Philipp Giesemann,[e] Martin I. Bidartondo,[b,c] Jeffrey G. Duckett,[d] Gerhard Gebauer,[e] William R. Rimington,[b,c,d] Sebastian Schornack,[f] Silvia Pressel,[d] and Katie J. Field[a,2,3]

[a]Centre for Plant Sciences, Faculty of Biological Sciences, University of Leeds, Leeds, LS2 9JT, United Kingdom
[b]Comparative Plant & Fungal Biology, Royal Botanic Gardens, Kew, Richmond TW9 3DS, United Kingdom
[c]Department of Life Sciences, Imperial College London, London, SW7 2AZ, United Kingdom
[d]Department of Life Sciences, Natural History Museum, London SW7 5BD, United Kingdom
[e]Laboratory of Isotope Biogeochemistry, Bayreuth Center of Ecology and Environmental Research, University of Bayreuth, 95440 Bayreuth, Germany
[f]Sainsbury Laboratory, University of Cambridge, Cambridge, CB2 1LR, United Kingdom

ORCID IDs: 0000-0002-3469-2549 (G.A.H.); 0000-0003-3172-3036 (M.I.B.); 0000-0003-1577-7501 (G.G.); 0000-0002-7836-5881 (S.S.); 0000-0001-9652-6338 (S.P.); 0000-0002-5196-2360 (K.J.F.).

Fungi and plants have engaged in intimate symbioses that are globally widespread and have driven terrestrial biogeochemical processes since plant terrestrialization >500 million years ago. Recently, hitherto unknown nutritional mutualisms involving ancient lineages of fungi and nonvascular plants have been discovered, although their extent and functional significance in vascular plants remain uncertain. Here, we provide evidence of carbon-for-nitrogen exchange between an early-diverging vascular plant (*Lycopodiella inundata*) and Mucoromycotina (Endogonales) fine root endophyte fungi. Furthermore, we demonstrate that the same fungal symbionts colonize neighboring nonvascular and flowering plants. These findings fundamentally change our understanding of the physiology, interrelationships, and ecology of underground plant–fungal symbioses in modern terrestrial ecosystems by revealing the nutritional role of Mucoromycotina fungal symbionts in vascular plants.

Plant terrestrialization >500 million years ago (Morris et al., 2018) was facilitated by the formation of mutualistic symbioses with fungi, through which the earliest plants gained access to mineral nutrients in exchange for photosynthetically fixed carbon (C). It was long hypothesized that this ancient mycorrhiza-like symbiosis was closely related to, and subsequently evolved into, widespread modern-day arbuscular mycorrhizas (AM) formed with plant roots by Glomeromycotina fungi (Pirozynski and Malloch, 1975; Redecker et al., 2000). However, recent molecular, cytological, physiological, and paleobotanical evidence has strongly indicated that early fungal associates were likely to be more diverse than has previously been assumed (Bidartondo et al., 2011; Field et al., 2015a, 2015b). Members of the earliest diverging clade of an ancient land plant lineage, Haplomitriopsida liverworts, are now known to form mycorrhiza-like associations with Mucoromycotina fungi (Bidartondo et al., 2011; Field et al., 2012, 2015b), which also colonize other early diverging plant lineages, namely hornworts, lycophytes, and ferns, sometimes co-occurring with Glomeromycotina fungi in the same plant host (Desirò et al., 2013; Rimington et al., 2015). Mucoromycotina represents an ancient fungal lineage considered to branch earlier than, or as a sister to, the Glomeromycotina AM fungi (James et al., 2006; Lin et al., 2014). The recent identification of Mucoromycotina in a range of modern nonvascular plants (Bidartondo et al., 2011) and plant fossils (Krings et al., 2007; Strullu-Derrien et al., 2014) supports the idea that the colonization of Earth's land masses by plants was facilitated not only

[1]This work was supported by the Natural Environment Research Council (NE/N00941X/1 to K.J.F., S.P., and S.S. and NE/N009665/1 to M.I.B.), the Leverhulme Trust (PLP-2017-079), the Biotechnology and Biological Sciences Research Council Translational Fellowship (BB/M026825/1 to K.J.F.), and the Natural Environment Research Council Doctoral Training Partnership (Science and Solutions for a Changing Planet studentship to W.W.R.).

[2]Author for contact: k.field@leeds.ac.uk.
[3]Senior author.

The author responsible for distribution of materials integral to the findings presented in this article in accordance with the policy described in the Instructions for Authors (www.plantphysiol.org) is: Katie J. Field (k.field@leeds.ac.uk).

K.J.F., S.P., S.S., M.I.B., and J.G.D. conceived and designed the investigation; S.P., J.K., J.G.D., M.I.B., A.S.J., G.G., and G.A.H. collected plant material; G.A.H. and K.J.F. undertook the physiological analyses; A.S.J., W.R.R., and M.I.B. undertook the molecular analyses; S.P. undertook the cytological analyses with assistance from J.K.; P.G. and G.G. analyzed and interpreted the stable isotope data; G.A.H. led the writing; all authors discussed results and commented on the article; K.J.F. agrees to serve as the author responsible for contact and ensure communication.

[OPEN]Articles can be viewed without a subscription.

www.plantphysiol.org/cgi/doi/10.1104/pp.19.00729

by Glomeromycotina AM, but also by Mucoromycotina fungal symbionts (Field et al., 2015a). The latest discoveries of putative Mucoromycotina fungi in vascular land plants (Rimington et al., 2015, 2016; Orchard et al., 2017a) indicate that root symbiotic versatility and diversity (Hoysted et al., 2018) has been grossly underestimated across extant plants.

Although Mucoromycotina fungal symbioses in nonvascular plants have received the most attention to date, there are now several reports of their occurrence in vascular plants (Rimington et al., 2015, 2016; Orchard et al., 2017a, 2017b; Hoysted et al., 2018). It has been suggested that the globally widespread, arbuscule-forming fine root endophytes (FREs) classified as *Glomus tenue* (or, more recently, *Planticonsortium tenue*; Walker et al., 2018), which occur across a wide range of vascular plant groups (Rimington et al., 2015; Orchard et al., 2017b), are closely related to the Mucoromycotina fungal symbionts of nonvascular plants (Field and Pressel, 2018; Hoysted et al., 2018). If true, there could be major ramifications for our understanding of the past and present diversity and function of plant–fungal nutritional symbioses (Field and Pressel, 2018), suggesting Mucoromycotina fungal symbiosis is not limited to ancient plant lineages but is in fact widespread throughout extant land plants. However, it remains unclear whether the putative Mucoromycotina FREs detected in vascular plants to date are comparable in terms of function and identity to the mutualistic Mucoromycotina fungal symbionts detected in nonvascular plants.

As lycophytes are considered to be the earliest divergent extant vascular plant lineage (Kenrick and Crane, 1997), the discovery of non-Glomeromycotina fungal associates in lycophyte roots and gametophytes is particularly important. For over 100 years, fungal associations in lycophytes have been thought of as being AM-like but with unique "lycopodioid" features (Duckett and Ligrone, 1992; Schmid and Oberwinkler, 1993). However, global analysis of fungal associates in 20 lycophytes (Rimington et al., 2016) has now shown their colonization is broadly similar to that of hornworts (Desirò et al., 2013), with many species forming single and/or dual associations with both Glomeromycotina AM fungi and Mucoromycotina FRE fungi (Rimington et al., 2016). Remarkably, every sample of *Lycopodiella inundata*—a species found in wet habitats across the northern Hemisphere—examined so far appears colonized exclusively by Mucoromycotina FRE fungi (Rimington et al., 2016). The fundamental obstacle to studying function of Mucoromycotina FREs has been finding any plants that are not co-colonized by coarse root endophytes (i.e. Glomeromycotina AM fungi). In fact, so far there is no evidence of nutritional mutualism between any vascular plant and Mucoromycotina FREs (Hoysted et al., 2018). Therefore, *L. inundata* provides a unique and important opportunity to dissect the symbiotic function of FREs in a vascular plant.

Here, we investigate the function, cytology, and occurrence of the fungal associates of *L. inundata* (Fig. 1). We use a combination of radio- and stable isotope tracers (Supplemental Figs. S1 and S2) to test physiology and functioning of vascular plant-Mucoromycotina fungal symbioses, detailed cytological analyses to characterize morphology and colonization patterns of Mucoromycotina fungi, and molecular techniques to identify the fungal associates of a range of vascular plants (including those used in our experiments) across several field sites. Furthermore, we used natural abundance $\delta^{13}C$ and $\delta^{15}N$ signatures to test under field conditions whether Mucoromycotina fungal association affects the direction of carbon and nitrogen fluxes between plants and associated fungi (Gebauer and Meyer, 2003). Specifically, we address the following questions:

(1) What is the function of Mucoromycotina fungal associations in lycophytes in terms of carbon-for-nutrient exchange?
(2) Are there characteristic cytological signatures or features of Mucoromycotina fungal associations in *L. inundata* and other vascular plants?
(3) Do Mucoromycotina fungal symbionts of *L. inundata* co-occur in neighboring angiosperm roots and nonvascular plants?

RESULTS

Mucoromycotina–*L. inundata* Symbioses Are Nutritional Mutualisms

Isotope tracing experiments conducted in controlled environment chambers confirmed carbon was transferred from field-collected *L. inundata* to extraradical hyphae of symbiotic Mucoromycotina FRE fungi (Fig. 2). Mucoromycotina fungal symbiont identity was confirmed using sequencing of the fungal 18S ribosomal RNA (rRNA) gene with the broad specificity fungal primer set NS1/EF3 and a semi-nested approach with Mucoromycotina- and Glomeromycotina-specific primers described in Desirò et al. (2013); Supplemental Fig. S3). Plants transferred an average of 79 μg ($\pm$49.3 SE) of recent photosynthate to the external fungal hyphal mycelium within the microcosm during the labeling period (Fig. 2A). This represents 0.28% ($\pm$0.14 SE) of the total amount of carbon that was fixed during the labeling period by *L. inundata* (Fig. 2B).

Mucoromycotina fungi within the experimental microcosms transferred between 3% and 9% of the supplied ^{33}P tracer and 0.6% to 1% of the supplied ^{15}N tracer to their plant hosts during the isotope labeling period (Fig. 2, C and D). Mucoromycotina FREs transferred significantly more ^{15}N than ^{33}P to *L. inundata* in terms of both absolute quantities (Fig. 2C, $P = 0.05$; Student's t test) and when normalized to plant biomass (Fig. 2D, $P = 0.03$, Student's t test).

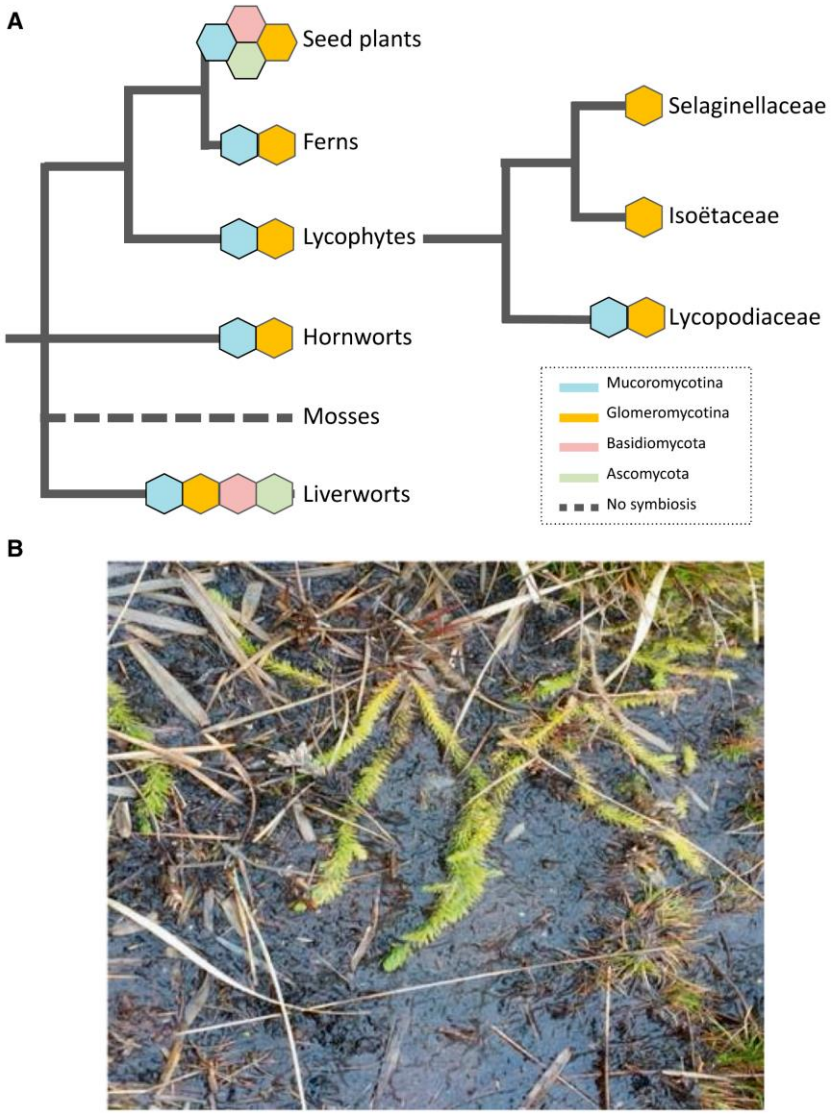

Figure 1. Land plant phylogeny and species used in this study. A, Land plant phylogeny showing key nodes alongside commonly associated fungal symbionts (Duckett and Ligrone, 1992; Duckett et al., 2006; James et al., 2006; Bidartondo et al., 2011). B, *L. inundata* at Thursley Common, Surrey, United Kingdom, June 2017.

To test the potential nutritional role of Mucoromycotina fungi in *L. inundata* in the field, we analyzed the natural abundance ^{13}C and ^{15}N stable isotope signatures of leaves and roots of *L. inundata* and *Juncus bulbosus*, both of which were shown to host Mucoromycotina FREs in their roots (Supplemental Figs. S4–S9). In addition, five plant species representing three different types of mycorrhizal associations were sampled to serve as reference plants: two ericoid mycorrhizal species (*Erica tetralix*, collected on six plots; *Calluna vulgaris*, collected on three plots), two ectomycorrhizal species (*Pinus sylvestris* and *Betula pendula* seedlings, both from one plot), and one arbuscular mycorrhizal species (*Molinia caerulea* from six plots).

All leaf $\delta^{13}C$ values from plants collected from the same site as those collected for our isotope tracing experiments ranged between −26.2 and −30.1% and root $\delta^{13}C$ values between −24.5 and −28.9%, whereas leaf $\delta^{15}N$ values ranged from 3.3 to −10.0% and root $\delta^{15}N$ values from 3.1 to −5.9% (Fig. 3). Leaves of the three groups, *L. inundata* ($n = 6$), *J. bulbosus* ($n = 6$), and reference plants, five species representing three types of mycorrhizal associations, i.e. arbuscular, ericoid, and ectomycorrhizal species ($n = 17$), also collected from the same site as plants used in our isotope tracing experiments, were significantly different in $\delta^{13}C$ ($H^2 = 8.758$; $P = 0.013$) and $\delta^{15}N$ ($H^2 = 21.434$; $P < 0.001$, Fig. 3A). *L. inundata* leaves were significantly depleted in ^{13}C compared to *J. bulbosus* leaves ($Q = 2.644$, $P < 0.05$) and a

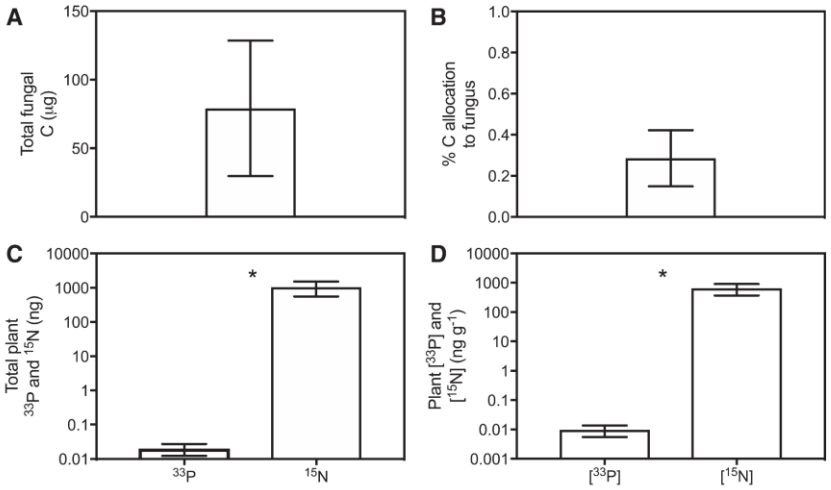

Figure 2. Carbon-for-nutrient exchange between *L. inundata* and Mucoromycotina fine root endophyte fungi. A, Total plant-fixed carbon transferred to Mucoromycotina FRE fungi by *L. inundata*. B, Percent allocation of plant-fixed carbon to Mucoromycotina FRE fungi. C and D, Total plant tissue phosphorus (^{33}P) and nitrogen (^{15}N) content in nanograms (C) and tissue concentration (ng g^{-1}) of fungal-acquired ^{33}P and ^{15}N in *L. inundata* tissue (D). In (A) and (B), $n = 20$; in (C) and (D), $n = 10$ (n indicates the number of biological replicates used during carbon-for-nutrient exchange experiments). Experiments were carried out three times. Asterisk (*) indicates where $P < 0.05$, Student's t test. Error bars = means ± SE.

significant depletion of *L. inundata* leaves compared to reference plant leaves ($Q = 2.662$, $P < 0.05$, Fig. 3A) was found. The *J. bulbosus* leaves were not significantly different from reference plants in δ^{13}C. No significant difference was discovered for δ^{15}N in *L. inundata* and *J. bulbosus* leaves ($Q = 1.017$, $P > 0.05$), while leaves of both species were significantly enriched in ^{15}N compared to the reference plants ($Q = 2.968$, $P < 0.05$; $Q = 4.205$, $P < 0.05$, Fig. 3A). For the roots, only δ^{15}N showed significant differences between the three groups under comparison ($F^2 = 34.815$; $P < 0.001$, Fig. 3B). The *L. inundata* and *J. bulbosus* roots were not significantly distinguished in δ^{15}N; however, roots of both species were significantly enriched in ^{15}N compared to reference plant roots ($Q = 10.109$, $P < 0.001$; $Q = 8.515$, $P < 0.001$, Fig. 3B).

Mucoromycotina FREs of *L. inundata* Show Distinctive Cytology

Trypan blue staining and scanning electron microscopy (SEM) of wild-collected plants (a liverwort, two grasses, and a rush) from the same site as the *L. inundata* plants used in our isotope tracer and stable isotope studies (except for the grass *Holcus lanatus*; see Supplemental Table S1), revealed two distinct fungal symbiont morphologies. These consisted of either coarse hyphae (>3-μm diameter) and large vesicles (>20-μm diameter) or fine branching hyphae (<2-μm diameter) with small swellings/vesicles (usually 5–10 but up to 15 μm in diameter; Figs. 4 and 5). Both morphologies were regularly observed, often co-occurring in the same sample, in the gametophyte of the liverwort *Fossombronia foveolata* (Figs. 4, A and B, and 5A; Supplemental Fig. S10A), in the roots of the grasses *H. lanatus* (Fig. 4F) and *M. caerulea* (Fig. 4, G and H), and the rush *J. bulbosus* (Fig. 5, H and I). In the colonized roots of both freshly collected *L. inundata* and those incubated in growth chambers, only fine hyphae with small swelling/vesicles were invariably detected (Figs. 4, C–E, and 5, F and G). As in the other plants analyzed, these fine hyphae were aseptate and formed both intercalary and terminal swellings/vesicles but, in contrast to the grasses (Supplemental Fig. S10B), never arbuscules. Similar fungal morphology was also observed in protocorm cells of newly developing sporophytes (Fig. 5, B and C) and in gametophytes of *L. inundata* (Supplemental Fig. S11). However, in these early developmental stages, fungal colonization consistently exhibits a distinct zonation: an outer intracellular zone and a more central, strictly intercellular zone (Fig. 5, D and E; Supplemental Fig. S11, B–G). In the intracellular zone, fungal colonization is the same as in the sporophyte roots and consists of fine hyphae with intercalary and terminal swellings/vesicles (Fig. 5, B and C; see also Supplemental Fig. S11I). Unique to the gametophyte generation, in the outermost cortical layers, the fungus also forms tightly wound coils (hyphae up to 2.5 μm in diameter) with larger vesicles (15–20 μm; Supplemental Fig. S11D), as described before in *Lycopodium clavatum* (Schmid and Oberwinkler, 1993). Both gametophyte and early developmental stages of the sporophyte generation develop a conspicuous central system of large, mucilage-filled intercellular spaces (ICSs). In this region, the fungus becomes strictly intercellular (Fig. 5, D and E; Supplemental Fig. S11, E–G). The intercellular hyphae are initially fine and with small swellings/vesicles (Fig. 5D; Supplemental Fig. S11E) as their intracellular counterparts, but soon enlarge and eventually reach diameters in excess of 3 μm (Supplemental Fig. S11F), with no swellings/vesicles present at this stage.

Mucoromycotina Fungal Symbionts Are Shared by Neighboring Angiosperms

Analysis of *L. inundata* plants collected from the same site, at the same time as plants used in the these

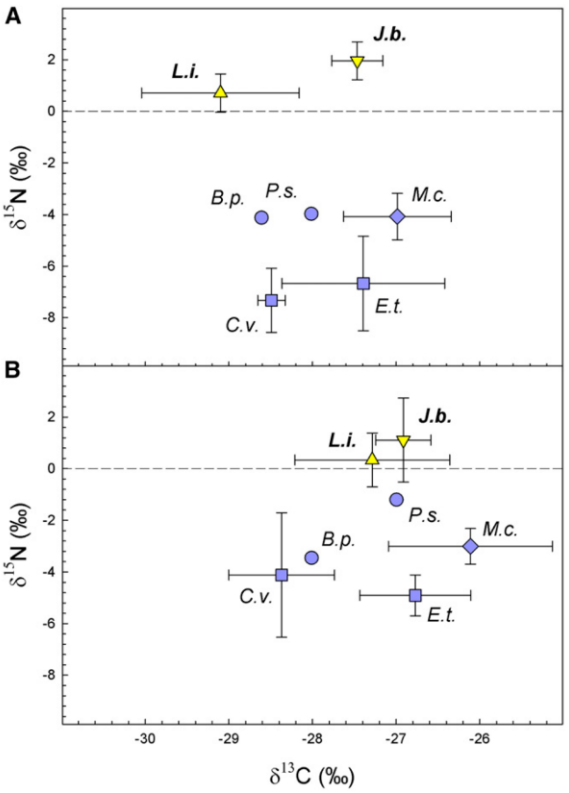

Figure 3. Carbon- and nitrogen-stable isotope natural abundance of *L. inundata* (L.i., $n = 6$), *J. bulbosus* (J.b., $n = 6$) and surrounding angiosperms (AM: *M. caerulea*, M.c., $n = 6$; ectomycorrhizal: *P. sylvestris*, P.s., $n = 1$; *B. pendula*, B.p., $n = 1$; ericoid mycorrhizal: *C. vulgaris*, C.v., $n = 3$, *E. tetralix*, E.t., $n = 6$) for leaf (A) and root (B) samples, respectively. Values = means ± SDs. One-tailed Kruskal–Wallis test, followed by Dunn's post hoc procedure, found significant differences ($P > 0.05$) among *L. inundata*, *J. bulbosus*, and surrounding angiosperms as references in leaf carbon- and nitrogen-stable isotope natural abundance and in root nitrogen-stable isotope natural abundance.

investigations, confirmed that they were colonized by Mucoromycotina fungi. Glomeromycotina sequences were not detected. Mucoromycotina operational taxonomic units (OTUs) were detected before and after the experiments (Supplemental Table S2); these same OTUs had previously been identified in wild-collected lycophytes from diverse locations (Rimington et al., 2015).

Diverse and shared Mucoromycotina fungi OTUs were detected in wild *L. inundata*, liverworts, and angiosperms growing adjacently in the same UK locations (Supplemental Table S2; Supplemental Figs. S2–S8) in the following combinations: *L. inundata*, *F. foveolata*, *M. caerulea*, and *J. bulbosus* (Thursley Common, Surrey); *L. inundata*, *F. foveolata*, and *J. bulbosus* (Norfolk); and *F. foveolata* and *H. lanatus* (Lynn Crafnant, Wales). Mucoromycotina OTUs were also detected in *L. inundata* from Studland Heath, Dorset.

DISCUSSION

Our results show that the symbiosis between *L. inundata* and Mucoromycotina FREs is nutritionally mutualistic, with the fungus gaining plant-fixed C and the plant gaining fungal-acquired N and P (Fig. 2; Supplemental Table S3). Cytological analyses of the fungus colonizing the roots of *L. inundata* revealed a characteristic morphology consisting invariably of fine, aseptate branching hyphae with terminal and intercalary swellings/vesicles. This morphology matches that described previously in a range of angiosperms colonized by FREs (Orchard et al., 2017a, 2017b) and here in grasses, a rush, and a liverwort, all harboring fungi identified molecularly as Mucoromycotina (Supplemental Fig. S3). Our results provide compelling evidence for Mucoromycotina FREs being shared by plants occupying key nodes in the land plant phylogeny—from early liverworts and vascular lycophytes to the later diverging angiosperms—and demonstrate that this association represents a nutritional mutualism as much in vascular plants as it does in nonvascular plants (Field et al., 2015b, 2016).

Our findings raise important questions regarding the ecology and evolution of mycorrhizal associations and the nature of widespread Mucoromycotina FRE fungal symbioses, chief among which is how have these associations persisted and why are they so widespread today? We can now begin to address this with the demonstration that a vascular plant assimilates relatively large amounts of ^{15}N tracer via its Mucoromycotina fungal symbiont when compared to the Mucoromycotina fungal-acquired ^{33}P tracer (Fig. 2C), suggesting a potential role for Mucoromycotina FREs in vascular plant nitrogen uptake, complementary to the role of Glomeromycotina AM fungi (Field et al., 2019). This nutritional role could help to explain the persistence of Mucoromycotina FREs across nearly all modern land plant lineages.

Costs and Benefits of Hosting Mucoromycotina Fungi

Our data demonstrate that *L. inundata* transfers carbon to symbiotic Mucoromycotina FRE (Fig. 2, A and B). However, when compared to other vascular plants with Glomeromycotina AM fungal associates in similar experimental systems (Field et al., 2012), it is clear that the relative C "cost" of maintaining Mucoromycotina fungal symbionts in *L. inundata* is at least on a par with, if not greater than, that of maintaining Glomeromycotina fungi. It is not entirely clear from our experiments why this might be and it is important to note that the C "cost" of hosting Mucoromycotina FREs has only been tested in one vascular plant species to date and thus represents an important area for future research. It is possible that the carbon-for-nutrient exchange dynamics between plant and Mucoromycotina FREs vary according to plant and fungal identity, in addition to abiotic factors, as

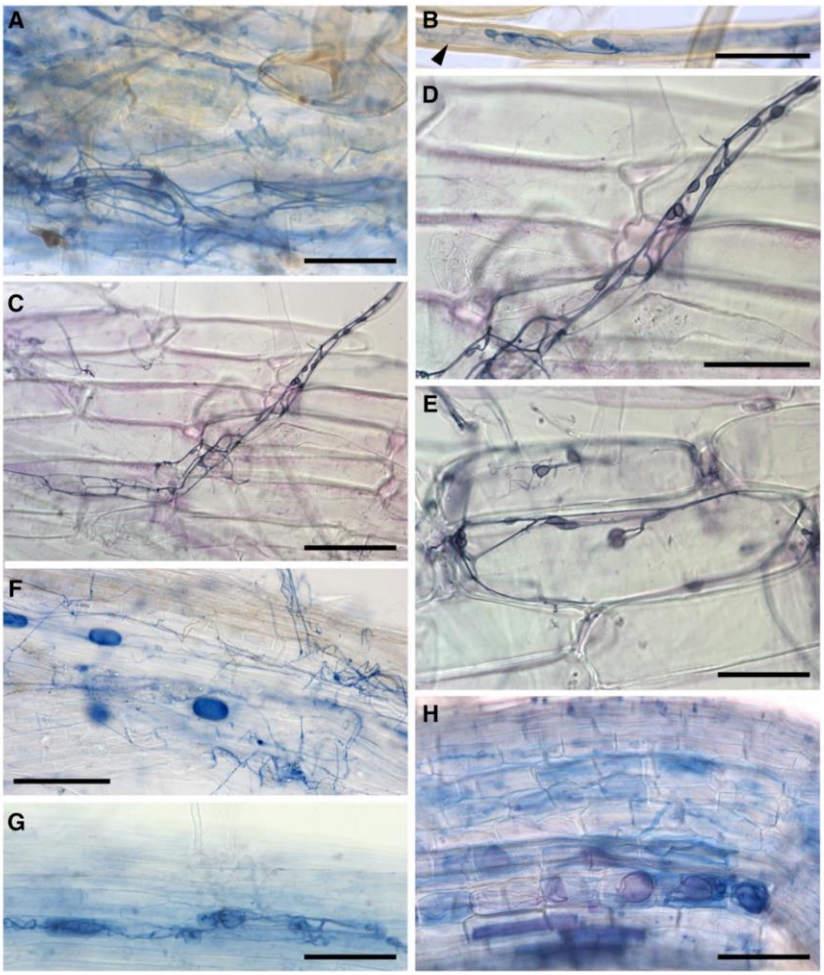

Figure 4. Light micrographs of trypan-blue–stained tissues. A and B, Branching fine hyphae with small swellings/vesicles in thallus cells (A) and rhizoid (B) of the liverwort *F. foveolata* (from Thursley Common) colonized by both Mucoromycotina FREs and Glomeromycotina; in (B) also note the coarse hyphae (arrowhead). C to E, Fine hyphae with small swellings/vesicles in the root hairs and root cells of the lycophyte *L. inundata* colonized by Mucoromycotina FREs only (field-collected specimens from Thursley Common). F, Fine hyphae with small swellings/vesicles and large vesicles in a root of the grass *H. lanatus* (from Lynn Crafnant, Wales) colonized by both Mucoromycotina FREs and Glomeromycotina. G and H, Roots of the grass *M. caerulea* (from Thursley Common) colonized by both Mucoromycotina FREs and Glomeromycotina, showing fine hyphae (G) and coarse hyphae with large vesicles (H). Scale bars = 50 μm (A and B, D–F); 100 μm (C, G, and H).

it does for Glomeromycotina AM (Field and Pressel, 2018).

Lycophytes represent a critical node in land plant phylogeny, widely considered as a diversification point in the mid-Paleozoic (480–360 million years ago) characterized by the evolution of roots, leaves, stomata, and associated vasculature (Kenrick and Crane, 1997). Given that all the plants sampled grew in close proximity and all follow the C_3 photosynthetic pathway, the trend for lower $\delta^{13}C$ values in root tissues versus leaves (Fig. 3) is most likely caused by systematic differences in ^{13}C abundance in photosynthetic versus nonphotosynthetic tissues (Gebauer and Schulze, 1991; Cernusak et al., 2009). The depletion of ^{13}C observed in the leaves of *L. inundata* (Fig. 3A) relative to the other, non-Mucoromycotina associated plants sampled is unlikely to be related to C gains from its Mucoromycotina fungal symbiont (Bago et al., 2000) as one would expect (myco)heterotrophic carbon gains to result in ^{13}C enrichment (Press et al., 1987; Schulze et al., 1991; Gebauer and Meyer, 2003); rather, it may indicate that *L. inundata* leaves regulate their stomata differently from *J. bulbosus* or the reference plants tested, as $\delta^{13}C$ in tissues of terrestrial plants is, among other factors, driven by the water use efficiency of the plant (Farquhar et al., 1982, 1989).

Alongside increased capacity for regulation of water relations and C capture and fixation, we hypothesize that the increasing size and structural complexity of land plants across the land plant phylogeny and evolutionary time (Field et al., 2012) result in greater plant nutrient demand. Glomeromycotina AM are associated with facilitation of plant P uptake and occur commonly in soils with low P availability (Smith et al., 2015; Albornoz et al., 2016). The amount of ^{33}P transferred to *L. inundata* plants in our experiments was much less than has previously been recorded for Mucoromycotina-associated liverworts (Field et al., 2016) or for Glomeromycotina-associated ferns and angiosperms (Field et al., 2012) despite the same amount of ^{33}P being made available in comparable experimental systems. This suggests Mucoromycotina

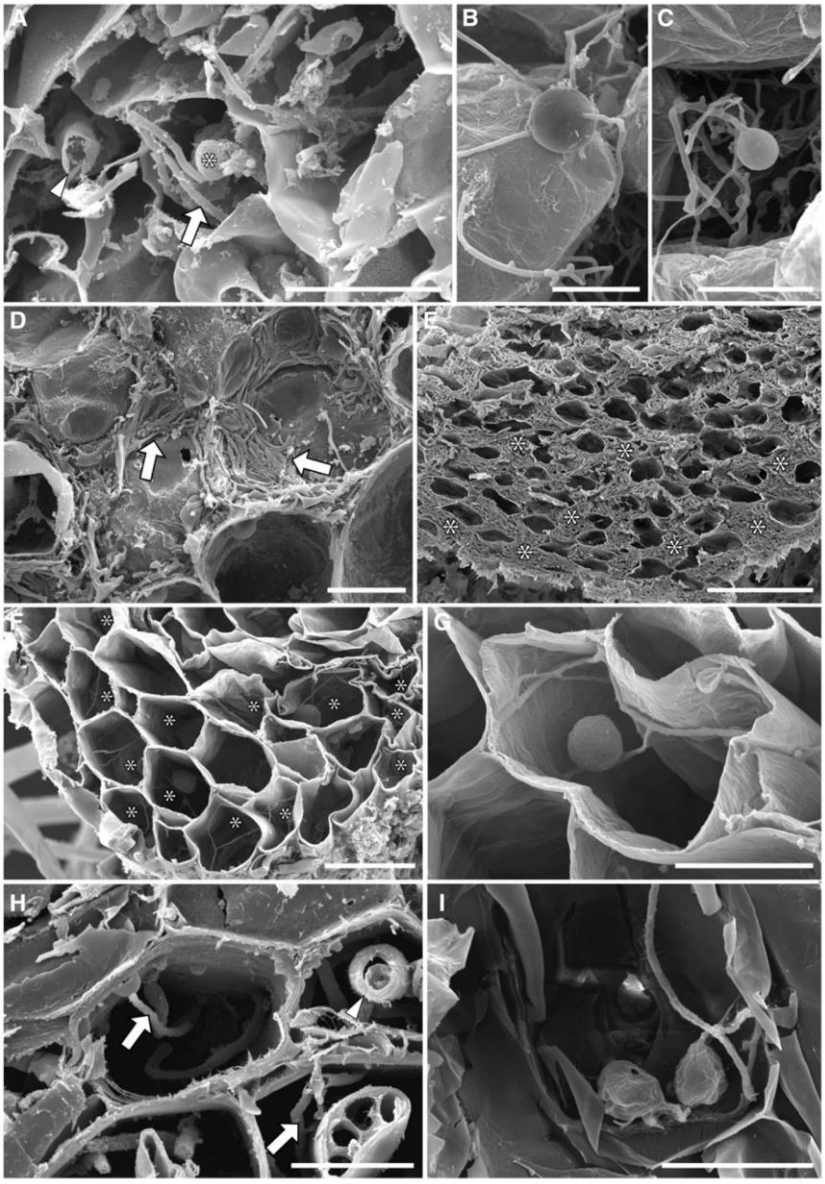

Figure 5. SEM images. A, Fine hyphae (arrows) with a small swelling/vesicle (*) in the thallus cells of *F. foveolata* (from Thursley Common); also note the much coarser hyphae (arrowheads). B to G, Fungal colonization in *L. inundata*. Intercalary (B) and terminal (C) small swellings/vesicles on fine hyphae in the ventral cell layers of a protocorm (from Thursley Common). Centrally and above this intracellular colonization zone, the fungus becomes exclusively intercellular, as evidenced by the presence of abundant, tightly-appressed hyphae surrounding the central protocorm cells (D, arrows) and eventually completely fills the large, mucilage-filled ICSs present in this zone (E, *). Cross sections of roots of experimental plants; several cells colonized exclusively (*) by branching fine hyphae with small swellings/vesicles (F), enlarged in (G). H and I, Cross sections of roots of *J. bulbosus* (from Thursley Common) showing fine (arrows) and coarse (arrowhead) hyphae (H) and a fine hypha with small swellings/vesicles (I). Scale bars = 20 μm (A, D, G, and I), 10 μm (B, C, and H), and 100 μm (E); 50 μm (F).

fungi may not play a critical role in lycophyte P nutrition. Our results contrast with the view that Mucoromycotina FREs enhance plant P uptake, at least in soils with very low P (Ryan and Kirkegaard, 2012; Orchard et al., 2017b). Previous experiments with Mucoromycotina fungi-associated liverworts suggest that in addition to supplying host plants with P, Mucoromycotina fungal associates also play a role in plant N nutrition (Field et al., 2015b, 2016, 2019).

Nitrogen is an essential element for plants that is available in soils in plant-inaccessible organic forms and as plant-accessible inorganic nitrate and ammonium (Krapp, 2015). Our results show that Mucoromycotina FRE symbionts transfer significantly more ^{15}N tracer compared to ^{33}P (Fig. 2, C and D). Up to 145 times more ^{15}N was transferred to *L. inundata* (0.3% to 1% of the supplied tracer) than to Haplomitriopsida liverworts in comparable experiments that assimilated between 0.05% and 0.2% of the supplied tracer (Field et al., 2016). Using analysis of natural abundance ^{15}N signatures, we show that Mucoromycotina FRE-associated *L. inundata* and *J. bulbosus* were ^{15}N enriched compared to co-occurring reference plants with different mycorrhizal fungal partners (Fig. 3). This ^{15}N enrichment could

be caused by temporal and spatial variations in N availability and changes in plant N demand over time (Gebauer and Meyer, 2003). However, these factors are unlikely in our case, because all plants sampled from this field collection grew in close spatial proximity and were collected at the same time. Presence of multiple N sources with distinct isotopic values and their utilization by different mycorrhizal associations are known as additional drivers of variations in plant ^{15}N isotope abundance (Bidartondo et al., 2004). While this distinction in N isotope abundance between plants with different mycorrhizas is almost or completely lost in conditions of high N availability (Gebauer and Meyer, 2003), it may become prominent under severe N limitation (Schulze et al., 1994). Given that our plants were collected at a heathland field site that was likely N-limited (von Oheimb et al., 2010) despite substantial atmospheric N deposition, the separation of *L. inundata* and *J. bulbosus* in their natural abundance ^{15}N from neighboring plants with other fungal associations supports our hypothesis that plants hosting Mucoromycotina symbionts benefit from fungal-acquired N.

Some Glomeromycotina AM fungi transfer N to their associated hosts (Leigh et al., 2009); however, the ecological relevance of AM-facilitated N uptake is widely debated, in particular the amounts of N transferred to hosts compared to the overall N requirements of the plant (Smith and Smith, 2011). Exclusive plant-Mucoromycotina FRE symbioses seem to be rare, having been reported before only in the earliest-diverging Haplomitriopsida liverworts (Field et al., 2015a, 2015b), while all other plants including other lycophytes (Rimington et al., 2015) that form associations with these fungi, appear able to do so also with Glomeromycotina, often simultaneously (Rimington et al., 2015). It is possible that the large input to *Lycopodiella* N-nutrition and minor contribution to P-nutrition by Mucoromycotina FREs reflect a specialized relationship, particularly pertinent when considering heathland habitats have very low plant-available N. Nevertheless, our present data combined with previous demonstrations of N transfer in liverwort-Mucoromycotina symbioses (Field et al., 2015b, 2016) and emerging evidence that Mucoromycotina FREs, but not Glomeromycotina AM fungi, are able to transfer N to host liverworts from organic sources (Field et al., 2019), all point to a critical role of Mucoromycotina FREs in host plant N nutrition. Indeed, our cytological analyses show that, differently from *Lycopodiella* roots where only fine endophytes were observed (Figs. 4 and 5; Table 1), all other co-occurring plants (*F. foveolata*, *J. bulbosus*, and *M. caerulea*) were also colonized by coarse endophytes with cytology typical of Glomeromycotina (Figs. 4 and 5; Table 1). The finer functional details, in terms of N and P transfer, of this partnership in other vascular plants from a broader range of habitats remain to be established; the challenge here will be to separate the nutritional contributions of Mucoromycotina FREs and Glomeromycotina to host plants that are cocolonized by both fungi (in addition to the contributions made by any mutualistic Ascomycetes and Basidiomycetes), as that seems to be the prevailing condition in vascular plants, especially angiosperms.

Mucoromycotina FREs

Mucoromycotina fungi within Endogonales colonizing the gametophytes of liverworts (*F. foveolata*) and lycophytes (*L. inundata*), the sporophytic protocorms and roots of lycophytes (*L. inundata*), and the roots of angiosperms (*J. bulbosus*, *M. caerulea*, and *H. lanatus*), all display the same characteristic morphology attributed previously to FREs (Orchard et al., 2017b; Walker et al., 2018). This contrasts with that typical of Glomeromycotina AM fungal associations, consisting of coarse hyphae (>3-μm diameter) and larger vesicles, which we observed in *Fossombronia*, *Juncus*, *Molinia*, and *Holcus* but not in *L. inundata* (Table 1). These observations, together with the molecular identification of Mucoromycotina clades shared by these phylogenetically distant plant lineages presented here, support previous suggestions that vascular plants' FREs are closely related to the Mucoromycotina mycorrhizal-like symbionts of nonvascular plants (Rimington et al., 2016). Here, we show that the same Mucoromycotina FREs have the capacity to be nutritionally mutualistic across different land plant phyla.

Our demonstration of an extensive intercellular phase of fungal colonization in the gametophytes and protocorms of *L. inundata* is in line with other lycophytes (Schmid and Oberwinkler, 1993; Rimington et al., 2015) and strongly recalls the gametophytes of the Haplomitriopsida liverwort *Treubia* (Duckett et al., 2006) and several hornworts (Desirò et al., 2013), all of which have also been shown to associate with Mucoromycotina fungi (Bidartondo et al., 2011; Desirò et al., 2013). Differently from their fine intracellular counterparts, intercellular hyphae become swollen, eventually reaching >3 μm in diameter. Tightly wound hyphal coils up to 2.5 μm in diameter with somewhat larger terminal vesicles (up to 20 μm in diameter) are also prominent in the outer cortical layers of *L. inundata* gametophytes but were not observed in either protocorms or roots. Thus, Mucoromycotina FREs display considerable phenotypic plasticity in their interactions with diverse lineages of land plants that appears to relate to the developmental stage of the host and whether it produces an extensive network of mucilage-filled ICSs. The putative occurrence of Mucoromycotina FREs in early land plants and their presence in both extant early and later diverging plant lineages now point to a prominent role of these fungi, not only in plant terrestrialization (Field et al., 2015a), but also in current ecosystem functioning. Indeed, Mucoromycotina FREs have been shown to occur worldwide across many ecosystems, particularly in the roots of crop and pasture species where colonization levels may be high, even as dense as the biomass of coarse Glomeromycotina arbuscular mycorrhizal fungi (Orchard et al., 2017b).

Table 1. *Cytology of colonization and fungal identity of study species compared to relevant examples from the literature referred to in "Discussion."* G = gametophyte generation; S= sporophyte generation.

Plant Group	G/S	Tissue/Location	Colonization	Morphology (Diameter)	Fungus ID	References
Liverworts						
Treubia	G	Several ventral cell layers	Intracellular	Coils (0.5–1.5 μm) with "lumps"/ swellings (up to 15 μm), arbuscule-like short-side branches on coiled hyphae	M	Duckett et al., 2006; Bidartondo et al., 2011
		Above intracellular zone	Intercellular: large mucilage-filled ICSs	Coarse hyphae 2–3 μm, thick-walled fungal structures		
Fossombronia	G	Thallus central strand	Intracellular	Coarse hyphae (2–3 μm); large vesicles (15–30 μm), coils (0.5–1 μm), fine hyphae (0.5–1.5 μm) with small swellings/ vesicles (5–10 μm), arbuscules	M&G	This study
Lycophytes						
Lycopodiella	G	Outer cortical cell layers	Intracellular	Coils (up to 2.5 μm) with vesicles (15–20 μm)	M	This study
		Several ventral cell layers	Intracellular	Fine hyphae (0.5–1.5 μm) with small swellings/vesicles (5–10 μm)		
		Above intracellular zone	Intercellular: large mucilage-filled ICSs	Coarse hyphae (2–>3 μm)		
	S	Protocorm:	Intracellular	Fine hyphae (0.5–1.5 μm) with small swellings/vesicles (5–10 μm)	M	This study
		Several ventral cell layers central, above intracellular zone	Intercellular: large mucilage-filled ICSs	Coarse hyphae (2–>3 μm)		
	S	Root	Intracellular and intercellular, small ICSs	Fine hyphae (0.5–1.5 μm) with small swellings/vesicles (5–15 μm)	M	Rimington et al., 2015; This study
Angiosperms						
Holcus	S	Root	Intracellular and intercellular, small ICSs	Coarse hyphae (>3 μm), large vesicles (20–40 μm), fine hyphae (0.5–1.5 μm) with small vesicles (5–10 μm), arbuscules/arbuscule-like structures	M&G	This study
Molinia	S	Root	Intracellular and intercellular, small ICSs	Coarse hyphae (>3 μm), large vesicles (20–40 μm), fine hyphae (0.5–1.5 μm) with small vesicles/ swellings (5–10 μm), arbuscules/ arbuscule-like structures	M&G	This study
Juncus	S	Root	intracellular and intercellular, small ICSs	Coarse hyphae (>3 μm), large vesicles (20–40 μm), fine hyphae (0.5–1.5 μm) with small vesicles (5–10 μm), arbuscules/arbuscule-like structures	M&G	This study
Trifolium	S	Root	intracellular and intercellular, small ICSs	Coarse hyphae (>3 μm), large vesicles (>30 μm) fine hyphae (>1.5 μm), intercalary and terminal vesicles/ swellings (5–10 μm) and arbuscules/arbuscule-like structures	M&G	Orchard et al., 2017a
Fossils						
Horneophyton	S	Aerial axes, cortical cells	intracellular	coarse hyphae (>3 μm), large vesicles (up to 50 μm), arbuscule-like structures	G	Strullu-Derrien et al., 2014
		Corm	intracellular and intercellular	intracellular coils, intercellular coarse hyphae (11–13 μm), thick-walled fungal structures	M	
Nothia	S	Aerial and prostrate axes	intercellular and intracellular	coarse hyphae (up to 15 μm) and intercellular vesicles (>50 μm)	Unidentified	Krings et al., 2007

CONCLUSION

More Ammunition for the Mycorrhizal Revolution

Our findings provide conclusive evidence that Mucoromycotina FREs form nutritional mutualisms not only with nonvascular liverworts (Field et al., 2015b, 2016), but also with a vascular plant. We have found that the Mucoromycotina FRE associates of *L. inundata* receive up to 189 times more photosynthesis-derived C from the plant than the Mucoromycotina fungal associates of nonvascular plants (Field et al., 2016). In return, *L. inundata* hosts receive a relatively large amount of N from their Mucoromycotina FRE partners—~145 times more than nonvascular plants receive from their Mucoromycotina fungal symbionts (Field et al., 2016). Together with our discovery that the same Mucoromycotina fungal symbionts are shared with neighboring grasses, rushes and liverworts, and recent findings of functional complementarity between Mucoromycotina FREs and Glomeromycotina AM (Field et al., 2019), our findings point toward a unique physiological niche for the persistence of Mucoromycotina fungi, both in single and dual colonizations with Glomeromycotina AM.

MATERIALS AND METHODS

Plant Material and Growth Conditions

Lycopodiella inundata, neighboring angiosperms (the grasses *Holcus lanatus*, *Molinia caerulea*, and the rush *Juncus bulbosus*), and a liverwort (*Fossombronia foveolata*) were collected from Thursley National Nature Reserve, Surrey, United Kingdom (SU 90081 39754), a heathland site, in June 2017. The *L. inundata* plants were planted directly into pots (90-mm diameter × 85-mm depth) containing a homogenous mixture of acid-washed silica sand and 5% pot volume compost (No. 2; Petersfield) to aid water-retention properties of the substrate and to provide minimal nutrients. Soil surrounding plant roots was left intact to prevent damage to the roots and to act as a natural inoculum, including symbiotic fungi and associated microorganisms. Pots were weeded regularly to remove other plant species. All plants used throughout this investigation were collected from the wild. Each microcosm was a homogenized mixture of acid-washed sand and soil collected from around the plant roots from the collection site. All plants used in this investigation (isotope tracing, cytology, and stable isotope studies) were collected from Thursley Nature Reserve, with additional plants from three other United Kingdom field sites (Supplemental Table S1), used for additional cytological and molecular analyses.

Based on the methods of Field et al. (2012, 2015a), three windowed cylindrical plastic cores covered in 10-μm nylon mesh (Supplemental Fig. S1) were inserted into the substrate within each experimental pot. Two of the cores were filled with the same substrate as the bulk soil within the pots, comprising a homogenous mixture of acid-washed silica sand and compost (No. 2; Petersfield), together making up 95% of the core volume, native soil gathered from around the roots of wild plants to ensure cores contained the same microbial communities as in bulk soil (4% core volume), and fine-ground tertiary basalt (1% core volume) to act as fungal bait. The third core was filled with glass wool to allow below-ground gas sampling throughout the ^{14}C-labeling period to monitor soil community respiration. Plants were watered every other day with no additional applications of nutrient solutions. Microcosms shared a common drip-tray within each cabinet throughout the acclimation period that ensured a common pool of rhizospheric microorganisms in each microcosm.

A total of 20 *L. inundata* microcosms were maintained in controlled environment chambers (model no. Micro Clima 1200; Snijders Labs) with a light cycle of 16-h daytime (20°C and 70% humidity) and 8-h night-time (at 15°C and 70% humidity). Day-time photosynthetically active radiation (PAR), supplied by LED lighting, was 225 μmol photons m^{-2} s^{-1}. Atmospheric CO_2 concentrations were set at 440 μL L^{-1}. Atmospheric [CO_2] was monitored using a sensor system (Vaisala), maintained through addition of gaseous CO_2. All pots were rotated within cabinets to control for cabinet and block effects. Plants were acclimated to chamber/growth regimes for four weeks to allow establishment of mycelial networks within pots and confirmed by hyphal extraction from soil and staining with trypan blue (Brundrett et al., 1996). Additionally, roots were stained with acidified ink for the presence of fungi, based on the methods of Brundrett et al. (1996).

Molecular Identification of Fungal Symbionts and Phylogenetic Analysis

All plants (Supplemental Table S1) were processed for molecular analyses within 1 week of collection. Genomic DNA extraction and purification from all specimens and subsequent amplification, cloning, and Sanger sequencing were performed according to methods from Rimington et al. (2015). The fungal 18S rRNA gene was targeted using the broad specificity fungal primer set NS1/EF3 and a semi-nested approach with Mucoromycotina- and Glomeromycotina-specific primers described in Desirò et al. (2013) for the experimental *L. inundata* plants and all other field-collected plant material. Resulting partial 18S rRNA sequences ~400–700 bp were edited and preliminarily identified with the tool "BLAST" (https://blast.ncbi.nlm.nih.gov/Blast.cgi) using the software "Geneious 8.1.7" (Kearse et al., 2012). Chimeric sequences were detected using the "UCHIME2" algorithm (Edgar, 2016) in conjunction with the most recent nonredundant small subunit SILVA database (small subunit Ref NR 132, December 2017; www.arb-silva.de). Sequences identified as Mucoromycotina sp were aligned with the tool "MAFFT" before removing unreliable columns using the default settings in the software "GUIDANCE2" (http://guidance.tau.ac.il). The best-fit nucleotide model for phylogenetic analysis was calculated using "Smart Model Selection" (Kumar et al., 2016). Maximum likelihood with 1,000 replicates was performed using the software "PhyML 3.0" (Guindon and Gascuel, 2003). Bayesian inference analysis was conducted in the software "MrBayes 3.2.6" (Ronquist and Huelsenbeck, 2003) with four Markov-chain Monte Carlo strands and 10^6 generations. Consensus trees were produced after excluding an initial burn-in of 25% of the samples (Supplemental Figs. S3–S9). Representative DNA sequences were deposited in the GenBank (see "Accession Numbers").

Cytological Analyses

L. inundata gametophytes (n = 15), young sporophytes (protocorms; n = 15), and roots of mature plants (both wild [n = 20] and experimental [n = 20]), roots of angiosperms (*H. lanatus*, *M. caerulea*, and *J. bulbosus*; n = 30 for each species), and liverwort gametophytes (*F. foveolata*; n = 30) were either stained with trypan blue (Brundrett et al., 1996) and photographed under an Axioscope (Zeiss) equipped with a digital camera (MRS Systems), or processed for SEM within 48 h of collection. For SEM, we followed the protocol of Duckett et al. (2006); see Supplemental Materials and Methods).

Quantification of C, ^{33}P, and ^{15}N Fluxes between Lycophytes and Fungi

After the 4-week acclimation period, microcosms were moved to individual drip-trays immediately before isotope labeling to avoid cross-contamination of the isotope tracers. One-hundred microliters of an aqueous mixture of ^{33}P-labeled orthophosphate (specific activity 111 TBq $mmol^{-1}$, 0.3 ng ^{33}P added; Hartmann Analytics) and ^{15}N-ammonium chloride (1 mg ml^{-1}; 0.1 mg ^{15}N added; Sigma-Aldrich) was introduced into one of the soil-filled mesh cores in each pot through the installed capillary tube (Supplemental Fig. S2A). In half (n = 10) of the pots, cores containing isotope tracers were left static to preserve direct hyphal connections with the lycophytes. Fungal access to isotope tracers was limited in the remaining half (n = 10) of the pots by rotating isotope tracer-containing cores through 90°, thereby severing the hyphal connections between the plants and core soil. These were rotated every second day thereafter, thus providing a control treatment that allows us to distinguish between fungal and microbial contributions to tracer uptake by plants. Assimilation of ^{33}P tracer into above-ground plant material was monitored daily using a hand-held Geiger counter held over the plant material.

At detection of peak activity in above-ground plant tissues (21 d after the addition of the ^{33}P and ^{15}N tracers), the tops of ^{33}P- and ^{15}N-labeled cores were sealed with plastic caps and anhydrous lanolin and the glass wool cores were sealed with rubber septa (SubaSeal; Sigma-Aldrich). Before cabinet

lights were turned on at 8 AM, each pot was sealed into a 3.5-L, gas-tight labeling chamber and 2 mL of 10% (w/v) lactic acid was added to 30 μL of $NaH^{14}CO_3$ (specific activity 1.621 GBq/mmol^{-1}; Hartmann Analytics), releasing a 1.1-MBq pulse of $^{14}CO_2$ gas into the headspace of the labeling chamber (Supplemental Fig. S2B). Pots were maintained under growth cabinet conditions, and 1 mL of headspace gas was sampled after 1 h and every 1.5 h thereafter. Below-ground respiration was monitored via gas sampling from within the glass-wool–filled core after 1 h and every 1.5 h thereafter for ~16 h.

Plant Harvest and Sample Analyses

Upon detection of maximum below-ground flux of ^{14}C, ~16 h after the release of the $^{14}CO_2$ pulse, each microcosm compartment (i.e. plant material and soil) was separated, freeze-dried, weighed, and homogenized. The ^{33}P activity in plant and soil samples was quantified by digesting in concentrated H_2SO_4 (Supplemental Materials and Methods) and liquid scintillation (Tricarb 3100TR liquid scintillation analyzer; Isotech). The quantity of ^{33}P tracer that was transferred to the plant by its fungal partner was then calculated using previously published equations (Cameron et al., 2007; see Supplemental Materials and Methods). To determine total symbiotic fungal-acquired ^{33}P transferred to *L. inundata*, the mean ^{33}P content of plants that did not have access to the tracer because cores into which the ^{33}P was introduced were rotated, was subtracted from the total ^{33}P in each plant that did have access to the isotopes within the core via intact fungal hyphal connections (i.e. static cores). This calculation controls for diffusion of isotopes and microbial nutrient cycling in pots, ensuring only ^{33}P gained by the plant via intact fungal hyphal connections is accounted for and therefore serves as a conservative measure of the minimum fungal transfer of tracer to the plant.

Between 2 and 4 mg of freeze-dried, homogenized plant tissue was weighed into 6 × 4 mm^2 tin capsules (Sercon) and ^{15}N abundance was determined using a continuous flow infrared mass spectormetry (IRMS; model no. PDZ 2020 IRMS; Sercon). Air was used as the reference standard, and the IRMS detector was regularly calibrated to commercially available reference gases. The ^{15}N transferred from fungus to plant was then calculated using equations published in Field et al. (2016); see Supplemental Materials and Methods). In a similar manner as for the ^{33}P tracer, the mean of the total ^{15}N in plants without access to the isotope because of broken hyphal connections between plant and core contents was subtracted from the total ^{15}N in each plant with intact hyphal connections to the mesh-covered core to give fungal-acquired ^{15}N. Again, this provides a conservative measure of ^{15}N transfer from fungus to plant as it ensures only ^{15}N gained by the plant via intact fungal hyphal connections is accounted for.

The ^{14}C activity of plant and soil samples was quantified through sample oxidation (307 Packard Sample Oxidizer, Isotech) followed by liquid scintillation. Total C ($^{12}C + {}^{14}C$) fixed by the plant and transferred to the fungal network was calculated as a function of the total volume and CO_2 content of the labeling chamber and the proportion of the supplied $^{14}CO_2$ label fixed by plants (see Supplemental Materials and Methods). The difference in total C between the values obtained for static and rotated core contents in each pot is considered equivalent to the total C transferred from plant to symbiotic fungus within the soil core for that microcosm, noting that a small proportion will be lost through soil microbial respiration. The total C budget for each experimental pot was calculated using equations from Cameron et al. (2006); see Supplemental Materials and Methods). Total percent allocation of plant-fixed C to extraradical symbiotic fungal hyphae was calculated by subtracting the activity (in becquerels) of rotated core samples from that detected in static core samples in each pot, dividing this by the sum of activity detected in all components of each microcosm, then multiplying it by 100.

Stable Isotope Signatures of Neighboring Plants

L. inundata and *J. bulbosus* were collected from Thursley National Nature Reserve, Surrey, together with co-occurring reference plants from six 1-m^2 plots in May 2018, following the sampling scheme of Gebauer and Meyer (2003). Five plant species representing three different types of mycorrhizal associations served as reference plants: two ericoid mycorrhizal species (*Erica tetralix*, collected on six plots; *Calluna vulgaris*, collected on three plots), two ectomycorrhizal species (*Pinus sylvestris* and *Betula pendula* seedlings, both from one plot), and one arbuscular mycorrhizal species (*M. caerulea* from six plots). Relative carbon and nitrogen isotope natural abundances of dried and ground leaf and root samples were measured in a dual element analysis mode with a model no. 1108 elemental analyzer (Carlo Erba Instruments) coupled to a DELTA S Continuous Flow Isotope Ratio Mass Spectrometer (using a Finnigan MAT; Thermo Fisher Scientific) via a ConFlo III open-split interface (Thermo Fisher Scientific), as described in Bidartondo et al. (2004). Relative isotope abundances (δ values) were calculated, calibrated, and checked for accuracy using methods detailed in Supplemental Materials and Methods.

Statistics

Isotope tracing data were checked for normality and differences between plant assimilation of ^{33}P and ^{15}N were tested using Student's t test with the software "SPSS v24" (IBM). Mean values are displayed in figures with SE. Stable isotope patterns between the groups of *L. inundata* (n = 6), *J. bulbosus* (n = 6), and surrounding angiosperms (n = 17) were tested for normality and equal variance. A one-tailed Kruskal–Wallis test (Q) was applied for nonparametric data followed by Dunn's post hoc procedure, while one-way ANOVA (F) was applied for parametric data followed by the Tukey post hoc procedure (q). Mean values are displayed in figures with SD.

Accession Numbers

Representative DNA sequences were deposited in the GenBank/EMBL data libraries under accession numbers MK673773–MK673803.

Supplemental Data

The following supplemental materials are available.

Supplemental Figure S1. Schematic diagram of mesh-covered core showing dimensions of window (not drawn to scale).

Supplemental Figure S2. Schematic diagrams of experimental microcosms showing N and P, and C isotope tracing.

Supplemental Figure S3. Phylogenetic relationships of Mucoromycotina OTUs associated with *L. inundata* grown for isotope tracing and cytology experiments in controlled environment growth chambers.

Supplemental Figure S4. An overview of phylogenetic relationships of Mucoromycotina OTUs associated with bryophytes, lycophytes, and angiosperms from various UK locations based on partial 18S gene sequences.

Supplemental Figure S5. Phylogenetic relationships of partial 18S DNA sequences classified as OTU 2, corresponding to "group A" in Desirò et al. (2013).

Supplemental Figure S6. Phylogenetic relationships of partial 18S DNA sequences classified as OTU 1, 3, and 4.

Supplemental Figure S7. Phylogenetic relationships of partial 18S DNA sequences clustering within OTU 5.

Supplemental Figure S8. Phylogenetic relationships of partial 18S DNA sequences classified as OTU 6, corresponding to "group B" in Desirò et al. (2013).

Supplemental Figure S9. Phylogenetic relationships of partial 18S DNA sequences clustering with OTU 7, corresponding to "group I" in Desirò et al. (2013).

Supplemental Figure S10. Micrographs showing morphology of fungal colonization in *F. foveolata* and *H. lanatus*.

Supplemental Figure S11. SEM images and light micrograph of toluidine blue stained semi-thin sections. Gametophyte morphologies in *L. inundata* (from Thursley Common).

Supplemental Table S1. Samples of lycophytes, liverworts, and angiosperms analyzed with their origin.

Supplemental Table S2. A summary of Mucoromycotina OTUs associated with liverworts, lycophytes, and angiosperms at four UK sites.

Supplemental Table S3. A summary of the amounts of C, ^{15}N, and ^{33}P detected in static and rotated core of microcosms used during carbon-for-nutrient experiments between *L. inundata* and Mucoromycotina FRE fungi.

Supplemental Materials and Methods. Detailed methods for mesh-covered core construction, calculation of carbon and nutrient fluxes between symbionts, molecular methods for fungal identification and cytological analyses of resin-embedded plant material.

ACKNOWLEDGMENTS

We thank James Giles (Natural England) for field support, Julia Masson and the Royal Society for the Protection of Birds for access to the Norfolk site, and The Species Recovery Trust for access to the Dorset site. We are grateful to the anonymous reviewers of this article and to the editor for their constructive comments.

Received June 17, 2019; accepted July 22, 2019; published July 29, 2019.

LITERATURE CITED

Albornoz FE, Lambers H, Turner BL, Teste FP, Laliberté E (2016) Shifts in symbiotic associations in plants capable of forming multiple root symbioses across a long-term soil chronosequence. Ecol Evol **6:** 2368–2377

Bago B, Pfeffer PE, Shachar-Hill Y (2000) Carbon metabolism and transport in arbuscular mycorrhizas. Plant Physiol **124:** 949–958

Bidartondo MI, Burghardt B, Gebauer G, Bruns TD, Read DJ (2004) Changing partners in the dark: Isotopic and molecular evidence of ectomycorrhizal liaisons between forest orchids and trees. Proc Biol Sci **271:** 1799–1806

Bidartondo MI, Read DJ, Trappe JM, Merckx V, Ligrone R, Duckett JG (2011) The dawn of symbiosis between plants and fungi. Biol Lett **7:** 574–577

Brundrett M, Bougher N, Dell B, Grove T, Malajczuk N (1996) Working with Mycorrhizas in Forestry and Agriculture. Monograph, **Australian Centre for International Agricultural Research**. Pirie Printers, Canberra

Cameron DD, Leake JR, Read DJ (2006) Mutualistic mycorrhiza in orchids: evidence from plant-fungus carbon and nitrogen transfers in the green-leaved terrestrial orchid *Goodyera repens*. New Phytol **171:** 405–416

Cameron DD, Johnson I, Leake JR, Read DJ (2007) Mycorrhizal acquisition of inorganic phosphorus by the green-leaved terrestrial orchid *Goodyera repens*. Ann Bot **99:** 831–834

Cernusak LA, Tcherkez G, Keitel C, Cornwell WK, Santiago LS, Knohl A, Barbour MM, Williams DG, Reich PB, Ellsworth DS et al (2009) Why are non-photosynthetic tissues generally ^{13}C enriched compared with leaves in C3 plants? Review and synthesis of current hypotheses. Funct Plant Biol **36:** 199–213

Desirò A, Duckett JG, Pressel S, Villarreal JC, Bidartondo MI (2013) Fungal symbioses in hornworts: A chequered history. Proc Biol Sci **280:** 20130207

Duckett JG, Ligrone R (1992) A light and electron microscope study of the fungal endophytes in the sporophyte and gametophyte of *Lycopodium cernuum* with observations on the gametophyte–sporophyte junction. Can J Bot **70:** 58–72

Duckett JG, Carafa A, Ligrone R (2006) A highly differentiated glomeromycotean association with the mucilage-secreting, primitive antipodean liverwort *Treubia* (Treubiaceae): Clues to the origins of mycorrhizas. Am J Bot **93:** 797–813

Edgar R (2016) UCHIME2: Improved chimera prediction for amplicon sequencing. bioRxiv doi:10.1101/074252

Farquhar GD, O'Leary MH, Berry JA (1982) On the relationship between carbon isotope discrimination and the intercellular carbon dioxide concentration in leaves. Funct Plant Biol **9:** 121–137

Farquhar GD, Ehleringer JR, Hubick KT (1989) Carbon isotope discrimination and photosynthesis. Annu Rev Plant Biol **40:** 503–537

Field KJ, Pressel S (2018) Unity in diversity: Structural and functional insights into the ancient partnerships between plants and fungi. New Phytol **220:** 996–1011

Field KJ, Cameron DD, Leake JR, Tille S, Bidartondo MI, Beerling DJ (2012) Contrasting arbuscular mycorrhizal responses of vascular and non-vascular plants to a simulated Palaeozoic CO_2 decline. Nat Commun **3:** 835

Field KJ, Pressel S, Duckett JG, Rimington WR, Bidartondo MI (2015a) Symbiotic options for the conquest of land. Trends Ecol Evol **30:** 477–486

Field KJ, Rimington WR, Bidartondo MI, Allinson KE, Beerling DJ, Cameron DD, Duckett JG, Leake JR, Pressel S (2015b) First evidence of mutualism between ancient plant lineages (Haplomitriopsida liverworts) and Mucoromycotina fungi and its response to simulated Palaeozoic changes in atmospheric CO_2. New Phytol **205:** 743–756

Field KJ, Rimington WR, Bidartondo MI, Allinson KE, Beerling DJ, Cameron DD, Duckett JG, Leake JR, Pressel S (2016) Functional analysis of liverworts in dual symbiosis with Glomeromycota and Mucoromycotina fungi under a simulated Palaeozoic CO_2 decline. ISME J **10:** 1514–1526

Field KJ, Bidartondo MI, Rimington WR, Hoysted GA, Beerling D, Cameron DD, Duckett JG, Leake JR, Pressel S (2019) Functional complementarity of ancient plant-fungal mutualisms: Contrasting nitrogen, phosphorus and carbon exchanges between Mucoromycotina and Glomeromycotina fungal symbionts of liverworts. New Phytol **223:** 908–921

Gebauer G, Meyer M (2003) ^{15}N and ^{13}C natural abundance of autotrophic and myco-heterotrophic orchids provides insight into nitrogen and carbon gain from fungal association. New Phytol **160:** 209–223

Gebauer G, Schulze E-D (1991) Carbon and nitrogen isotope ratios in different compartments of a healthy and a declining *Picea abies* forest in the Fichtelgebirge, NE Bavaria. Oecologia **87:** 198–207

Guindon S, Gascuel O (2003) A simple, fast, and accurate algorithm to estimate large phylogenies by maximum likelihood. Syst Biol **52:** 696–704

Hoysted GA, Kowal J, Jacob A, Rimington WR, Duckett JG, Pressel S, Orchard S, Ryan MH, Field KJ, Bidartondo MI (2018) A mycorrhizal revolution. Curr Opin Plant Biol **44:** 1–6

James TY, Kauff F, Schoch CL, Matheny PB, Hofstetter V, Cox CJ, Celio G, Gueidan C, Fraker E, Miadlikowska J, et al (2006) Reconstructing the early evolution of fungi using a six-gene phylogeny. Nature **443:** 818–822

Kearse M, Moir R, Wilson A, Stones-Havas S, Cheung M, Sturrock S, Buxton S, Cooper A, Markowitz S, Duran C, et al (2012) Geneious Basic: An integrated and extendable desktop software platform for the organization and analysis of sequence data. Bioinformatics **28:** 1647–1649

Kenrick P, Crane PR (1997) The origin and early evolution of plants on land. Nature **389:** 33

Krapp A (2015) Plant nitrogen assimilation and its regulation: A complex puzzle with missing pieces. Curr Opin Plant Biol **25:** 115–122

Krings M, Taylor TN, Hass H, Kerp H, Dotzler N, Hermsen EJ (2007) An alternative mode of early land plant colonization by putative endomycorrhizal fungi. Plant Signal Behav **2:** 125–126

Kumar S, Stecher G, Tamura K (2016) MEGA7: Molecular evolutionary genetics analysis version 7.0 for bigger datasets. Mol Biol Evol **33:** 1870–1874

Leigh J., Hodge A., Fitter A. H. (2009) Arbuscular mycorrhizal fungi can transfer substantial amounts of nitrogen to their host plant from organic material. New Phytol **181:** 199–207

Lin K, Limpens E, Zhang Z, Ivanov S, Saunders DG, Mu D, Pang E, Cao H, Cha H, Lin T, et al (2014) Single nucleus genome sequencing reveals high similarity among nuclei of an endomycorrhizal fungus. PLoS Genet **10:** e1004078

Morris JL, Puttick MN, Clark JW, Edwards D, Kenrick P, Pressel S, Wellman CH, Yang Z, Schneider H, Donoghue PC (2018) The timescale of early land plant evolution. Proc Natl Acad Sci USA **115:** E2274–E2283

Orchard S, Hilton S, Bending GD, Dickie IA, Standish RJ, Gleeson DB, Jeffery RP, Powell JR, Walker C, Bass D, et al (2017a) Fine endophytes (*Glomus tenue*) are related to Mucoromycotina, not Glomeromycota. New Phytol **213:** 481–486

Orchard S, Standish RJ, Dickie IA, Renton M, Walker C, Moot D, Ryan MH (2017b) Fine root endophytes under scrutiny: A review of the literature on arbuscule-producing fungi recently suggested to belong to the Mucoromycotina. Mycorrhiza **27:** 619–638

Pirozynski KA, Malloch DW (1975) The origin of land plants: A matter of mycotrophism. Biosystems **6:** 153–164

Press MC, Shah N, Tuohy JM, Stewart GR (1987) Carbon isotope ratios demonstrate carbon flux from C(4) host to C(3) parasite. Plant Physiol **85:** 1143–1145

Redecker D, Kodner R, Graham LE (2000) Glomalean fungi from the Ordovician. Science **289:** 1920–1921

Rimington WR, Pressel S, Duckett JG, Bidartondo MI (2015) Fungal associations of basal vascular plants: Reopening a closed book? New Phytol **205:** 1394–1398

Rimington WR, Pressel S, Field KJ, Strullu-Derrien C, Duckett JG, Bidartondo MI (2016) Chapter 2: Reappraising the origin of mycorrhizas. *In* F Martin, ed, Molecular Mycorrhizal Symbiosis. John Wiley & Sons, New York, pp 31–32

Ronquist F, Huelsenbeck JP (2003) MrBayes 3: Bayesian phylogenetic inference under mixed models. Bioinformatics **19:** 1572–1574

Ryan MH, Kirkegaard JA (2012) The agronomic relevance of arbuscular mycorrhizas in the fertility of Australian extensive cropping systems. Agric Ecosyst Environ **163:** 37–53

Schmid E, Oberwinkler F (1993) Mycorrhiza-like interaction between the achlorophyllous gametophyte of *Lycopodium clavatum* L. and its fungal endophyte studied by light and electron microscopy. New Phytol **124:** 69–81

Schulze E-D, Lange OL, Ziegler H, Gebauer G (1991) Carbon and nitrogen isotope ratios of mistletoes growing on nitrogen and non-nitrogen fixing hosts and on CAM plants in the Namib desert confirm partial heterotrophy. Oecologia **88:** 457–462

Schulze E-D, Chapin III FS, Gebauer G (1994) Nitrogen nutrition and isotope differences among life forms at the northern treeline of Alaska. Oecologia **100:** 406–412

Smith SE, Smith FA (2011) Roles of arbuscular mycorrhizas in plant nutrition and growth: New paradigms from cellular to ecosystem scales. Annu Rev Plant Biol **62:** 227–250

Smith SE, Anderson IC, Smith FA (2015) Mycorrhizal associations and phosphorus acquisition: From cells to ecosystems. Ann Plant Rev **48:** 409–440

Strullu-Derrien C, Kenrick P, Pressel S, Duckett JG, Rioult JP, Strullu DG (2014) Fungal associations in *Horneophyton ligneri* from the Rhynie Chert (c. 407 million year old) closely resemble those in extant lower land plants: Novel insights into ancestral plant-fungus symbioses. New Phytol **203:** 964–979

von Oheimb G, Power SA, Falk K, Friedrich U, Mohamed A, Krug A, Boschatzke N, Härdtle W (2010) N:P ratio and the nature of nutrient limitation in Calluna-dominated heathlands. Ecosystems **13:** 317–327

Walker C, Gollotte A, Redecker D (2018) A new genus, Planticonsortium (Mucoromycotina), and new combination (*P. tenue*), for the fine root endophyte, *Glomus tenue* (basionym *Rhizophagus tenuis*). Mycorrhiza **28:** 213–219

Plant Physiology Supporting Information

Mucoromycotina fine root endophyte fungi form nutritional mutualisms with vascular plants.

Grace A. Hoysted, Alison S. Jacob, Jill Kowal, Philipp Giesemann, Martin I. Bidartondo, Jeffrey G. Duckett, Gerhard Gebauer, William R. Rimington, Sebastian Schornack, Silvia Pressel and Katie J. Field

The following Supporting Information is available for this article:

Supplemental text specific details on methods (mesh-covered core construction, equations, molecular methods for fungal identification).

Figure S1 Schematic diagram of mesh-covered core showing dimensions of window

Figure S2 Experimental microcosm showing (a) ^{15}N and ^{33}P and (b) ^{14}C isotope tracing.

Figure S3-S9 Phylogenetic relationships.

Figure S10-S11 Scanning electron micrograph and light micrographs of trypan blue stained roots.

Table S1 Plant samples with their origin.

Table S2 A summary of Mucoromycotina OUTs associated with plant samples at four UK sites.

Table S3 A summary of the amounts of carbon, ^{15}N and ^{33}P detected in static and rotated cores of microcosms.

Respective references

Supplementary Information Text

Summary

This file provides specific details on methods referred to in the main text of the above article, including mesh-covered core construction, equations for calculation of carbon and nutrient fluxes between symbionts and molecular methods for fungal identification. Cytological analyses of resin-embedded plant material are also included. Figures S1 and S2 illustrate experimental systems; Figures S3 to S9 are phylogenetic trees of Endogonales (Mucoromycotina) detected in plants. Figures S10 and S11 provide additional light and scanning electron micrographs of targeted plant species colonized by Mucoromycotina fine root endophytes (FRE), which complement those in the main text. Table S1 refers to the lycophytes, liverworts and angiosperms used throughout this study and their original location, Table S2 includes a summary of Mucoromycotina OTUs in lycophytes, liverworts and angiosperms and Table S3 includes a summary of the amounts of carbon, ^{15}N, ^{33}P in static and rotated cores within experimental microcosms used during the carbon-for-nutrient exchange experiments.

Materials and Methods

Plant growth conditions

Lycopodiella inundata plants were maintained in controlled environment chambers (Micro Clima 1200, Snijders Labs, Netherlands) with settings chosen to simulate the plant's natural environment: 70% RH, 16 hr/8 hr day/night, 20°C day/ 15°C night, 100.1 μmol m^{-2} s^{-1} irradiance.

Cytological analysis

For trypan blue staining, plant tissues were cleared in 5% KOH at 90°C for 3 h, acidified in 2% HCl for 1-2 min, stained in 0.05% trypan blue, de-stained in 50% glycerin for 24 h before viewing under a light microscope. For SEM, tissues were fixed in 3% glutaraldehyde, dehydrated through an ethanol series, critical-point dried using CO_2 as transfusion fluid, sputter coated with 390 nm palladium-gold and viewed using a FEI Quanta scanning electron microscope (FEI, Hillsboro, OR, USA).

For light microscopy, *L. inundata* gametophytes and the protocorms of young sporophytes were processed according to Ligrone and Duckett (1994). Briefly, specimens were fixed in 3% glutaraldehyde, 1% freshly prepared formaldehyde and 0.75% tannic acid in 0.05 M Na–cacodylate buffer, pH 7, for 3 h at room temperature. After several rinses in 0.1 M buffer, samples were post-fixed in buffered (0.1 M, pH 6.8) 1% osmium tetroxide overnight at 48° C, dehydrated in an ethanol series and embedded in Spurr's resin via ethanol, and 0.5 mm thick sections were cut with a diamond histo-knife, stained with 0.5% toluidine blue and photographed under a Zeiss Axioscope light microscope equipped with an MRc digital camera

^{33}P sample analysis

After harvest and freeze-drying, 10-50 mg of homogenised plant and soil materials were digested in 500 µl of concentrated H_2SO_4. These were heated to 365°C for 15 min, and 50 µl H_2O_2 were added to each sample when cool. Samples were reheated to 365°C for one minute, producing a clear digest solution which was then cooled and diluted to 5 ml with distilled water. One ml of each diluted digest was then added to 10 ml of the scintillation cocktail Emulsify-safe (Perkin Elmer, Beaconsfield, UK) before liquid scintillation counting.

^{14}C sample analysis

Approximately 10-20 mg of scintillation of sample was weighed into Combusto-cones (Perkin Elmer) which were then oxidised. CO_2 released through oxidation was trapped in 10 ml Carbosorb (Perkin Elmer, UK) prior to mixing with the scintillation cocktail 10 ml Permaflour (Perkin Elmer, UK). Total carbon (^{12}C + ^{14}C) fixed by the plant and transferred to the fungal network was calculated as a function of the total volume and CO_2 content of the labelling chamber and the proportion of the supplied $^{14}CO_2$ label fixed by plants. The difference in carbon between the static and rotated cores is considered equivalent to the total C transferred from plant to symbiotic fungus within the soil core, noting that a small proportion will be lost through soil microbial respiration. The total carbon budget for each experimental pot was calculated using equations from Cameron *et al.* (2007) (see below).

Stable isotope signatures of neighbouring plants

Leaf and root samples were washed, dried to constant weight at 105°C and ground to a fine powder in a ball mill (Retsch Schwingmühle MM2, Haan, Germany). Relative C and N isotope natural abundances of the leaf and root samples were measured in a dual element analysis mode with an elemental analyser (Carlo Erba Instruments 1108, Milan, Italy) coupled to a continuous flow isotope ratio mass spectrometer (delta S, Finnigan MAT, Bremen, Germany) via a ConFlo III open-split interface (Thermo Fisher Scientific, Bremen, Germany) as described in Bidartondo *et al.* (2004). Relative isotope abundances are denoted as δ values calculated according to the following equation: $\delta^{13}C$ or $\delta^{15}N = (R_{sample}/R_{standard} - 1) \times 1000$ [‰], where R_{sample} and $R_{standard}$ are the ratios of heavy to light isotope of the samples and the respective standard. Standard gases were calibrated with respect to international standards (CO_2 vs PDB, N_2 vs N_2 in air) with the reference substances ANU sucrose and NBS18 for the carbon isotopes and N1 and N2 for the nitrogen isotopes (International Atomic Energy Agency, Vienna, Austria). Reproducibility and accuracy of the C and N isotope abundance measurements were routinely controlled by measuring the laboratory standard acetanilide. In relative C and N isotope natural abundance analyses, acetanilide was routinely analyzed with variable sample weight at least six times within a batch of 50 samples. The maximum variation of $\delta^{13}C$ and $\delta^{15}N$ was always below 0.2‰.

Construction of mesh-covered cores

Based on the methods of Field *et al.* (2012) two windows (20 mm x 50 mm, Supplementary Figure S1) were cut into the below-ground portion of each core. The windows and base were covered with nylon mesh (10 μm pore size) and sealed with a fast-setting acrylic adhesive (Tensol 12, Bostok Limited, UK). This mesh size is fine enough to exclude lycophyte roots but allows the ingrowth of fungal hyphae. We perforated a fine-bore capillary tube using a needle and installed it to run the full-length of each of the cores (100 mm in length, 1.02 mm internal diameter; Portex, UK). The tubing ensured isotope solution was introduced and distributed evenly throughout the core volume. We sealed the capillary tube using acrylic adhesive 5 mm from the bottom of the core in order to prevent excess isotope leaching from the bottom of the core.

Sampling of lycophytes, liverworts and angiosperms

Sampling sites for *Lycopodiella inundata* and adjacent liverworts and angiosperms are listed in Supplementary Table 1 (S1).

Plant harvest and sample analyses

Upon detection of maximal belowground ^{14}C flux following release of $^{14}CO_2$, 3ml of 2 M KOH was introduced to each chamber to trap residual $^{14}CO_2$ gas in the chamber headspace. One ml of each 'used' KOH trap was transferred to vials containing 10 ml of the scintillation cocktail Ultima Gold (Perkin Elmer, Beaconsfield, UK) and the radioactivity of each sample determined through liquid scintillation. These data were used to calculate carbon budgets for each experimental pot (see below for equations).

Plant and soil materials were separated, freeze-dried, weighed and homogenised using a Tissue Lyser LT (Qiagen, UK).

^{33}P transfer from fungus to plant

The ^{33}P transferred from fungus to plant was determined using equation 1 (Cameron *et al.*, 2007):

$$M^{33}\mathrm{P} = \{[\frac{A}{S\mathrm{Act}}]M\mathrm{wt}\}\, Df$$

Where M^{33}P = Mass of ^{33}P, A = radioactivity of the tissue sample (Bq), SAct = specific activity of the source (Bq mmol^{-1}), Df = dilution factor and Mwt = molecular mass of P.

Carbon transfer from plant to fungus

The difference in carbon between the static and rotated cores is taken to be equivalent to the total C transferred from plant to symbiotic fungus within the soil core. Total carbon transferred by the plant to the fungus was calculated using equation 2:

$$M_C = \left(\left(\frac{A}{S\mathrm{Act}}\right)M14C\right) + (P_r\, x\, M\mathrm{wt}_c)$$

Where M_C = Mass of carbon transferred from plant to fungus, A = radioactivity of the tissue sample (Bq); SAct = specific activity of the source (Bq Mol^{-1}), $M^{14}C$ = atomic mass of ^{14}C, P_r = proportion of the total ^{14}C label supplied present in the tissue; $M\mathrm{wt}_C$ = mass of C in the CO_2 present in the labelling chamber (g) (from the ideal gas law; Equation 3):

$$m_{cd} = M_{cd}\left(\frac{PV_{CD}}{RT}\right) \therefore m_{c} = m_{cd} \text{ x } 0.27292$$

Where m_{cd} = mass of CO_2 (g), M_{cd} = molecular mass of CO_2 (44.01 g mol^{-1}) P = total pressure (kPa); V_{cd} = volume of CO_2 in the chamber (0.003 m^3); R = universal gas constant (J K^{-1} mol^{-1}); T, absolute temperature (K); m_c, mass of C in the CO_2 present in the labelling chamber (g), where 0.27292 is the proportion of C in CO_2 on a mass fraction basis (Cameron *et al.*, 2006).

Suppliers and addresses

Petersfield no.2 compost, Leicester, UK; Snijder Labs, Netherlands; Vaisala, Birmingham, UK; Zeiss, Germany; Sigma, UK; Hartmann Analytics, Germany; Isotech, Chesterfield, UK; Sercon Ltd., Crewe, UK; Carlo Erba Instruments, Milan, Italy; delta S, Finnigan MAT, Bremen, Germany; Thermo Fisher Scientific, Bremen, Germany; IBM Analytics, New York, USA

Supplementary figures

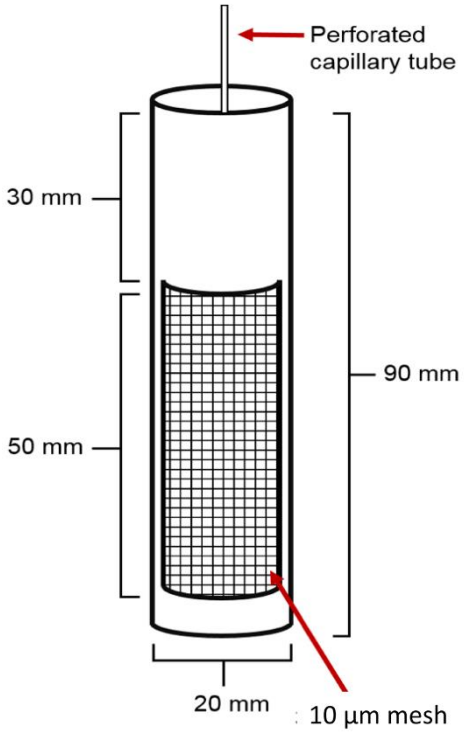

Figure S1 Schematic diagram of mesh-covered core showing dimensions of window (not drawn to scale).

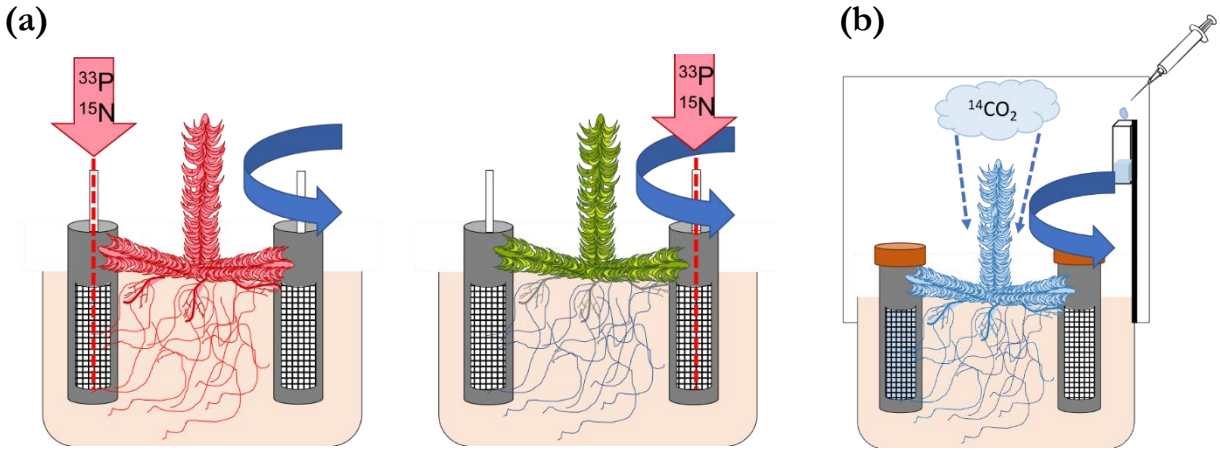

Figure S2 Experimental microcosm showing (a) ^{15}N and ^{33}P and (b) ^{14}C isotope tracing.

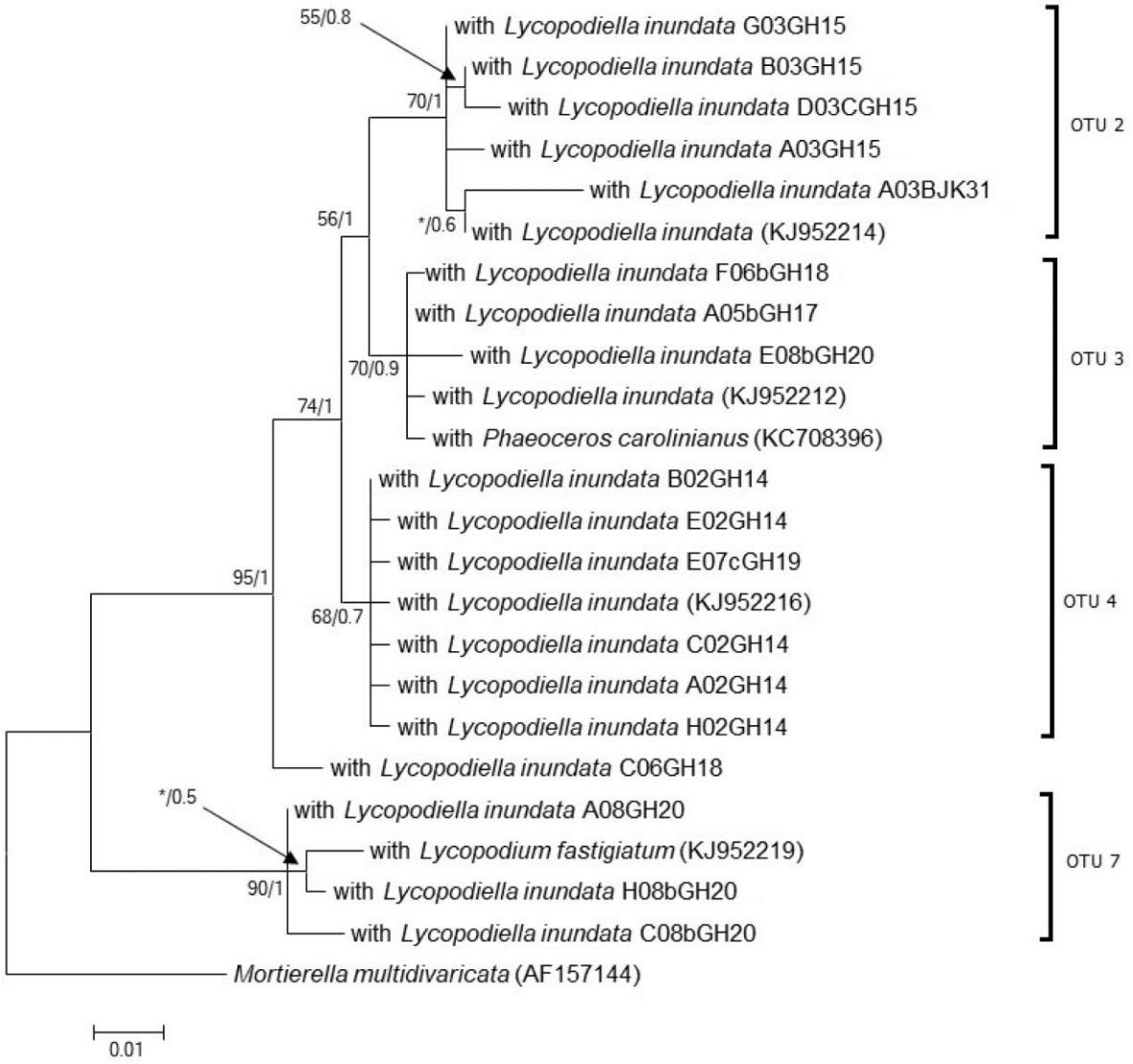

Figure S3 Phylogenetic relationships of Mucoromycotina OTUs associated with *Lycopodiella inundata* grown for isotope tracing and cytology experiments in controlled environment growth chambers. The final alignment consisted of 24 taxa and 397 characters. The TN93 + G model was used for analysis. The ML tree is shown. The values adjacent to each node correspond to the bootstrap support and posterior probabilities, respectively. An asterisk denotes a bootstrap value <50% or posterior probability <0.5.

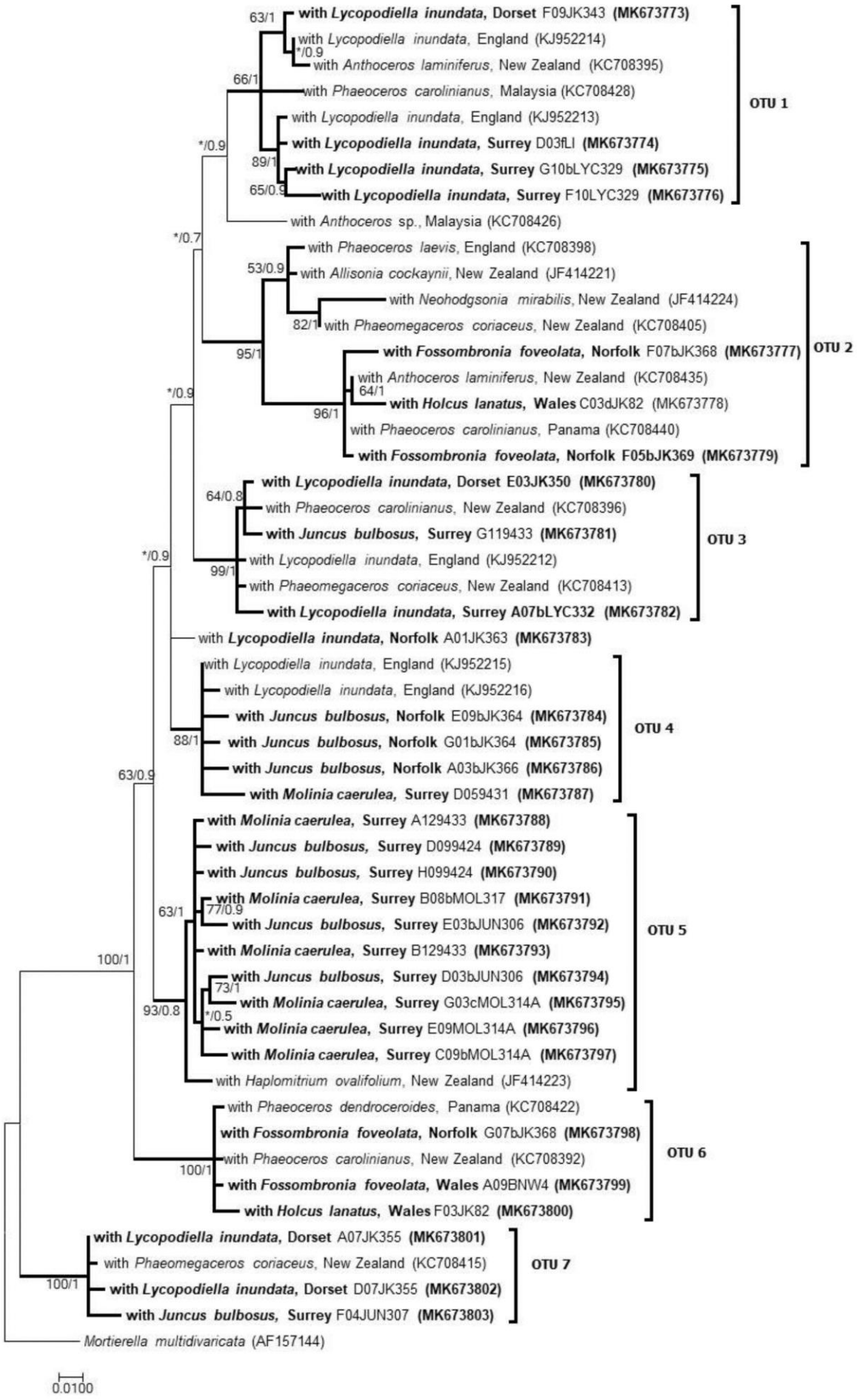
63/1
with Lycopodiella inundata, Dorset F09JK343 (MK673773)
with Lycopodiella inundata, England (KJ952214)
*/0.9
with Anthoceros laminiferus, New Zealand (KC708395)
66/1
with Phaeoceros carolinianus, Malaysia (KC708428)
with Lycopodiella inundata, England (KJ952213)
with Lycopodiella inundata, Surrey D03fLI (MK673774)
*/0.9
89/1
with Lycopodiella inundata, Surrey G10bLYC329 (MK673775)
65/0.9
with Lycopodiella inundata, Surrey F10LYC329 (MK673776)
OTU 1
with Anthoceros sp., Malaysia (KC708426)
*/0.7
with Phaeoceros laevis, England (KC708398)
53/0.9
with Allisonia cockaynii, New Zealand (JF414221)
with Neohodgsonia mirabilis, New Zealand (JF414224)
82/1
with Phaeomegaceros coriaceus, New Zealand (KC708405)
95/1
with Fossombronia foveolata, Norfolk F07bJK368 (MK673777)
with Anthoceros laminiferus, New Zealand (KC708435)
*/0.9
64/1
with Holcus lanatus, Wales C03dJK82 (MK673778)
96/1
with Phaeoceros carolinianus, Panama (KC708440)
with Fossombronia foveolata, Norfolk F05bJK369 (MK673779)
OTU 2
with Lycopodiella inundata, Dorset E03JK350 (MK673780)
64/0.8
with Phaeoceros carolinianus, New Zealand (KC708396)
with Juncus bulbosus, Surrey G119433 (MK673781)
*/0.9
with Lycopodiella inundata, England (KJ952212)
99/1
with Phaeomegaceros coriaceus, New Zealand (KC708413)
with Lycopodiella inundata, Surrey A07bLYC332 (MK673782)
OTU 3
with Lycopodiella inundata, Norfolk A01JK363 (MK673783)
with Lycopodiella inundata, England (KJ952215)
with Lycopodiella inundata, England (KJ952216)
with Juncus bulbosus, Norfolk E09bJK364 (MK673784)
88/1
with Juncus bulbosus, Norfolk G01bJK364 (MK673785)
63/0.9
with Juncus bulbosus, Norfolk A03bJK366 (MK673786)
with Molinia caerulea, Surrey D059431 (MK673787)
OTU 4
with Molinia caerulea, Surrey A129433 (MK673788)
with Juncus bulbosus, Surrey D099424 (MK673789)
with Juncus bulbosus, Surrey H099424 (MK673790)
with Molinia caerulea, Surrey B08bMOL317 (MK673791)
63/1
77/0.9
with Juncus bulbosus, Surrey E03bJUN306 (MK673792)
with Molinia caerulea, Surrey B129433 (MK673793)
100/1
with Juncus bulbosus, Surrey D03bJUN306 (MK673794)
73/1
with Molinia caerulea, Surrey G03cMOL314A (MK673795)
93/0.8
*/0.5
with Molinia caerulea, Surrey E09MOL314A (MK673796)
with Molinia caerulea, Surrey C09bMOL314A (MK673797)
OTU 5
with Haplomitrium ovalifolium, New Zealand (JF414223)
with Phaeoceros dendroceroides, Panama (KC708422)
with Fossombronia foveolata, Norfolk G07bJK368 (MK673798)
100/1
with Phaeoceros carolinianus, New Zealand (KC708392)
with Fossombronia foveolata, Wales A09BNW4 (MK673799)
with Holcus lanatus, Wales F03JK82 (MK673800)
OTU 6
with Lycopodiella inundata, Dorset A07JK355 (MK673801)
with Phaeomegaceros coriaceus, New Zealand (KC708415)
100/1
with Lycopodiella inundata, Dorset D07JK355 (MK673802)
with Juncus bulbosus, Surrey F04JUN307 (MK673803)
OTU 7
Mortierella multidivaricata (AF157144)
0.0100

Figure S4 An overview of phylogenetic relationships of Mucoromycotina OTUs associated with bryophytes, lycophytes and angiosperms from various UK locations based on partial 18S gene sequences. Only the subset of representative OTUs relevant to this study are shown. Genbank accession numbers (MK673773-MK673803) of selected sequences from this study are shown in parentheses, Codes after plant names refer to the clone identity. Our sequences lie within the *Densosporaceae* which is sister to the *Endogonaceae* (Desirò *et al.* 2013). The final alignment consisted of 94 taxa and 693 characters. Sequences shorter than 690 bp were excluded from the analysis. The model selected for analysis was TN93 + G + I. The tree shown is that inferred from the ML analysis. The values adjacent to each node correspond to the bootstrap support and posterior probabilities, respectively. An asterisk denotes a bootstrap value <50% or posterior probability <0.5.

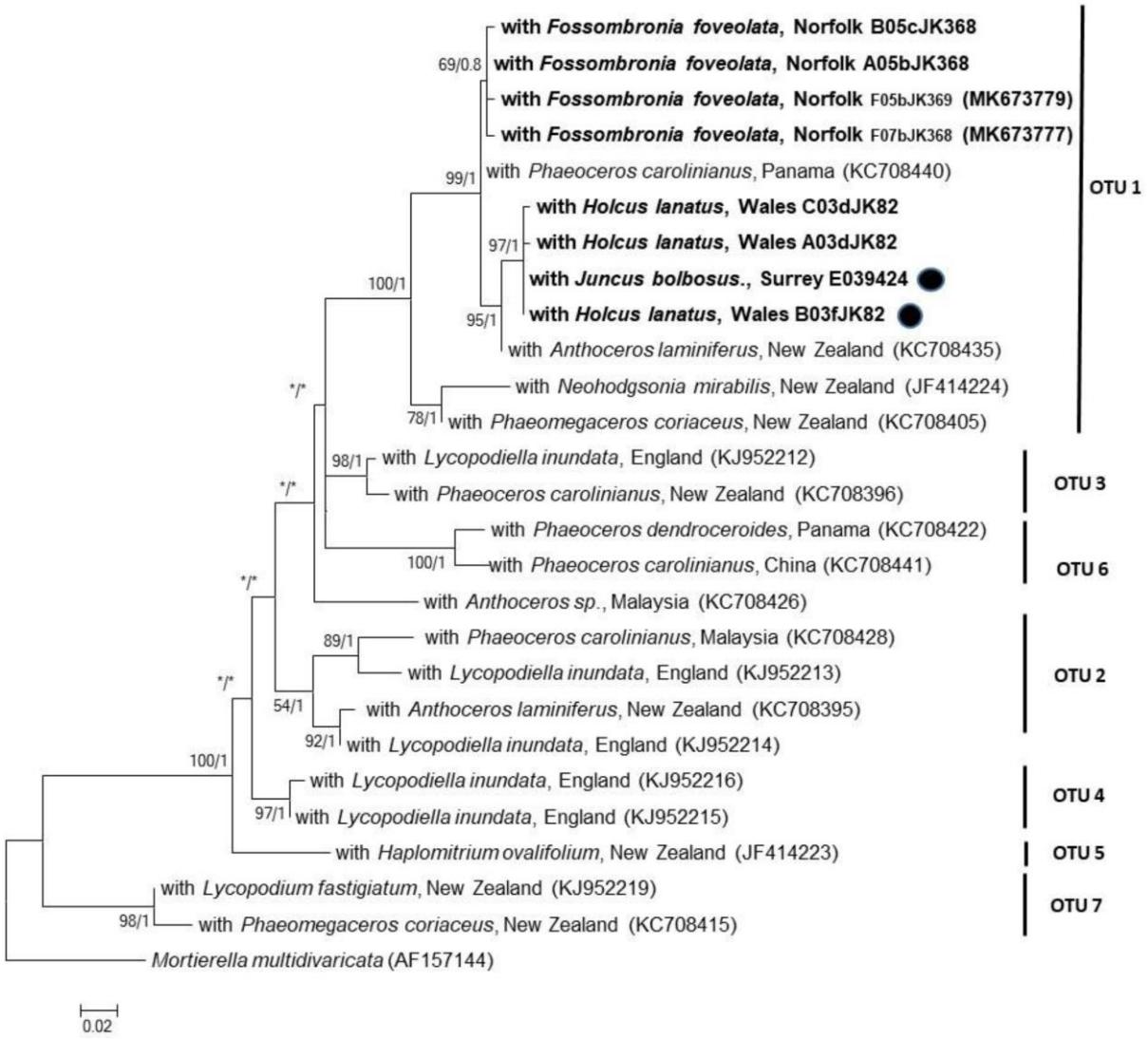

Figure S5 Phylogenetic relationships of partial 18S DNA sequences classified as OTU 2, corresponding to "group A" in Desirò *et al.* (2013). Black dots indicate identical sequences isolated from different plant species. The ML tree is shown. Values at nodes refer to ML/Bayesian inference. The final alignment consisted of 731 characters and analysis was conducted using the TN93 + G + I substitution model.

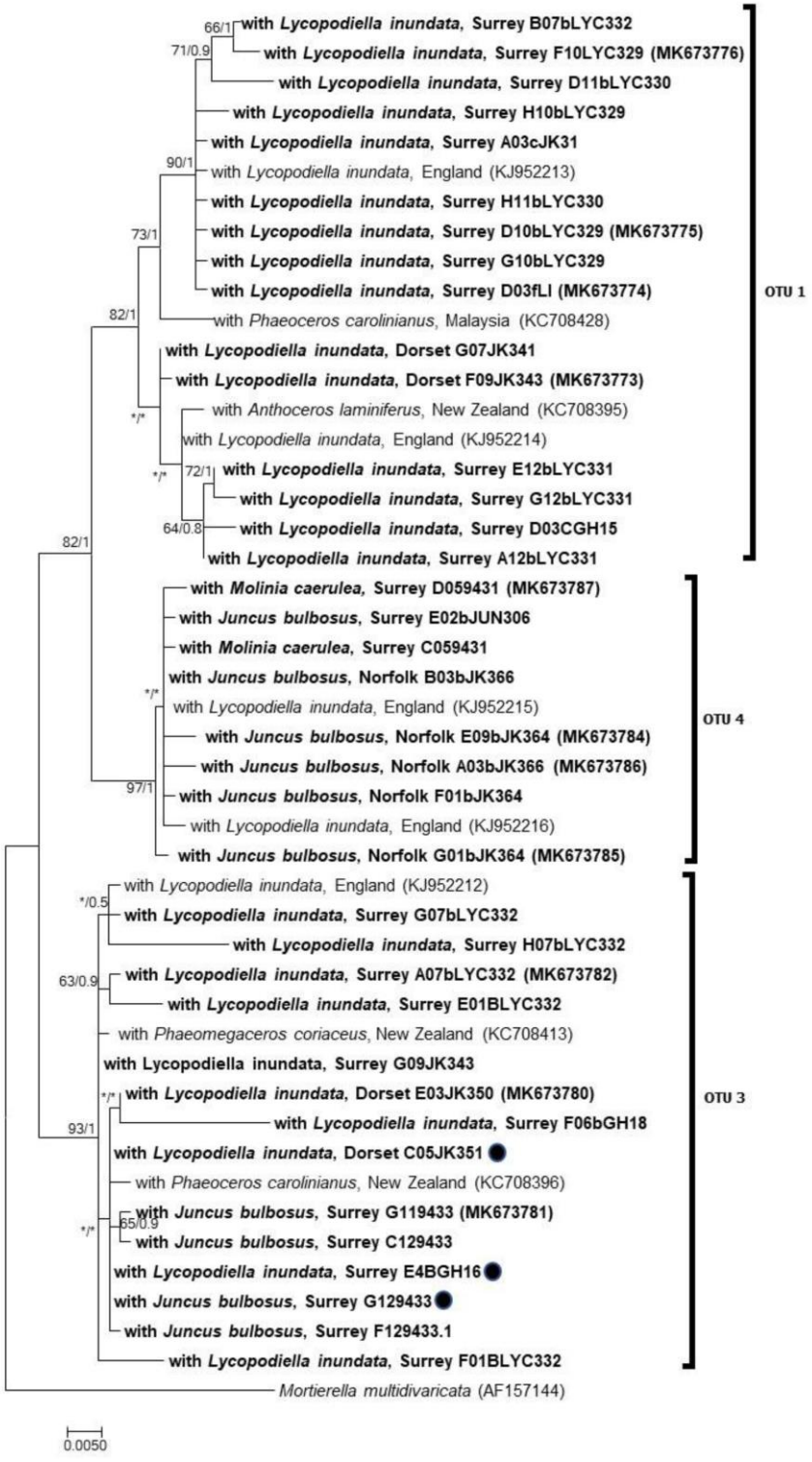

Figure S6 Phylogenetic relationships of partial 18S DNA sequences classified as OTU 1,3 and 4. The ML tree is shown. Black dots indicate identical sequences isolated from different plant species or locations. The final alignment consists of 681 characters and phylogenetic analysis was conducted using the best fit model, TN93 + G + I, as explained in materials and methods except that 2,000,000 generations were run for Bayesian analysis. The values adjacent to each node correspond to the bootstrap support and posterior probabilities, respectively. An asterisk denotes a bootstrap value <50% or posterior probability <0.5.

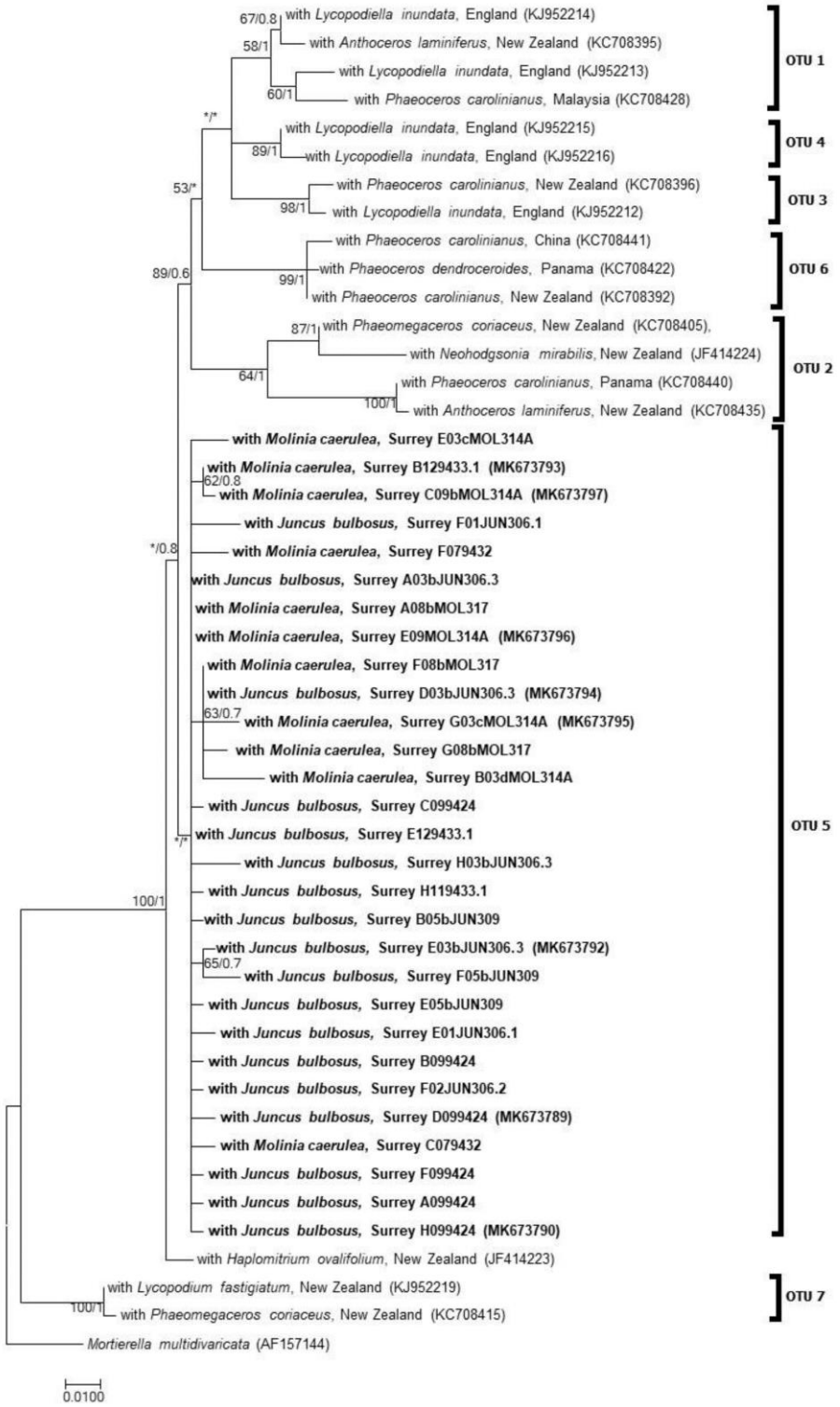

Figure S7 Phylogenetic relationships of partial 18S DNA sequences clustering within OTU 5. The final alignment comprised 649 characters and used the TN93 +G + I substitution model. The ML tree is featured. The values adjacent to each node correspond to the bootstrap support and posterior probabilities, respectively. An asterisk denotes a bootstrap value <50% or posterior probability <0.5.

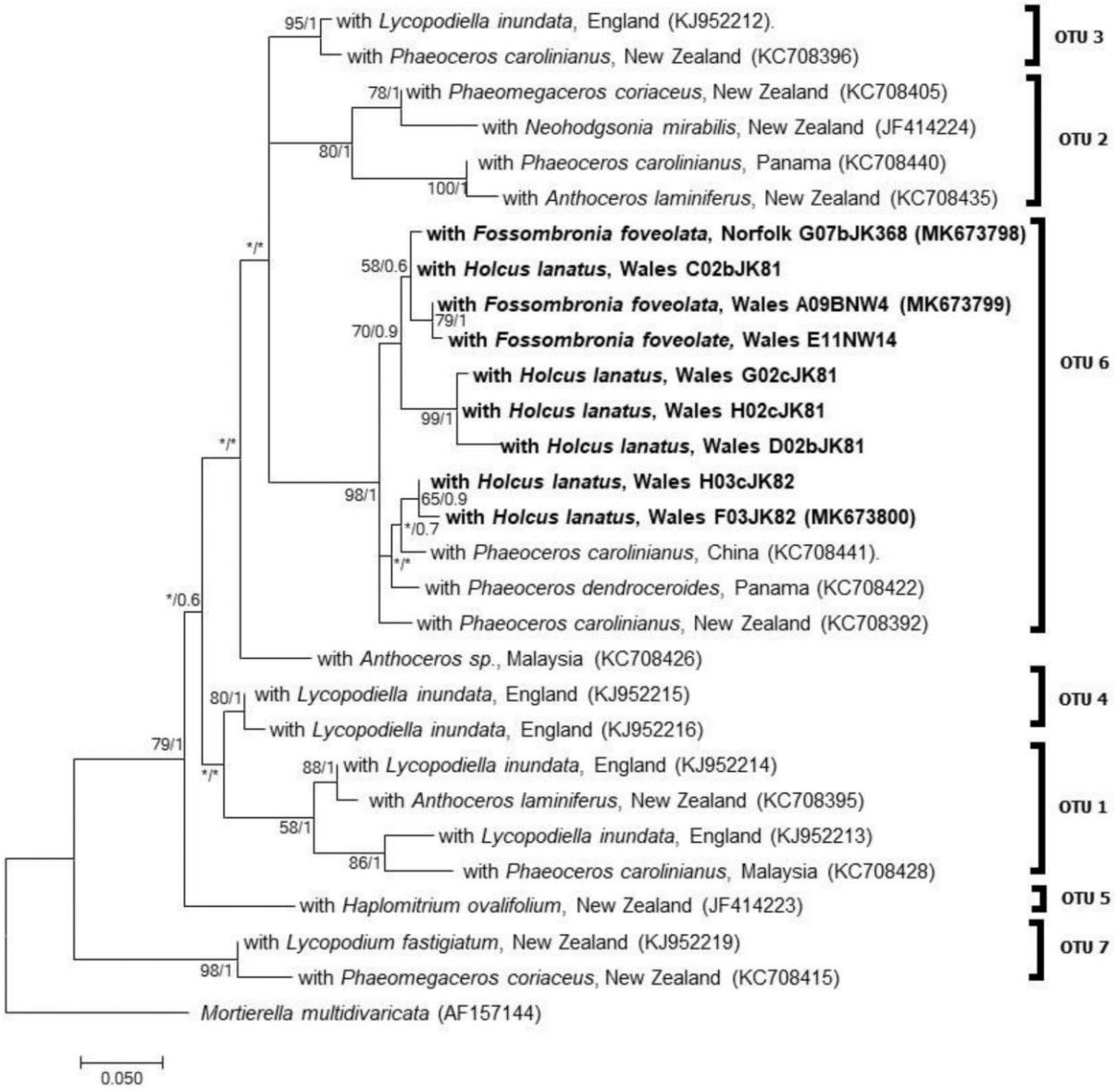

Figure S8 Phylogenetic relationships of partial 18S DNA sequences classified as OTU 6, corresponding to "group B" in Desirò *et al.* (2013). The ML tree is displayed. Black dots indicate identical sequences isolated from different plant species or locations. The final dataset consisted of 622 characters and was analysed using the TN93 + G + I substitution model. Values at the nodes indicate ML/Bayesian inference values. An asterisk denotes a bootstrap value <50% or posterior probability <0.5.

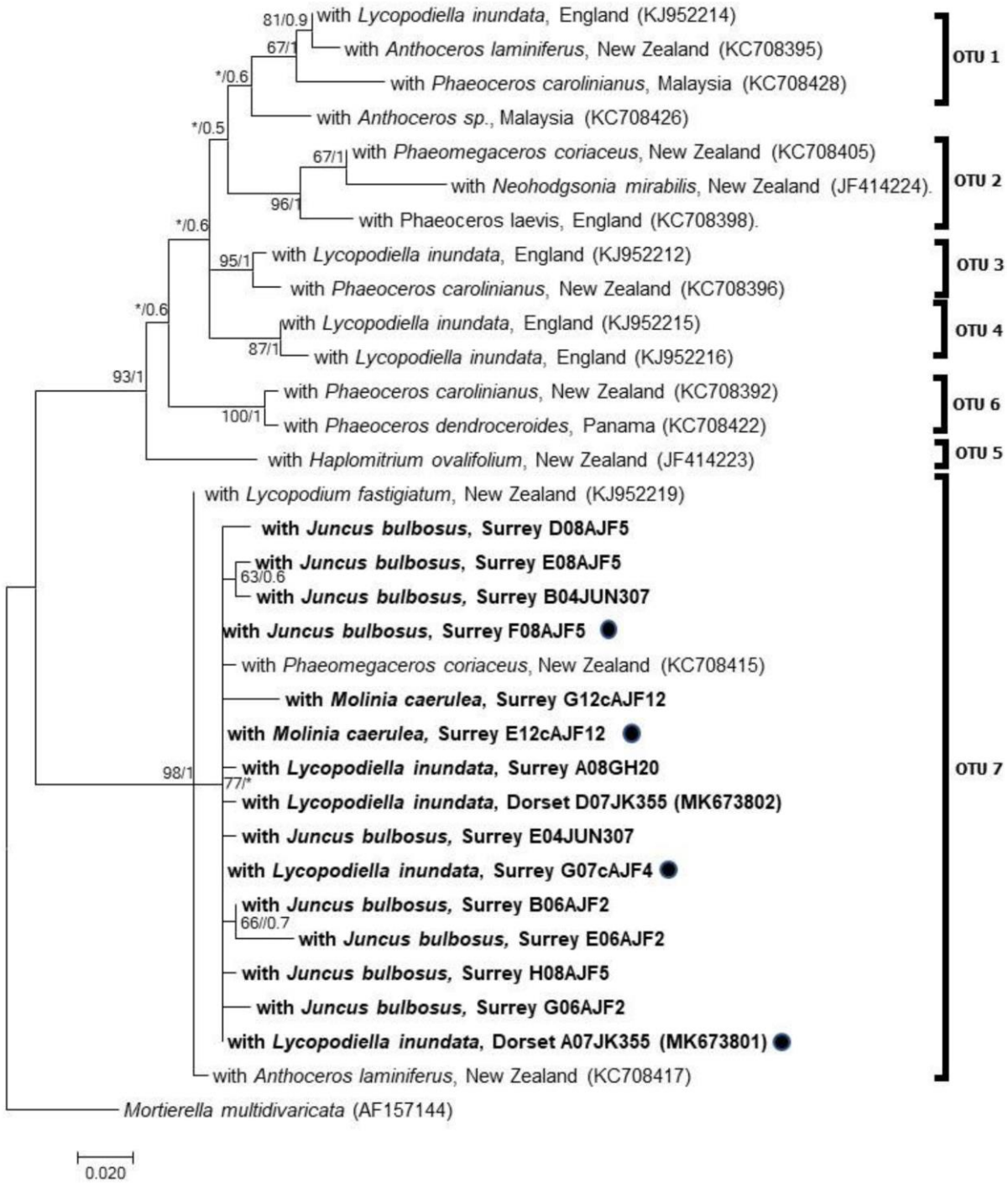

Figure S9 Phylogenetic relationships of partial 18S DNA sequences clustering with OTU 7, corresponding to "group I" in Desirò *et al.* (2013). The ML tree is shown. The final alignment comprised 580 characters and the substitution model used for the analysis was TN93 + G + I. Values at the nodes indicate ML/Bayesian inference values. An asterisk denotes a bootstrap value <50% or posterior probability <0.5.

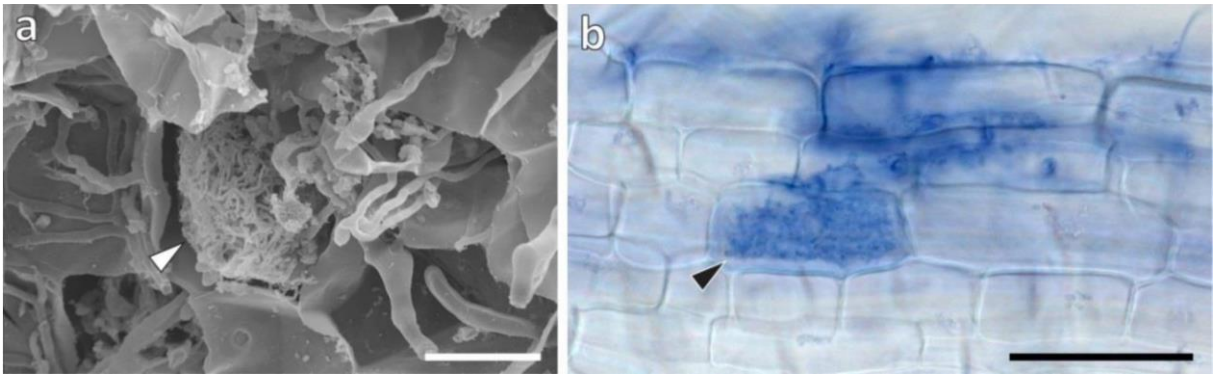

Figure S10 (a) Scanning electron micrograph of *Fossombronia foveolata* thallus (from Thursley Common*)* showing coil of fine hyphae (arrowhead) and coarse hyphae in surrounding cells; **(b)** Light micrograph of trypan blue stained root of *Holcus lanatus* (from Lynn Crafnant) showing fine hyphae and an arbuscule-like structure (arrowhead). Scale bars: **(b)** 50 μm, **(a)** 20 μm.

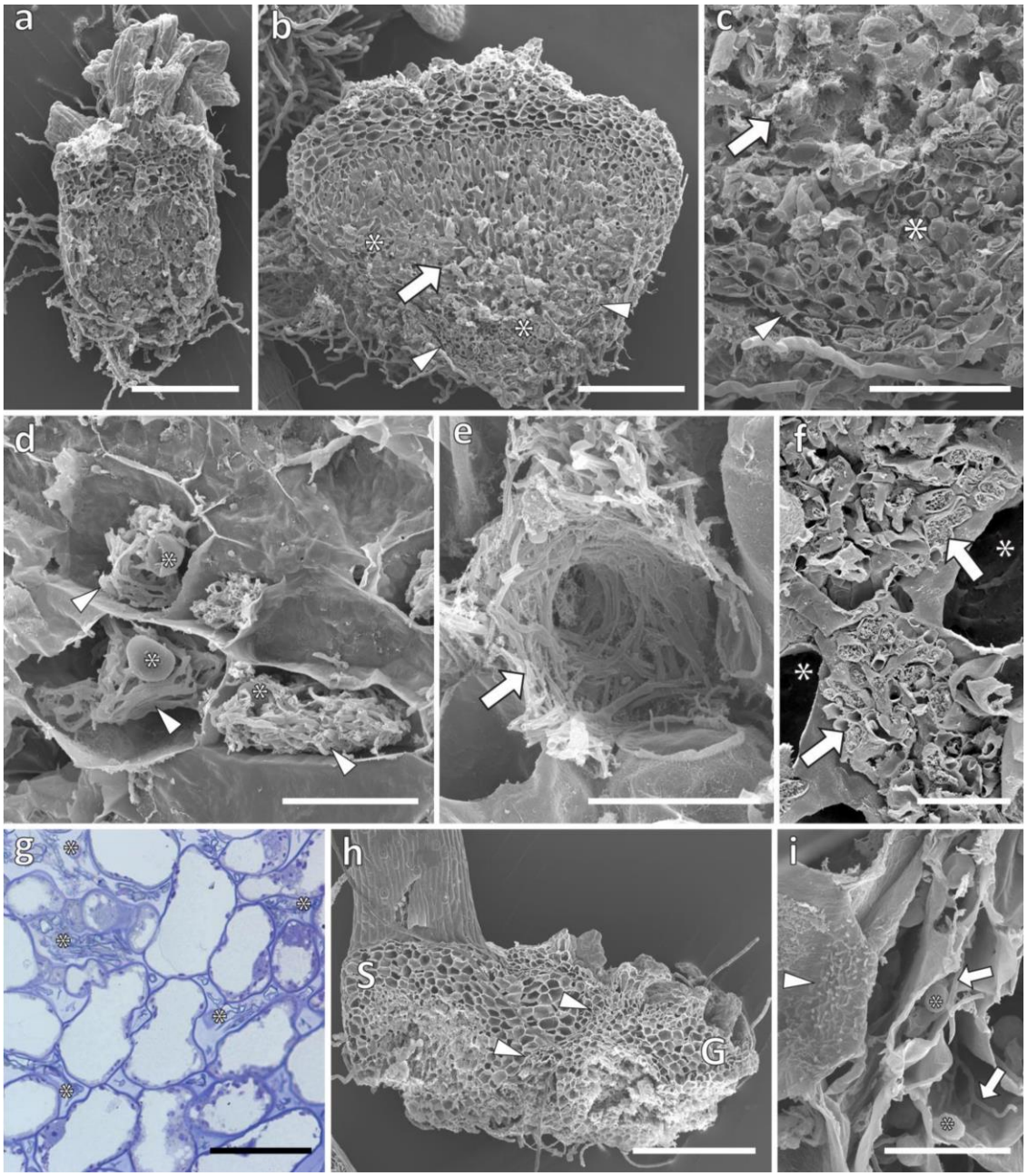

Figure S11 Scanning electron micrographs, except **(g)** light micrograph of toluidine blue stained semi-thin sections. Gametophyte morphologies in *Lycopodiella inundata* (from Thursley Common) **(a, b), (b, c)** zonation of fungal colonization in a gametophyte: intracellular in the outer cortical layers (arrowheads) and surrounding tissue (*), and strictly intercellular in the central region characterized by large, mucilage-filled, intercellular spaces (arrows); **(d)** hyphal coils (arrowheads) and vesicles (*) in the outer cortical layers; **(e, f)** centrally, the fungus colonizes the system of large intercellular spaces between the host cells (* in f); here the fine hyphae (arrows) **(e)** eventually become swollen, reaching diameters of > 3 µm (arrows) **(f); (g)** intercellular fungal proliferation (*), note the non-colonized, living host cells in this zone; **(h)** young sporophyte (S) attached to gametophyte (G), arrowheads point to the sporophyte-gametophyte junction, enlarged in **(i).** Note that the gametophyte fungus, which is intracellular at the S-G junction and consists of fine hyphae (arrows) and small vesicles (*) does not cross the placenta identifiable by its numerous wall ingrowths (arrowhead). Scale bars: **(a, b, h)** 500 µm, **(c)** 200 µm, **(d, g)** 50 µm, **(e, f, i)** 20 µm.

Table S1 Samples of lycophytes, liverworts and angiosperms analysed with their origin.

Sample species	**Samples analysed**	**Origin**
Lycophytes		
Lycopodiella inundata (L.) Holub	24	Thursley Common, Surrey; England
Lycopodiella inundata (L.) Holub	16	Studland Heath, Dorset; England
Lycopodiella inundata (L.) Holub	4	confidential site, Norfolk; England
Liverworts		
Fossombronia foveolata Lindb.	1	Thursley Common, Surrey; England
Fossombronia foveolata Lindb.	3	confidential location, Norfolk; England
Fossombronia foveolata Lindb.	6	Lynn Crafnant; Wales
Angiosperms		
Molinia caerulea (L.) Moench	28	Thursley Common, Surrey; England
Juncus bulbosus L.	30	Thursley Common, Surrey; England
Juncus bulbosus L.	3	confidential location, Norfolk; England
Holcus lanatus L.	3	Lynn Crafnant; Wales

Table S2 A summary of Mucoromycotina OTUs associated with liverworts, lycophytes and angiosperms at four UK sites. The numbers within each column represent the number of partial 18S sequences that cluster within each OTU.

Species	**Location**	**OTU 1**	**OUT 2**	**OUT 3**	**OUT 4**	**OUT 5**	**OUT 6**	**OUT 7**	**ND[1]**
Lycopodiella inundata (*n* = 4)	Dorset	2	0	4	0	0	0	3	0
Fossombronia foveolata (*n* = 2)	Norfolk	0	4	0	0	0	1	0	0
Juncus bulbosus (*n* = 2)	Norfolk	0	0	0	5	0	0	0	0
Lycopodiella inundata (*n* = 1)	Norfolk	0	0	0	0	0	0	0	1
Lycopodiella inundata (*n* = 6)	Surrey	13	0	7	0	0	0	4	0
Juncus bulbosus (*n* = 12)	Surrey	0	1	4	13	31	0	16	0
Molinia caerulea (*n* = 8)	Surrey	0	0	0	9	19	0	12	0
Fossombronia foveolata (*n* = 2)	Wales	0	0	0	0	0	4	0	0
Holcus lanatus (*n* = 2)	Wales	0	6	0	0	0	8	0	0

[1]ND = not determined, singleton OTU.

Table S3 A summary of the amounts of carbon, ^{15}N and ^{33}P detected in static and rotated core of microcosms used during carbon-for-nutrient experiments between *Lycopodiella inundata* and Mucoromycotina FRE fungi. SEM = standard error of the mean.

	Static Core				Rotated Core			
	%		SEM		%		SEM	
Carbon allocated to fungus	1.13		0.74		0.65		0.59	
	ng	SEM	ng/g^{-1}	SEM	ng	SEM	ng/g^{-1}	SEM
Carbon in fungus	4481	2019.30	680.20	410.49	1549.23	968.53	94.14	30.64
^{15}N in plant tissue	1434.62	480.76	1077.47	329.93	294.39	177.49	360.50	149.08
^{33}P in plant tissue	0.022	0.007	0.015	0.004	0.003	0.001	0.009	0.005

Respective references

Bidartondo MI, Burghardt B, Gebauer G, Bruns TD, Read DJ (2004) Changing partners in the dark: isotopic and molecular evidence of ectomycorrhizal liaisons between forest orchids and trees. Proc Biol Sci **271**: 1799-1806.

Cameron DD, Johnson I, Leake JR, Read DJ (2007) Mycorrhizal acquisition of inorganic phosphorus by the green-leaved terrestrial orchid *Goodyera repens*. Ann Bot **99**: 831-834.

Cameron DD, Leake JR, Read DJ (2006) Mutualistic mycorrhiza in orchids: evidence from plant–fungus carbon and nitrogen transfers in the green-leaved terrestrial orchid *Goodyera repens*. New Phytol **171**: 405-416.

Desirò A, Duckett JG, Pressel S, Villarreal JC, Bidartondo MI (2013) Fungal symbioses in hornworts: a chequered history. Proc Biol Sci **280**: 20130207.

Field KJ, Cameron DD, Leake JR, Tille S, Bidartondo MI, Beerling DJ (2012) Contrasting arbuscular mycorrhizal responses of vascular and non-vascular plants to a simulated Palaeozoic CO_2 decline. Nat Commun **3**: 835.

Ligrone R, Duckett JG (1994) Cytoplasmic polarity and endoplasmic microtubules associated with the nucleus and organelles are ubiquitous features of food-conducting cells in bryoid mosses (Bryophyta). New Phytol **127**: 601-614.

Declaration

(Eidesstattliche) Versicherungen und Erklärung

(§ 9 Satz 2 Nr. 3 PromO BayNAT)

Hiermit versichere ich eidesstattlich, dass ich die Arbeit selbstständig verfasst und keine anderen als die von mir angegebenen Quellen und Hilfsmittel benutzt habe (vgl. Art. 64 Abs. 1 Satz 6 BayHSchG).

(§ 9 Satz 2 Nr. 3 PromO BayNAT)

Hiermit erkläre ich, dass ich die Dissertation nicht bereits zur Erlangung eines akademischen Grades eingereicht habe und dass ich nicht bereits diese oder eine gleichartige Doktorprüfung endgültig nicht bestanden habe.

(§ 9 Satz 2 Nr. 4 PromO BayNAT)

Hiermit erkläre ich, dass ich Hilfe von gewerblichen Promotionsberatern bzw. -vermittlern oder ähnlichen Dienstleistern weder bisher in Anspruch genommen habe noch künftig in Anspruch nehmen werde.

(§ 9 Satz 2 Nr. 7 PromO BayNAT)

Hiermit erkläre ich mein Einverständnis, dass die elektronische Fassung meiner Dissertation unter Wahrung meiner Urheberrechte und des Datenschutzes einer gesonderten Überprüfung unterzogen werden kann.

(§ 9 Satz 2 Nr. 8 PromO BayNAT)

Hiermit erkläre ich mein Einverständnis, dass bei Verdacht wissenschaftlichen Fehlverhaltens Ermittlungen durch universitätsinterne Organe der wissenschaftlichen Selbstkontrolle stattfinden können.

_____

Ort, Datum, Unterschrift